Université de Lille

McMaster University

Co-tutorial Doctoral Thesis

Computational Actinide Chemistry:
Structure, Bonding and Thermodynamics

Author:

Sophie KERVAZO

A thesis submitted in fulfillment of the requirements
for the degree of Doctor of Philosophy
in:

Physics - Diluted medium and fundamental optics
in the doctoral school

Sciences de la Matière, du rayonnement et de l'environnement
in:

Laboratoire Physique des Lasers, Atomes et Molécules
Department of Chemistry and Chemical Biology
Defense October 26th 2018

Protractors
Pr. Nathalie GUIHERY   Université P. Sabatier Toulouse III
Dr. Emmanuel FROMAGER   Université de Strasbourg
Examiners
Pr. Laurent MARON   Université P. Sabatier Toulouse III
Dr. Dominique GUILLAUMONT   CEA Marcoule
Supervisors
Dr. Valérie VALLET   Université de Lille
Pr. Paul AYERS   McMaster University
Co-supervisors
Dr. Florent REAL   Université de Lille
Dr. André SEVERO PEREIRA   Université de Lille
GOMES

This page intentionally left blank

Computational Actinide Chemistry:
Structure, Bonding and Thermodynamics

Auteur:

Sophie KERVAZO

En vue de l'obtention du

DOCTORAT DE L'UNIVERSITÉ DE LILLE

en

PHYSIQUE: MILIEUX DILUÉS ET OPTIQUE FONDAMENTAL

de l'école doctorale

Sciences de la Matière, du rayonnement et de l'environnement

au sein des laboratoires:

Laboratoire Physique des Lasers, Atomes et Molécules

Department of Chemistry and Chemical Biology

Défence: 26/10/2018

iv

This page intentionally left blank

ABSTRACT

The main question of this thesis is: do we have today the tools to efficiently describe the structure, the bonding and the thermodynamics of actinide systems? This broad question is answered thanks to three studies. The first two are directly applied to the plastic industry and the nuclear plant safety. The last one, more fundamental, concerns the benchmarking of newly developed theoretical approach on f-element systems. First, actinides and transition metal arene-coordinated alkyl cations have been recently proven to be efficient catalysts for ethylene polymerizations. Interestingly, thorium, uranium and zirconium alkyl cations? catalytic activity depends on the solvent. To understand these behaviors and to confirm the tendency of these complexes to engage in unusual-arene coordination, relativistic DFT calculations combined with a characterization of the interaction thanks to the ETS-NOCV method are used. Second, in accident scenario along the reprocessing of spent nuclear fuel, plutonium can be released in various volatile forms (PuO_2, PuO_3 or $PuO_2(OH)_2$, ...). The exploration of these scenarios by the use of simulations requires, among the various parameters, the knowledge of the thermodynamic properties of the possibly formed elements. Our in-silico study focusses on the determination of the enthalpies of formation of the former two species for which experimental uncertainties remain, using multi-configurational relativistic wavefunction method. The last part of the thesis focusses on the benchmark of the B2-PLYP functional for f-element systems, which turns out quite accurate with respect to the experimental data and the gold-standard CCSD(T) method.

ABSTRACT

La question générale traitée dans cette thèse est de déterminer si, aujourd'hui, nous disposons d óutils théoriques efficaces pour d' écrire la structure, la liaison et les propriétés thermodynamiques de système comprenant un actinide. Cette large question va être abordée à láide de trois études différentes. Les deux premières sont directement liées à l?industrie plastique et à la sureté nucléaire. La dernière, plus fondamentale concerne une analyse comparative d?une approche théorique nouvellement développée sur des systèmes comprenant des éléments f. Tout dábord, les cations alkyles contenant un actinide (Th, U) ou un métal de transition (Zr) coordonné à un arène se sont révélés efficaces pour la catalyse de la synthèse du polyéthylène. étonnamment, les activités catalytiques des cations alkyles dépendent du solvant. Pour comprendre cela et confirmer la tendance quónt ces complexes à se lier à l?arène, une étude en DFT dans un contexte relativiste combinée à une caractérisation de liaison avec la méthode ETS-NOCV fut faite. La deuxième étude vise à étoffer les bases de données thermodynamiques qui servent à explorer numériquement les scénarios d?accidents. Notre étude in silico porte sur la détermination des enthalpies de formation des deux espèces pour lesquelles des incertitudes expérimentales subsistent (PuO_3 ou $PuO_2(OH)_2$, ...), en utilisant une méthode quantique multiconfigurationnelle et relativiste. La dernière partie de la théorie se concentre sur l?estimation de la précision de la fonctionnelle B2-PLYP pour les éléments f, qui sávère assez précise en comparaison aux données expérimentales et à la méthode de référence CCSD(T).

Acknowledgements

First, I want to thank the protractors Emmanuel Fromager and Nathalie Guihery the jury Dominique Guillaumont and Laurent Maron who take the time to read, listen and give me a feedback on my work. I would like to acknowledge David Emslie et Randy Dumont for getting up so early to attend my PhD defence. My directors also need to be thanked, the four of them is the perfect mixture and is the whole spectrum in their scientific knowledges, listening, advices and managing skills. In science, collaboration is a key to success and I was lucky enough to work with amazing searchers: Françis Virot, David Emslie, Stefan Knecht, Leon Freitag and Benjamin Helmich-Paris.

A french comedian Pierre Desproges in one of his chronicles of ordinary hatred said the humanity is divided in four categories: relations, friends, close friends and people you do not know. The the people I do not know, thank you for reading this lines. I hope it can help for your project or to fight insomnia.

Friends/ colleagues: during a PhD, the time spend with friends being inversely proportional to that spend with the colleagues so I thank you all for enlightening scientific conversions, nice beers or a nice scientific conversions with enlightening beers. Family (not describe by Desproges): I have the luck to have a great family, always there when needed or just to share a slice of pizza. Thank you for being here, it is also a pleasure to go home thanks to you all. Close friend: Desproges said that you can count them on the Baron Empain's hand or Django Reihart's for the most misanthrope of us. Nonetheless, you are still being here, thank you !

Desproges was then adding the woman he loved. I will just change the gender to thank to man who is here for me day after day. Finally I think Desproges forget another type of people: the mothers. I thank mine for always supporting me and being there.

REMERCIEMENTS

Contents

xiv

List of Figures

List of Tables

List of Abbreviations

AMFI	**A**verage **M**ean Field Integrals
ANO	**A**tomic **N**atural **O**rbitals
ASTEC	**A**ccident **S**ource **T**erm **E**valuation **C**ode
BSSE	**B**asis **S**ets **S**uperpositon **E**rror
CASSCF	**C**omplete **Actif S**pace **S**elf **C**onsistent **F**ield
CASPT2	**C**omplete **Actif S**pace **P**erturbation **T**heory at the **2**nd order
CBS	**C**omplete **B**asis **S**et
CC	**C**oupled **C**luster
CCSD(T)	**C**oupled **C**luster with **S**ingles and **D**ouble and **T**riple
CI	**C**onfiguration **I**nteraction
CPP	**C**ore **P**olarisation **P**otential
CSF	**C**onfiguration **S**tate **F**unction
DFT	**D**ensity **F**unctional **T**heory
DKH	**D**ouglas **K**roll **H**ess
DMRG	**D**ensity **M**atrix **R**enormalisation **G**roup
EA	**E**lectronic **A**finity
ECP	**E**ffective **C**ore **P**otential
EOM	**E**quation **O**f **M**otion
ETS	**E**xtended **T**ransition **S**tate
FCI	**F**ull **C**onfiguration **I**nteraction
FORA	**F**irst **O**rder **R**egular **A**pproximation
GGA	**G**eneralized **G**radient **A**pproximation
HF	**H**artree **F**ock
IP	**I**onisation **P**otential
IRSN	**I**nstitut **R**adioprotection et de **S**ureté **N**ucléaire
KS	**K**ohn **S**ham
GTO	**G**aussian **T**ype **O**rbitals
LCAO	**L**inear **C**ombimaison of **A**tomic **O**rbitals
LDA	**L**ocal **D**ensity **A**pproximation
MAD	**M**ean **A**verage **D**eviation
MO	**M**olecular **O**rbital

MP	**M**øller-**P**lesset
MP2	**M**øller-**P**lesset at the **2**nd order
NEVPT2	**N** -**E**lectron **V**alence state **P**erturbation **T**heory at the **2**nd order
NOCV	**N**atural **O**rital for **C**hemical **V**alence
PE	**P**oly**E**tylene
PT	**P**erturbation **T**heory
PUREX	**P**lutonium **U**ranium **R**edox **EX**traction
RASSI	**R**estricted **Actif S**pace **S**tate **I**nteraction
RECP	**R**elativistic **E**ffective **C**ore **P**otential
RHF	**R**estricted **H**artree **F**ock
SA	**S**tate **A**verage
SCF	**S**elf **C**onsistent **F**ield
SF	**S**pin **F**ree
SO	**S**pin **O**rbit
SOC	**S**pin **O**rbit **C**oupling
SR	**S**calar **R**elativistic
SS	**S**tate **S**pecific
STO	**S**later **T**ype **O**rbitals
TDDFT	**T**ime **D**ependent **D**ensity **F**unctional **T**heory
TPH	**T**tetra-**P**ropylene
UCCSD(T)	**U**nrestricted **C**oupled **C**luster with **S**ingle **D**ouble and (**T**riple)
UHF	**U**nrestricted **H**artree **F**ock
ZORA	**Z**eroth **O**rder **R**egular **A**pproximation
ZPE	**Z**ero **P**otential **E**nergy

Chapter 1

General Introduction

Actinides are located in the last row of the periodic table, with an atomic number of 89 to 103 and even if they are large atoms with limited natural availability, for some of them, their use are present in our daily life. The plastic piece holding this pages together and the electric power used to write them do not contain actinides but could be the result of the daily exploitation of actinides complexes.

As quantum chemist, the modelling actinides can be a challenge for two main reasons. The first is the inclusion of relativistic effects, the second is how to properly take into account the electronic correlation within the partially occupied 7s, 5f and 6d valence orbitals of actinides. The main question of this thesis is: do we have today the tools to efficiently describe the structure, the bonding and the thermodynamics of actinide systems ?

This broad question is answered thanks to three studies. The two first are directly applied to the plastic industry and the nuclear plant safety. The last one, more fundamental, concerns the benchmarking of double hybrid functional on f-element systems.

The first applied use of actinides we are interested in is the use of actinides complexes as catalyst for the ethylene polymerisation. As with many great discoveries in chemistry, and sciences in general, polyethylene (PE) was first synthesised in Germany by accident in 1898 by Hans von Pechmann. It has now an important position in our daily life since it is used in many plastic items such as plastic bags, bottles, etc...

The most widely used ethylene polymerisation catalysis process is the Ziegler-Natta that allows an ethylene coordination and 1,2 insertion [1] in arene solvent in industry [2] or alkane one in academic laboratory [3]. Many patents are filled as the industrial application of new and better catalysts for ethylene polymerisation could really

be lucrative. The most interesting patent here was filled by Dow Chemical Company in 1987 in order to base, for the first time, the polymerisation of ethylene on actinides and more precisely on a mixture of bis(metallocene) precursor $[Cp^*_2AnX_2]$ and $[Cp^*AnX_3]$ (An = Th, U and X = Cl, Me, CH_2SiMe_3) with different activating agents.

With the goal of improving the polymerisation of polyethylene, Pr David Emslie and his former PhD student Nicholas R. Andreychuk at McMaster University worked on new compounds based on actinides as catalysts. They could obtain the arene-coordinated alkyl cations $[(XA_2)An(CH2SiMe_3)(arene)]^+$ with (An = Th, U; XA_2 = 4,5-bis(2,6-diisopropylanilido)-2,7-di-*tert*-butyl-9,9-dimethylxanthene); arene = benzene, toluene, bromobenzene or fluorobenzene) (Figure 1.1) and $[B(C_6F_5)_4]^-$ as counter ion and the close equivalent $[(XN_2)Zr(CH_2SiMe_3)(arene)]^+$ with the same arenes and (XN_2) being the 4,5-bis(2,4,6-triisopropylanilido)-2,7-di-*tert*-butyl-9,9-dimethylxanthene.
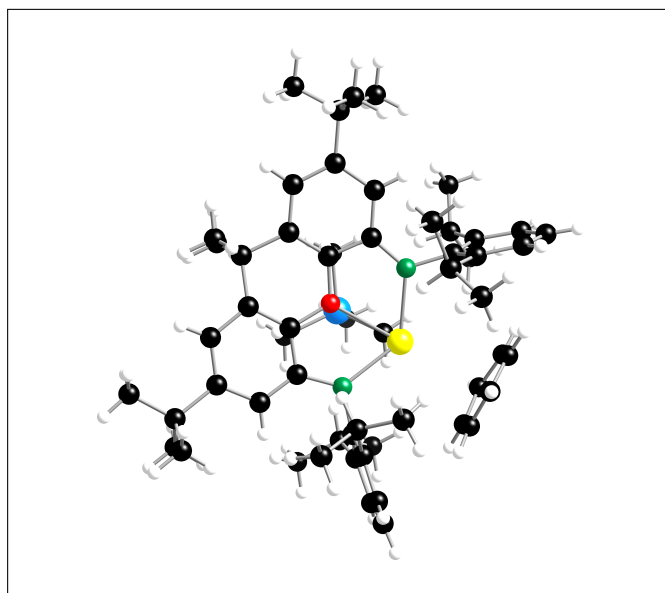
FIGURE 1.1: $(XA_2)U(CH2SiMe_3)(benzene)^+$

The activity of the catalyst does not only dependent on the arene but also of the metallic center. Our theoretical contribution, presented in Chapter 3 aims at understanding the mechanism of the catalysis by an in-depth study of the bond between the arene and the transition metal Zr or an actinide (Th or U) center

As second study, we worked with the French Radioprotection and Nuclear Safety agency (IRSN). While in the past decades the climate change and the future nuclear plants are at the heart of political debate, it is important to recall that no matter the prospective political decisions, nuclear safety must be addressed now. One of the challenge of nuclear power plants is the recycling of the nuclear fuel. Wordwide

the chosen recycling process is the PUREX (Plutonium Uranium Redox EXtraction) one. It uses a liquid-liquid extraction in order to separate the fission products from Plutonium and Uranium in order to reinject the former in the nuclear cycle. The problem with PUREX process is that the solvent tetra-propylene (TPH) could ignite itself and lead to a release, among numerous species, of gaseous plutonium in the atmosphere. This actually happened three times, twice at Savannah River (USA) in 1953 and 1975 and at Tomsk (Russia) in 1993. Even if the plutonium species only represents 0.9% of the fission products it is still responsible for 50% of the radio-toxicity after 100 years (see Figure 1.2).
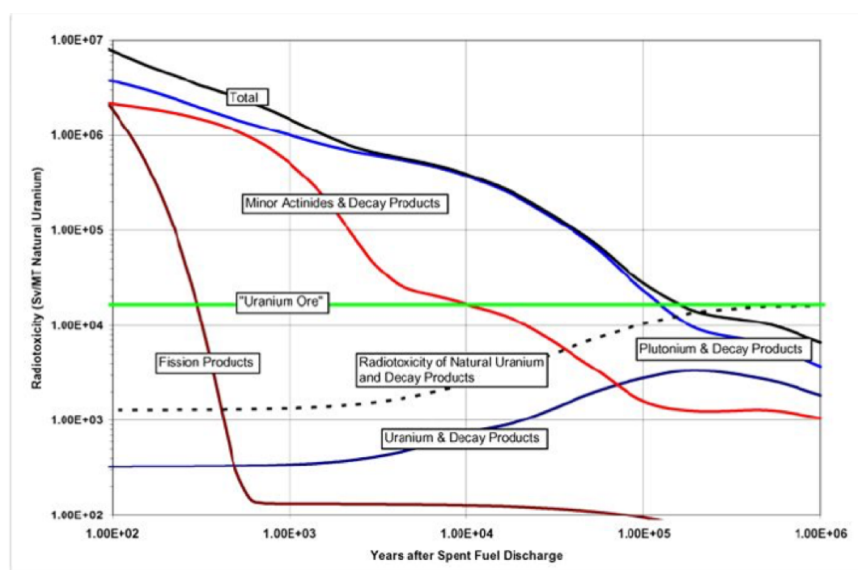
FIGURE 1.2: Radiotoxicity of spend nuclear fuel [4]

To perform nuclear safety analysis, the chemical behaviour of the Pu species need to be known. Experimental studies are complicated to pursue for safety reason. Since Pu can have multiple degrees of oxidation including (VI) it cannot be replaced by the less radioactive Th or Ce for the experiments. The volatile species expected to be formed in the contact with oxygen are the dioxide PuO_2, trioxide PuO_3 and oxy-hydroxide ($PuO_2(OH)_2$) of plutonium. Horeover, the experiments conducted in the past 30 years disagree on the formation of PuO_3 *i.e.* some analysis of experimental data proposed that PuO3 could be formed along the chemical processes, while others do not. Thus theoretical simulations of an accident is the best solution to answer this question. The ASTEC (Accident Source Term Evaluation Code) simulator code, developed by the IRSN, can simulate the accident condition of pression and temperature but precise thermodynamic data such as heat capacities, entropies and enthalpies of formation of the different species involved are needed as input parameters. This study will limit itself to the plutonium oxides PuO_2 and PuO_3 and the

oxyhydroxide $PuO_2(OH)_2$. Those thermodynamic values can be obtained computationally thanks to a detailed knowledge of their electronic structure which implies to take into account thoroughly relativistic effects and electronic correlation. The challenging aspect of this work as detailed in Chapter 4, is the multiconfigurational character of the ground-state wave function.

The treatment of electronic correlation is still source of new developments in quantum chemistry. For the past 10 years, the DFT community tried to better account for electronic correlation in the functionals by proposing new approaches. One of them is the so-called double-hybrid method, which is based on the use of a hybrid functional combined with the MP2 correlated method. This family of functionals has proven its efficiency for a lot of system but so far it was never applied to f-elements. During this thesis, one double hybrid (B2-PLYP) was tested for f-elements systems and representative chemical reaction in Chapter 5

In this thesis the general methods of quantum chemistry are first presented in Chapter 2. These will be followed in Chapter 3 by the exploration of the bonding between alkyl cations and arenes to rationalise the catalytic process of polyethylen. A third part (Chapter 4) will be devoted to the determination of thermodynamic properties of plutonium oxides and oxyhydroxide. The last chapter (Chapter 5) will evaluate the performances of double hybrid functional B2-PLYP for the determination of thermodynamic properties of f-elements containing systems. We will close this manuscript with general conclusions and perspectives.

Chapter 2

Methods

2.1 Introduction to Quantum Chemistry

As discussed in the introduction, the experimental expertise is complementary to theoretical studies. In this chapter, I will define all the necessary tools to understand what is solved from a computational point of view and all the important concepts that were used during my PhD work. As we already mentioned, the context of this study implies accounting for relativistic effects due to the presence of actinides. However, for the sake of clarity, we will start with the presentation of quantum chemical mechanics notions in a non-relativistic framework before introducing the relativistic Dirac equation and the other flavors of relativistic approximate Hamiltonians. Last but not least the concept of basis sets will be presented.

2.1.1 Schrödinger equation

The time-dependent Schrödinger equation describes the physics of a molecular system with respect to time [5]:

$$\hat{H}\psi = i\hbar\frac{\partial\psi}{\partial t}$$

(2.1)

Where ψ(t) is the wave function of the state under consideration, in general the ground state (or an excited state), $\hat{H}$ the Hamiltonian operator, i the imaginary number and $\hbar$ the Planck contants divided by 2π. The first approximation is to consister the system as stationary at a moment t [6] and thus the equation becomes an eigenvalue equation, independent of time:

$$\hat{H}(\boldsymbol{r}, \boldsymbol{R})\psi(\boldsymbol{r}, \boldsymbol{R}) = E\psi(\boldsymbol{r}, \boldsymbol{R})$$

(2.2)

with $\psi(\boldsymbol{r}, \boldsymbol{R})$ the wave function of the system made on our case of electrons at positions { $\boldsymbol{r} = r_1, ..., r_n$} and nuclei at the positions {$\boldsymbol{R} = R_1, ..., R_N$} and E being the total energy. $\hat{H}$ is written for a molecule, in atomic units as:

$$\hat{H} = -\sum_i \frac{1}{2} \bigtriangledown_i^2 - \sum_A \frac{1}{2M_A} \bigtriangledown_A^2 - \sum_{i,A} \frac{Z_A}{r_{iA}} + \frac{1}{2} \sum_{i \neq j} \frac{1}{r_{ij}} + \frac{1}{2} \sum_{A \neq B} \frac{Z_A Z_B}{R_{AB}} \qquad (2.3)$$

i and j are indices running over the electrons while A and B indices are related to the nuclei. r_{ij} is the distance between the electron i and j , r_{iA} the one between an electron i and a nucleus A and R_{AB} is the distance between two nuclei. Finally, Z_A is the atomic number of nucleus A. The two-first terms of equation 2.3 represent the kinetic energies terms of the electrons and the nuclei, respectively. The last three terms are the standard Coulomb interaction potential terms for electron-nucleus, electron-electron and nucleus-nucleus interactions.

2.1.2   Born-Oppenheimer approximation

As a proton is heavier than an electron (mass ratio of 1 836) the velocity of the nucleus considered to be negligible. Thus, it is possible to decouple the Hamiltonian as a sum of the electronic Hamiltonian $\hat{H}^{el}$ and the nuclear one $\hat{H}^{nuc}$

$$\hat{H} = \hat{H}^{el} + \hat{H}^{nuc} \qquad (2.4)$$

In the adiabatic approximation [7] or Born-Oppenheimer approximation, the wave function $\psi(\boldsymbol{r}, \boldsymbol{R})$ can be written as a product of the electronic contribution, ψ^{el}, and the nuclear one ψ^{nuc}:

$$\psi(\boldsymbol{r}, \boldsymbol{R}) = \psi_{\boldsymbol{R}}^{el}(\boldsymbol{r}) \psi^{nuc}(\boldsymbol{R}) \qquad (2.5)$$

The electronic Hamiltonian operator is define as:

$$\hat{H}^{el} = -\sum_i \frac{1}{2} \bigtriangledown_i^2 - \sum_{i,A} \frac{Z_A}{r_{iA}} + \frac{1}{2} \sum_{i \neq j} \frac{1}{r_{ij}} + \frac{1}{2} \sum_{A \neq B} \frac{Z_A Z_B}{R_{AB}} \qquad (2.6)$$

It can be shown that the contribution of the nucleus-nucleus interaction term is just a constant in the total energy calculation. The eigenvectors are the electronic wave functions $\psi_{\boldsymbol{R}}^{el}(\boldsymbol{r})$ that depend parametrically on $\boldsymbol{R}$. Therefore, the electrons move on a potential energy surface (PES), $E_{\boldsymbol{R}}^{el}$, that can be obtained by solving the following:

$$\hat{H}^{el}\psi_{\boldsymbol{R}}^{el} = E_{\boldsymbol{R}}^{el}\psi_{\boldsymbol{R}}^{el} \tag{2.7}$$

The methods presented in the following pages have for purpose to solve this eigenvalue problem.

2.1.3 Constraints on the wave-function

The first hypothesis is to consider the electrons as independent particules. Thus the n-particule wave function can be written as the product of N one-particule orbitals ϕ (see Section 2.5.1).

$$\psi(r_1, r_2, ..., r_N) = \phi_1(r_1)...\phi_N(r_N) \tag{2.8}$$

A prerequisite for the form of the electronic wave function (now written as ψ), because it characterises fermion particules, is its anti-symmetric character with respect to the particle exchange:

$$\psi(i, j) = -\psi(j, i) \tag{2.9}$$

A a manifestation of the Pauli exclusion principle [8], which states that two fermions cannot occupied the same quantum state, *i.e.* they cannot have the same four quantum numbers (n, l, m and s).

A trial wave function that satisfies both criteria is the Slater determinant [9] composed of orthonormal spin orbitals.

$$\psi(r_1, r_2, ..., r_N) = \frac{1}{\sqrt{N!}} \begin{vmatrix} \phi_1(r_1) & \phi_2(r_1) & ... & \phi_N(r_1) \\ \phi_1(r_2) & \phi_2(r_2) & ... & \phi_N(r_2) \\ \vdots & \vdots & \ddots & \vdots \\ \phi_1(r_N) & \phi_2(r_N) & ... & \phi_N(r_N) \end{vmatrix} \tag{2.10}$$

with the spin orbitals in column and the electron coordinates in row. From now on, ψ will denote Slater determinants.
One can notice:

- The anti-symmetry of the wave-function is present since the exchange of two rows changes the sign of the determinant.

- The Pauli principle and the indiscernibility of the electrons remains. Indeed, having two electrons in the same state will give a determinant equals to zero since two columns will be equal.

- The normalisation constant is $\frac{1}{\sqrt{N!}}$.

2.2   Single-Reference Methods

In this section, the methods common to the three thesis projects using the single-reference approximation will be presented. The specific methods proper to each of them are introduced in the chapter in question.

2.2.1   Hartree-Fock method

In the context of Wave Function Theory, equation 2.10 can be solved thanks to different approximations. The Hartree-Fock approach [10] is the foundation of many other methods and more specifically the so-called *post* Hartree-Fock methods, presented later. It rests on the mean-field approximation which assumes that a given electron is sujected to the average potential (which as discussed below, consists of a classical (electrostatic) and a non-classical (exchange) interaction) of the other electrons, rather than the individual electron-electron interactions. The Hartree-Fock wave function is determined by the variation principle by minimising the energy of the system:

$$E_{HF} = \frac{\langle \Phi | H^{el} | \Phi \rangle}{\langle \Phi | \Phi \rangle} \geq E \tag{2.11}$$

E_{HF} being the HF energy and E the exact total energy of the system. Since the N-electrons problem can be decomposed in N one-electron problems, the solution Φ can be described by a Slater determinant built from the orbitals ϕ_i. The variational conditions on the orbitals lead to a new effective one-electron operator, the Fock operator [6] $\hat{F}_i$.

$$\hat{F}_i \phi_i = \epsilon_i \phi_i \tag{2.12}$$

Its eigenvector, ϕ_i is the molecular spin-orbital of the electron i and its eigenvalue ϵ_i the corresponding orbital energy. The Fock operator can be written as:

$$\hat{F}_i(r) = \hat{h}_i(r) + \sum_{j=1}^{N} |\hat{J}_j(r) - \hat{K}_j(r)| \tag{2.13}$$

The one-electron core Hamiltonian $\hat{h}_i(\mathbf{r})$ is composed of the kinetic energy of the electron i and the nucleus-electron potential energy:

$$\hat{h}_i(\mathbf{r}) = -\frac{1}{2}\nabla_i^2 - \sum_{K=1}^{N}\frac{Z_K}{r_{iK}} \tag{2.14}$$

The second part of the equation 2.13 is composed by the two one-electron operators. The Coulomb operator J_j, corresponds to the classic representation of the repulsion between two electrons (i and j). The second operator is the non-classical exchange operator and arises from the indiscernability of the electrons and the anti-symmetry of the wave-function. It forbids electrons with identical spins to occupy the same spatial position. Applying the exchange and Coulomb operators on ϕ_j gives:

$$\hat{J}_j\phi_i(\mathbf{r_i}) = \left[\int \frac{\phi_j^*(\mathbf{r_j})\phi_j(\mathbf{r_j})}{r_{ij}}d\mathbf{r_j}\right]\phi_i(\mathbf{r_i}) \tag{2.15}$$

$$\hat{K}_j\phi_i(\mathbf{r_i}) = \left[\int \frac{\phi_j^*(\mathbf{r_j})\phi_i(\mathbf{r_j})}{r_{ij}}d\mathbf{r_j}\right]\phi_j(\mathbf{r_i}) \tag{2.16}$$

Thus the eigenvalue ϵ_i of the eigenfunction ϕ_i in the equation 2.12 is:

$$\epsilon_i = \langle\phi_i|\,\hat{F_i}\,|\phi_i\rangle = \langle\phi_i|\,\hat{h_i}\,|\phi_i\rangle + \langle\phi_i|\sum_{j=1}^{N}(\hat{J}_j - \hat{K}_j)\,|\phi_i\rangle \tag{2.17}$$

Finally, the whole energy Hartree-Fock is:

$$\mathbf{E}_{HF} = \sum_{i=1}^{N}h_{ii} + \frac{1}{2}\sum_{i=1}^{N}\sum_{j=1}^{N}(\mathbf{J}_{ij} - \mathbf{K}_{ij}) = \sum_{i=1}^{N}[\epsilon_i - \frac{1}{2}\sum_{j=1}^{N}(\mathbf{J}_{ij} - \mathbf{K}_{ij})] \tag{2.18}$$

Where N remains the number of electrons and ϵ_i, $\mathbf{J}_{ij}$ and $\mathbf{K}_{ij}$ follow the description of the equations 2.17 and:

$$\mathbf{J}_{ij} = \int \phi_i^*\hat{J}_i\phi_i;\, \mathbf{K}_{ij} = \int \phi_i^*\hat{K}_i\phi_i \tag{2.19}$$

One can note that the total energy Hartree-Fock is not the sum or the energy of the spin-orbitals of the equation 2.17 otherwise the electronic repulsion would be counted twice for each electron.

2.2.2   The problem of Electron Correlation

Definition

As mentioned above, in the HF approximation, the instantaneous electron-electron interaction was replaced by an average potential while this approximation can yield to a fairly good representation of the physical systems. It is, nevertheless, still far from the exact solution as far as physico-chemical process are concerned. The missing interactions are what is referred as electronic correlation E_{corr} [11] which is defined as the difference between the total exact non relativistic energy of the system E_{tot} and the Hartree-Fock one E_{HF} (for a given basis set limit, see Section 2.5):

$$E_{corr} = E_{tot} - E_{HF} \tag{2.20}$$

Though electron correlation represents only 5 to 10% of the total energy of the system it can change the whole picture of the wave function and impact molecular properties and thus cannot be neglected [12]. From a physical point of view, electronic correlation is due to two types of instantaneous repulsions. The first one is the repulsion between the two negative charges, leading to the Coulomb hole. The second type of repulsion prevents two particles with the same spin to be at the same position corresponding to the Fermi hole.

One can distinguish between the dynamical and non-dynamical (or static) electronic correlation. The static correlation, occurring in case of near orbitals degeneracy, implies that the wave function has to be described by more than one Slater determinant. The dynamical correlation, is connected to the instantaneous correlation of the electron motions and is accounted for by post-Hartree-Fock methods discussed after.

Møller-Plesset Perturbation Theory

In order to include dynamical correlation into a single reference wavefunction, Perturbation Theory (PT) [13] can be used. One can rewrite the Schrödinger equation as:

$$\hat{H}\psi = E\psi \tag{2.21}$$

with :

$$\hat{H} = \hat{H}_0 + \hat{H}' \tag{2.22}$$

where $\hat{H}_0$ is the HF Hamiltonian and $\hat{H}'$ the perturbation one defined in the equation 2.26.

The energy and the wave function can be written as Taylor expansion of λ (being the strength of the perturbation) since E_{PT} and ψ are continuous functions between zero and infinity:

$$E_{PT} = \lambda^{(0)} E_0 + \lambda^{(1)} E_1 + \lambda^{(2)} E_2 + ... \tag{2.23}$$

$$\psi = \lambda^{(0)} \psi_0 + \lambda^{(1)} \psi_1 + \lambda^{(2)} \psi_2 + ... \tag{2.24}$$

If $\lambda = 1$, the n-th order energy and wavefunction are of all the terms with indices $\leq$ n.

In the Møller-Plesser (MP) Perturbation Theory, $\hat{H}_0 = \hat{H}_{HF}$ thus it consists in the introduction of a perturbation to a reference (HF) wave function. In other words, excited Slater determinants are included.

We will focus on Møller-Plesset to the 2nd order (MP2), for which double excitations are included. Since it is easily proven that MP1 (Møller-Plesser to the 1st order) is actually equivalent to HF [10] with the Brillouin theorem. The Brillouin theorem stating that the singly excited configurations do not contribute to the 1st order correction to the wave function. By single excitation, one has to understand the promotion of one electron to an unoccupied orbital is allowed (see Figure 2.1), for double excitations, it is two electrons. The number of excited determinants is directly linked to the size of the basis set implying that, the computational cost will be also dependent on it (see Table 2.1 and Section 2.5.1 for the definition of a basis set). Let us have a look at E_{MP2} starting from $\lambda = 1$ and equation 2.23 .

$$E_{MP2} = E_0 + E_1 + E_2 = \sum_i \epsilon_i - \frac{1}{2} \sum_{ij} \langle ij | |ij \rangle \tag{2.25}$$

As mentioned before, MP2 includes single and double excitations (if non-canonical/open-shell orbitals are used). The matrix elements with singly excited determinants Φ_i^a are:

$$
\begin{aligned}
\langle \Phi_0 | \hat{H}' | \Phi_i^a \rangle &= \langle \Phi_0 | \hat{H}_0 - \sum_j^{N_{elec}} \hat{\boldsymbol{F}}_j | \Phi_i^a \rangle \\
&= \langle \Phi_0 | \hat{H}_0 | \Phi_i^a \rangle - \langle \Phi_0 | \sum_j^{N_{elec}} \hat{\boldsymbol{F}}_j | \Phi_i^a \rangle \\
&= \langle \Phi_0 | \hat{H}_0 | \Phi_i^a \rangle - \left(\sum_j^{N_{elec}} \epsilon_j \right) \langle \Phi_0 | \Phi_i^a \rangle
\end{aligned}
\tag{2.26}
$$

Where the subscript of Φ, $i, j, ...$ are the occupied orbitals the electron is promoted from and $a, b, ...$ the virtual orbitals. Φ_0 and Φ_i^a are two orthogonal states so the

second term is equals to zero. For the first term, the Brillouin theorem [14] states that (for closed shell systems) if two orthogonal states satisfying HF equation are different by only one orbital then: $\langle \Phi_0 | \hat{H}_0 | \Phi_i^a \rangle = 0$, so that $\langle \Phi_0 | \hat{H}' | \Phi_i^a \rangle = 0$. Thus, E_2 only involves doubly excited determinants:

$$E_2 = \sum_{i<j}^{occ} \sum_{a<b}^{vir} \frac{\langle \Phi_0 | \hat{H}' | \Phi_{ij}^{ab} \rangle \langle \Phi_{ij}^{ab} | \hat{H}' | \Phi_0 \rangle}{E_0 - \epsilon_{ij}^{ab}} \tag{2.27}$$

Because of the Koopmans' Theorem [15] the difference in total energy between two Slater determinants is the difference in Molecular Orbitals (MO) energies thus the second-order energy for a closed-shell system can be written with a sum over the spatial orbitals a, b, r and s as:

$$E(MP2) = 2 \sum_{abrs}^{N/2} \frac{\langle ab | | rs \rangle - \langle rs | | ab \rangle}{\epsilon_a + \epsilon_b - \epsilon_r - \epsilon_s} - \sum_{abrs}^{N/2} \frac{\langle ab | | rs \rangle - \langle rs | | ba \rangle}{\epsilon_a + \epsilon_b - \epsilon_r - \epsilon_s} \tag{2.28}$$

The two main advantages of MP2 are the low computational cost compared to variational methods (such as CI see Section 4.2.1) and its size extensivity [1].

Higher orders of perturbation such as MP3 (with the third order energy) or MP4 (with the fourth order energy) allow to include more dynamical correlation but at a greater cost. However, it has been shown that MP perturbation theory may not always converge [17], converge slowly or even oscillate. The issue of convergence, as well as the fact that other approaches such as coupled cluster have a similar cost than MP3, MP4 etc... but are more reliable, means that these approaches are mow seldom used.

TABLE 2.1: Computational Cost and Amount of Correlation Included In the different Møller-Plesser Perturbation Theories. (see section 2.5.1 for the definition of M_{basis})

Method	Computational Cost	Amount of Correlation Included
MP2	M_{basis}^5	80 - 90 %
MP3	M_{basis}^6	90 - 95 %
MP4	M_{basis}^7	95 - 97 %

---

[1]Size-extensivity is a mathematical concept introduced by Bartlett [16] to characterised a method with a linear scaling between the energy and the number of electrons. The size consistency is also a property of a method, refering to the fact that if A and B are two subsystems sharing no electrons the following equality is true: E(A + B) = E(A) + E(B).This property is particularly important when a dissociation curve is explored.
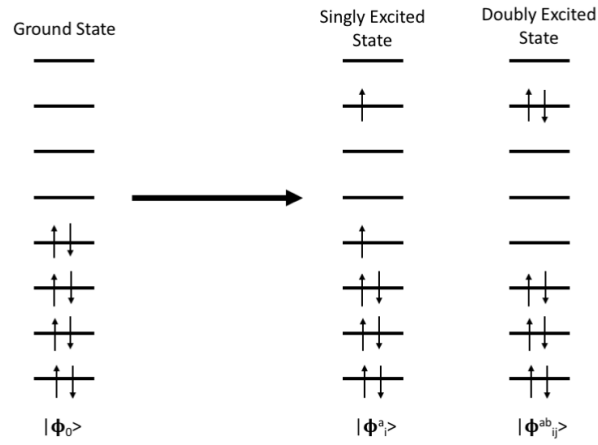
Figure 2.1: Single Excitation from a Ground State [17]

Coupled Cluster Method

The coupled cluster (CC) method [18–21] is an approach based on the Many-Body Perturbation Theory where high-order excitations are included efficiently. Thus, the Schrödinger equation can be written as:

$$\hat{H}\Psi_{CC} = E\Psi_{CC} \tag{2.29}$$

Ψ_{CC} is defined with an excitation operator $\hat{T}$ acting on a reference wave function:

$$\Psi_{CC} = e^{\hat{T}}\Psi_0 \tag{2.30}$$

The exponential term can be expanded as:

$$e^{\hat{T}} = 1 + \hat{T} + \frac{1}{2!}\hat{T}^2 + \frac{1}{3!}\hat{T}^3 + ... = \sum_{k=0}^{\infty} \frac{1}{k!}\hat{T}_k \tag{2.31}$$

the excitation operator $\hat{T}$ is the sum:

$$\hat{T} = \sum_{i=1}^{N} \hat{T}_i \tag{2.32}$$

the subscript being the excitation order and N the number of electrons in the system. The excitation order corresponds to the number of electrons excited from an

occupied to an unoccupied orbital, for example:

$$\hat{T}_1 \Psi_0 = \sum_i^{occ} \sum_a^{virtual} t_i^a \Phi_i^a \tag{2.33}$$

and

$$\hat{T}_2 \Psi_0 = \sum_{i<j}^{occ} \sum_{a<b}^{virtual} t_{ij}^{ab} \Phi_{ij}^{ab} \tag{2.34}$$

represent single and double excitations, where t_i^a and t_{ij}^{ab} are the amplitudes of the excitations and so on. Here, the variational principle generally used to find the energy cannot be applied. Indeed, non-vanishing terms all the way up to the order of N arise because of the expansion in equation 2.31. Therefore, the energy is determined by projecting equation 2.29 onto the reference wave function Φ_0. The coupled-cluster E_{CC} energy is then expressed as:

$$E_{CC} = \langle \Phi_0 | e^{-\hat{T}} \hat{H} e^{\hat{T}} | \Phi_0 \rangle \tag{2.35}$$

This method, similar to MP2 in the idea, retrieves the dynamical correlation of the system but still describes it with a single reference determinant. However, in contrast to MP2, the single excited T_1 operators are known to introduce orbital relaxation [22] and make CC method more reliable than MP2 in cases the HF orbitals are not optimal

If no constraints on the excitation order are put in place, one would arrive at the FCI calculation and the method 4.2.1 would only be applicable for very small systems, so a truncated form was developed including only the single and double electrons excitations [23]. This truncated CC, called CCSD, remains size extensive and affordable for medium systems. Higher-order truncations are available such as CCSDT[24] including explicitly the triple excitations or CCSDTQ adding the quadruple ones, but they are too expensive for the gain in electronic correlation retrieved. The triple excitations, that might be important for the description of some wave functions, are then included perturbatively, leading to CCSD(T) being the most wisely used triple variant [25][2].

Unfortunately, the restricted CCSD(T) depicted above is inadequate to describe open-shell molecules such as the ones under study. Thus, one must turn to the unrestricted version of this method UCCSD(T). The first formulations of it [16, 27, 28] use an

---

[2]CCSD(T) is different from CCSD[T] were the contribution of the single excitations are not taken into account and from CCSD-T where triples corrections are computed as defined by M. J. O. Deegan *et al.*[26]

Unrestricted-HF (UHF) reference wave function. However this idea has the disadvantages of being expensive and leading to spin contamination (artificial mixing of multiple electronic spin states). This is why different studies decided to start with a restricted HF reference [29, 30] but the spin contamination of the wave-function was still present. In 1993, Knowles *et al.* [20, 21] proposed a RHF-UCCSD formulation.

Today, UCCSD(T) is considered as the "gold standard" for single reference cases, but may fail for multi-reference ones. The T_1 [31] and D_1 diagnostics [32, 33] can be used to qualitatively spot a multi-reference character. Defining T_1 with the one-electron excitation amplitudes t_1:

$$T_1 = \frac{||t_1||}{\sqrt{N}} \tag{2.36}$$

And the D_1 for open-shell [34]:

$$D_1 = max(||f_i^a||_2, ||f_x^a||_2, ||f_i^x||_2) \tag{2.37}$$

where the 2-norm of a matrix, $||R||_2$, is the maximum Euclidean norm of the vectors formed by the multiplication of R with a unit vector [35], and the f amplitudes being linked to the t amplitudes by:

$$f_i^a = \frac{t_{i\alpha}^{a\alpha} + t_{i\beta}^{a\beta}}{2} \tag{2.38}$$

$$f_x^a = \frac{t_{x\alpha}^{a\alpha}}{\sqrt{2}} \tag{2.39}$$

$$f_i^x = \frac{t_{i\beta}^{x\beta}}{\sqrt{2}} \tag{2.40}$$

If for lighter elements a T_1 diagnostic higher than 0.02 is usually a sign of multi-reference character the value is raised at 0.05 [36, 37] for systems with transition metals and other heavy elements.

2.3 Density Functional Theory

At the birth of quantum chemistry in the 1960's, the limited computational power raised difficulties to perform accurate calculations using large basis sets (see Section 2.5.1) or including many atoms with HF method. In this context, the great adventure of Density Functional Theory (DFT) started in 1964 with Hohenberg and Kohn [38]

when they demonstrated that the exact energy of the ground state of any electron gas in an external potential is a functional of the density F [ρ].

$$E[\rho] \equiv \int v(\boldsymbol{r})\rho(\boldsymbol{r})d\boldsymbol{r} + F[\rho] \qquad (2.41)$$

where v would be the Coulomb attraction between the nuclei and the electrons. ρ, the total electron density of N electrons is defined as:

$$\rho(\boldsymbol{r}) = N \int ... \int |\Psi(\boldsymbol{x}_1, \boldsymbol{x}_2, ... \boldsymbol{x}_n)|^2 d\sigma d\boldsymbol{x}_2 ... d\boldsymbol{x}_N \qquad (2.42)$$

σ being the arbitrary spin of the electron one, $\boldsymbol{x}_i$ being the map of the spin-spatial coordinated of the other N-1 electrons.

F[ρ] is a universal functional of the total electron density ρ that corresponds to the sum of the two electron energy functional W[ρ] and the kinetic energy terms T[ρ]. Considering F[ρ], it can be rewritten as:

$$F[\rho] = T[\rho] + W[\rho] \qquad (2.43)$$

Thus the "only" down side is the determination of the universal functional F[ρ], since the energy is simply obtained by the variational principle. Hohenberg and Kohn stated themselves the problem of obtaining this universal functional in the conclusion of their paper: *"We have developed a theory of electronic ground state which is exact in two cases : The case of a nearly constant density [...] and the case of a slowly varying density. Actual electronic systems do not belong to either of them."*

The answer to this problem arrived one year later in 1965, with Kohn and Sham [39] by proposing that the exchange-correlation term, at the heart of the problem of Hohenberg and Kohn (and more generally in quantum chemistry), can be approximate by using the true chemical potential $\mu(\rho)$ of the homogeneous interacting electron gas.

$$\frac{\delta E}{\delta \rho} = \mu \qquad (2.44)$$

First, the density is rewritten as a slater determinant of spin orbitals ϕ_i for a non interacting reference system.

$$\rho(\boldsymbol{r}) = \sum_i^N \phi_i^*(\boldsymbol{r})\phi_i(\boldsymbol{r}) \qquad (2.45)$$

Then, the variational principle is applied to equation 2.41 in order to obtain N coupled one-particle equations for the non-interacting electrons, the so-called the Kohn-Sham equations:

$$\left\{ -\frac{1}{2m}\bigtriangledown^2 + \phi(\boldsymbol{r_i}) + v_{xc}(\rho(\boldsymbol{r_i})) \right\} |\phi_i\rangle = \epsilon_i |\phi_i\rangle \tag{2.46}$$

with:

$$\phi(\boldsymbol{r}) = v_{ext}(\boldsymbol{r}) + \int \frac{\rho(\boldsymbol{r'})}{|\boldsymbol{r} - \boldsymbol{r'}|} d\boldsymbol{r'} \tag{2.47}$$

and

$$v_{xc}(\rho(\boldsymbol{r})) = \frac{\delta E_{xc}[\rho]}{\delta\rho(\boldsymbol{r})} \tag{2.48}$$

Here, the issue is the formulation of E_{xc}. In practice, the exact functional is replaced by an approximated one with a certain number of exact conditions being enforced [10] as listed below:

- For a hydrogen-like system the functional should give the exact exchange energy and a correlation energy equals to zero.

- For solid-state physics, it is important to recover the electron gas solution when the density becomes constant. However, it is less true for molecular densities since as the electron gas model does not properly describe a molecular system.

- Multiplying by a constant factor the molecular coordinates ($\rho\lambda(x,y,z) = \lambda^3\rho(\lambda x, \lambda y, \lambda z)$) should result in a linear scaling of the exchange energy. $E_x[\rho_\lambda] = \lambda E_x[\rho]$.

- On the contrary, there is no full scaling concerning the correlation energy.

- The exact functional should fulfill the Lieb-Oxford inequality saying that $E_x[\rho] \geq E_{xc}[\rho] \geq 2.273 \, E_x^{LDA}[\rho]$ (see Section 2.3.1).

- As $\boldsymbol{r}$ tends to infinity the exchange potential should have an asymptotic behaviour in $-r^{-1}$ while the correlation potential shows a $-\frac{1}{2}\alpha r^{-4}$ behaviour (α being the polarisability of the N_{elec} - 1 system).

A good starting point to find the universal or approximate functional is to separate the exchange term from the correlation one in equation ??, such as $E_{xc}[\rho] = E_x[\rho] + E_c[\rho]$, with :

$$E_x[\rho] = \int \rho(\boldsymbol{r})\epsilon_x([\rho], \boldsymbol{r}) d\boldsymbol{r} \tag{2.49}$$

$$E_c[\rho] = \int \rho(\boldsymbol{r})\epsilon_c([\rho], \boldsymbol{r}) d\boldsymbol{r} \tag{2.50}$$

The exchange energy, by definition, involves only electrons with identical spins while the correlation due to electrons with the same spin is different, and thus separable, from the correlation from electrons with opposite spins:

$$E_x[\rho] = E_x^\alpha[\rho_\alpha] + E_x^\beta[\rho_\beta] \tag{2.51}$$

$$E_c[\rho] = E_c^{\alpha\alpha}[\rho_\alpha] + E_c^{\beta\beta}[\rho_\beta] + E_c^{\alpha\beta}[\rho_\alpha, \rho_\beta] \tag{2.52}$$

With $\rho = \rho_\alpha + \rho_\beta$ and $\rho_\alpha = \rho_\beta$ for a closed-shell singlet state.

Now that the basis of DFT are exposed, the next part will focus of the expressions of $E_x[\rho]$ and $E_c[\rho]$ and the approximations leading to their formulations.

2.3.1   Local Density Approximation

In the Local Density Approximation (LDA)[39–41], the exchange energy is given by the Dirac formula:

$$E_x^{LDA}[\rho] = -C_x \int \rho(\boldsymbol{r})^{\frac{4}{3}} d^3\boldsymbol{r} \tag{2.53}$$

In the case of an open-shell system where α and β densities are different, LSDA (Local Spin Density Approximation) is used, the exchange energy reads :

$$E_x^{LSDA}[\rho] = -C_x \int (\rho_\alpha(\boldsymbol{r})^{\frac{4}{3}} + \rho_\beta(\boldsymbol{r})^{\frac{4}{3}}) d^3\boldsymbol{r} \tag{2.54}$$

Concerning the correlation part, it is fitted on high precision calculations performed with Quantum Monte Carlo method to a uniform electron gas. The analytic interpolation formula used for this fit defines the functional, for example Vosko, Wilk and Nusair' one [41] (VWN) or the popular PW92 constructed by Perdew and Wang in 1992 [40].

2.3.2   Generalised Gradient Approximation

The goal of the Generalised Gradient Approximation's (GGA) [42] is to improve the exchange and correlation energies by including the electron density and its derivative, at given point (removing the *local* or homogeneous character of LDA) in the functional. For example, in this thesis, we have used the Perdew-Burke-Ernzerhof (PBE) [43] GGA functional defined by its exchange functional:

$$\epsilon_x^{PBE} = \epsilon_x^{LDA} F(x) \tag{2.55}$$

where x is a gradient of the density:

$$x = \frac{|\nabla \rho|}{\rho^{\frac{4}{3}}} \tag{2.56}$$

and

$$F(x) = 1 + a - \frac{a}{1 + bx^2} \tag{2.57}$$

a and b being parameters. The correlation part is expressed as:

$$\epsilon_c^{PBE} = \epsilon_c^{LDA} H(x) \tag{2.58}$$

$$H(x) = cf_3^3 \ln\left[1 + dt^2\left(\frac{1 + At^2}{1 + At^2 + A^2t^4}\right)\right] \tag{2.59}$$

$$A = d\left[exp\left(-\frac{\epsilon_c^{PBE}}{cf_3^3}\right) - 1\right]^{-1} \tag{2.60}$$

$$f_3(\zeta) = \frac{1}{2}\left[(1+\zeta)^{\frac{2}{3}} + (1-\zeta)^{\frac{2}{3}}\right] \tag{2.61}$$

$$t = \left[2(3\pi^3)^{\frac{1}{3}}f_3\right]^{-1} x \tag{2.62}$$

The parameters a, b and c are determined in a non-empirical way. ζ is the relative spin polarisation (= $(n_\uparrow$ - $n_\downarrow)$ /n with $n = 3/4$ π r_s^3, r_s being the Wigner-Seitz radius that is the radius of a sphere whose volume is equal to the mean volume per atom in a solid).

2.3.3 Hybrid-Generalised Gradient Approximation

Hybrid-GGA functionals combine a LDA part, a GGA part and an exact HF exchange weighted in order to fit experimental data. For example in this work, the well-used B3LYP [44] and PBE0 [45, 46] functionals have been used. The B3LYP functional is:

$$E_{xc}^{B3LYP} = (1-a)E_x^{LSDA} + aE_x^{exact} + b\delta E_x^{B88} + (1-c)E_c^{LSDA} + cE_c^{LYP} \tag{2.63}$$

The LYP and B88 part of the correlation and exchange energies are obtained with the GGA approximtion. E_x^{exact} is obtained when the KS orbitals used are identical to HF one. E_x^{LSDA} is described in the equation 2.54. The default values for a, b and c are 0.2, 0.7 and 0.8 respectively, however most of the quantum chemistry codes allow the user to modify these values. The defaults values are kept in the present work.

PBE0 consists in the addition of 25% of E_x^{exact} to the PBE functional presented in the previous paragraph.

2.3.4   Strengths and Weaknesses of DFT

As one understood, DFT is a great tool for quantum chemists. It is fast and black box once the functional is (smartly) chosen. Its computational cost scales as N^3 (N being the number of orbitals). On the other side, the impossibility to systematically improve results and the problem of describing spin states are severe drawbacks [47, 48]. In a vision restricted to the treatment of actinides, the main deficiency of DFT is its single determinant description, while the large number of unpaired f, s and d actinides electrons may results in a strongly multi-determinantal wave-function.

We can also point out that the exchange-correlation functional does not account for long-range ($\frac{C_6}{R_6}$) correlation corresponding to the London part of the dispersion energy notably present when Van der Waals interaction are important.

Dispersion can be patched to KS energies as proposed by Grimme *et al.* [49–51] with the D3 empirical correction:

$$E_{disp} = E^{(2)} + E^{(3)} \tag{2.64}$$

With the two-body $E^{(2)}$ term defined as:

$$E^{(2)} = \sum_{AB} \sum_{n=6,8,10} s_n \frac{C_n^{AB}}{r_{AB}^n} f_{d,n}(r_{AB}) \tag{2.65}$$

with

$$f_{d,n}(r_{AB}) = \frac{1}{1 + 6(\frac{r_{AB}}{s_{r,n} R_0^{AB}})^{-\alpha_n}} \tag{2.66}$$

C_n^{AB} are tabulated for atom pairs, s_n and $s_{r,n}$ are a scaling factor adjusted for each functional and R_0^{AB} is the cutoff radii

The three-body $E^{(3)}$ term is:

$$E^{(3)} = \sum_{ABC} f_{d,(3)}(\bar{r}_{ABC}) E^{ABC} \tag{2.67}$$

$\bar{r}_{ABC}$ being the geometrically averaged radii of atoms A, B and C and E^{ABC} the triple dispersion term:

$$E^{ABC} = \frac{C_9^{ABC}(3cos\theta_a cos\theta_b cos\theta_c + 1)}{(r_{AB}r_{BC}r_{CA})^3} \quad (2.68)$$

where C_9^{ABC} is a constant and θ_a, θ_b and θ_c are the internal angles of the triangle formed by r_{AB}, r_{BC} and r_{CA}

This dispersion correction can be efficient but still relies on empirical corrections. A second solution is a new type of functionals, the Double Hybrids described in Chapter 5.

2.4 Treatment of relativistic effects

All the methods presented so far were based on the non-relativistic Schrödinger equation. For relatively light atoms (Z < 36), this approximation is fully legitimate but increasing the atomic number of the atom implies for the electrons closer to the nucleus to have a velocity approaching the speed of light [52], making relativistic effects no longer negligible and affecting their electronic structure.

Relativistic effects can be separated in two types: those independent of the electron spin (or scalar) and those dependent of the electron spin (or spin-orbit). The first steams from the fact that, because of the stronger nuclear attraction (as Z increases), the inner electrons are accelerated and get closer to the nucleus. The consequence is, the contraction and the stabilisation of the *s* and *p* orbitals. Furthermore, as the inner *s* and *p* electrons are drawn towards the core, they increasingly more effective in screening outer shells and as consequence, the *d* and *f* electrons are destabilised. The second category, the spin-orbit one, can be seen, in a classic representation, as the interaction of the electron magnetic moment and the magnetic induction created by the kinetic orbital motion and results in the splitting of orbitals with angular momenta greater than 0.

2.4.1 Dirac equation

According to relativistic theory, since the speed of light and the Physics laws are the same in all inertial frames, the researched equation must be invariant under Lorentz transformation [53][3]. We see, for instance, the time-dependent Schrödinger equation:

$$\frac{-\hbar}{2m}\left[\frac{\partial^2\psi(\boldsymbol{r},t)}{\partial x^2} + \frac{\partial^2\psi(\boldsymbol{r},t)}{\partial y^2} + \frac{\partial^2\psi(\boldsymbol{r},t)}{\partial z^2}\right] = -i\hbar\frac{\partial\psi(\boldsymbol{r},t)}{\partial t} \quad (2.69)$$

---

[3]Invariant under Lorentz transformation means that the value of a quantity is the same in all Galileen referentials

does not fulfil this requirement, since the spatial coordinates x, y and z appear as quadratic derivatives while the time appears as its first derivative.

Paul. A. M. Dirac [54] suggested instead an Hamiltonian with linear derivatives of both time and space, introducing the algebraic quantities α and β. The Dirac equation, in an external electromagnetic potential describes the relativistic motion of an electron as:

$$\left(\beta m_0 c^2 + e\phi + \boldsymbol{\alpha}.\boldsymbol{\pi} - ih\frac{\partial}{\partial t} \right) \psi = 0 \tag{2.70}$$

with

$$\boldsymbol{\pi} = \boldsymbol{p} + e\boldsymbol{A} \tag{2.71}$$

recalling :

$$\boldsymbol{p} \to \boldsymbol{p} - q\boldsymbol{A}; E \to -q\phi \tag{2.72}$$

ϕ being the scalar potential and $\boldsymbol{A}$ the vector potential describing the magnetic field and q = -e for an electron and q = +e for a positon. α retains the information about the spin of the particle. Both α and β are 4 x 4 matrices defined as:

$$\alpha_x = \begin{pmatrix} 0 & 0 & 0 & 1 \\ 0 & 0 & 1 & 0 \\ 0 & 1 & 0 & 0 \\ 1 & 0 & 0 & 0 \end{pmatrix}, \alpha_y = \begin{pmatrix} 0 & 0 & 0 & -i \\ 0 & 0 & i & 0 \\ 0 & -i & 0 & 0 \\ i & 0 & 0 & 0 \end{pmatrix}, \alpha_z = \begin{pmatrix} 0 & 0 & 1 & 0 \\ 0 & 0 & 0 & -1 \\ 1 & 0 & 0 & 0 \\ 0 & 1 & 0 & 0 \end{pmatrix} \tag{2.73}$$

$$\beta = \begin{pmatrix} 1 & 0 & 0 & 0 \\ 0 & 1 & 0 & 0 \\ 0 & 0 & -1 & 0 \\ 0 & 0 & 0 & -1 \end{pmatrix} \tag{2.74}$$

This can be rewritten with the Pauli matrices, the zero 2 x 2 matrix 0_2 and the 2 x 2 Identity matrix 1_2:

$$\alpha_x = \begin{pmatrix} 0_2 & \sigma_x \\ \sigma_x & 0_2 \end{pmatrix}, \alpha_y = \begin{pmatrix} 0_2 & \sigma_y \\ \sigma_y & 0_2 \end{pmatrix}, \alpha_z = \begin{pmatrix} 0_2 & \sigma_z \\ \sigma_z & 0_2 \end{pmatrix} \tag{2.75}$$

$$\beta = \begin{pmatrix} 1_2 & 0_2 \\ 0_2 & -1_2 \end{pmatrix} \tag{2.76}$$

The Pauli matrices being:

$$\sigma_x = \begin{pmatrix} 0 & 1 \\ 1 & 0 \end{pmatrix}, \sigma_y = \begin{pmatrix} 0 & -i \\ i & 0 \end{pmatrix}, \sigma_z = \begin{pmatrix} 1 & 0 \\ 0 & -1 \end{pmatrix} \tag{2.77}$$

Since α and β appears in the equation 2.70 as 4 x 4 matrices the wave function must be a four-component vector:

$$\psi(r,t) = \begin{pmatrix} \psi_1(r,t) \\ \psi_2(r,t) \\ \psi_3(r,t) \\ \psi_4(r,t) \end{pmatrix} \tag{2.78}$$

Among the four components, two (one for the spin α and one for the β) are the large (L) ones and the other two are the small (S) components (also one for the spin α and one for the β) we can rewrite $\psi(r, t)$ as:

$$\psi(r,t) = \begin{pmatrix} \psi^L(r,t) \\ \psi^S(r,t) \end{pmatrix} = \begin{pmatrix} \psi_\alpha^L(r,t) \\ \psi_\beta^L(r,t) \\ \psi_\alpha^S(r,t) \\ \psi_\beta^S(r,t) \end{pmatrix} \tag{2.79}$$

The solution of the time-independent Dirac equation for a free electron can then be found by solving the matrix equation:

$$\begin{pmatrix} mc^2 - E & c(\boldsymbol{\sigma}.\boldsymbol{p}) \\ c(\boldsymbol{\sigma}.\boldsymbol{p}) & -mc^2 - E \end{pmatrix} \begin{pmatrix} \psi^L \\ \psi^S \end{pmatrix} = 0 \tag{2.80}$$

leading to the four two-fold degenerate solutions, corresponding to the large and small components:

$$E^+ = +\sqrt{c^2 p^2 + m^2 c^4} \tag{2.81}$$

and

$$E^- = -\sqrt{c^2 p^2 + m^2 c^4} \tag{2.82}$$

indicating that an electron could occupy a positive or negative state. Since the physical meaning of the former states would be a problem, Dirac supposed all the negative states to be occupied [55], That so the electrons would not be able to occupy them

due to the Pauli principle. In the presence of a potential such as the nucleus (V = e$\phi = \frac{-Z}{r}$ see equation 2.71), two continuum of states appear, with one corresponding to electronic (positive) states and one for the negative solutions, and bound states in between the continuum.

In this formalism only the one electron equation can be exactly resolved, therefore, some approximations must be made to describe many-electrons systems.

2.4.2 Dirac-Coulomb-Breit Hamiltonian

While multiple electrons are present their motions are dependent from each other. Thus we introduce the many-electron Dirac-Coulomb-Breit Hamiltonian $\hat{H}^{DCB}$ as the sum of the Dirac one-electronic Hamiltonian and the two-electronic Breit correction term g_{ij}^B:

$$\hat{H}^{DCB} = \sum_{i=1}^{N} \hat{h}_i + \sum_{i<j} \hat{g}_{ij}^B \tag{2.83}$$

where

$$\hat{g}_{ij}^B = -\frac{1}{2r_{ij}} \left(\boldsymbol{\alpha}_i.\boldsymbol{\alpha}_j + \frac{(\boldsymbol{\alpha}_i.\boldsymbol{r}_{ij})(\boldsymbol{\alpha}_i.\boldsymbol{r}_{ij})}{r_{ij}^2} \right) \tag{2.84}$$

the first term in parenthesis being the Gaunt interaction [56] and the second the retarded effect important for long distance interactions [57, 58].

2.4.3 Dirac Equation approximations

Since working with the four-component framework can be expensive even for relatively small systems, simplifying the Dirac equation by keeping only two components, the large ones, could save a lot of computational effort. To do so, the large and small components must be separated. It can be done with the elimination of the small components or by decoupling the small and large components with a unitary transformation.

Small Components elimination

In a similar way than in equation 2.80, the time independent Dirac equation for one free electron can be written to take into account an external potential V (shifting by

-mc^2 to set the electronic solutions to zero):

$$
\begin{pmatrix} V - E & c(\boldsymbol{\sigma}.\boldsymbol{p}) \\ c(\boldsymbol{\sigma}.\boldsymbol{p}) & V - 2mc^2 - E \end{pmatrix} \begin{pmatrix} \psi^L \\ \psi^S \end{pmatrix} = 0 \tag{2.85}
$$

which is equivalent to resolve the two equations system:

$$
\begin{aligned}
c(\boldsymbol{\sigma}.\boldsymbol{p})\psi^S + V\psi^L &= E\psi^L \\
c(\boldsymbol{\sigma}.\boldsymbol{p})\psi^L + (V - 2mc^2)\psi^S &= E\psi^S
\end{aligned} \tag{2.86}
$$

Thus it is possible to express ψ^S as a function of ψ^L:

$$
\psi^S = K(E)\frac{\boldsymbol{\sigma}.\boldsymbol{p}}{2mc}\psi^L \tag{2.87}
$$

with K(E) a local multiplicative operator that depends on the electron energy:

$$
K(E) = \left(1 - \frac{V - E}{2mc^2}\right)^{-1} \tag{2.88}
$$

By inserting equation 2.87 in the first equation 2.86 we obtained the 2-component equation:

$$
\left(\frac{1}{2m}(\boldsymbol{\sigma}.\boldsymbol{p})K(E)(\boldsymbol{\sigma}.\boldsymbol{p}) + V\right)\psi^L = E\psi^L \tag{2.89}
$$

This equation allows to retrieve the Schrödinger equation in the non-relativistic limit ($c \to \infty$ and $K \to 1$).

Pauli Hamiltonian

The K(E) term can be expanded as a geometric series as:

$$
K(E) = \sum_{k=0}^{\infty} \left(\frac{V - E}{2mc^2}\right)^k \tag{2.90}
$$

The Pauli approximation is obtained by retaining the two first terms of the series:

$$
K(E) \approx K^{Pauli}(E) = 1 + \frac{V - E}{2mc^2} \tag{2.91}
$$

This expansion is only valid if

$$|V - E| << 2mc^2$$

but is not the case in the region close to the nucleus. As r $\to$ 0 and V = $\frac{-Z}{r} \to \infty$, making the condition |V - E| << 2mc^2 not true. Away from the nucleus, K(E) can be expanded to the first order leading to the Pauli Hamiltonian $\hat{H}^{Pauli}$ [59, 60]:

$$\hat{H}^{Pauli} = \hat{T} + V - \frac{1}{8m^2c^2}\boldsymbol{p}^4 + \frac{\hbar^2}{8m^3c^2}(\nabla^2 V) + \frac{\hbar}{4m^2c^2}\boldsymbol{\sigma}.(\nabla V) \times \boldsymbol{p} \qquad (2.92)$$

$\hat{T}$ being the kinetic energy operator, V remains the potential created by the nucleus $(-\frac{Ze^2}{r})$ the third term being the mass-speed correction term coming from the relativistic variation of the mass with the speed. The fourth term is a correction due to the fast oscillation of the electron around its mean position. It is also called the Darwin term. Finally the last term is the spin-orbit coupling.

Zeroth Order Relativistic Approximation Hamiltonian

To obtain an approximate Hamiltonian valid in all regions of space one can expanded K(E) differently as:

$$K(E) = \left[1 + \frac{E}{2mc^2 - V}\right]^{-1} = 1 - \frac{E}{2mc^2 - V} + \left[\frac{E}{2mc^2 - V}\right]^2 + ... \qquad (2.93)$$

Thus, by keeping the zeroth order of expansion 2.93, we obtain the Zeroth Order Relativistic Approximation (ZORA) Hamiltonian:

$$\hat{H}^{ZORA} = V + (\boldsymbol{\sigma}.\boldsymbol{p})\frac{c^2}{2mc^2 - V}(\boldsymbol{\sigma}.\boldsymbol{p}) \qquad (2.94)$$

Of course, this formulation retains the spin-orbit coupling in $\boldsymbol{\sigma}.\boldsymbol{p}$, it is easy to disregard this part to obtain the Scalar Relativistic (SR) ZORA Hamiltonian. In 1998, Christoph van Wüllen [61] showed that the scalar relativistic effects could be fully included in a kinetic operator $\hat{T}^{ZORA}_{SR}$:

$$\hat{T}^{ZORA}_{SR} = \boldsymbol{p}\frac{c^2}{2mc^2 - V}\boldsymbol{p} \qquad (2.95)$$

This new operator is really useful when the SOC is small enough to be disregarded and allows to decrease the computational cost.

Decoupling small and large components with unitary transform: the Douglas-Kroll-Hess Hamiltonian

The Douglas-Kroll-Hess (DKH) [62, 63] Hamiltonian does not rely on the elimination of the small components as before but is derived from a unitary transformation U, acting on the Dirac-Coulomb Breit Hamiltonian $\hat{H}^{DCB}$, in order to obtain a diagonal Hamiltonian:

$$U^{\dagger}\hat{H}^{DCB}U = \begin{pmatrix} h_+ & 0 \\ 0 & h_- \end{pmatrix} \tag{2.96}$$

with $U^{\dagger}U = 1$.

The first transformation in the DKH approximation is actually the Foldy Wouthuysen transformation [64] in a free particule case.

$$\hat{U}^{(0)} = \hat{A}_i(a + \boldsymbol{\beta\alpha P}_i) \tag{2.97}$$

with

$$\hat{A}_i = \sqrt{\frac{\hat{E}_i + m_e c^2}{2\hat{E}_i}}; \boldsymbol{P}_i = \frac{c\boldsymbol{p}_i}{\hat{E}_i + m_e c^2} \tag{2.98}$$

with $\hat{E}_i$ the kinetic energy operator for the positive energy states, defined as:

$$\hat{E}_i = \sqrt{m_e^2 c^4 + p_i^2 c^2} \tag{2.99}$$

After this first transformation the resulting Hamiltonian matrix, $\hat{H}^{DKH1}$ is not diagonal but the coupling is already reduced. The potential $\hat{V}$ needs to be now added and the decomposition to be pushed one step further.

$$\hat{U}^{(1)} = \sqrt{1 + \hat{W}_1^2} + \hat{W}_1 \tag{2.100}$$

with

$$\hat{W}_1(i) = \hat{W}_1 \phi(\boldsymbol{p}_i) = \int d^3 p_j \hat{W}(\boldsymbol{p}_i, \boldsymbol{p}_j) \phi(\boldsymbol{p}_j) \tag{2.101}$$

where:

$$\hat{W}(\boldsymbol{p}_i, \boldsymbol{p}_j) = \int d^3 p_j \hat{A}_i(\boldsymbol{\sigma P}_i - \boldsymbol{\sigma P}_j) \hat{A}_j \frac{\hat{V}(\boldsymbol{p}_i, \boldsymbol{p}_j)}{\hat{E}_i + \hat{E}_j} \phi(\boldsymbol{p}_j) \tag{2.102}$$

$\hat{V}(\boldsymbol{p}_i, \boldsymbol{p}_j)$ being the the Fourier transform of the potential energy and $\phi(p_i)$ the (bispinor) wave function associated to an electron having the momentum $\boldsymbol{p}_i$. The decoupled Hamiltonian for two particles is thus:

$$\hat{H}^{Decoupled} = \beta\hat{E}_i + \hat{A}_i(\hat{V} + \boldsymbol{\sigma}\boldsymbol{P}_i\hat{V}\boldsymbol{\sigma}\boldsymbol{P}_i)\hat{A}_i - \beta(\hat{W}_1\hat{E}_i\hat{W}_1 + \frac{1}{2}[\hat{W}_1^2, \hat{E}_i]_+) \qquad (2.103)$$

Using the Dirac relation $((\boldsymbol{\sigma}.\boldsymbol{u})(\boldsymbol{\sigma}.\boldsymbol{v}) = \boldsymbol{u}.\boldsymbol{v} + \mathrm{i}\,\boldsymbol{\alpha}(\boldsymbol{u}\times\boldsymbol{v}))$, it is possible to separate the terms spin-independent to the spin-dependent leading to the $\hat{H}^{SF}$ and $\hat{H}^{SO}$, respectively.

$$\hat{H}^{SF} = \sum_i \hat{E}_i + \sum_i \hat{V}_{eff}^{SF}(i) + \sum_{i<j} \frac{1}{r_{ij}} \qquad (2.104)$$

with

$$\hat{V}_{eff}^{SF}(i) = -\hat{A}_i[V(i) + \boldsymbol{P}_iV(i)\boldsymbol{P}_i]\hat{A}_i - \hat{W}_1(i)\hat{E}_i\hat{W}_1(i) - \frac{1}{2}[\hat{W}_1^2(i), \hat{E}_i]$$

$$V(i) = \sum_\alpha \frac{Z_\alpha}{r_{i\alpha}} \qquad (2.105)$$

and $\hat{H}^{SO}$:

$$\begin{aligned}\hat{H}^{SO} =\alpha\hbar c\Bigg\{ &\sum_i\sum_a Z_a \frac{\hat{A}_i}{\hat{E}_i + m_ec^2}\boldsymbol{\sigma}_i\Big(\frac{\boldsymbol{r}_{ia}}{r_{ia}^3}\times\boldsymbol{p}_i\Big)\frac{\hat{A}_i}{\hat{E}_i + m_ec^2}\\ &-\sum_{i\neq j}\frac{\hat{A}_i\hat{A}_j}{\hat{E}_i + m_ec^2}.(\boldsymbol{\sigma}_i\frac{\boldsymbol{r}_{ij}}{r_{ij}^3}\times\boldsymbol{p}_i)\frac{\hat{A}_i\hat{A}_j}{\hat{E}_i + m_ec^2} - 2\boldsymbol{\sigma}_i\Big(\frac{\boldsymbol{r}_{ij}}{r_{ij}^3}\times\boldsymbol{p}_i\Big)\frac{\hat{A}_i\hat{A}_j}{\hat{E}_i + m_ec^2}\Bigg\}\end{aligned} \qquad (2.106)$$

This SO Hamiltonian is the sum of one-electron and two-electrons terms. The matrix elements of the SO operator are still expensive to calculate. A solution is to approximate this Hamiltonian. The Atomic Mean Field Approximation (AMFI) is used to reduce the number of integrals to calculate using a "simple" idea since the SO interaction is short range as it behaves (as $\frac{1}{r^3}$), it is relevant to disregard all multi-center two-electron SO integrals [65]. For a balanced treatment of SO effects, it is also appropriate to only include one-center one-electron SO integrals.

To simplify the SO Hamiltonian in a context of CI-SO coupling, Hess *et al.*[65] showed that the doubly excited determinants SO contributions can be negligible if the matrix elements of the SO operator between two Slater determinant that differ from only one single-excitation (from the spin orbital i to the spin orbital j) are modified

in a way that defines the effective mean field one-electronic operator as:

$$\hat{H}_{ij}^{SO} = \langle \phi_i(1) | \hat{h}^{SO}(1) | \phi_j(2) \rangle + \frac{1}{2} \sum_k n_k \Bigg\{ \langle \phi_i(1) | \widetilde{H}_{kk}^{SO}(1) | \phi_j(1) \rangle$$
$$- \langle \phi_i(1) | \widetilde{H}_{kj}^{SO}(1) | \phi_k(1) \rangle - \langle \phi_k(1) | \widetilde{H}_{ik}^{SO}(1) | \phi_j(1) \rangle \Bigg\}$$

(2.107)

with

$$\langle \phi_i(1) | \widetilde{H}_{kk}^{SO}(1) | \phi_j(1) \rangle = \langle \phi_i(1)[\phi_k(2) | \widetilde{H}_{1,2}^{SO} | \phi_k(2)] \phi_j(1) \rangle \quad (2.108)$$

$$\langle \phi_i(1) | \widetilde{H}_{kj}^{SO}(1) | \phi_k(1) \rangle = \langle \phi_i(1)[\phi_k(2) | \widetilde{H}_{1,2}^{SO} | \phi_j(2)] \phi_k(1) \rangle \quad (2.109)$$

$$\langle \phi_k(1) | \widetilde{H}_{ik}^{SO}(1) | \phi_j(1) \rangle = \langle \phi_k(1)[\phi_i(2) | \widetilde{H}_{1,2}^{SO} | \phi_k(2)] \phi_j(1) \rangle \quad (2.110)$$

and :

$$\hat{h}^{SO}(1) = \alpha \hbar c \Bigg\{ \sum_a Z_\alpha \frac{\hat{A}_1}{\hat{E}_1 + m_e c^2} \boldsymbol{\sigma}_1 \Big(\frac{\boldsymbol{r}_{1a}}{r_{1a}^3} \times \boldsymbol{p}_1 \Big) \frac{\hat{A}_1}{\hat{E}_1 + m_e c^2} \Bigg\} \quad (2.111)$$

$$\widetilde{H}_{1,2}^{SO} = \alpha \hbar c \Bigg\{ \frac{\hat{A}_1 \hat{A}_2}{\hat{E}_1 + m_e c^2} \cdot \Big(\boldsymbol{\sigma}_1 \frac{\boldsymbol{r}_{12}}{r_{12}^3} \times \boldsymbol{p}_1 \Big) \frac{\hat{A}_1 \hat{A}_2}{\hat{E}_1 + m_e c^2} - 2\boldsymbol{\sigma}_1 \Big(\frac{\boldsymbol{r}_{12}}{r_{12}^3} \times \boldsymbol{p}_1 \Big) \frac{\hat{A}_1 \hat{A}_2}{\hat{E}_1 + m_e c^2} \Bigg\} \quad (2.112)$$

n_k is the occupation of spin-orbital k, ϕ_i an occupied and ϕ_j a virtual orbital. Since equation 2.107 describes the valence electrons in a field created by the electrons in the orbitals k $\neq$ i, n_k and ϕ_k must have a physical meaning. For this reason, the AMFI module must be used with atomic natural orbitals such as the relativistic contracted ANO-RCC basis sets (see Section 2.5.1).

2.4.4 Relativistic Effective Core Potential

In chemistry, many molecule's properties involve the valence electrons and eventually the sub-valence shells. It is then possible to speed up the calculation by replacing the core electrons by an effective core potential (ECP) [66]. Since the number of electrons is smaller and the number of functional basis can be reduced, the calculation becomes less expensive. The second advantage of ECP is its convenience because it can be used with DFT and wave function methods. The Hamiltonian is reduced to the sum of the interaction between the valence electrons and the interaction of the former with the nucleus/core electrons and called the valence Hamiltonian $\hat{H}^v$:

$$\hat{H}^v = \sum_i^{n_{valence}} -\frac{1}{2} \hat{\nabla}_i^2 + \sum_{i<j}^{n_{valence}} \frac{1}{r_{ij}} + \sum_i^{n_{valence}} \sum_I^N V_{cv}^I(i) + \sum_{I<J}^N \frac{Q_I Q_J}{R_{IJ}} + V_{CPP} \quad (2.113)$$

The first term is the kinetic energy of the valence electrons. The second is the interaction between the valence electrons, the third one is the interaction between the electron/nuclei and valence electrons. The fourth term is the repulsion between effective cores. The last term is the core polarisation potential (CPP). V_{cv} in equation 2.113 is parametrised to include not only to the scalar relativistic effects but also the spin-orbit relativistic effects so it is adjusted to reproduce data with great accuracy.

$$V_{cv}^I(i) = \sum_{i}^{n_{valence}} \frac{Q_I}{r_{iI}} + \sum_{i}^{n_{valence}} V_{PP}^I(i) \tag{2.114}$$

The name of the ECP is given under the form ECPnXY where usually XY represents the level of the fully relativistic method used to generate the target all-electron data to which the ECP parameters are adjusted: MWB for multi-configurational Wood-Boring or MDF for multi-configuration Dirac-Fock [67].

2.5   Basis Sets, Basis Sets Superposition Error and Complete Basis Set Extrapolation

2.5.1   Basis Sets

Back to equation 2.10, the wave-function is described by a Slater determinant composed of orthonormal spin-orbitals. In a molecule, each spin-orbital represents a molecular orbital (MO) ϕ_i which can be represented by a Linear Combination of Atomic Orbitals (LCAO) [68], χ_k.

$$\phi_i = \sum_{j}^{N_{AO}} c_{ij}\psi_i = \sum_{j}^{N_{AO}} c_{ij} \sum_{k}^{Nb} d_{jk}\chi_k \tag{2.115}$$

d_{jk} being the expansion coefficients, χ_k the atomic basis functions, and Nb the number of the basis function used. A minimum basis set contains roughly[4] as much basis function as there are atomic orbitals.

The only restriction for mathematical functions to be used as basis functions is to decay to zero as the distance between the nuclei and the electron increases. In practice, two families of orbitals are used: the Slater Type Orbitals (STO) [69] and the Gaussian Type Orbitals (GTO) [70] both products of a radial part $\mathcal{R}_l(r)$ and a spherical harmonic function $Y_{lm_l}(\theta\phi)$.

---

[4]sometimes extra orbitals are added for polarization

- Slater Type Orbitals

Slater-type orbitals, the radial part only depends on n as

$$\mathcal{R}_n = N_{Slater} r^{n-1} e^{-\zeta r} \tag{2.116}$$

n being the principal quantum number, N_{Slater} the normalisation constant, r is the distance between the electron and the nucleus and ζ a constant related to the effective charge of the nucleus Z^* such that the energy level of this orbital equals to

$$E_n = \frac{1}{2}\left(\frac{Z^*}{n}\right)^2 \tag{2.117}$$

STO basis are successful for atoms as they describe the cusp at the nucleus. However, their limitation is that two-electrons integrals involving 3 or 4 centres cannot be computed analytically.

- Gaussian Type Orbitals

To overcome the integration issue, GTO (Gaussian Type Orbitals) were introduced defined as:

$$\mathcal{R}_n = N_6(\alpha) r^{n-1} e^{-\alpha r^2} \tag{2.118}$$

for their radial part. If the GTOs allow the calculations to be performed faster, the r^2 dependency alter the description of the electron behaviour near the nucleus [10]. Therefore a larger basis will be needed to reach the same accuracy as with an STO.

Linear combinations (contractions) of primitive GTOs functions are able to approximate the nodal structures of atomic orbitals (AO). The quality of a basis set is linked to the number of Gaussian primitives and to the optimisation of the contraction coefficients.

In the current work, we aim at computing reaction energies with an accuracy of a few kJ.mol^{-1}. Thus the choice of the atomic basis set is crucial. In all the PhD projects, basis sets of at least triple-ζ quality were used to determine the optimal geometries, using correlation consistent Dunning's basis sets [71, 72], aug-cc-pVTZ/aug-cc-pVQZ, and the proper small-core RECP basis sets for the heavy elements. For the largest molecular complexes (See Chapter 3), efficient computational speed up was achieved with the resolution of the identity algorithm, using Ahlrichs def2-TZVP basis sets and their auxiliary counterparts [73, 74]. Note that for heavy elements, the def2-basis sets are bound to small-core RECPs.

To reach chemical accuracy (or higher) for thermodynamics properties of plutonium gas-phase molecules, the electronic energies were extrapolated to the complete basis set limit, from calculations with the extended all-electron atomic natural orbital relativistic correlation consistent (ANO-RCC) Roos's basis sets [75–77], which offer from triple to quadruple-ζ quality expansions in the Douglas-Kroll-Hess relativistic framework [78].

We will comment on the choice of the basis sets in the appropriate introductory sections of each research project.

2.5.2   Basis Sets Superposition Error

The Basis Sets Superposition Error (BSSE) introduced by Boys and Bernardi [79] occurs when 2 atoms (A and B) are close to each other. The basis set of the atom A will be superposed with the basis set of the atom B describing twice the same stabilising energy. Thus, the total energy is lower than what it should be and must be corrected.

$$E_{corrected} = E_{uncorrected} + E_{BSSE} \tag{2.119}$$

In order to compute the corrected total energy, the energy of atom A has to be calculated in the presence of the basis of the atom B and the energy of atom B in the presence of the basis of the atom A.

$$E_{BSSE} = E_A^A - E_A^{AB} + E_B^B - E_B^{AB} \tag{2.120}$$

where the superscripts refers to the basis set used and the subscripts the atom.

2.5.3   Complete Basis Set Extrapolation

A way to avoid BSSE, among others, is to extrapolate the energy to the Complete Basis Set (CBS) limit *i.e.* to approach the results with infinite basis sets (see Figure 2.2).

In this work we compared two ways of extrapolating energies, one by extrapolating the total energy, the second by extrapolating separately the SCF energy and the correlated energy before summing the two.

FIGURE 2.2: Theoretical convergence to the complete basis set limite
with increasing the number of basis functions
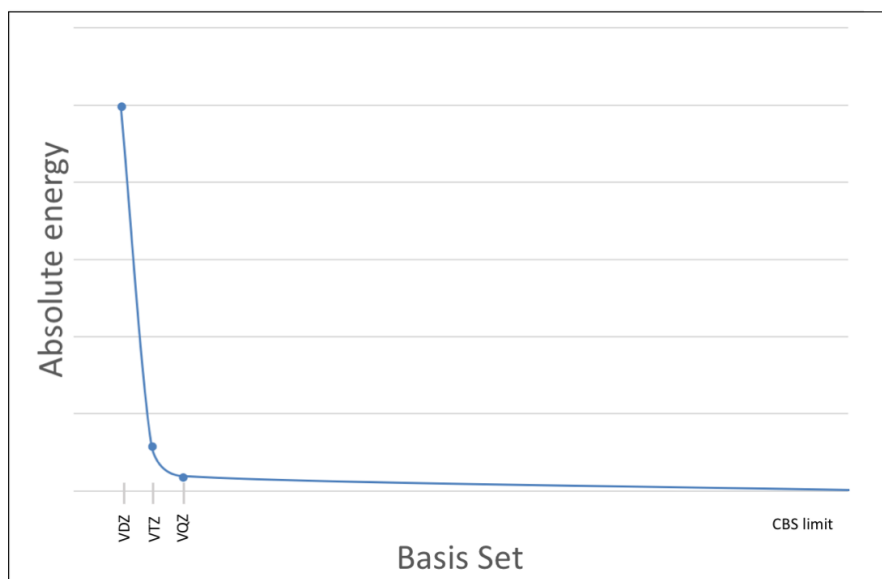
The total energy CBS value can be derived from a two-points extrapolation formula
[80]:

$$E_{XY}^{CBS} = \frac{X^3 E_X - Y^3 E_Y}{X^3 - Y^3} \tag{2.121}$$

where X and Y are the size of the basis sets (typically n=3 and n=4 for triple and
quadruple-ζ basis sets).

Peterson *et. al.* [81] proposed specific formulas for the uncorrelated energy E_{CBS}^{SCF} and
the correlated energy E_{CBS}^{Corr} extrapolations:

$$E_n^{SCF} = E_{CBS}^{SCF} + A(n+1)e^{-6.57\sqrt{n}} \tag{2.122}$$

$$E_n^{corr} = E_{CBS}^{corr} + \frac{B}{(n+\frac{1}{2})^4} \tag{2.123}$$

In these formulas n is the size of the basis set (typically n=3 and n=4 for triple and
quadruple-ζ basis sets), E^{SCF} is either the SCF or CASSCF energy and E^{corr} the cor-
relation part of the total energy.

2.6   Conclusion

As mentioned before, only a few and basic methods of Quantum Chemistry were depicted here. Nonetheless, it already triggers some general questions at the heart of the modelling of Actinides.

How to properly describe the relativistic effects ?

How the retrieve electronic correlation ?

If the first question is almost answered in the present section, the former question will be addressed more particularly in the Chapter 4. Indeed, a good way to describe the static correlation is to use methods including multiple Slater determinants in the wave function. These methods are called "multi-reference" quantum chemical methods.

Chapter 3

Coordination of Alkyl cations [(XA$_2$)X(CH$_2$SiMe$_3$)] (X = Th, U) or[(XN$_2$)Zr(CH$_3$)] with an arene for Ethylene polymerisation: Exploration of the bonding

3.1 Introduction

The amount of polyethylene produced every year implies a constant need for improving the industrial production process. Since the pioneering process by Karl Ziegler and Giulio Natta in the early 1950's on the polymerisation of simple olefins, there had been intense interest in the application of early transition metal catalysts for the selective polymerisation of inexpensive olefins. Following to Ziegler-Natta catalysts [82] , metallocene catalysts were discovered in the late 1980's and resulted in numerous industrial processes for improving the properties of polyolefinic materials along with performance parameters. In particular, beside the requirement of higher activity, research have focused on the control of particle size, particle size distribution, and the morphology of the resultant polyolefin (number of carbon in the chain). In the metallocene family, group 4 transition metal metallocene complexes have the largest activity, such as [Cp$_2$ZrMe][B(C$_6$F$_4$TBS)$_4$] synthesised by Marks and co-workers [83–91] 1.1 x 10^{7}g of polyethylene.(mol of M=Zr)$^{-1}$.h^{-1}.atm^{-1}[92]). The brother complex with Th was also synthesised but is an order of magnitude less active than the Zr-complex (9.2 x 10^{5}g of polyethylene.(mol of Th)$^{-1}$.h^{-1}.atm^{-1}), suggesting that the nature of the metallic centre may play a key role in the catalytic

activity. In the 1990s, new catalysts with well-defined metal complexes and other ligand motifs were summarised as the "post metallocenes" family [93].

During my first-year PhD stay at Mc Master University in Hamilton (Ontario, Canada), discussions were initiated with David Emslie's research group, currently working on the synthesis of cationic metal alkyl complexes, that are open post-metallocene catalysts of electropositive metals. These are typically generated by reaction of a neutral dialkyl complex with strong electrophiles such as $[CPh_3][B(C_6F_5)_4]$, $[HNMe_2Ph][B(C_6F_5)_4]$, $B(C_6F_5)_3$ or $(Al(CH_3)xOy)n$ (Methylaluminoxane-MAO). The subsequent polymerisation is achieved by repeated ethylene coordination and 1,2-insertion steps [1]. These activation and polymerization reactions are commonly conducted in arene or alkane solvents; the former is standard in academic laboratories [2], while the latter is favoured in industry [3, 94]. However, in sterically open post-metallocene catalysts of electropositive metals, arene solvents have significant potential to coordinate, negatively impacting ethylene polymerisation activity. At the same time arene coordination is known to increase the thermal stability of metal alkyl cations prior to exposure to ethylene, which is of key importance for industrial polymerisation processes often conducted at elevated temperatures (140 °C). Therefore, Emslie's group has explored, in a systematic fashion, the suitability of tetravalent actinides, namely Thorium and Uranium, to create thermally robust and highly reactive cationic monoalkyl derivatives, as an alternative to the Zirconium based ones.

The chapter begins with a review of all the Zr, Th, and U complexes that were synthesised and crystallised when possible for structural characterisation. We will also present the evaluated ethylene polymerisation activities at room and elevated (70-80 °C) temperatures. The experimental work scanned several arene solvents, from benzene, toluene, to halogenated derivatives of benzene (bromo-benzene, fluorobenzene and di fluorobenzene), with different electron donor capabilities, noting for example that Hayes *et al.* showed a good activity for a scandium complex in Bromobenzene [95, 96]. In an attempt to link the catalytic properties with the complexes structures and coordination, the second part will present the quantum chemical calculations that allow an in-depth discussion of the influence of the cation and the impact of arene solvent coordination. We finally investigate the strength of the interaction between cationic metal alkyl complex with ethylene to shed some light on the competition between ethylene and arene coordination in the initial steps of the catalytic reaction.

3.2 Systems presentation and theoretical studies

3.2.1 Catalysts synthesis strategy, structures and catalytic power

Using a neutral dialkyl **1-X** (X = Th, U or Zr) the arene-coordinated alkyl cations could be derived, where the arene (benzene, toluene, bromo-benzene, fluorobenzene or the (o)-difluoro-benzene) is introduced by the solvent. The catalytic power and the robustness of the compounds were tested by exposing them to ethylene during 30 min at temperatures between 20 and 70 °C (80 °C for **n-Zr**). It is important to note that early transition metal and f-element olefin polymerisation catalysts are frequently generated *in situ* without isolation and characterisation, this lack of information is the main source of uncertainties in the mechanism.

TABLE 3.1: Name of the different ligands, counter ion and arene of the compounds discussed in this Chapter

	Formula	Name
Ligands	XA_2	4,5-bis(2,6-diisopropylanido)-2,7-di-tert-butyl-9,9-dimethylxanthene
Ligands	XN_2	4,5-bis(2,4,6-triisopropylanido)-2,7-di-tert-butyl-9,9-dimethylxanthene
	CH_2SiMe_3	(trimethylsilyl)methyl
Counter ion	$B(C_6F_5)_4{}^-$	diskal tetrakis(pentafluorophenyl)borate
Arene	C_6H_6	Benzene
	$C_6H_5CH_3$	Toluene
	C_6H_5Br	Bromobenzene
	C_6H_5F	Fluorobenzene
	$C_6H_5F_2$	Difluorobenzene
	C_2H_2	Ethylene

The different metallic centres are chosen first because the literature reports their efficiency (see Section 3.1) and because of their electronic structure in the tetravalent oxidation state. Zr(IV) is a $4d^0$-element with the smallest ionic radius, while Th(IV) is a $5f^0$-element and U(IV) a $5f^2$-element with larger ionic radii (see Table 3.3). In the actinides, while the 5f-orbitals are expected to participate into the bonding, the 6d-orbitals in U(IV) complexes may also play a role in the bonding, allowing back donation electron transfer [97].

The choice of the arene is made in order to tune the donating capacity. This donating power is directly connected to the strength of the cation arene bond. If too strong it could hinder or even shutter ethylene coordination and impact the catalytic activity (see Section 3.2.2).

We start the a survey on Emslie's work with the cation derivatives of the neutral dialkyl **1-Th**. **2-Th**, **3-Th** and **5-Th** cations [99–102]. All of them could be synthesised but only **2-Th** could be characterised with X-ray diffraction (see Figure 3.1). Unfortunately only **5-Th** exhibits a catalytic power but it is not thermally robust (see Table

TABLE 3.2: Numbers and Formula of the different compounds of the present Chapter

Number	Formula	X-ray structure
1-U	$[(XA_2)U(CH_2SiMe_3)_2]$	yes
2-U	$[(XA_2)U(CH_2SiMe_3)(C_6H_6)]^+[B(C_6F_5)_4]^-$	yes
3-U	$[(XA_2)U(CH_2SiMe_3)(C_6H_5CH_3)]^+[B(C_6F_5)_4]^-$	yes
4-U	$[(XA_2)U(CH_2SiMe_3)(C_6H_5Br)]^+[B(C_6F_5)_4]^-$	no
5-U	$[(XA_2)U(CH_2SiMe_3)(C_6H_5F)]^+[B(C_6F_5)_4]^-$	yes
6-U	$[(XA_2)U(CH_2SiMe_3)(C_6H_4F_2)]^+[B(C_6F_5)_4]^-$	no
E-U	$[(XA_2)U(CH_2SiMe_3)(C_2H_2)]^+[B(C_6F_5)_4]^-$	not synthesised
1-Th	$[(XA_2)Th(CH_2SiMe_3)_2]$	no
2-Th	$[(XA_2)Th(CH_2SiMe_3)(C_6H_6)]^+[B(C_6F_5)_4]^-$	yes
3-Th	$[(XA_2)Th(CH_2SiMe_3)(C_6H_5CH_3)]^+[B(C_6F_5)_4]^-$	no
4-Th	$[(XA_2)Th(CH_2SiMe_3)(C_6H_5Br)]^+[B(C_6F_5)_4]^-$	not synthesised
5-Th	$[(XA_2)Th(CH_2SiMe_3)(C_6H_5F)]^+[B(C_6F_5)_4]^-$	no
6-Th	$[(XA_2)Th(CH_2SiMe_3)(C_6H_4F_2)]^+[B(C_6F_5)_4]^-$	not synthesised
2'-Th	$[(XN_2)Th(CH_3)(C_6H_6)]^+[B(C_6F_5)_4]^-$	not synthesised
E-Th	$[(XA_2)Th(CH_2SiMe_3)(C_2H_2)]^+[B(C_6F_5)_4]^-$	not synthesised
2-Zr	$[(XA_2)Zr(CH_2SiMe_3)((C_6H_5CH_3))]^+[B(C_6F_5)_4]^-$	not synthesised
2'-Zr	$[(XN_2)Zr(CH_3)(C_6H_6)]^+[B(C_6F_5)_4]^-$	no
3'-Zr	$[(XN_2)Zr(CH_3)(C_6H_5CH_3)]^+[B(C_6F_5)_4]^-$	yes
4'-Zr	$[(XN_2)Zr(CH_3)(C_6H_5Br)]^+[B(C_6F_5)_4]^-$	no
5'-Zr	$[(XN_2)Zr(CH_3)(C_6H_5F)]^+[B(C_6F_5)_4]^-$	not synthesised
6'-Zr	$[(XN_2)Zr(CH_3)(C_6H_4F_2)]^+[B(C_6F_5)_4]^-$	not synthesised
E'-Zr	$[((XN_2)Zr(CH_3)(C_2H_2)]^+[B(C_6F_5)_4]^-$	not synthesised

TABLE 3.3: Ionic Radii of metallic center in Å from [98]

Element	Ionic Radius
Zr	0.72
Th	0.94
U	0.89

3.5). **4-Th** could not be synthesised and no attempt was made for the generation of **6-Th**.

The benzene **2-U** and toluene **3-U** derivatives of **1-U**, are more soluble than their thorium equivalents [103–107]. Thus it could be crystallised to obtain a deep brown solids (see Figures 3.2 and 3.3 for structure). The distances are, as expected from the ionic radii, shorter in the uranium complexes than in the thorium ones (see Table 3.4). **4-U** (bromobenzene) was readily obtained but not structurally characterised
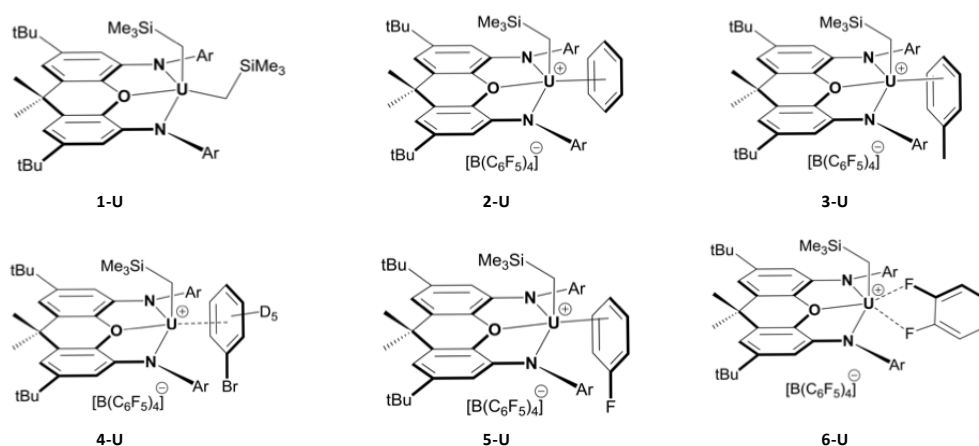
FIGURE 3.1: Structures of the catalysts containing uranium, thorium ones are strictly equivalent.

and catalytically silent.

TABLE 3.4: Important bond lengths in Å and angles in degree for the neutral **1-U** and the cationic **2-U**, **2-Th**, **3-U**, **3'-Zr** and **5-U** given by X-ray diffraction [108].

Compounds	**1-U**	**2-U**	**2-Th**
An-O	2.484(5), 2.504(4)	2.441(2)	2.496(5)
An-N	2.261(5), 2.262(5),	2.224(2), 2.236(6)	2.278(3), 2.288(3)
	2.272(5), 2.280(5)		
An-C_{arene}	–	3.099(3) - 3.248(3)	3.18 - 3.31
$N_1 \ldots N_2$	4.00, 4.02	3.94	4.04
Arene Bend			
Angle [1]	17.5, 18.8	18.9	8.7
O-An-C_{apical}	94.8(2),95.0(2)	87.26(8)	91.3(1)
An-C-Si	128.2(3), 130.4(3),	133.7(2)	131.0(2)
	130.5(4), 130.8(3)		
Compounds	**3-U**	**3'-Zr**	**5-U**
An-O	2.417(9)	2.220	2.431(3)
An-N	2.21(1), 2.22(1)	2.138; 2.122	2.215(3), 2.218(3)
An-C_{arene}	3.05(2) - 3.78(2)	2.697 - 2.840	3.129(5) - 3.598(6)
$N_1 \ldots N_2$	3.98	3.91	3.98
Arene Bend			
Angle[1]	5.9		7.2
O-An-C_{apical}	88.8(4)		89.6(1)
An-C-Si	136.8(7)	–	134.8(2)

[1] Angle between the carbons of the arene and the planar ligand.
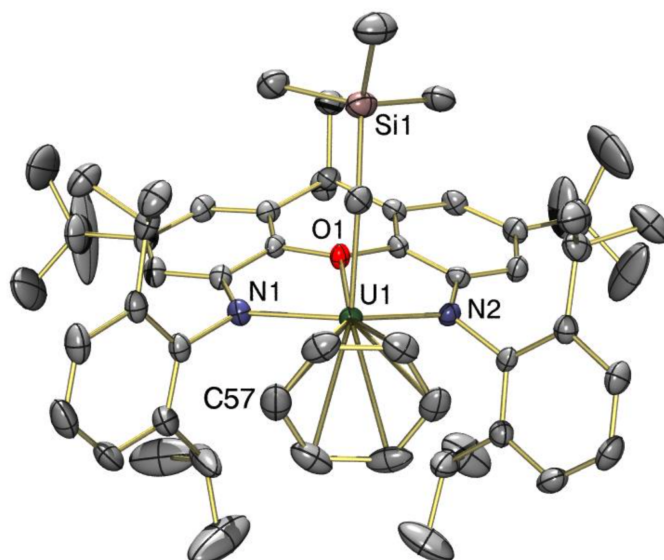
FIGURE 3.2: X-ray crystal structure of η^6-**2-U** [108]. Hydrogen atoms are not represented
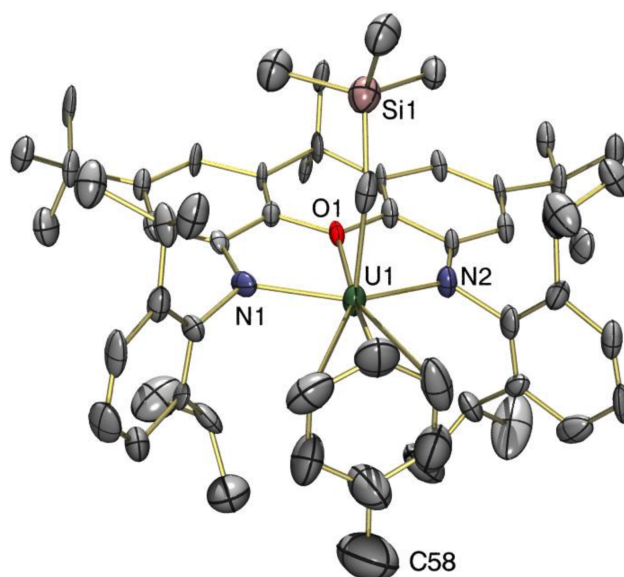
FIGURE 3.3: X-ray crystal structure of η^6-**3-U** [108]. Hydrogen atoms are not represented

Bromobenzene was then exchanged (conceptually) with fluorobenzene to have an expected less donating ligand character, leading to **5-U** which could be X-ray analysed (see Figure 3.4). This makes it the first 5*f*-element complex bearing a π-coordinated

fluoroarene ligand crystallographically characterised. Table 3.4 shows a ressemblance between **5-U** and **3-U** with the same distance N_{1-2} (3.98 Å) and the smallest arene bend angle (7.2 °and 5.9°, respectively).
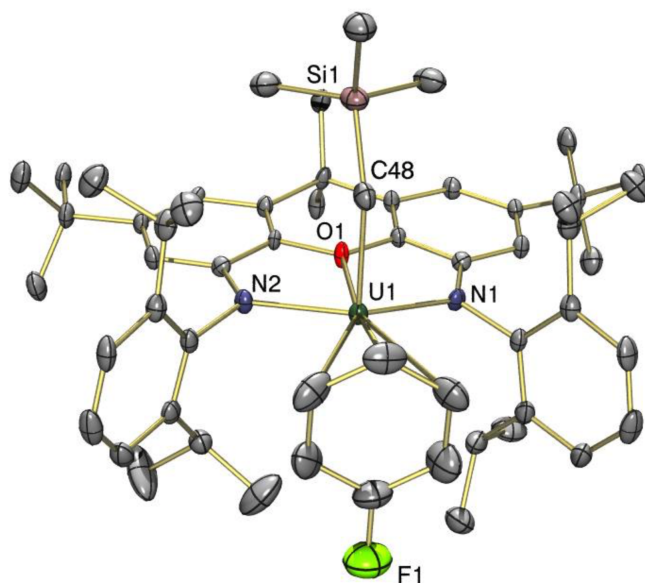
FIGURE 3.4: X-ray crystal structure of η^6-**5-U** [108]. Hydrogen atoms are not represented

In order to further decrease the coordination between arene and the uranium metalic center, the cation with *o*-difluorobenzene was synthesised but could not be crystallised.

The activity of **5-U** is slightly larger than **6-U**, 1.12 x 10^4g of polyethylene.(mol of U)$^{-1}$.h^{-1}.atm^{-1} at 20 °C (see Table 3.5). However, at higher temperature (70 °C) no polymerisation is observed, indicating that **6-U** has a reduced thermal stability. An attempt was made to use the *m*-difluorobenzene, unfortunately no polyethylene was formed after 30 minutes at 20 °C.

At the same time, close equivalents were synthesised with a zirconium center [109].

2'-Zr polymerises so slowly that its activity is negligible. **3'-Zr** presents excellent performance with an activity of 2.73 x 10^5g.mol $^{-1}$.h^{-1}.atm^{-1} observed after 30 minutes at 20 °C and 1.11 x 10^5g.mol $^{-1}$.h^{-1}.atm^{-1} observed after 30 minutes at 80 °C. The decrease of the activity as the temperature increases can probably be explained by the decomposition of the catalyst. **4'-Zr** could be obtained (see Figure 3.6) and presents an activity close to that of **3'-Zr**. Its structure could not be resolved since

TABLE 3.5: Activities of complexes at and 1 atm in g of polyethylene.(mol of X=Th, U or Zr)$^{-1}$.h^{-1}.atm^{-1} and after 30 min of ethylene exposure.

Complex	Activity (20°C)	Activity (70°C)[1]
2-U	0	0
3-U	0	0
4-U	0	0
5-U	12 800	39 200
6-U	11 200	0
2-Th	0	0
3-Th	0	0
5-Th	16 800	57 600
2'-Zr	NA	NA
3'-Zr	273 000	113 000
4'-Zr	52 200	NA
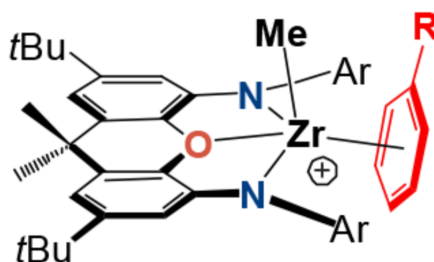
FIGURE 3.5: Structures of the compounds containing zirconium, with R = H, CH$_3$, F, Br .

the synthesis leads to a mixture of two isomers (see Figure 3.6). There is no report of synthesis concerning **5'-Zr** or **6'-Zr** yet.
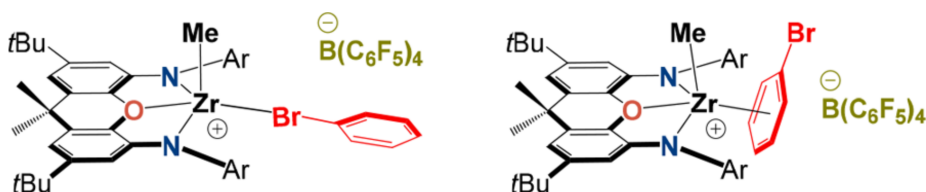
FIGURE 3.6: Possible structures of **4'-Zr** [109]

3.2.2 Finding the catalytic mechanism

The rationalisation of the catalytic mechanism is not easy since several hypotheses can be put forward:

- First, is it a concerted mechanism like in Figure 3.7 where both arene and ethylene are bonded at the same time to the metallic center or not ?

- If not, the relative bonding strengths of ethylene versus arene with the metal will be important. If the arene-metal bond is too strong, the ethylene will not be able to insert itself and the catalysis will not occur.

The success of the zirconium complexes over the actinides ones raises the question on the nature of the arene bonds to the metals. Having the smallest ionic radius Zr could be expected to form stronger bonds than the Th and U, contradicting the observed efficiency.

Gardner *et al.* [110] reported a larger catalytic power for Th complexes ([Th{N(CH$_2$CH$_2$NSiPri$_3$)$_2$(CH$_2$CH$_2$NSiPri$_2$C[H]MeCH$_2$)}]) than for the U ones (as for **5-U** and **5-Th**), and proposed as an explanation that electrostatic interactions are dominant in Th-complexes making the Th-ligand bond reacting more easily than the U-ligand one. Conversely, Domeshek *et al.* [111], in their complexes bis(N,N'-bis(trimethylsilyl)-2-pyridylami-dinate)An(μ-Cl)$_2$Li(TMEDA) (An = Th, U) found that U-complexes are more efficient than the Th ones. They proposed three explanations. The first is that the 5f^2 electrons of uranium can participate to a back-donation leading to an improved coordination to the olefin facilitating the activation of the double bond. The second is that the thorium complexes form stronger bonds with the arene making the insertion of ethylene harder. Another explanation is that the 5f orbitals in the U complex could stabilise the 4-member transition state (Figure 3.7), thus facilitating the catalysis [112].
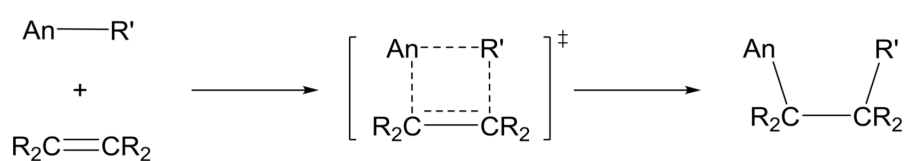
FIGURE 3.7: Four-center transition state in neutral organoactinide-mediated transformation where R' is the arene [108]

The last explanation appears as the simplest, as the larger size of Th(IV) might make it sterically more accessible than the U(IV) .

Of course, the true explanation can be a mixture of these hypothesis calling for a theoretical study of the systems to rationalise their catalytic activities and the mechanism of polymerisation by answering the following questions:

- Why do Zr complexes present such short bonds between the arene and the metal?

- What is the dominant nature of the bonding (electrostatic, covalent?...)?

- What is the participation of d and f orbitals into the bonding?

- What is the strength of the ethylene-metal versus the arene-metal bond?

3.2.3 Theoretical Studies of the Th, U and Zr cationic complexes

The theoretical studies of the complexes cited in the previous section are very limited. One theoretical study explored the catalysis reaction path [110]. It includes a full geometry optimisation followed by an anharmonic frequency calculation with the B3PW91 [113, 114] functional. Scalar relativistic effects were included by the Stuttgart-Dresden RECP [115, 116] and the corresponding basis sets. These articles emphasised the important role of the 5f-orbitals of thorium [110] and uranium [110, 117].

This study confirm that the explanations proposed by experimentalists such as electrostatic interaction, back-donation and strength of the bonds must be tested and assessed by an in-depth exploration of the bond between the various metallic centre and the arene solvents. In this context, we have used the ETS-NOCV bonding analysis [118, 119] that has been proven useful to elucidate the nature of the bonding interaction in multiple transition metal complexes [97, 120–129].

We start by optimising the structures of the complexes and compare the computed geometries to X-ray data, when available. Ultimately our results should address the previous and the following questions:

- How well do quantum chemistry structures agree with X-ray data?

- Is it possible to predict the geometries of the uncrystallised complexes?

- What are the driving forces of the cation interactions? How do they relate to the catalytic activity?

3.3 Optimisation of the Arene-Coordinated Uranium, Thorium or Zirconium Alkyl Cations

The complexes were optimised at the DFT level with the TURBOMOLE package [130]. Def-TZVP with RECP [131] was used for U, Th and Zr, and def2-TZVP basis

set [73] for all the other atoms. The resolution of identity for the Coulomb integrals was used to reduce the computational cost. We first considered the pure GGA PBE functional but it was not satisfying. Indeed in the η^6-**2-U** and η^6-**2-Th** benzene complexes, the benzene ended up being tilted in the optimised structured deviating from its expected orientation observed in the crystal. The hybrid PBE0 [45] functional previously reported good geometrical agreement with the experimental data for Actinides containing molecules [132] . In our case PBE0 brought the theoretical structure in excellent agreement with the experimental one. All the geometries provided by Emslie's team are available in Appendix A. The inclusion of the solvent effect with the COSMO continuum solvent model marginally affected the geometries while significantly increasing the computational time. This lead us to consider only gas-phase optimised geometries.

3.3.1 Optimisation of Benzene-Coordinated Alkyl Cations

For η^6-**2-Th** and η^6-**2-U**, X-ray structures were available and were used as starting points (see Table 3.2). For the **2'-Zr** no X-ray structure was available. Thus the X-ray structure of η^6-**3'-Zr** was used by substituting the methyl group of toluene by a hydrogen atom. As a complement of information concerning the influence of the (trimethylsilyl)methyl group, the structure η^6-**2-Zr**, being the strict equivalent of η^6-**2-Th** and the structure η^6-**2'-Th** being the strict equivalent of η^6-**2'-Zr**, were optimised. The starting points of those optimisations were the optimised η^6-**2-Th** and η^6-**2'-Zr** geometries where the Th atom was substituted by a Zr atom and vice versa respectively..

3.3.2 Optimisation of Toluene-Coordinated Alkyl Cations

For η^6-**3-U** and η^6-**3'-Zr**, X-ray structures were available and were used as starting points. Since the X-ray data of η^6-**3-U** and η^6-**3'-Zr** present the arene facing the metallic center (as in the benzene complexes), we only tested the orientation of the methyl group of the arene for the toluene structure η^6-**3-Th**. By convention, as in [96], we will name as "exo" structure the structure where the methyl group is on the same side as the CH$_2$SiMe$_3$ group and as "endo" structure, the structure where the methyl group sits on the opposite side of CH$_2$SiMe$_3$ as illustrated by Figure 3.8.
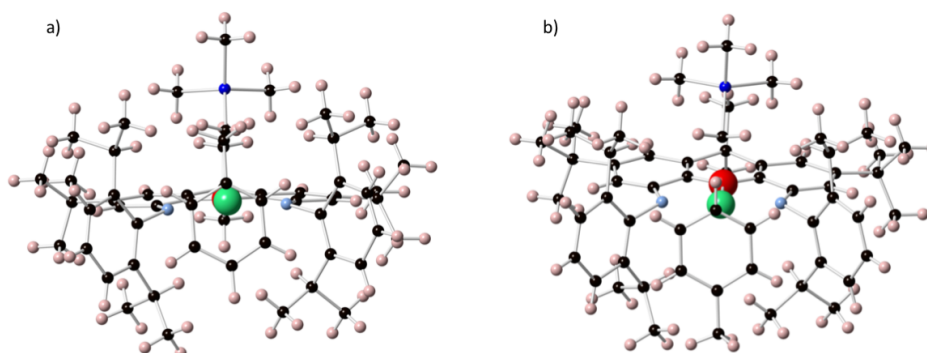
FIGURE 3.8: Starting geometries for the optimisation of the toluene
complex η^6-**3-Th** with a) the "exo" starting point b) the "endo" starting
point.

3.3.3   Optimisation of Halogeno-Coordinated Alkyl Cations

The X-ray structure of fluorobenzene, η^6-**5-U**, is also presenting a "endo" structure.
Thus we also expect a "endo" structure for η^6-**5-Th**. We also explored the orientation
of the arene in the fluorobenzene complexes η^1-**5-Th** and η^1-**5'-Zr** having the fluo-
robenzene of the arene ring facing the metallic centre, with the "horizontal" and the
"vertical" orientations as shown in Figure 3.9.

The bromo-benzene **4-U** and fluorobenzene **5-U** were optimised with the η^6-**5-U** X-
ray structure as starting point substituting fluorine by bromine.

The η^6-**3-Th**, η^6-**3-U** and η^6-**5-U** have a similar orientation of the methyl group of the
toluene or the fluor of the fluorobenzene; all are in the "endo" orientation. Thus the
bromo-benzene η^6-**4-Th** and η^6-**4-U** were optimised in the "endo" convention.

For the **4'-Zr**, Motolko *et al.* [109] reported the "exo" and the "horizontal" structures
as possible structures and probably a mixing of the two. Thus we tested these two
orientations presented in Figure 3.10.

3.3.4   Optimisation of Difluoro-Coordinated Alkyl Cations

For difluoro-benzene complexes, only the **6-Th** was optimised so far. There are no
X-ray data for any of the metallic center thus, five orientations were tested. Three
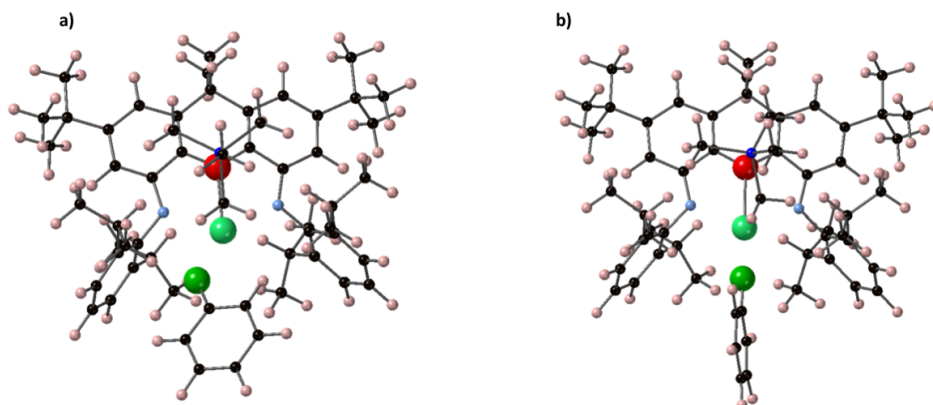
FIGURE 3.9: Starting geometries for the optimisation of η^1-**5-Th** with
a) the "horizontal" starting point and b) the "vertical" starting point.
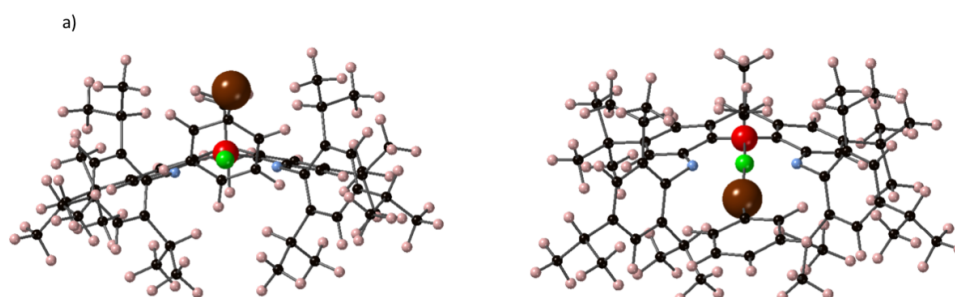
FIGURE 3.10: Starting geometries for the optimisation of the bro-
mobenzene complex **4′-Zr** with a) the "exo" starting point and b) the
"horizontal" starting point.

correspond to the arene facing Th with different initial positions of the two fluor
atoms. Again, we kept the "exo" and "endo" notations, adding the label "side" to the
third possibility as it can be seen in Figure 3.11. The last two starting points are the
"horizontal" and the "vertical" presented earlier.
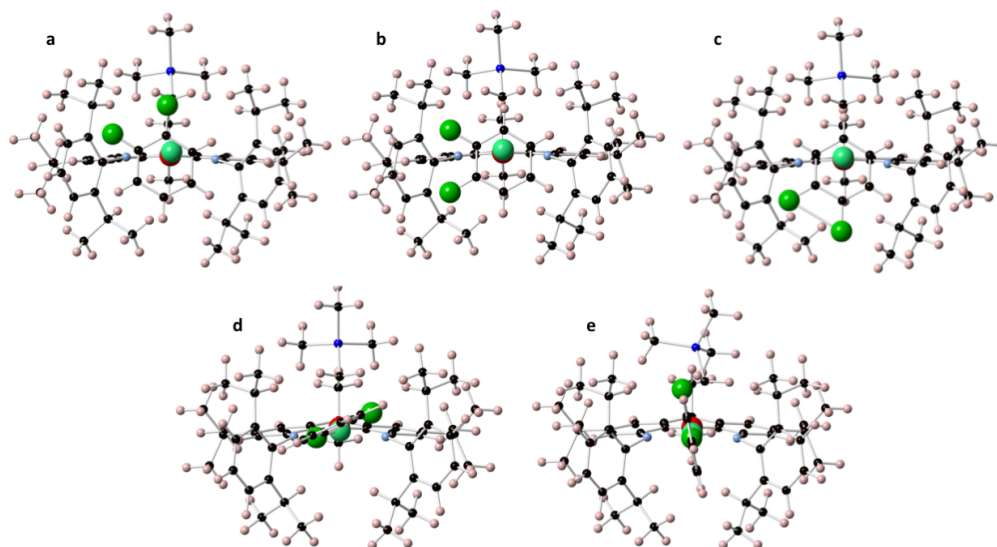
FIGURE 3.11: Starting geometries for the optimisation of **6-Th**: (a) η^6-**6-Th-exo**, (b) η^6-**6-Th-side**, (c) η^6-**6-Th-endo**, (d) η^1-**6-Th-horizontal** and (e) η^1-**6-Th-vertical**.

3.3.5   Optimisation of Ethylene-Coordinated Alkyl Cations

The **E'-Zr**, **E-Th** and **E-U** are optimised with two starting points, one with CH_2 pointing to the metal one with the two carbons of the ethylene facing the metal/actinide centre. The starting structures are the optimised structures of the benzene **2'-Zr**, **2-Th** and **2-U**.
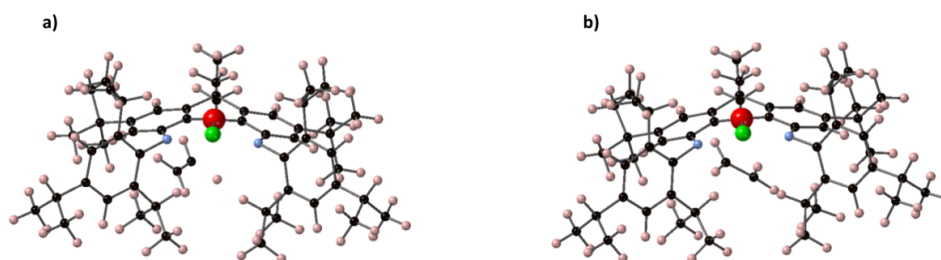
FIGURE 3.12: Starting geometries for the optimisation of **E'-Zr**: (a) η^1-**E'-Zr** and (b) η^2-**E'-Zr**.

3.4 Bonding studies

3.4.1 Dissociation curves - Benzene-Coordinated Alkyl Cations

For the benzene complexes, to quantify the strength and the nature of the benzene cation bonds, interaction curves were computed scanning the cation benzene distance from 2.7 Å to 4.0 Å for Th and U and from 2.2 Å to 3.4 Å in steps of 0.1 Å plus additional points at 4.5, 5, 6 and 10 Å.

Since the curves were smooth and presented only a single minimum (see Figure 3.17), the estimation of the binding energy was done at the structures accounting for the BSSE correction as described in the following paragraph.

3.4.2 Estimation of the binding energies at the equilibrium including BSSE and dispersion

For the BSSE calculation, the complex is divided into two fragments the first one (A) being composed of the catalyst and the second fragment (B) corresponding to the arene. If all the setup from the previous calculation was kept (DFT-TURBOMOLE-PBE0), tests on basis sets, using larger ones, such as def2-QZVP, def2-TZVPP and aug-cc-pVTZ for **2'-Zr** were performed. The interaction energies changed by a few kJ/mol with a largest basis sets proving that def2-TZVP is sufficiently accurate.

Because of the π-coordination of the arene to the metallic center, dispersion effects might be important. They can be captured by the MP2 method at considerable computational cost, or with a DFT-based approach with an empirical dispersion correction, namely the D3 correction [50].

3.4.3 Decomposition of the bond energy: the ETS-NOCV method

The ETS-NOCV method [118, 119], implemented in the ADF package, decomposes the interaction between two fragments within a system chosen by the user, to offer a quantitative picture of the chemical bond.

ETS - Extended Transition State decomposition analysis

The total energy between the interacting fragments is divided in 4 components [133]:

$$\Delta E_{tot} = \Delta E_{dist} + \Delta E_{elstat} + \Delta E_{Pauli} + \Delta E_{orb} \tag{3.1}$$

- ΔE_{dist}: the distorsion term corresponding to the energy between the free fragments and their geometry within the complex.

- ΔE_{elstat}: the electrostatic stabilising interaction between the 2 fragments when they are brought to their position in the final complex.

- ΔE_{Pauli}: the destabilising repulsive interaction between the occupied orbitals of the 2 fragments.

- ΔE_{orb}: the stabilising interaction between the occupied orbitals of one fragment and the unoccupied orbitals of the other one and the mixing of the unoccupied and occupied orbitals of a same fragment (intrafragment polarisation) once the two fragments have been united.

The change in the electronic density $\Delta\rho$ responsible for ΔE_{orb} can be written as:

$$\Delta\rho(1) = \sum_{\lambda}\sum_{\nu} \Delta P_{\lambda\nu}\lambda(1)\nu(1) \tag{3.2}$$

With "(1)" corresponding to the molecular orbital, λ are the occupied orbitals and ν the unoccupied orbitals of the 2 fragments and $\Delta P_{\lambda\nu}$ the deformation density function of λ and ν. Then ΔE_{orb} can be written as:

$$\Delta E_{orb} = \sum_{\lambda}\sum_{\nu} \Delta P_{\lambda\nu} F_{\lambda\nu}^{TS} \tag{3.3}$$

where $F_{\lambda\nu}^{TS}$ is the Kohn-Sham Fock matrix element that can be defined in terms of potential (transition state -TS) that is midway between the combined fragments and the final molecule (this is why it is called transition state).

NOCV - Natural orbitals for chemical valence

Derived from Nalewajski-Mrozek valence theory [134, 135], the deformation density is defined as :

$$\Delta\rho(r) = \rho^{system} - \sum_i \rho_i^{frag}(r) \tag{3.4}$$

The deformation density $\Delta\rho$ can be expanded as a sum of pairs of (Ψ_{-k}, Ψ_k) the natural orbitals for chemical valence (NOCV) that provide an orbital representation of the deformation density:

$$\Delta\rho(r) = \sum_{k=1}^{M/2} \nu_k[-\Psi_{-k}^2(r) + \Psi_k^2(r)] = \sum_{k=1}^{M/2} \Delta\rho_k(r) \tag{3.5}$$

In equation 3.5, Ψ_{-k} and Ψ_k NOCV are the eigenvectors of the ΔP matrix corresponding to eigenvalues $\pm \nu_k$, where $\Delta P = P_{AB}$ - $(P_A + P_B)$, and P_{AB}, P_A and P_B are the molecular, and the fragment charge and bond order matrices [134, 135].

As a result the orbital interaction can be expressed in terms of the NOCV orbitals as:

$$\Delta E_{orb} = \sum_{k=1}^{M/2} \Delta E_{orb}(k) = \sum_{k=1}^{M/2} \nu_k[-F_{-k,-k}^{TS}(r) + F_{k,k}^{TS}(r)] \tag{3.6}$$

where $F_{-k,-k}^{TS}$ and $F_{k,k}^{TS}$ are the diagonal Kohn-Sham matrix elements defined over NOCVs with respect to the TS density. In this expression, only few complementary NOCV pairs (often 2 to 4) contribute significantly to ΔE_{orb}. Each pair represents one charge-transfer contribution $\Delta\rho_k$, with its energy contribution $\Delta E_{orb}(k)$. To discuss trends across complexes the same fragment types must be used *i.e.* the fragments A and B must describe the same parts of the molecule.

ETS-NOCV calculations were performed for all the benzene complexes with the PBE0 functional, QZ4P basis sets and included scalar relativistic effects with the ZORA Hamiltonian. As for the BSSE calculation, the first fragment includes the cationic complex and the second one the arene. One has to note that ETS-NOCV analysis cannot be performed with spin-orbit coupling. Nevertheless, for benzene complexes a simple-point calculation with Spin-Orbit ZORA Hamiltonian was ran showing that spin-orbit coupling has no effect on the interaction energy.

3.5 Results and discussions

3.5.1 Geometries of the arene-coordinated uranium, thorium or zirconium alkyl cation with the arene solvent

Geometries of benzene-coordinated alkyl cations

Table 3.6 gathers all the results for the benzene complexes. The distances between the metal centres and both the oxygen and nitrogen atoms of the XA_2 (4,5-bis(2,4,6-triisopropylanilido)-2,7-di-tert-butyl-9,9-dimethylxanthene) group almost perfectly vary with respect to the ionic radii variations; for instance the Th-O distance in η^6-**2-Th** comes out 0.22 Å longer the Zr-O one in η^6-**2-Zr**, and 0.06 Å longer than the U-O one in η^6-**2-U**. Contrariwise the metal-arene distances do not follow the ionic radii trends since the Th-C_{arene} distance are about 0.47 Å and 0.17 Å longer than the Zr-C_{arene} and U-C_{arene} ones respectively, suggesting that the various cations interact differently with the benzene ring. The computed structure of η^6-**2'-Zr** is also reported though it could not be crystallised by Emslie *et al.* The difference between η^6-**2'-Zr** and η^6-**2-Zr** is that a methyl group is attached to Zr in the former while the latter carries a bulkier CH_2SiMe_3 group. This is confirmed by the fact that η^6-**2'-Th** present similar O-M-C_{apical} angle and arene bend angle than η^6-**2'-Zr**. As consequences, η^6-**2'-Th** also present a short distance M-Arene Centroid than η^6-**2-Th**. Albeit Zr-O and Zr-N distances are nearly the same in both η^6-**2-Zr** and η^6-**2'-Zr** complexes, the Zr-C_{arene} distance is shorter in the former than in the latter.
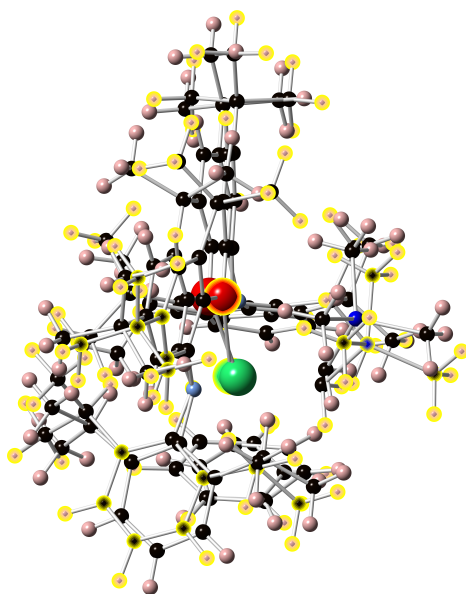
FIGURE 3.13: Superposition of the X-ray and the optimised (yellow atoms) structures of η^6-**2-Th**

TABLE 3.6: Important bond lengths in Å and angles in degree for η^6-**2-U** (X-ray and optimised structures), η^6-**2-Th** (X-ray and optimised structures),η^6-**2′-Th** (optimised structure), η^6-**2′-Zr** (optimised structure) and η^6-**2-Zr** (optimised structure).

Compounds	η^6-**2-U** X-ray	η^6-**2-U** opt	η^6-**2-Th** X-ray	η^6-**2-Th** opt
M-O	2.441(2)	2.428	2.496(5)	2.487
M-N	2.224(2), 2.236(6)	2.222, 2.231	2.278(3), 2.288(3)	2.278, 2.282
M-C$_{arene}$	3.099(3) - 3.248(3)	3.028 - 3.795	3.18 - 3.31	3.19 - 3.41
M-Arene Centroid	2.932	3.136	2.950	2.999
$N_1 \ldots N_2$	3.94	3.99	4.04	4.02
Arene Bend				
Angle[1]	18.9	23.5	8.7	10.8
O-M-C$_{apical}$	87.26(8)	91.90	91.3(1)	91.4
M-C-Si	133.7(2)	135.7	131.0(2)	132.4

Compounds	η^6-**2′-Th**	η^6-**2′-Zr** opt	η^6-**2-Zr** opt
M-O	2.500	2.248	2.263
M-N	2.273, 2.274	2.144, 2.149	2.103, 2.099
M-C$_{arene}$	3.171-3.302	2.781 - 2.881	4.43 - 2.699
M-Arene Centroid	2.925	2.470	3.403
$N_1 \ldots N_2$	3.963	3.87	3.829
Arene Bend			
Angle[1]	0.8	2.4	30.1
O-M-C$_{apical}$	82.8	82.2	96.2
M-C-Si	–	–	132.3

[1] Angle between the carbons of the arene and the planar ligand.
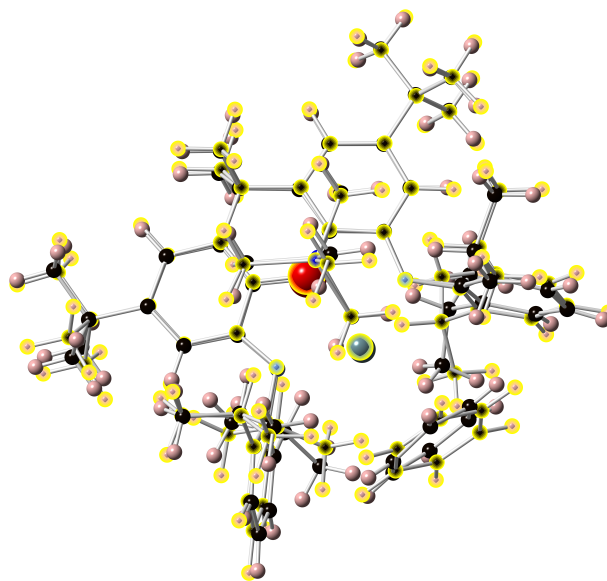
FIGURE 3.14: Superposition of the X-ray and the optimised (yellow atoms) structures of η^6-**2-U**

Geometries of toluene-coordinated alkyl cations

TABLE 3.7: Important bond lengths in Å and angles in degree for η^6-**3-U** (X-ray structures), η^6-**2-Th** (optimised structure) and η^6-**3'-Zr** (X-ray and optimised structures).

Compounds	η^6-**3-U-endo** X-ray	η^6-**3-Th-endo** opt	η^6-**3'-Zr-exo** opt	η^6-**3'-Zr-exo** X-ray
M-O	2.480	2.417(9)	2.247	2.220
M-N	2.21(1), 2.22(1)	2.277, 2.273	2.161, 2.148	2.138, 2.142
M-C$_{arene}$	3.05(2) - 3.78(2)	3.084 - 4.005	2.747 - 2.908	2.697 - 2.840
M-Arene Centroid	3.138	3.271	2.449	2.383
N$_1$ ... N$_2$	3.98	4.04	3.91	3.91
Arene Bend Angle[1]	11.8	13.4	12.7	
O-M-C$_{apical}$	5.9	92.20	87.7	81.0
M-C-Si	136.8(7)	133.8	–	–

[1] Angle between the carbons of the arene and the planar ligand.

The structures of η^6-**3-U-endo** and η^6-**3-Th-exo** are not be obtained yet. For those available the computed geometries agree well with the available crystallographic data (see Table 3.7). The main observation is that the M-C$_{arene}$ distances in toluene complexes are slightly shorter than in the benzene ones.

Geometries of halogeno-coordinated alkyl cations

The structures of bromobenzene η^6-**4-U** and the fluorobenzene η^6-**5-U** and η^1-**5-Th-horizontal** are not reported yet.

The fluorobenzene η^6-**5'-Zr-exo** is slightly more stable than η^1-**5-Th-vertical** with a difference in energy of 0.35 kJ.mol^{-1}. This difference is so small that both structures will be kept for the rest of the study. The η^1-**5'-Zr-vertical** relaxed to an "horizontal" orientation but forming an important tilt angle with the molecular plane. The most stable is the optimised **5'-Zr-vertical**, with an energy 4.2 kJ.mol^{-1} lower than that obtained with the η^1-**5'-Zr-horizontal**. The last isomer, η^6-**5'-Zr-exo** is the least stable lying 15.7 kJ.mol^{-1} above η^1-**5'-Zr-vertical**. Nevertheless, as the structures are close in energy both the η^1-**5'-Zr-horizontal** (from the optimised $\eta^{'}$-**5'-Zr-vertical** starting point) and η^1-**5'-Zr-exo** are kept for the next steps of the study. The currently optimised structures cannot be compared to crystal data, though, they reveal very

similar bond distances to the toluene ones.

TABLE 3.8: Important bond lengths in Å and angles in degree for η^6-**5-U** (optimised and X-ray structures), η^6-**5-Th** (optimised structure), η^6-**5'-Zr** (optimised structure) and η^1-**5'-Zr** **-horizontal** (optimised structure) and the relative energy ΔE in kJ.mol^{-1} with respect to the most stable isomer.

Compounds	η^6-**5-U** X-ray	η^6-**5-Th-endo** opt	η^1-**5-Th-vertical**
M-O	2.431	2.477	2.476
M-N	2.215, 2.218	2.267, 2.275	2.267, 2.270
M-C$_{arene}$	3.128 - 3.598	3.140 - 3.822	–
M-Arene Centroid	3.077	3.204	–
N$_1$...N$_2$	3.98	4.033	4.040
Arene Bend Angle [1]	1.6	8.4	78.9
O-M-C$_{apical}$	89.6	92.3	94.9
M-C-Si	134.8	133.2	132.5
ΔE		0.0	0.3

Compounds	η^6-**5'-Zr-exo** opt	η^1-**5'-Zr** **-horizontal** opt	
M-O	2.277	2.257	
M-N	2.088, 2.082	2.068, 2.070	
M-C$_{arene}$	2.687 - 4.417	–	
M-Arene Centroid	3.401	–	
N$_1$...N$_2$	3.790	3.813	
Arene Bend Angle [1]	10.7	11.1	
O-M-C$_{apical}$	91.3	101.5	
M-C-Si	–	–	
ΔE	15.7	0.0	

[1] Angle between the carbons of the arene and the planar ligand.
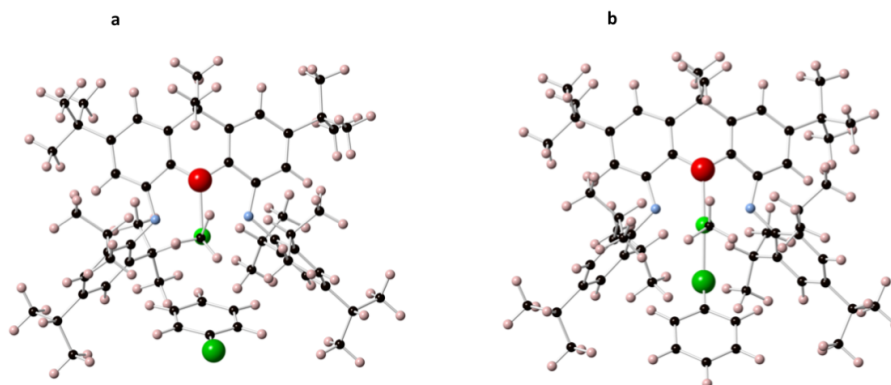
FIGURE 3.15: Optimised geometries for a) η^6-**5'-Zr-exo**, b) η^1-**5'-Zr-horizontal**

TABLE 3.9: Important bond lengths in Å and angles in degree for η^6-**4-Th** (optimised structure) and **4'-Zr** (optimised structures) and the relative energy ΔE in kJ.mol^{-1} with respect to the most stable isomers.

Compounds	η^6-**4-Th-endo** opt	η^6-**4'-Zr-exo** opt	η^1-**4'-Zr-horizontal** opt
M-O	2.472	2.276	2.260
M-N	2.263, 2.263	2.082, 2.088	2.069, 2.077
M-C$_{arene}$	3.058 - 4.335	2.697 - 4.406	–
M-Arene Centroid	3.481	3.390	–
N$_1$ ... N$_2$	4.03	3.789	3.789
Arene Bend			
Angle [1]	4.9	11.4	13.5
O-M-C$_{apical}$	92.9	91.1	90.8
M-C-Si	133.3	–	–
ΔE		0.0	9.7

[1] The angle between the carbons of the arene and the planar ligand.

In the case of bromobenzene isomers, η^6-**4'-Zr-exo** is more stable than η^1-**4'-Zr-horizontal** by 9.7 kJ.mol^{-1} but since David Emslie suspected the presence of these two isomers from NMR analysis [109], both will be kept for the next steps of the bonding study.

Geometries of difluorobenzene-coordinated alkyl cations

η^1-**6-Th-vertical** and η^1-**6-Th-horizontal** are converging to the same η^1-**6-Th-vertical** structure, thus only this one will be kept for the results. The most stable isomer is the η^1-**6-Th-vertical** and the other three are less than 15 kJ.mol^{-1} higher in energy, forcing us to consider all of them. Nonetheless the final structure of η^1-**6-Th-horizontal**
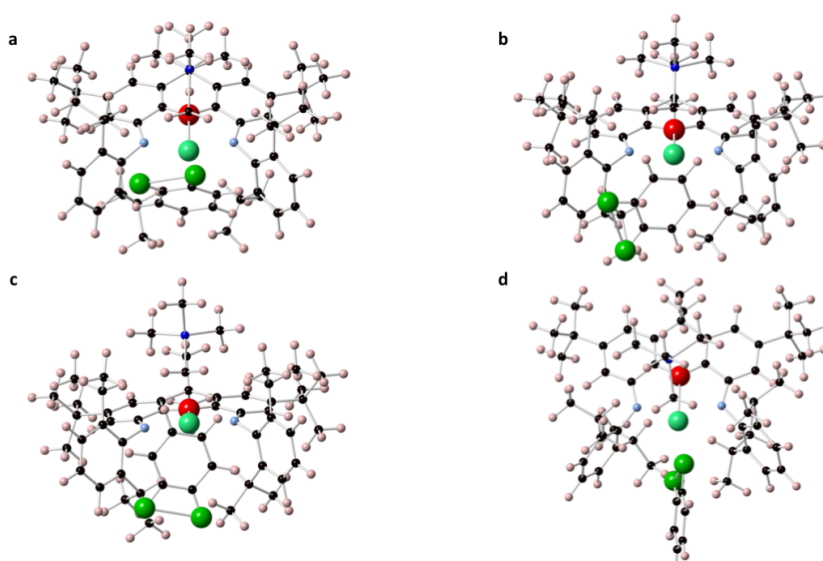
FIGURE 3.16: Optimised geometries for a) η^6-**6-Th-exo**, b) η^6-**6-Th-side**, c) η^6-**6-Th-endo** and, d) η^1-**6-Th-vertical**

TABLE 3.10: Important bond lengths in Å and angles in degree for η^6-**6-Th-exo**, η^6-**6-Th-side**, η^6-**6-Th-endo**, η^1-**6-Th-horizontal** and η^1-**6-Th-vertical** optimised structures and the relative energies ΔE in kJ.mol^{-1} with respect to the most stable isomer.

Compounds	η^1-**6-Th-vertical** opt	η^6-**6-Th-exo** opt	η^6-**6-Th-side** opt	η^6-**6-Th-endo** opt
M-O	2.46	2.492	2.477	2.475
M-N	2.252, 2.254	2.279, 2.280	2.259, 2.258	2.262, 2.258
M-C$_{arene}$	–	3.060 - 4.298	3.107 - 4.373	3.030 - 4.326
M-Arene Centroid	–	3.461	3.531	3.464
N$_1 \ldots$ N$_2$	4.000	4.036	4.004	4.014
Arene Bend Angle [1]	–	28.6	24.9	13.0
O-M-C$_{apical}$	93.6	93.5	93.3	93.5
M-C-Si	132.3	133.8	132.4	132.3
ΔE	0.0	12.4	15.5	9.6

[1] The angle between the carbons of the arene and the planar ligand.

The arene bend angles in the η^6-**6-Th-exo** and η^6-**6-Th-side** isomers are larger than in the η^6-**6-Th-endo** one because of the steric repulsion of the two fluorine atoms.

Optimisation of Ethylene-Coordinated Alkyl Cations

The **E'-Zr** optimised structures with both starting points are giving the same result with the two carbons of the ethylene facing the zirconium atom. For this reason, for U and Th complexes, the optimisation where the CH_2 is pointing to the actinide is disregarded. The important information on the complexes can be found in Table 3.11

TABLE 3.11: Important bond lengths in Å and angles in degree for η^2-**E'-Zr** and η^2-**E-Th** optimised structures.

Compounds	E'-Zr	E-Th
M-O	2.268	2.467
M-N	2.070, 2.076	2.251, 2.254
M-C$_{ethylene}$	2.796, 2.842	3.113, 3.094
N$_1$ ... N$_2$	3.790	4.005
Ethylene Bend Angle [1]	37.4	12.9
O-M-C$_{apical}$	92.1	95.6
M-C-Si	–	131.4

[1] The angle between the carbons of the ethylene and the planar ligand.

All the distance M-C$_{ethylene}$ are shorter than in the other complexes thus a stronger bond could be expected. Unfortunately, as I write this lines, no result about η^2-**E-U** is available.

3.5.2 Bonding studies

Dissociation curves - Benzene-Coordinated Alkyl Cations

Figure 3.17 presents the results for the dissociation of benzene from the alkyl Zr, Th and U cations. The curves display only one minimum corresponding to the distance benzene - metallic center found in the geometry optimisations. The bonding energies derived from the curves are -145.5 kJ.mol^{-1}, -90.4 kJ.mol^{-1} and -80.3 kJ.mol^{-1} for η^6-**2'-Zr**, η^6-**2-Th** and η^6-**2-U**, respectively.
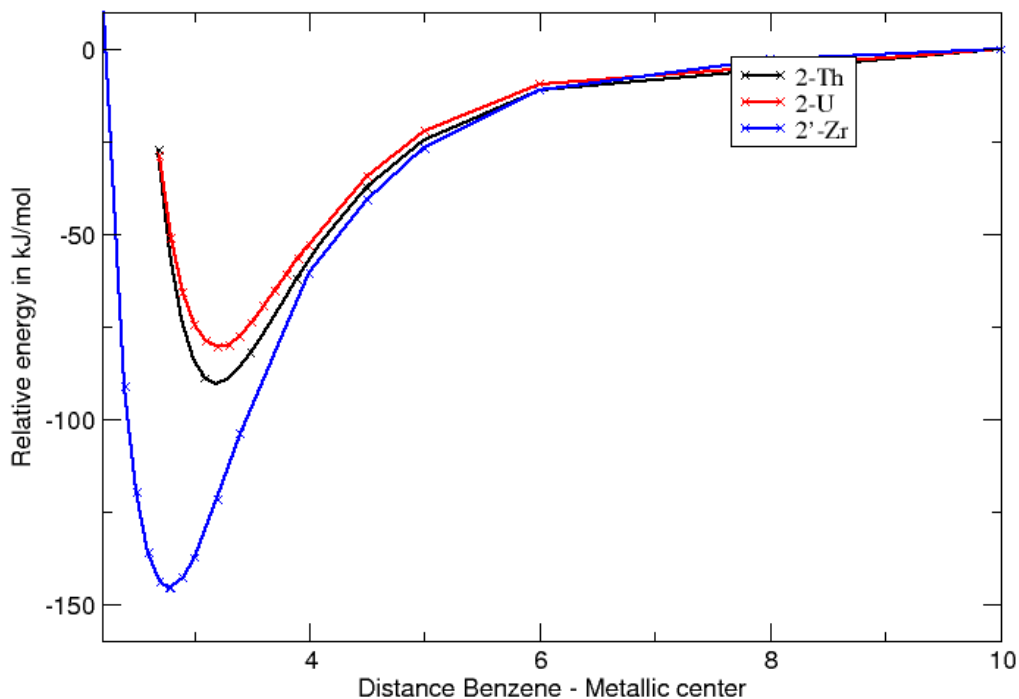
FIGURE 3.17: Dissociation curves for η^6-**2-Th** (black), η^6-**2-U** (red)
and η^6-**2'-Zr** (blue) for a benzene - metallic center distance between
2.2 Å and 10 Å

TABLE 3.12: BSSE corrections (in kJ.mol^{-1}) to the benzene interaction
energies in η^6-**2'-Zr** computed at different levels of calculation with
different basis sets.

	ΔE	ΔE(BSSE)	$\Delta E_{corrected}$
PBE0-def2-TZVP	-147.4	-4.6	-142.8
(PBE0 + D3)-def2-TZVP	-204.4	-4.6	-199.9
MP2-def2-TZVP	-281.9	-42.2	-239.7
MP2-def2-TZVPP	-289.4	-36.9	-252.6
MP2-aug-cc-pVTZ	-305.2	-45.0	-260.2

BSSE corrections and decompositions of the bond energies: an ETS-NOCV study

To evaluate the accuracy of the QM methods on the bonding energies, we have per-
formed PBE0, PBE0 + D3 and MP2 calculations for the η^6-**2'-Zr** complex (see Table
3.12). MP2 energies are somewhat sensitive to the size of the basis set; increasing

the basis quality from def2-TZVP to def2-TZVPP and aug-cc-PVTZ increases the binding energy by 13 and 20 kJ.mol^{-1} (< 10% of the total interaction energy), respectively, while expanding significantly the computational time. Thus, the def2-TZVP basis sets are kept for all other complexes.

TABLE 3.13: Bonding energies in kJ.mol^{-1} for the benzene molecules η^6-**2'-Zr**, η^6-**2-Zr**, η^6-**2-Th** and η^6-**2-U** at PBE0, PBE0 + D3 and MP2 levels.

	ΔE			ΔE(BSSE)			$\Delta E_{corrected}$		
	PBE0	PBE0 + D3	MP2	PBE0	PBE0 + D3	MP2	PBE0	PBE0 + D3	MP2
η^6-**2'-Zr**	-147.4	-204.4	-305.2	-4.6	-4.6	-45.0	-142.8	-199.9	-260.2
η^6-**2-Zr**	-92.8	-147.1	-190.5	-3.2	-3.2	-29.1	-89.6	-143.8	-161.5
η^6-**2-Th**	-92.5	-141.7	-189.7	-3.5	-3.5	-25.7	-89.0	-138.1	-164.1
η^6-**2-U**	-77.8	-128.0		-3.5	0.2		-74.2	-128.2	

From Table 3.13, we note that for both Zr and Th complexes, the MP2 energies are larger than the PBE0 ones. Assuming that PBE0 with D3 correction captures most of the dispersion effects, it is interesting to note that the PBE0 trends across the metal centres match the MP2 ones. However, the MP2 values come out lower than the PBE0 + D3 ones, which is in line with the fact that MP2 is known to overestimate

dispersion contributions [136, 137].

TABLE 3.14: Bonding energy decomposition in kJ.mol^{-1} for the zirconium cations with the ETS-NOCV method .

	η^2-**E'-Zr**	η^6-**2'-Zr**	η^6-**2-Zr**	η^6-**3'-Zr-exo**
ΔE_{Dist}	29.7	95.4	38.1	112.0
ΔE_{Pauli}	130.8	296.4	137.6	311.7
ΔE_{elstat}[1]	-119.3 (54%)	-200.5 (45%)	-105.6 (45%)	-217.6 (45%)
ΔE_{orb}[1]	-99.6 (46%)	-242.2 (55%)	-126.3 (55%)	-263.2 (55%)
ΔE^{σ}_{orb}[2]	-62.8 (63%)	-45.2 (19%)	–	-46.0 (19%)
$\Delta E^{\pi 1}_{orb}$[2]	-12.5 (13%)	-60.2 (25 %)	-71.1 (56%)	-66.1 (25%)
$\Delta E^{\pi 2}_{orb}$[2]	–	-63.2 (26%)	-13.0 (10%)	-66.9 (25%)
ΔE^{other}_{orb}[2]	-24.7 (24%)	-77.0 (30%)	-41.0 (32%)	-84.1 (31%)
ΔE^{PBE0}_{int}	-88.1	-146.3	-94.3	-169.2
ΔE_{Disp}[3]	-33.1	-52.5	-51.0	-61.9
$\Delta E^{PBE0+D3}_{int}$	**-91.5**	**-103.4**	**-107.2**not finish	**-119.1**

	η^6-**4'-Zr-exo**[*]	η^1-**4'-Zr-horizontal**	η^6-**5'-Zr-exo**	η^1-**5'-Zr-horizontal**
ΔE_{Dist}	36.3	29.1	30.7	22.3
ΔE_{Pauli}	133.3	115.3	136.7	100.3
ΔE_{elstat}[1]	-95.1 (43%)	-97.5 (48%)	-103.0 (45%)	-108.7 (54%)
ΔE_{orb}[1]	-125.6 (57%)	-105.9 (52%)	-125.3 (55%)	-91.7 (44%)
ΔE^{σ}_{orb}[2]	-73.6 (59%)	-65.5 (62%)	-74.5 (59%)	-44.5 (49%)
$\Delta E^{\pi 1}_{orb}$[2]	-10.5 (8%)	-10.8 (10%)	-9.6 (8%)	-14.2 (15%)
$\Delta E^{\pi 2}_{orb}$[2]	-8.4 (7%)	–	-8.4 (7%)	-9.6 (10%)
ΔE^{other}_{orb}[2]	-33.4 (26%)	-30.2 (28%)	-33.1 (24%)	-23.8 (26%)
ΔE^{PBE0}_{int}	-87.3	-88.1	-91.5	-100.0
ΔE_{Disp}[3]	-55.5	-47.3	-52.5	-36.8
$\Delta E^{PBE0+D3}_{int}$	**-106.5**	**-106.3**	**-113.0**	**-114.5**

[*] Most stable isomers.

[1] Values in parenthesis give the percentage contribution to the total attractive interaction (ΔE_{elstat} +ΔE_{orb}).

[2] Values in parenthesis give the percentage contribution to the total orbital energy for the σ- and π-donor NOCV-pair contributions.

[3] ΔE_{Disp} is the difference between ΔE^{PBE0}_{int} and $\Delta E^{PBE0+D3}_{int}$ with the BSSE correction.

Tables 3.14 and 3.15 summarise the energy decomposition analysis performed at the PBE0 level and the dispersion contributions that range from 40 to 70 kJ.mol^{-1}, representing at least 27% of the bonding energy. Thus, dispersion does not change the trends observed but is not negligible. Comparing the benzene η^6-**2'-Zr** and the

toluene η^6-**3'-Zr-exo** in Table 3.14, we see that the η^6-**3'-Zr-exo**, which is catalytically more active than η^6-**2'-Zr**, exhibits a stronger bond between Zr and the toluene solvent, which is counter intuitive with the hypothetical mechanism. η^6-**2-Zr** does not present an important σ interaction while η^6-**2'-Zr** does. It can come from the fact that η^6-**2-Zr** presents a large arene bond angle (30.1°) which prevents σ overlaps.

Fluorobenzene **5'-Zr** forms the weakest arene bond to zirconium. In case of the η^6-**5'-Zr-exo** isomer, it can be explained by the fact that the center of the fluorobenzene ring is shifted upwards as a result of hydrogen bonding between fluorine and a hydrogen atom of the CH_2SiMe_3 group.

The weakest bond is observed between the ethylene and the zirconium. Such a weak bond discredits the hypothesis of a competition between the arene from solvent and the ethylene. Nonetheless, the ethylene complexe is presenting a bond different from the one between the arene and the zirconium. Indeed, in present a σ donation from the ethylene carbons to the 4d and 5s orbitals of the zirconium and a π-retrodonation from the 2p orbitals of the carbons around Zr to the 2p orbitals of the ethylene carbons (see Figure **??**). Further explorations of possible transition states involving both

ethylene and the arene are foreseen.

TABLE 3.15: Bonding energy decomposition in kJ.mol^{-1} for the thorium cations with the ETS-NOCV method.

	η^2-**E-Th**	η^6-**2-Th**	η^6-**2′-Th**	η^6-**3-Th-endo**
ΔE_{Dist}	1.4	15.5	29.8	17.3
ΔE_{Pauli}	90.4	143.9	153.5	119.7
ΔE_{elstat} [1]	-87.6 (56%)	-115.6 (49%)	-120.8 (48%)	-102.0 (49%)
ΔE_{orb} [1]	-69.3 ((44%))	-120.9 (51%)	-130.3 (52%)	-104.9 (51%)
ΔE^{σ}_{orb} [2]	-43.1(62%)	-22.6 (19%)	-24.5 (19%)	-10.5 (10%)
$\Delta E^{\pi 1}_{orb}$ [2]	-8.7 (12%)	-33.0 (27%)	-35.6 (27%)	-39.7 (38%)
$\Delta E^{\pi 2}_{orb}$ [2]	–	-26.4 (22%)	-28.5 (22%)	-20.9 (20%)
ΔE^{other}_{orb} [2]	-17.8 (26%)	-39.7 (33%)	-42.6 (32%)	-34.2 (32%)
ΔE^{PBE0}_{int}	-66.5	-92.6	-97.6	-87.1
ΔE_{Disp} [3]	-25.2	-45.6	-50.5	-52.1
$\Delta E^{PBE0+D3}_{int}$	**-90.2**	**-122.7**	**-118.3**	**-121.9**

	η^6-**4-Th-endo**	η^6-**5-Th-endo**	η^1-**5-Th-verical**	
ΔE_{Dist}	8.1	-0.6	-6.1	
ΔE_{Pauli}	94.4	113.1	63.4	
ΔE_{elstat} [1]	-72.7 (45%)	-91.4 (48%)	-72.4 (55%)	
ΔE_{orb} [1]	-87.8 (55%)	-97.8 (52%)	-59.3 (45%)	
ΔE^{σ}_{orb} [2]	–	-11.7 (12%)	–	
$\Delta E^{\pi 1}_{orb}$ [2]	–	-33.5 (34%)	–	
$\Delta E^{\pi 2}_{orb}$ [2]	–	-21.3 (22%)	–	
ΔE^{other}_{orb} [2]	-87.8 (100%)	-32.1 (32%)	-59.3 (100%)	
ΔE^{PBE0}_{int}	-66.1	-76.1	-68.3	
ΔE_{Disp} [3]	-50.8	-48.7	-21.3	
$\Delta E^{PBE0+D3}_{int}$	**-108.8**	**-125.4**	**-95.7**	

	η^1-**6-Th-vertical**[*]	η^6-**6-Th-exo**	η^6-**6-Th-side**	η^6-**6-Th-endo**
ΔE_{Dist}	6.5	6.8	6.8	31.8
ΔE_{Pauli}	70.2	97.3	89.6	93.2
ΔE_{elstat} [1]	-80.2 (56%)	-71.4 (45%)	-68.6 (45%)	-69.8 (44%)
ΔE_{orb} [1]	-62.0 (44%)	-87.0 (55%)	-82.2 (55%)	-89.0 (56%)
ΔE^{σ}_{orb} [2]		– -15.5 (18%)	-38.0 (46%)	-41.4 (47%)
$\Delta E^{\pi 1}_{orb}$ [2]	–	-39.7 (46%)	-16.2 (20%)	-13.8 (16%)
$\Delta E^{\pi 2}_{orb}$ [2]	–	–	–	–
ΔE^{other}_{orb} [2]	-62.0 (100%)	-32.3 (37%)	-28.6 (34%)	-34.4 (37%)
ΔE^{PBE0}_{int}	-72.0	-61.1	-61.2	-65.6
ΔE_{Disp} [3]	-22.7	-45.9	-44.2	-44.4
$\Delta E^{PBE0+D3}_{int}$	**-88.2**	**-100.2**	**-98.6**	**-78.2**

[*] Most stable isomers.

[1] Values in parenthesis give the percentage contribution to the total attractive interaction (ΔE_{elstat} +ΔE_{orb}).

[2] Values in parenthesis give the percentage contribution to the total ornital energy

We can see that the bonding interaction decreases along the arene series of the Th-complexes (see Table 3.15); as the bonding strength decreases, so does the 7s and 5f characters of the acceptor orbital while the 6d character increase in the main deformation densities contributions (See figure 3.18, **??** and the Appendix C).

Regarding the **6-Th** isomers, η^6-**6-Th-vertical** is the most stable one and presents the strongest arene-metal interaction. In η^1-**6-Th-vertical** and η^6-**6-Th-endo** the orbital interaction is composed of multiple small interactions. In η^1-**6-Th-vertical**, the arene ring orientation does not favour any bonding symmetry, while η^6-**6-Th-endo**, the arene ring is shifted perpendicularly to the molecular plane. Just as in Zr complexes, η^2-**E-Th** presents the weakest bond and the π retrodonation from the 2p orbitals of the carbons close to the Th center and the 4d orbitals of the thorium to the 2p orbitals of the ethylene carbons. The same exploration of transition state must then be done to shed light on the mechanism.

Finally the useful complexes to compare the metals are the η^6-**2-Th**, η^6-**2-Zr**, η^6-**2'-Th** and η^6-**2'-Zr** ones (see Tables 3.14 and 3.15 and Figures 3.18, **??**, 3.19 and **??**). The interaction strength is roughly the same comparing metals but the Zr benzene bond is somewhat more covalent than the Th-benzene one (larger ΔE_{orb} percentage). Again the absence of σ interaction in **2-Zr** is explained by the large arene bend angle. Being smaller in the thorium equivalent, the σ donation contributions into the 6d and 5f orbitals of Th amounts to 20% while π-type interactions sums up to 49% of the covalent contribution.

3.6 Conclusion and Perspectives

Although a lot of information have been already collected, the catalytic mechanism could not be revealed. So far we have shown that our QM calculations are able to reproduce X-ray data and certainly predict the geometries of uncrystallised complexes. We have seen that the Zr-cations have a bonding interaction slightly more covalent than the Th-ones, in which the arene interaction is electrostatically driven. The stronger bonds in thorium systems mainly involve 7s and 5f orbitals while the weakest involve mainly 6d orbitals. The study of hypothetic transition states will be done to explore the possible reaction paths.
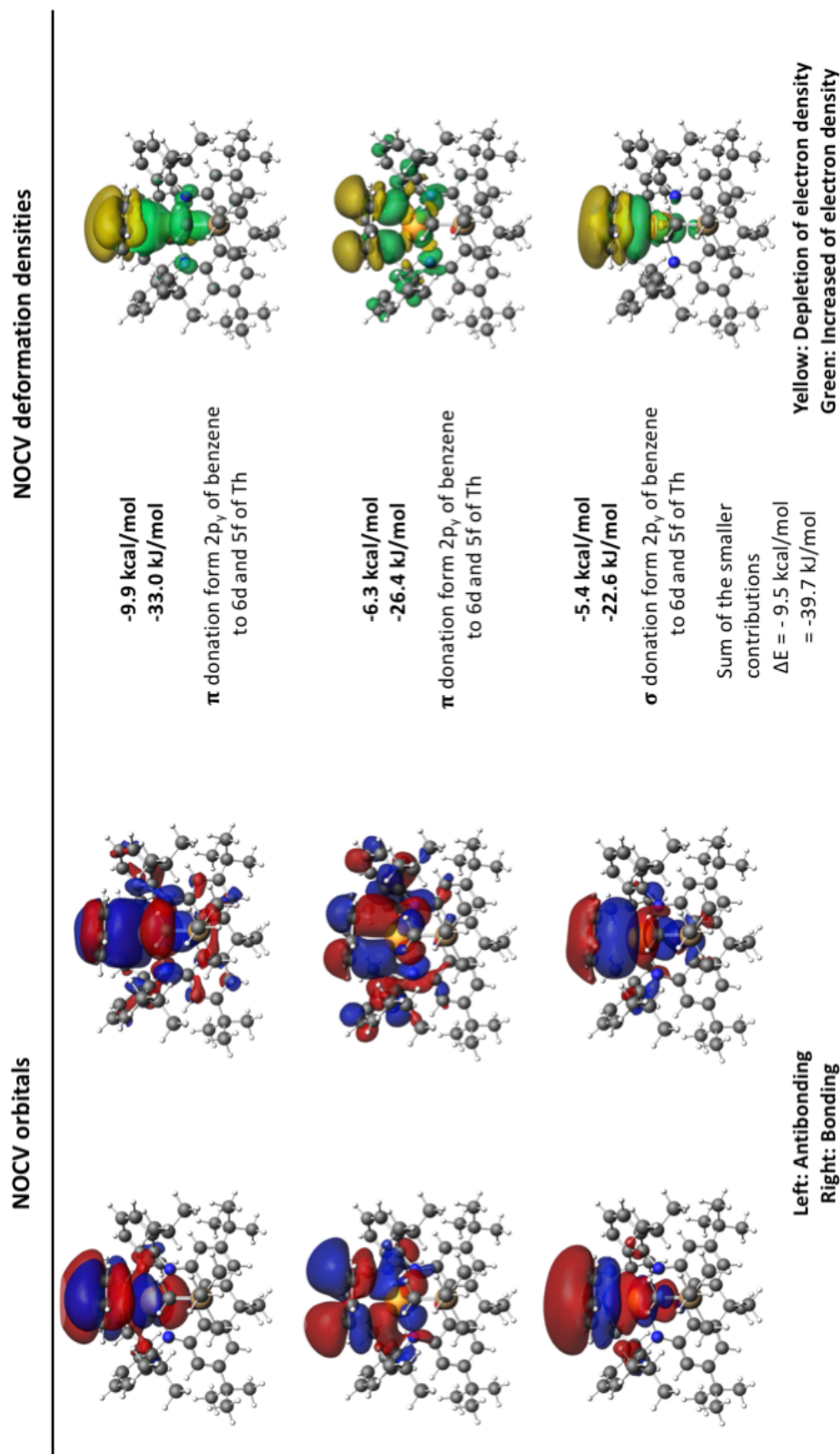
FIGURE 3.18: On the left hand side: the NOCV Orbitals (with isosurfaces set to 0.01) and on the right hand side ETS-NOCV deformation density contributions, Increased (green) and decreased (yellow) electron density is presented relative to that in the isolated fragments (isosurfaces are set to 0.0001) for the molecule η^6-**2-Th**.

NOCV deformation densities

NOCV orbitals

-17.5 kcal/mol
-71.1 kJ/mol

π donation form $2p_y$ of benzene to 5s and 4d of Zr

-3.1 kcal/mol
- 13.0 kJ/mol

π donation form $2p_y$ of benzene to 4d of Zr

Sum of the smaller contributions

ΔE = - 9.8 kcal/mol
= - 41.0kJ/mol

Yellow: Depletion of electron density
Green: Increased of electron density

Left: Antibonding
Right: Bonding
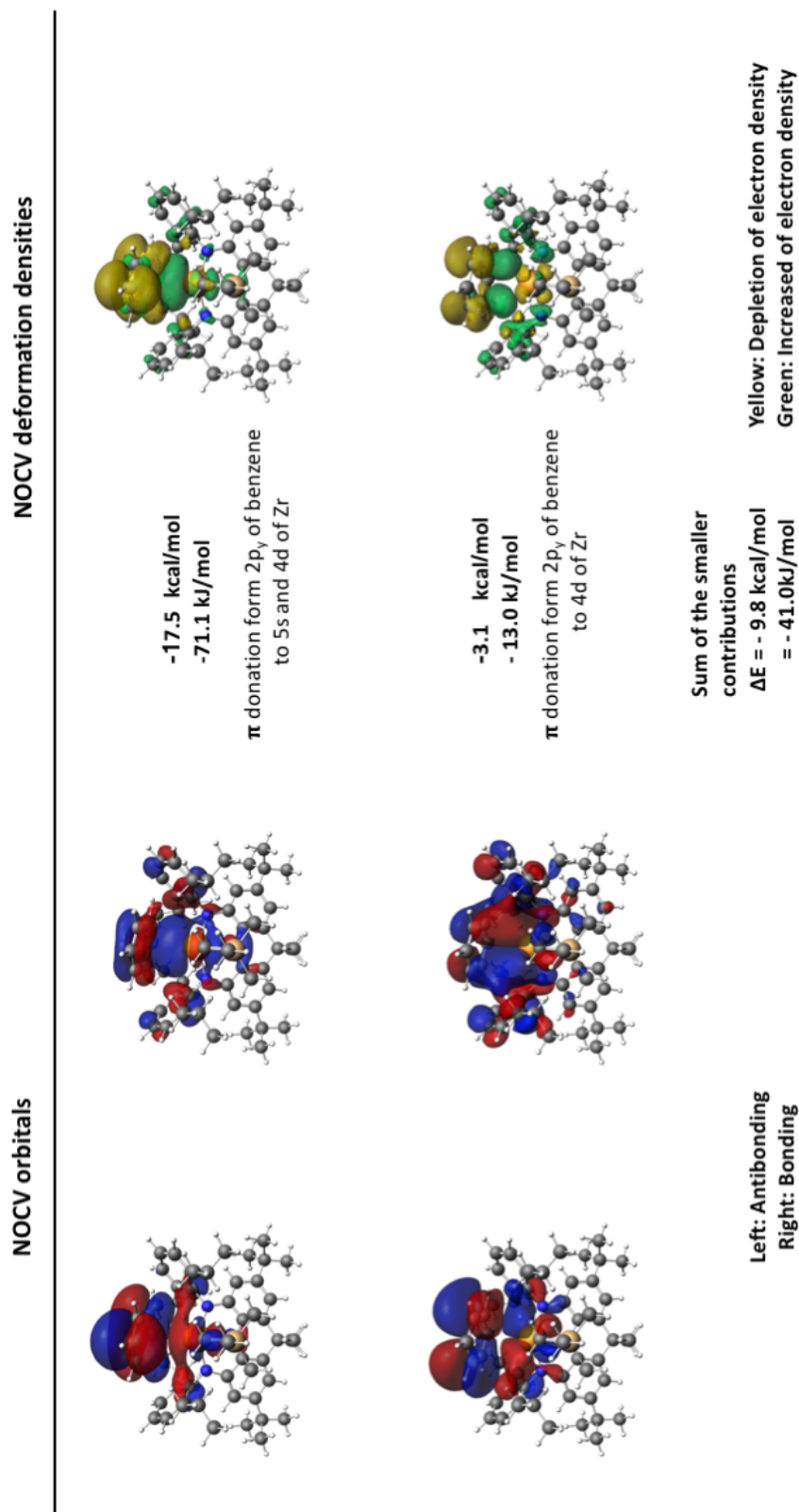
FIGURE 3.19: On the left hand side: the NOCV Orbitals (with isosurfaces set to 0.01) and on the right hand side ETS-NOCV deformation density contributions, Increased (green) and decreased (yellow) electron density is presented relative to that in the isolated fragments (isosurfaces are set to 0.0001) for the molecule η^6-**2-Zr**.
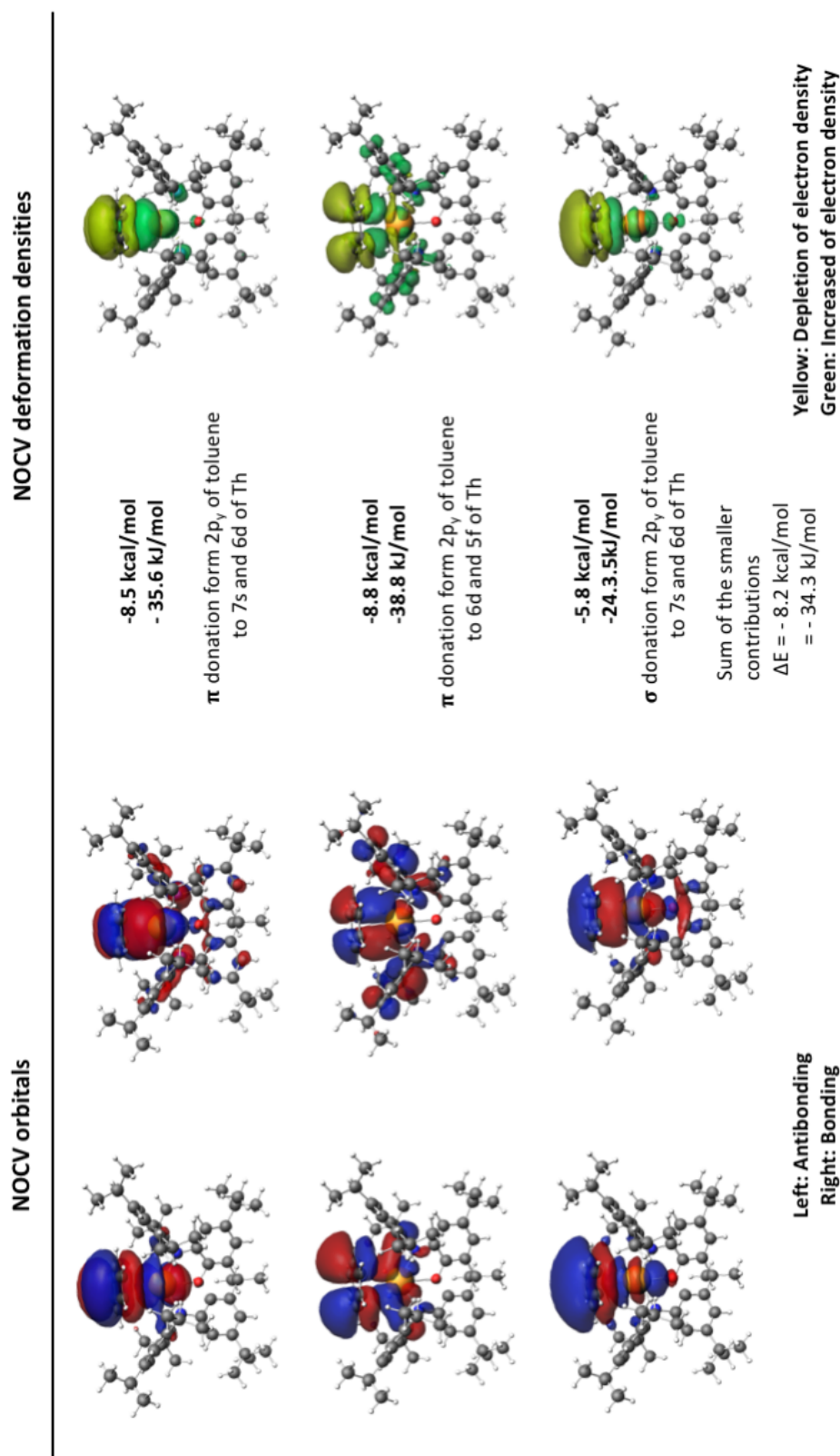
FIGURE 3.20: On the left hand side: the NOCV Orbitals (with isosurfaces set to 0.01) and on the right hand side ETS-NOCV deformation density contributions, Increased (green) and decreased (yellow) electron density is presented relative to that in the isolated fragments (isosurfaces are set to 0.0001) for the molecule η^6**2′-Th.**

NOCV deformation densities

-14.4 kcal/mol
-60.2 kJ/mol

π donation form $2p_y$ of benzene
to 4d and 5s of Zr

-15.1 kcal/mol
- 63,2 kJ/mol

π donation form $2p_y$ of benzene
to 4d and 5s of Zr

-10.8 kcal/mol
-45.2 kJ/mol

σ donation form $2p_y$ of benzene
to 4d and 5s of Zr

Sum of the smaller
contributions

ΔE = - 18.4 kcal/mol
= - 77.0kJ/mol

Yellow: Depletion of electron density
Green: Increased of electron density

NOCV orbitals

Left: Antibonding
Right: Bonding
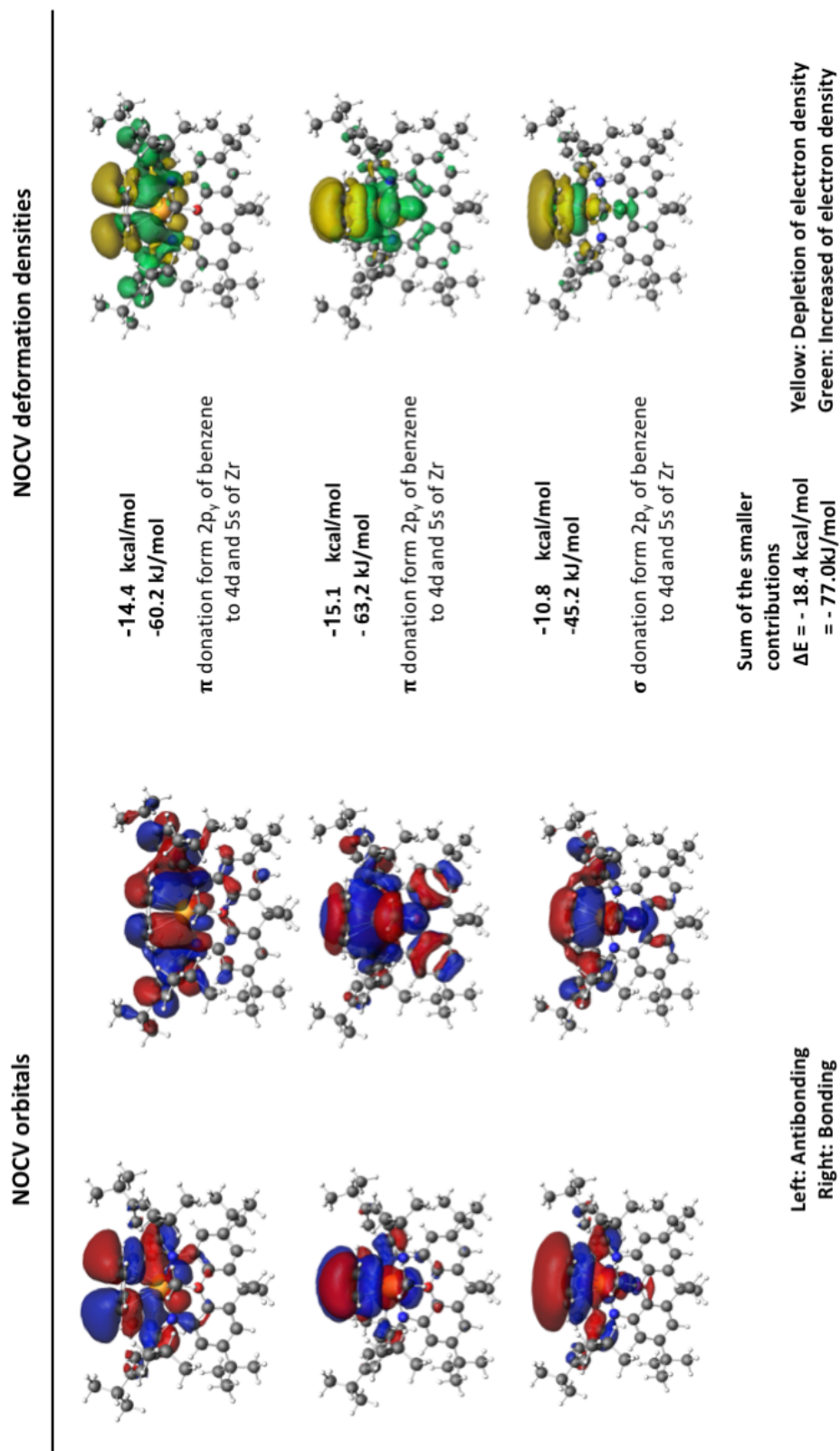
FIGURE 3.21: On the left hand side: the NOCV Orbitals (with isosurfaces set to 0.01) and on the right hand side ETS-NOCV deformation density contributions, Increased (green) and decreased (yellow) electron density is presented relative to that in the isolated fragments (isosurfaces are set to 0.0001) for the molecule η^6**2-Zr**.

NOCV deformation densities

NOCV orbitals

-15.0 kcal/mol
-62.8kJ/mol

σ donation form 2p of ethylene
to 4d and 5s of Zr

-3.0 kcal/mol
- 12.5 kJ/mol

π donation form 2p of C
close to Zr and 4d of Zr
to 2p of C of ethylene

Sum of the smaller
contributions
ΔE = - 5.9 kcal/mol
= - 24.7 kJ/mol

Yellow: Depletion of electron density
Green: Increased of electron density

Left: Antibonding
Right: Bonding
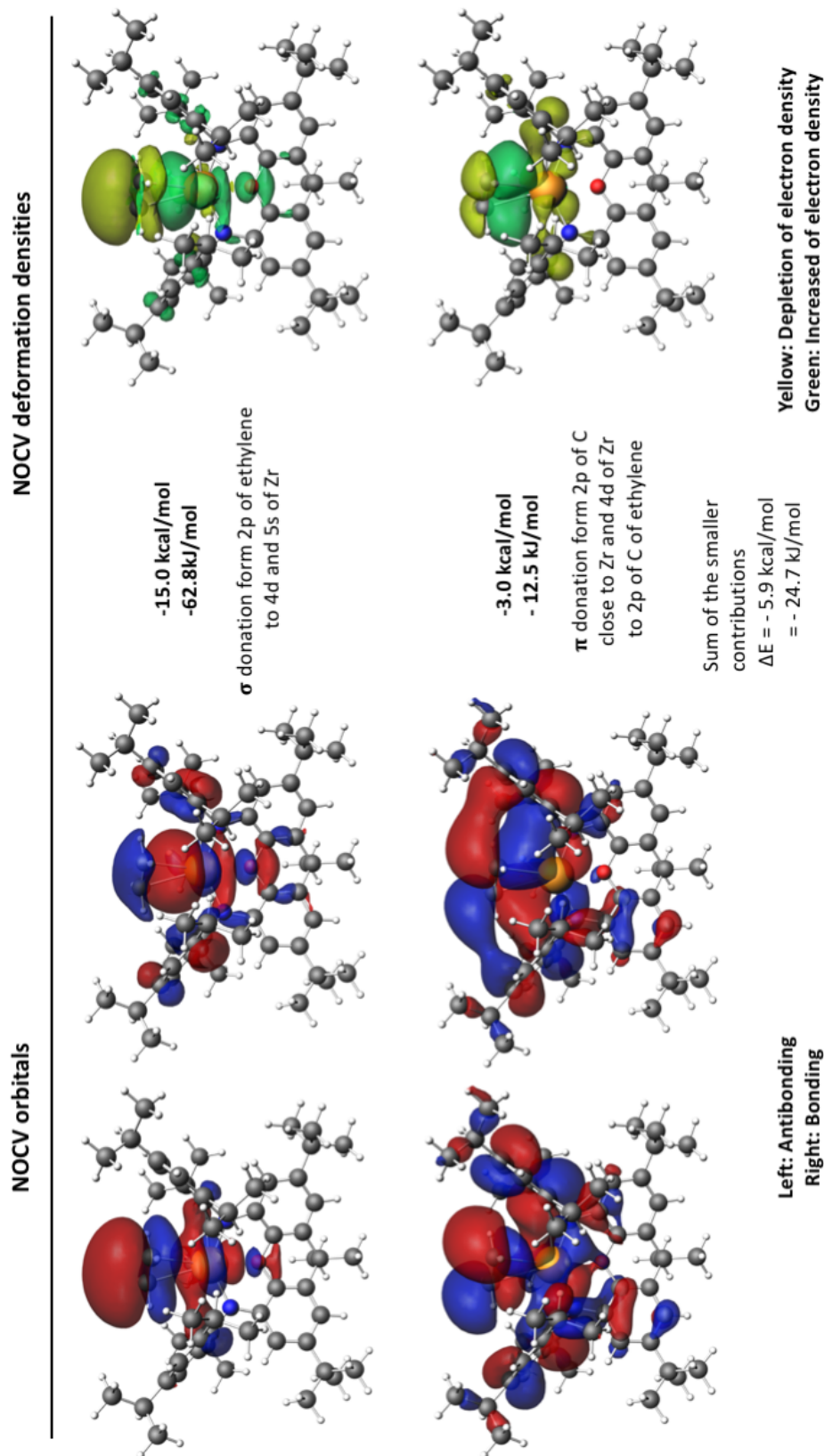
FIGURE 3.22: On the left hand side: the NOCV Orbitals (with isosurfaces set to 0.01) and on the right hand side ETS-NOCV deformation density contributions, Increased (green) and decreased (yellow) electron density is presented relative to that in the isolated fragments (isosurfaces are set to 0.0001) for the molecule η^2-**E′-Zr**.
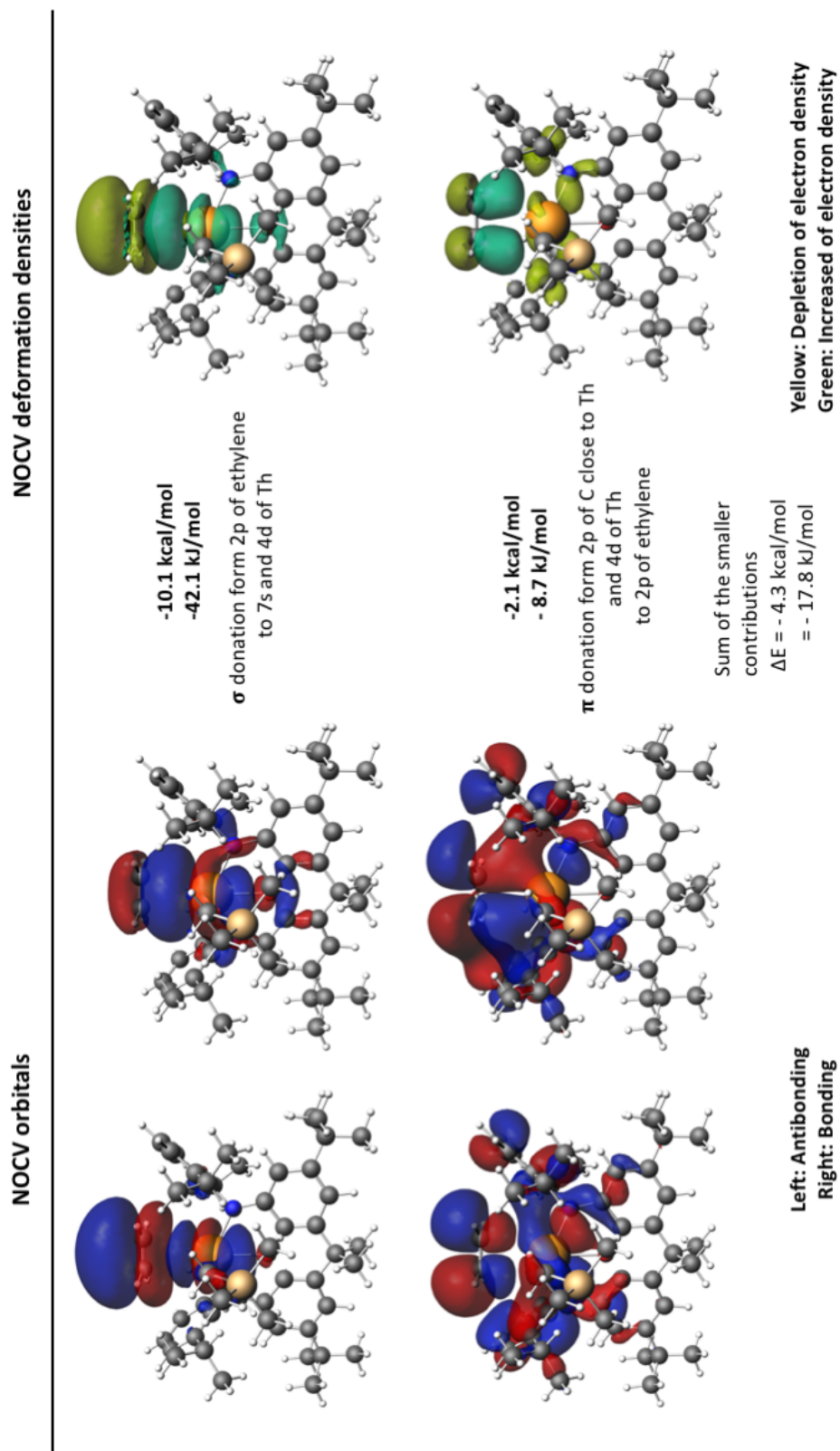
FIGURE 3.23: On the left hand side: the NOCV Orbitals (with isosurfaces set to 0.01) and on the right hand side ETS-NOCV deformation density contributions, Increased (green) and decreased (yellow) electron density is presented relative to that in the isolated fragments (isosurfaces are set to 0.0001) for the molecule η^2-**E-Th**.

Chapter 4

Thermodynamic properties and electronic structures of Plutonium Oxides

Contents

As mentioned previously a nuclear accident would release numerous compounds. To confine this compounds would first imply to know the amount of the species released. This is what the IRSN (French Institute for Radioprotection and Nuclear Safety) aims to do. They decided to focused on Plutonium and its oxide because of its toxicity and volatility mentioned in the Introduction. In order to make a good prediction, the enthalpies of formation, the heat capacity and the entropy of each molecule involved must be known with the highest possible accuracy. In this Chapter, the enthalpies of formation of PuO_2, PuO_3 and $PuO_2(OH)_2$ will be discussed. Before a discussion of the computational protocol used and of the results obtained for these species, the existing experimental and theoretical results are reviewed below.

4.1   Review of available data for Plutonium Oxides

4.1.1   Experimental data

From a number of experimental investigations on PuO_2 [138–144], the most rescent which adresses the determination of $\Delta_f H^\ominus$ is that of Gotcu-Freis *et al.* [138]. They carried out the measurements of the vapour pressure with a Knudsen cell coupled with a quadrupole mass spectrometer. This apparatus is designed for the study of radioactive materials at high temperature and built in a glove box shielded by 5 cm thick lead bricks. This simple description of the experimental setup is enough to emphasize the difficulty of manipulating plutonium. Gotcu-Freis *et al.* extracted the values $\Delta_f H^\ominus$ = -(428.7 ± 7.0) kJ.mol^{-1} and $\Delta_f H^\ominus$ = -(440± 7.0) kJ.mol^{-1}, using the 2nd and 3rd law of thermodynamics, respectively. Previously the values reported in the thermodynamic databases were slightly higher $\Delta_f H^\ominus$ = -(412 ± 20.0) kJ.mol^{-1} [139] and $\Delta_f H^\ominus$ = -(410± 20.0) kJ.mol^{-1} [140]. Konings in his 2014's review [141] selected $\Delta_f H^\ominus$ = -(428.7 ± 20.0) kJ.mol^{-1} as the preferred value.

Unfortunately, the thermodynamic properties of PuO_3 and $PuO_2(OH)_2$ are not as much documented (see Table 4.1). The first molecule was observed in a small amount by Ronchi *et al.* [145] after sublimation of free surfaces of PuO_2 in presence of oxygen but no thermodynamic data was reported. Krikorian *et al.* [146] favoured the transpiration method starting from a PuO_2 solid sample and flows of O_2 or H_2O to generate PuO_3 and $PuO_2(OH)_2$ molecules respectively. They reported the values of standard enthalpy of formation of -(562.8 ± 5.0) kJ.mol^{-1} for PuO_3 and -(1 018.2 ± 3.3) kJ.mol^{-1} for $PuO_2(OH)_2$. This study is the unique source of experimental data

for $PuO_2(OH)_2$. Konings *et al.* [141] reported the value of $\Delta_f H^\ominus$ = -(567.6 $\pm$ 15.0) kJ.mol^{-1} for PuO_3. One can note that the measurement of $\Delta_f H^\ominus$ is never direct as they are derives from measured reaction quantities (such as the partial vapour pression) for a given chemical reaction. Thus the validity of the results on $PuO_2(OH)_2$ and PuO_3 needs to be confirmed.

Accounting for the fact that the manipulation plutonium is neither easy or safe, a reasonable alternative is to determine the enthalpies of formation with accurate relativistic correlated quantum chemical methods.

However, simulations of such systems remain challenging and to prove the capabilities of *ab initio* methods one has to answer to the following questions:

- Is it possible to reproduce the $\Delta_f H^\ominus$ value for PuO_2 ?

- Can we confirm the values of $\Delta_f H^\ominus$ for PuO_3 and $PuO_2(OH)_2$?

4.1.2 Computational protocol for prediction of thermochemistry data

On the quantum chemical side, these molecules have been studied from a structural point of view but, predictions of enthalpies of formation are lacking, justifying our study.

Since our goal is to calculate the enthalpies of formation $\Delta_f H^\ominus$ of different species, we need to define the target quantities. The enthalpy H is defined as:

$$H = U + pV \tag{4.1}$$

U being the internal energy of the system, p its pressure and V its volume. The enthalpy of formation of a molecule is then the change in enthalpy to form one mole of the molecule. Hess law states that the enthalpy of a given reaction is the sum of standard enthalpies of formation of products minus the sum of the reactants.

$$\Delta_r H^\ominus = \sum_i \nu_i \Delta_f H^\ominus \tag{4.2}$$

with ν_i the stoechiometric number.

In practice $\Delta_r H^\ominus$ is calculated as:

$$\Delta_r H^\ominus = \sum_i (E_i + ZPE_i + H_{corr,i}) \tag{4.3}$$

summing up the electronic energy E_i, the Zero Point Energy (ZPE) and the thermal correction to enthalpy $H_{corr,i}$.

The enthalpy of formation of the molecule of interest can thus be extracted by the computation of the $\Delta_r H^{\ominus}$ for a chosen reaction as in the equation 4.4 and the subtraction of the known $\Delta_f H^{\ominus}$ of the other reactants and products (see Table 4.2). For example for the reaction : A + Pu $\rightarrow$ PuX + C we can obtain $\Delta_f H^{\ominus}$ as:

$$\Delta_f H^{\ominus}(PuX) = \Delta_r H^{\ominus} - \Delta_f H^{\ominus}(A) - \Delta_f H^{\ominus}(Pu) + \Delta_f H^{\ominus}(C) \qquad (4.4)$$

where $\Delta_f H^{\ominus}$(Pu), $\Delta_f H^{\ominus}$(A) and $\Delta_f H^{\ominus}$(C) are tabulated. Sing the enthalpy of formation is path independent, the results from the reactions R_1 to R_5 should be close to each other. The average of the results will be our final $\Delta_f H^{\ominus}$ and the mean deviation the reported error.

Since it is established that DFT is able, even for open-shell systems, to yield good geometries and vibrational frequencies that contribute to the Zero Point Energy (ZPE) and the thermal correction to the enthalpy (H_{corr}), this will be the method of choice to estimate these thermodynamic contributions. However, the accurate estimation of the electronic energy of each molecules remains the most sensitive part, in particular for Pu and its derivatives since one can expect large contributions of the electron correlation as well as the relativistic effects. This will thus concentrate most of our attention in the following paragraphs.

Among the prior theoretical investigations on Pu oxides [147–152], the only one that focussed on the trioxide and oxyhydroxide molecules is that of Boguslawski *et al.* [147] employing the spin-free DMRG method which underlines the complexity of the electronic structure of $PuO_2(OH)_2$, PuO_2 and PuO_3. This method, allowing to include all the valence orbitals in the active space for the DMRG wave-function, can indicate which orbitals are important for the description of the correlation *via* an entanglement figure (see section 4.2.3). The entanglement diagrams show that the 5f-orbitals plutonium orbitals and the p-orbitals of bonded oxygens are important for the description of the non-dynamical correlation and that the wave-function has a strong multi-reference character.

This study, however, only provides a partial picture of the problem as it lacks the treatment of SOC in order to establish the true nature of the ground state.

While there are no subsequent theoretical investigations for $PuO_2(OH)_2$ reported in the literature, for PuO_3, a study, based on CASSCF/CASPT2 + RASSI simulations by Kovacs *et al.* [148] represents a priori a good starting point for a deeper understanding of its electronic structure. Despite a different active space from what

Boguslawski *et al.* predicted, they reached an agreement on the nature ground state (spin-free $^3B_2$ in the symmetry C_{2v}).

Concerning PuO_2, its electronic structure was studied by Liao *et al.* [149], Moskaleva *et al.* [152] and Archibong *et al.* [150] using single reference approaches, U-DFT for the two first and U-CCSD(T) for the last one, and only including the scalar relativistic effects. The only theoretical study of PuO_2 including the SOC was carried out by La Macchia *et al.* [151]. While all spin-free studies (i.e all aforementioned papers including the one using DMRG) proposed that the lowest $^5\Sigma_g$ state as the molecule's ground state, La Macchia *et al.* found that the SOC effect is so important that the ground state is no longer mainly composed of the $^5\Sigma_g$, as there is a strong contribution of the $^5\Phi_u$, and that the geometry of the molecule is strongly modified compared to the spin-free on, with SOC being responsible for a decrease of the Pu-O bond length of 0.048 Å.

TABLE 4.1: $\Delta_f H^\ominus$ (kJ/mol) of the different compounds given in the literature.

Molecule	References	$\Delta_f H^\ominus$
PuO_2	Gotcu-Freis *et al.* [138]	-(428.7 ± 7)
	Gotcu-Freis *et al.* [138]	-(440 ± 7)
	Glushko *et al.* [139]	-(412 ± 20)
	Cordfunke *et al.* [140]	-(4120 ± 20)
	Konings *et al.* [141]	-(428.7 ± 20)
PuO_3	Krikorian *et al.* [146]	-(562.8 ± 5)
	Konings *et al.* [141]	-(567.6 ± 15)
$PuO_2(OH)_2$	Krikorian *et al.* [146]	-(1 018.2 ± 3.3)

The results discussed above raise a few questions that will condition our capability of computing the desired thermodynamics:

- What is the geometry and nature of ground state of PuO_2 ?

- What is the ground state electronic structure of PuO_3 and $PuO_2(OH)_2$?

- Have static and dynamical correlation effects been treated properly before?

An appealing choice would be to use four-component-based multireference methods, such as 4c-FSCC [153–155] or EOM-CC [156] to answer these questions. Unfortunately, the relativistic FSCC implementation at our disposal at this time, cannot be used to investigate PuO_3 and $PuO_2(OH)_2$; it requires that the reference wave function to be a single determinant. For these systems, such a reference is a very poor choice. For PuO_2, on the other hand, once SOC is included self-consistently in the calculation as it is done in four-component approach, the ground state can be represented by a single determinant and the CCSD(T) method (and EOM-CC) applied.

Another option would be to extend the work of Boguslawski *et al.* and include a better description of the electronic correlation, in particular the dynamic contribution, and also include the effect of the spin-orbit coupling. Recent developments make it now possible to use DMRG-SCF and DMRG-NEVPT2 to include, respectively static and dynamic correlation, with an active space up to 50 electrons in 50 orbitals. Though, SOC is still only included via State Interaction (see Section 4.2.2). Preliminary calculations, however, were not successful and require further investigation that will pursued beyond this thesis.

For these reasons, the only generally applicable method to treat such highly correlated systems in a relativistic framework is the CASPT2 method, combined with a posteriori treatment of SOC.

In this chapter, we provide a detailed description of the CASSCF approach that relies on the selection of important orbitals (active space) for the treatment of the static correlation. The choice of the active space is at the heart of this work and will be discussed in details for the three molecules.

4.2 Multireference Approaches

All the quantum chemical methods listed so far in Chapter 2 refer to single determinant wave function, thus not applicable for the foreseen multi-reference gas-phase plutonium molecules. Indeed, partial population of the valence 7s, 5f and 6d orbitals can induce significant multi-reference contributions to the wave functions and connected to the presence of quasi-degenerated electronic states, reflected by strong static correlation. We will now describe the various multi-reference methods that can account for static and dynamical correlation.

4.2.1 The ideal multi reference method: Full Configuration Interaction

The most complete way to capture electronic correlation, for the ground state or excited states, is to use the Full Configuration Interaction (FCI) method, for which the wave function is written as a linear combination of all the possible determinants created by single up to N-excitations from the HF determinant, N being the number of electrons:

$$|\psi_{FCI}\rangle = c_0 \, |\Phi_{HF}\rangle + \sum_{a,r} c_a^r \, |\Phi_a^r\rangle + \sum_{\substack{a<b \\ r<s}} c_{ab}^{rs} \, |\Phi_{ab}^{rs}\rangle + \sum_{\substack{a<b<c \\ r<s<t}} c_{abc}^{rst} \, |\Phi_{abc}^{rst}\rangle + ... \qquad (4.5)$$

One recognises Φ_{HF} the HF solution the excited determinants from the HF one. Φ_a^r is a singly excited (S-type) determinant generated by the promotion of one electron from the spin orbital a to the spin orbital r; the ψ_{ab}^{rs} is a doubly excited (D-type) determinant created by the promotion of two electrons from the spin orbitals a and b to the spin orbitals r and s etc...
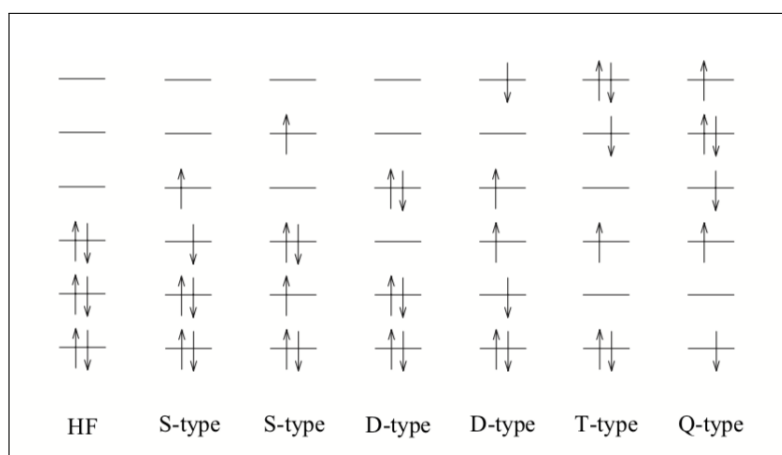
FIGURE 4.1: Various Excited Slater determinants generated from a HF reference [10]

The expansion coefficients are determined from a variational procedure in order to minimise the energy. In order to find the expansion coefficients all the possible excited determinants must be generated but also all the combinaisons of them : the Configurational State Functions (CSFs). It is the number of CSFs that will limit the use of this method. Indeed it was shown [10] that just for singlet the number of generated CSFs is:

$$\frac{M!(M+1)!}{\left(\frac{N}{2}\right)!\left(\frac{N}{2}+1\right)!\left(M-\frac{N}{2}\right)!\left(M-\frac{N}{2}+1\right)!} \tag{4.6}$$

M being the number of basis functions and N the number of electrons. If one takes the plutonium atom as example, the number of electron is 94 and the chosen basis set is the contracted ANO-RCC-TZP corresponding to 87 basis functions, the number of CSFs is 4.4614245×10^{48} only for singlet configurations (!!). For this reason, one is forced to cut the number of excitations to obtain a *truncated*-CI expansion or reduce the number of determinants by selecting the orbitals that can participate into the excited determinants.

4.2.2   Multiple-steps correlated methods

Inclusion of static correlation: Complete Active Space Self Consistent Field

The main idea of the Complete Active Space Self Consistent Field (CASSCF) method is to proceed to a FCI calculation but only with a set of selected orbitals forming the so-called active space. The molecular orbitals are thus divided in three groups: the inactive orbitals, lowest in energy and doubly occupied, the active space containing at most 18 electrons in 18 active orbitals. The occupations of the active orbitals can vary between zero and two electrons. The third and last type of orbitals are the unoccupied orbitals also called virtual orbitals (see Figure 4.2) which will remain unoccupied.

CASSCF is far from "black box" being a method since the selection of the active space is in general not trivial especially due to the constraint of the number of electrons and the active obitals. The choice of active space, and making sure it accurately represents the physics of the system, represent the main challenges if this type of calculation. That said, one can follow the rules proposed by Roos *et al.* [157] to built an active space suitable for the ground state or excited states of a given system:

- the orbitals participating to the target state.

- the valence orbitals (*i.e.* first row for light atoms; 7s, 5f and 6d for an actinide atom).

- orbitals with an occupation between 0.05 and 1.95 electron from the MP2 first-order density matrix.

- if bonding orbitals are taken, the corresponding anti-bonding should be included as well.

Certainly, the number of electrons and orbitals corresponding to the point above can quickly be greater than 18. So, the choice of the orbitals to exclude is left to the appreciation of the user, nonetheless, this choice must be argued.

One solution to extend the size of the active space is to use the Restricted Active Space Self Consistent Field (RASSCF) method, Figure 4.2. The RAS1 is composed of doubly occupied orbitals, the RAS2 is the full CI active space and RAS3 includes unoccupied orbitals. A FCI will be done in the RAS2 space and excitations from RAS1 orbitals to RAS3 ones are added with a user-defined constrain on the maximum numbers of holes and particles in RAS1 and RAS3, respectively.

In order to compute the Spin-Orbit Coupling (SOC) in the system not only the ground state is needed but also some of the excited states (this need will be explain in the
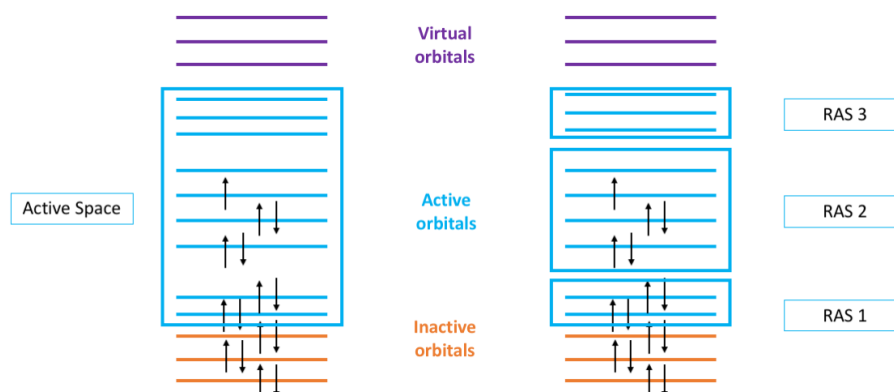
FIGURE 4.2: Representation of the CASSCF and RASSCF approaches. On the left hand side, the CASSCF method within the active space (9;9) on the right hand side, the RASSCF method with the active spaces: RAS1(4;2), RAS2(5;4);, RAS3(0,3).

section 4.2.2) that can be coupled by the SO operator. If only one state is computed at a time, we refer to a State Specific (SS) calculation, for a ground or excited state. The SS approach has the main disadvantages to be computationally expensive since a specific set of orbitals is optimised for each state. Instead, it is faster to use the SA procedure for which a set of common orbitals to several state sharing the same multiplicity and symmetry is optimised.

Note that SA-CASSCF energies will be higher than the SS ones but as we often only consider energy differences, the errors on the individual energies will compensate.

This multi-reference method CASSCF or RASSCF thoroughly includes the static electronic correlation but only a limited part of the dynamical correlation, since only double excitations are included within the active space. A rather economical way of including dynamical correlation, due to the excitations from active space to the virtual orbitals, is to use second-order perturbation theory.

Multi-Reference Perturbation Theory at the 2nd order

The Complete Active Space Perturbation Theory at the 2nd order or CASPT2 is, as indicated by his name a perturbative method. It allows to account for the dynamical correlation to the wave function, starting from a CASSCF calculation by adapting the MP2 approach introduced in Section 2.2.2. The contributing single and double excitations are represented in Figure 4.3. They are classified according to the number of holes and particles. It is useful to by-pass the diagonalisation problem of the

operator $\hat{H}'$. Instead of the diagonalisation of the full $\hat{H}'$ will be done by block *i.e.* for each excitation type at a time.
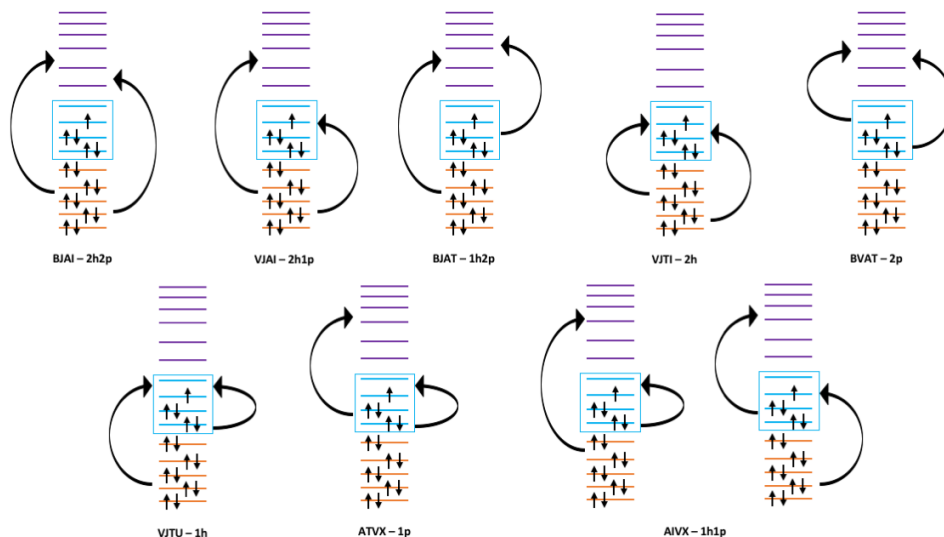
FIGURE 4.3: Representation of the possible di-excitation in CASPT2 method. NAME of the excitation in CASPT2 method - number of *h*oles (electron(s) outside the active space promoted to the active or virtual orbitals) number of *p*articule (electron occupying a virtual orbital - outside the active space - after the perturbation).

Originally, the Hamiltonian used was the Zeroth-Order Hamiltonian with the standard Fock matrix formulation [158]:

$$\hat{H}_0 = \hat{P}_0 \hat{F} \hat{P}_0 + \hat{P}_k \hat{F} \hat{P}_k + \hat{P}_{SD} \hat{F} \hat{P}_{SD} + \hat{P}_{TQ...} \hat{F} \hat{P}_{TQ...} \qquad (4.7)$$

where $\hat{P}_0$ in the projector on the one-dimensional space V_0, spanned by the CAS reference wave function ϕ_0 under consideration, $\hat{P}_k$ is the projector on the space V_k, spanned by the orthogonal complement to ϕ_0 in the restricted FCI subspace used to generate the CAS wave function. $\hat{P}_{SD}$ is the projector on the space V_{SD}, spanned by all the single and double replacement states generated from V_0, finally $\hat{P}_{TQ...}$ in the projector on the space V_{TQ}, spanned by all higher excitation not included in V_k and V_{SD}.

This formulation raises the intruder state problem [159]. When excited determinants are close in energy to the reference ones, their contribution will diverge due to a denominator approaching zero. Those intruder states can be spotted by a low (< 0.60)

value of the weight of the CAS/RAS wave function in the final wave function. To eliminate this problem a level shift of the active orbitals was introduced. Based on the Ionisation Potential (IP) and Electronic affinity (EA) [160], the IPEA shift was determined thanks to a benchmark on atomic data. During our study IPEA value was kept at its default value: 0.25 a.u.. Since it is known that the higher states are much more sensitive to the value of the level shift [159] it was decided to use the available "imaginary shift". It actually uses real quantities to treat the potential energy function differently from the IPEA level shift in order to reduce the sensitivity of the energies to the size of the imaginary shift. It was fixed at 0.05 a.u., the smallest value reported by Forsberg *et al.* [159] to reach accurate results.

Finally, another possibility to fix the problem of intruder states is to use the Hamiltonian by Angeli *et al.* [161] which is based on the generalised zeroth order Hamiltonian by Dyall [162]. It behaves as a true many-body Hamiltonian inside the CAS subspace, including all two-electrons interactions, while the CASPT2 method uses the monoelectronic Fock Hamiltonian. N-Electron Valence state Perturbation Theory at the 2nd order (NEVPT2) method is intrinsically intruder state free; however, current implementations limit its use to active spaces of 14 electrons in 14 orbitals, thus inapplicable to our systems.

A *posteriori* treatment of spin orbit coupling : the RASSI method

The Restricted Active Space State Interaction (RASSI) methods is able to compute the coupling elements for any one-electron operator between CASSCF/RASSCF wavefunction that can be non-orthogonal. In our case, the one-electron operator is SOC, computed with the atomic mean field spin-orbit operator described by equation 2.106 in Section 2.4.3, that couples states of different spins and spatial symmetries. In order to also include the dynamical correlation, the method was adapted by Malmqvist *et al.* [163] to use the CASPT2 wave-functions as basis. So the diagonal RASSI matrix [65] is dressed with the CASPT2 energies while the spin orbit matrix elements (V_{SO}) appear as off-diagonal elements. The so-constructed matrix is diagonalised to obtain the SO-eigenstates.

The lowest eigenvalue is the energy of ground state at spin-orbit CASPT2 (SO-CASPT2) level. Every SO-state is expressed as a linear combinaison of the Spin-Free (SF) states that constituted the basis. The SOC contribution to the molecule total energy is thus energy difference between the lowest SO state and the lowest SF state.
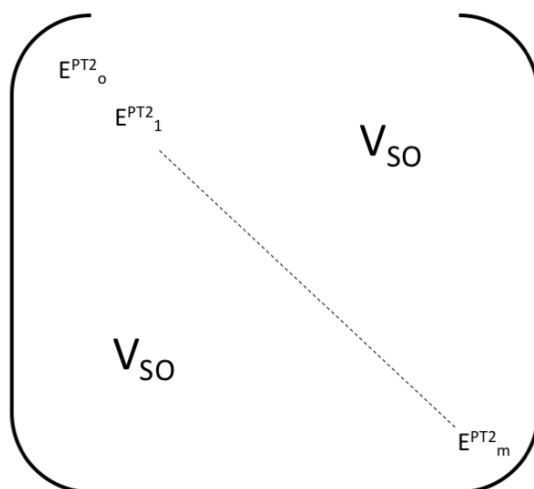
FIGURE 4.4: Matrix representation with, in diagonal, the CASPT2 energies and outside the diagonal, the spin orbit element.

4.2.3 Opening the active spaces to include electronic correlation: the Density Matrix Renormalisation Group

TABLE 4.2: $\Delta_f H^\ominus$ of the different compounds given in kJ/mol

Species	$\Delta_f H^\ominus$	$\Delta\Delta_f H^\ominus$
O (^{3}P)	249.23 [164]	0.00
H (^{1}S)	218.00 [165]	0.01
Pu (^{5}F)	349.00 [166]	3.0
H_2 (1S)	0.00 [165]	0
H_2O	-241.81 [164]	0.03
H_2O_2	-135.88 [167]	
O_2	0.00 [165]	0.00
OH	37.36 [164]	0.13

4.3 Technical Considerations and Computational details

4.3.1 Geometries, enthalpic corrections and basis sets

The first information a computational chemist needs is the geometry of the system under study. In our case, all the geometries (except PuO_2 see section 4.3.1) were optimised with DFT (see section 2.3) and the B3LYP functional [168, 169] using the GAUSSIAN09 [170] package. The plutonium atom was described by a relativistic effective core potential (RECP) ECP60MWB [171] with the corresponding basis set of

TABLE 4.3: Reactions used to calculate $\Delta_r H^\ominus$

	PuO_2	PuO_3	$PuO_2(OH)_2$
R_1	$Pu + O_2 \longrightarrow PuO_2$	$Pu + \frac{3}{2} O_2 \longrightarrow PuO_3$	$Pu + O_2 + 2 H_2 \longrightarrow PuO_2(OH)_2$
R_2	$Pu + 2 O \longrightarrow PuO_2$	$Pu + 3 O \longrightarrow PuO_3$	$Pu + 4 O + 2 H \longrightarrow PuO_2(OH)_2$
R_3	$Pu + H_2O_2 \longrightarrow PuO_2 + H_2$	$Pu + \frac{3}{2} H_2O_2 \longrightarrow PuO_3 + \frac{3}{2} H_2O$	$Pu + 3 H_2O_2 \longrightarrow PuO_2(OH)_2 + 2 H_2O$
R_4	$Pu + OH \longrightarrow PuO_2 + 2 H$	$Pu + 3 OH \longrightarrow PuO_3 + 3 H$	$Pu + 4 OH \longrightarrow PuO_2(OH)_2 + 2 H$
R_5	$Pu + 2 H_2O \longrightarrow PuO_2 + 2 H_2$	$Pu + 3 H_2O \longrightarrow PuO_3 + 3 H_2$	$Pu + 4 H_2O \longrightarrow PuO_2(OH)_2 + 2 H_2$

quadruple ζ [71] quality, while for the lighter atoms by augmented triple ζ (aug-cc-pVTZ) basis sets were used. This basis set quality is known to reproduce properly the geometries and the enthalpic corrections. All the geometries are available in Annex A. The calculation of harmonic frequencies is necessary to compute the zero point energy (ZPE) and the thermal corrections to the enthalpy of equation 4.3 and the entropy. Anharmonic frequencies were also computed but no significant difference in the value of the entropies S were seen in comparison to the harmonic ones, thus only contributions obtained at the harmonic level were kept.

Once the geometries of the different molecules were obtained and to reach accurate electronic energies for the determination of $\Delta_f H^\ominus$, two methods were used. The first is the UCCSD(T) method which represents the gold standard for single-reference wave function. The second is the multi-reference wave-function method that involves CASSCF plus CASPT2 calculations to check whether the wave function has a multi-reference character or not. In both cases, the scalar relativistic effects are included via the DKH2 Hamiltonian and the SOC was calculating with the RASSI procedure and added to the UCCSD(T) and CASPT2 spin free energies. All atoms are described with the ANO-RCC basis sets [172, 173] with qualities sequentially increased from triple-ζ (n=3) to quadruple-ζ (n=4) to extrapolate the energies to the CBS limit with the total energy extrapolation (CBS-TE) and the extrapolation separating the uncorrelated and correlated energies (CBS-CE). The two extrapolation methods yield to small differences of a few kJ.mol^{-1} for the reaction energies.

Geometry of PuO$_2$

Because of disagreement in literature [147, 149, 152, 174] concerning the distance Pu-O and the nature of the ground state, a more accurate exploration of the potential energy surface was needed. It was first done with the State Specific-Spin-Free-CASPT2 method for the lowest quintet A$_g$ and A$_u$ states in D$_{2u}$ symmetry. Scanning distances from 1.724Å to 1.884Å in steps of 0.02 Å.

In addition to the CASPT2 calculations, Andre Gomes performed calculations based on the molecular mean-field [175] approximation to the Dirac–Coulomb (^{2}DC^M)

Hamiltonian, at MP2, CCSD and CCSD(T) [176, 177] levels of theory with the DIRAC electronic structure code [178] using $D_{\infty h}$ symmetry. The Dyall basis sets [179, 180] of triple- and quadruple-zeta qualities were employed for the plutonium atom, and Dunning's aug-cc-pVXZ (X=T, Q) sets[181] for the oxygen atoms. In all calculations, the $(SS|SS)$-type two-electron integrals were approximated by a point-charge model [182]. Electrons in molecular spinors with energies comprised between -3 and 100 au were included in the correlated treatment, which amounted to correlating 28 electrons for PuO_2.

The SCF calculations were closed-shell ones, with 52 and 58 electrons in *g* and *u* irreducible representations, respectively. The equilibrium structure and spectroscopic constants for each electronic structure method were determined via a polynomial fit of the potential energy surface constructed from single-point calculations for Pu-O internuclear distances between 1.750 Å and 1.880, in steps of 0.005. Energies and potential energy curves at the complete basis set limit were obtained with the two-point extrapolation (see equation 2.121).

4.3.2 Results of the single-reference gold standard method: UCCSD(T)

The UCCSD(T) [183] calculations were performed with the Molpro Quantum Chemistry software [156]. The frozen orbitals were the 1*s* orbital of O and 1*s* to 5*d* (included) orbitals of Pu. No core-valence correlation was considered here due to the excessive computational cost and that we expect them not to exeed few $kJ\,mol^{-1}$ for actinide molecules [184].

In order to look at the influence of the inclusion of the spin-orbit *a priori*, $^2DC^M$-CCSD(T) calculation were performed (by Andre Gomes). It could be done on Pu, PuO_2, H_2, OH, H_2O and H_2O_2 allowing us to obtain the energies for reactions R_3, R_4 and R_5 for PuO_2. The setup from the PES exploration of PuO_2 was kept (see Section 4.3.1).

In addition, thanks to the recent implementation made by Andre Gomes used recent implementation in DIRAC code [185] of variant of EOM-CCSD, we were able to compute the ionization potential for atomic Pu and PuO_2 (EOM-IP-CCSD) and the excitation energies (EOM-EE-CCSD) for PuO_2.

In the case of EOM-IP-CCSD for Pu, we requested the number of states as follows: five $\Omega = 1/2_g$, two $\Omega = 3/2_g$, one $\Omega = 5/2_g$, three $\Omega = 1/2_u$, two $\Omega = 3/2_u$ and one $\Omega = 5/2_u$, whereas for PuO_2 we requested two $\Omega = 1/2_g$, one $\Omega = 3/2_g$, three $\Omega = 1/2_u$, two $\Omega = 3/2_u$ and one $\Omega = 5/2_u$ states. In the case of EOM-EE-CCSD

we requested the number of states as follows: six $\Omega = 0_g$, four $\Omega = 1_g$, three $\Omega = 2_g$, two $\Omega = 3_g$, one $\Omega = 4_g$, one $\Omega = 5_g$, ten $\Omega = 0_u$, nine $\Omega = 1_u$, seven $\Omega = 2_u$, five $\Omega = 3_u$, three $\Omega = 4_u$, and one $\Omega = 5_u$.

4.3.3 Multi-reference calculations: Actives Spaces, Number of States and Shifts

Actives spaces

All the multi-reference wave-function calculations were performed with the MOL-CAS software [186]. As previously mentioned the choice of active space is crucial since a poor choice of active space can lead not only to poor accuracy but to false results. The easiest choice of active space is the one for the atomic plutonium. One would be tempted to wisely but simply consider the 5f-orbitals. The Paris-Sud database [167] reports the nonet ^9H, involving the 6d and 7s orbitals, as the closest in energy to the septuplet ground state. Thus the former orbitals were also included to lead to an active space of 8 electrons in 13 orbitals (8,13). First calculations yield for the appearance of a spurious orbital in the CAS, making us reconsider our previous active space. Finally, we proposed the following organisation: the 7s orbital in the RAS1 with 1 hole allowed, the 5f orbitals in the RAS2 and the 6d orbitals in the RAS3 with one particule permitted. Concerning the molecules with no plutonium atom, the active space is simply composed of the oxygen valence orbitals. For those molecules, spin-orbit coupling was not imputed as it is expected to be negligible.

Concerning the plutonium oxides and oxyhydroxides, the choice of the active space was guided by the DMRG study of Boguslawski *et al.* [147], to which our research team contributed. This study followed the rules laid out in the Section 4.2.2 to define the 'full valence" space. The analysis of the entanglement diagrams lead to the definition of "optimal active spaces" listed in Table 4.4.

TABLE 4.4: Full active space and optimal active space presented in the article of Boguslawski *et al.* [147]

Molecules	Full Valence	Optimal Active Space
PuO_2	(28,25)	(18,17)
PuO_3	(34,26)	(14,14)
$PuO_2(OH)_2$	(42,35)	(20,22)

Note that neither orbital optimisation nor SOC were included in [147]. The suggested optimal active space for $PuO_2(OH)_2$ is too large for the CASSCF method.

Instead, we restricted ourselves to a minimal active space of 2 electrons in 4 orbitals (see Figure 4.5). Concerning PuO_3 and PuO_2 attempts to use the optimal active spaces was made but turned out unsuccessful as these are suited for the ground state only but do not apply for the excited states. Thus the active spaces had to be modified.
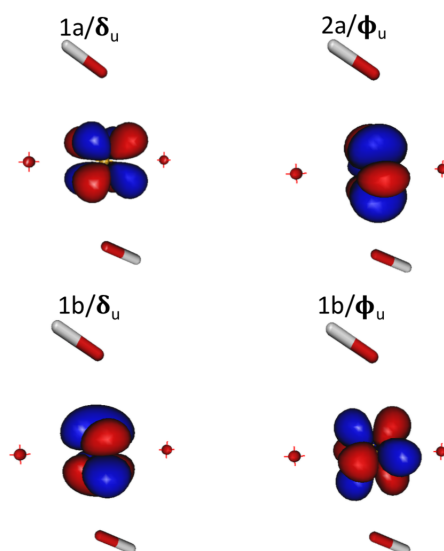
FIGURE 4.5: Molecular orbitals of $PuO_2(OH)_2$ at the CASSCF level. Isosurface = 0.05 a.u.

- **PuO_2 active space**

For PuO_2, the optimal active space matches the MO diagram of the uranyl moleculeproposed by Denning *et al.* [187]. This paper emphasised the mixing of the 5f, 6d and the 2p-orbitals of the oxygens, thus a chemically relevant model should include (14, 18) which is already approaching the limit of the CASSCF code. Moreover we would like to add the 7s orbitals that have been proven important for the description of plutonium and for PuO_2 [147], bringing the active space to 16 electrons in 19 orbitals, which is undoable.

After a close look at the DFT-B3LYP results for PuO_2, it appears that the lowest orbitals of the (16;19) active space are the degenerate π_g orbitals formed by the combination of Pu's 6d and oxygen 2p-orbitals. These orbitals did not appear as strongly entangled to the other valence orbitals in the entanglement diagram on the Figure 3 in [147] and can thus be eliminated from the active space cutting it down to a CAS(12, 17) (see Table 4.5 for details). This is slightly larger than the one used in the study of La Macchia *et al.* but the results can still be comparable.
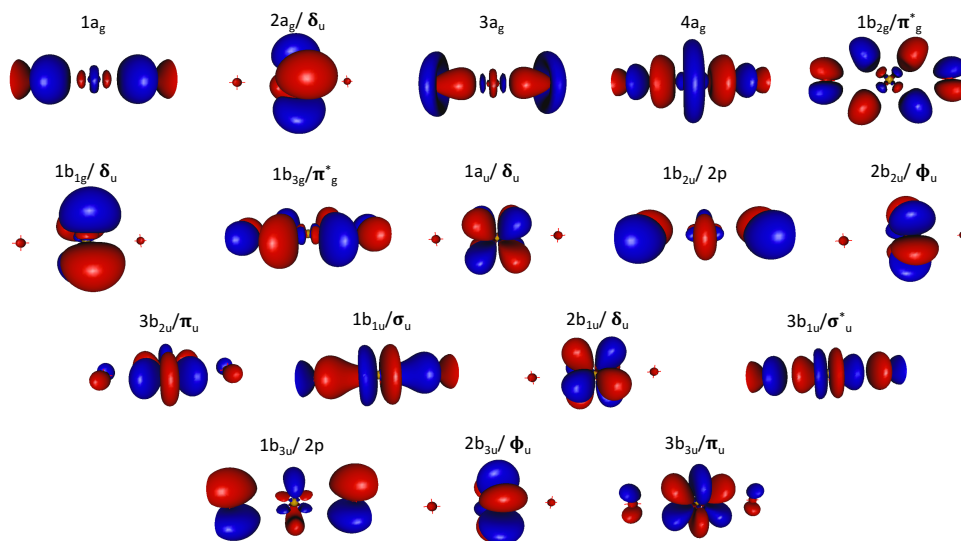
FIGURE 4.6: Molecular orbitals of PuO_2 at the CASSCF level; Isosurface = 0.05 a.u.

TABLE 4.5: Active spaces for the various plutonium oxides and oxyhydroxides.

Molecule	Active Space (electron, orbitals)	Orbitals
PuO_2	(12,17)	$\pi_u(2), \pi_g(2), \sigma_g, \sigma_u, \pi_u^*(2), \pi_g^*(2), \sigma_g^*, \sigma_u^*, f_\delta(2), f_\phi(2)$
PuO_3	(14,13)	$1a_1, 2a_1/\pi_u, 2a_1, 4a_1/p_x^o, 5a_1/\phi_u, 6a_1/\pi_u, 1b_1/\phi_u,$
		$2b_1/\pi_u, 1b_2/p_z^o, 2b_2/\sigma_u, 3b_2/\delta_u, 4b_2/\sigma_u^*, 1a_2/\delta_u$
$PuO_2(OH)_2$	(4,4)	$1a/\delta, 2a/\phi, 1b/\delta, 2b/\phi$
Pu	(8,13)	7s, 5f, 6d
O	(6,4)	$2s, 2p_x, 2p_y, 2p_z$
O_2	(12, 8)	$\sigma_{2s}, \sigma_{2s}^*, \sigma_{2p}(3), \sigma_{2p}^*(3)$
OH	(7,5)	$\sigma, \sigma_{nb}, 2p_x^O, 2p_y^O, \sigma^*,$
H_2O_2	(14, 10)	$1\,\sigma^{O-O}, 1\,\sigma^{*O-O}, \sigma^{O-H}(2), 2\,\sigma^{O-O}, \pi^{O-O}, 2p^O,$
		$1\sigma^{*O-O}, \sigma^{O-H}(2)$
H_2O	(8,6)	$2a_1, 1b_2, 3a_1, 1b_1, 4a_1, 1b_2$
H_2	(2, 2)	σ, σ^*
H	(1,1)	1s

- **PuO$_3$ active space**

Concerning PuO_3, from a chemical view point, assuming Pu to be in oxidation state (VI), we can depict it as a plutonyl PuO_2^{2+} in interaction with a O^{2-} anion. Thus from the PuO_2 active space we selected all the orbitals that could mix with the 2p-orbitals of the apical oxygen, leading to an active space of 12 electrons in 10 orbitals ($2p_x$ and $2p_z$ of the oxygen plus the $2b_{2u}/\phi_u$, $2b_{3u}/\phi_u$, $1b_{1u}/\sigma_u$, $2b_{1u}/\delta_u$, $3b_{1u}/\sigma_u^*$, $1a_u/\delta_u$,

TABLE 4.6: Totale energy of the ground state of Pu, PuO_3 and $PuO_2(OH)_2$ for different value of the imaginary shift.

Molecule	0.01	0.05	0.01	No Imaginary shift
Pu	-29539.80490586	-29539.80507744	-29539.80592767	-29539.80604535
PuO_3	-29765.45793749	-29765.45814830	-29765.45837134	-29765.45737950
$PuO_2(OH)_2$	-29841.93260283	-29841.93266384	-29841.93267515	-29841.93267545

$3b_{3u}/\pi_u$ and $3b_{3u}/\pi_u$ of PuO_2). It is enough for the description of the ground state but not for the excited states. Thus, 2 electrons and 3 orbitals (corresponding to the $1a_g$, $1b_{2u}/2p$ and the visible of Figure 4.6 and the $1a_g$ of Figure 4.7) were added to obtain the active space mentionned in the Table 4.5 or in Figure 4.7.
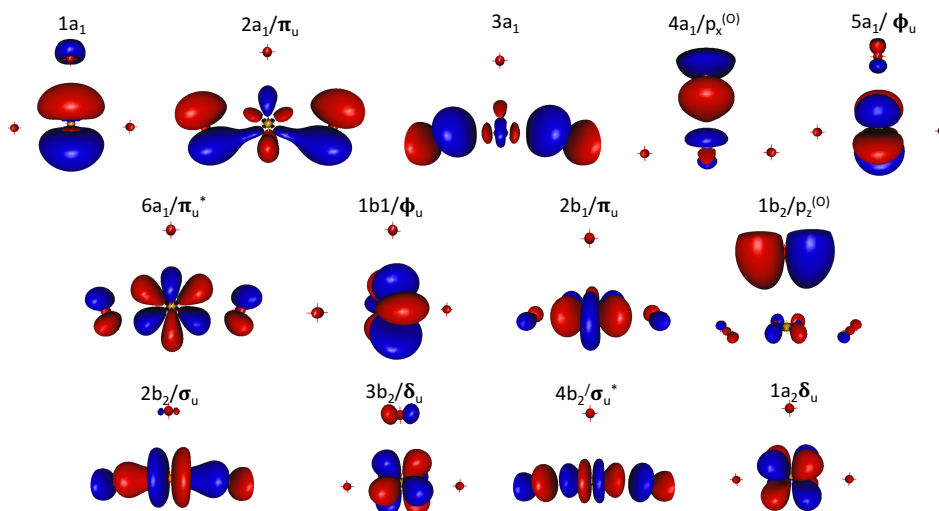
FIGURE 4.7: Active CASSCF orbitals of PuO_3 at the CASSCF level; Isosurface = 0.05 a.u.

- **CASPT2 - Numbers of state computed**

The number of states that are computed at CASSCF levels was dependent on the number of states that could be described properly (with a significant (> 0.6) reference weight) at the CASPT2 level. To keep high reference weights, beside the default IPEA value (0.25 a.u.), an imaginary shift had to be added. Indeed the Molcas manual recommends its use to improve the description of CASPT2 excited states results when transition metals or actinides are involved to avoid intruder state problems. Since the computation of PuO_2 is quite expensive, tests on the value of the imaginary shift was done on Pu, PuO_3 and $PuO_2(OH)_2$ only with smaller active spaces, (6,7), (12,10) and (2,4) for Pu, PuO_3 and $PuO_2(OH)_2$, respectively.

As shown in [159] the total energy is barely modified and the minimal value of the shift with noticeable effect on the description of the excited states is 0.05 a.u.. This

is the value kept in all the CASPT2 calculations since the 0.01 does not increase the number of states properly described and the value 0.1 impact the total energies and the excitation energies.

TABLE 4.7: Number of electronic states at CASSCF level of calculations

Multiplicity	Pu (C_i)	PuO$_2$ (D$_{2h}$)								PuO$_3$ (C$_{2v}$)				PuO$_2$(OH)$_2$ (C$_2$)	
symmetry	A$_g$	A$_g$	B$_{2g}$	B$_{1g}$	B$_{3g}$	A$_u$	B$_{2u}$	B$_{1u}$	B$_{3u}$	A$_1$	B$_1$	B$_2$	A$_2$	A	B
Singulet	0	5	5	5	5	5	5	5	5	20	20	20	20	7	4
Triplet	50	5	10	10	10	7	10	7	10	20	20	20	20	2	4
Quintuplet	120	5	5	5	5	5	5	5	5	20	20	20	20	0	0
Septuplet	110	0	0	0	0	0	0	0	0	0	0	0	0	0	0
Nonet	35	0	0	0	0	0	0	0	0	0	0	0	0	0	0

TABLE 4.8: Number of electronic states at CASPT2 level of calculations

Multiplicity	Pu (C_i)	PuO$_2$ (D$_{2h}$)								PuO$_3$ (C$_{2v}$)				PuO$_2$(OH)$_2$ (C$_2$)	
symmetry	A$_g$	A$_g$	B$_{2g}$	B$_{1g}$	B$_{3g}$	A$_u$	B$_{2u}$	B$_{1u}$	B$_{3u}$	A$_1$	B$_1$	B$_2$	A$_2$	A	B
Singulet	0	2	0	2	0	3	3	3	3	10	9	7	7	7	4
Triplet	27	2	3	3	3	6	7	6	7	16	15	13	14	2	4
Quintuplet	113	4	3	2	3	4	4	4	4	8	7	6	7	0	0
Septuplet	103	0	0	0	0	0	0	0	0	0	0	0	0	0	0
Nonet	35	0	0	0	0	0	0	0	0	0	0	0	0	0	0

Concerning the number of states included in the CASPT2, all of the 16 states were incorporated for PuO$_2$(OH)$_2$. Nonetheless, it was not possible for the atom of Pu or for the di and tri oxides (see Table 4.9). Thus we set a limit at 3 eV from the ground state for PuO$_3$ and only 2 eV for Pu and PuO$_2$. Even if these limits can seem arbitrary, they ensure a good description of all states introduced in the SO-RASSI calculations and which couple to the spin-free ground states.

TABLE 4.9: Number of states available for computation and states taken for computation for the plutonium atom and the various plutonium oxides and oxyhydroxides.

	Pu	PuO$_2$	PuO$_2$(OH)$_2$	PuO$_3$
Number of available states	20 825	136 634 576	16	2 740 106
Number of states included in RASSI	278	81	16	119

TABLE 4.10: Fine structure transition energies (cm^{-1}) of atomic Pu computed at the SO-CASPT2 with the ANO-RCC-TZVP basis set, and analysis of the various *J*-states in terms of the dominating *LS* terms.

Exp.[188–190]	This work	*J*-value	Weight of *LS* states
0	0	0	54% ^7F , 38% ^5D , 7% ^3P
2204	1806	1	64% ^7F , 32% ^5D
4300	4208	2	82% ^7F , 17% ^5D
6145	6353	3	88% ^7F , 10% ^5D
7775	8091	4	93% ^7F
9179	9552	5	90% ^7F
10 238	11 010	6	85% ^7F , 10% ^5G
9773	12 499	0	44% ^7F , 21% ^5D , 8% ^3P
13 528	13 612	1	66% ^9H , 9% ^7F , 7% ^7G

4.4 Results and Discussions

4.4.1 Electronic Structures Analysis

Atomic Pu

To compute the enthalpies of formation of the plutonium molecules, an accurate description of the plutonium atom, i.e. its electronic structure, is mandatory. Thus, in Table 4.10 (the higher excited states can be found in the Appendix B), the SO-CASPT2 calculations are reported and compared to available data from the literature [188–190]. The *ab initio* energy levels are able to accurately reproduce the experimental assignments with errors between 91 and 397 cm^{-1} for the first five excited states under 9500 cm^{-1}. Deviations between our results and the available data appear after the sixth state. The experimental assignment predicts the sixth state at 9773 cm^{-1} with a $J = 0$ while such state is found at 12 488 cm^{-1} in the current study though uncertainties remain for the attribution of this electronic state. The computed seventh state with $J = 6$ is about 800 cm^{-1} higher energy than the experimental value. Looking closely at the nature of the Pu low-lying states, one can first notice the remarkable mixing between the ^7F, ^5D and ^3P spin-orbit free states and that the contribution of the ^5D state decreases as the energy increases. Finally, the most important result is the overall good reproduction of the SO splitting of ^7F spin-free state, making us confident for the exploration of the other plutonium molecules.

PuO$_3$ and PuO$_2$(OH)$_2$

For PuO$_3$, at the spin-orbit level, we report the description of the ground state and the six lowest excited states in Table **??**, (the higher excited states can be found in the Appendix B). It is noteworthy that the 1a$_g$, 2a$_g$/δ_u and 3a$_g$ orbitals are doubly occupied in all the calculated spin-free states. The PuO$_3$ orbitals are composed of a mixture of orbitals belonging to the plutonyl subunit and the distant oxygen. Thus, for the sake of clarity, we labelled these orbitals with the labels associated to those of the PuO$_2^{2+}$ ion (with linear energy D_{2h} notations), and those of the distant oxygen atom are denoted by p$_{x,y,z}^{(O)}$. The SO ground state is composed of 47% ^{3}B$_2$, 24% ^{3}A$_2$ and 14% ^{3}B$_1$ spin-free states. The composition is similar to the one previously reported by Kovács [191] (52% ^{3}B$_2$ and 24% ^{3}A$_2$). More striking is the difference between our computed vertical excitation energies with that of Kovács's SO-CASPT2 spectrum [191]. While we predict the first excited state to be at 1235 cm^{-1}, he places it at 471 cm^{-1}. The overall determined spectrum from our calculations is much denser and lower by about 4000 cm^{-1} than his. Such discrepancy may find its origin in the description of the spin-free states. We agree with Kovács that the spin-free ground state has ^{3}B$_2$ symmetry, though with a different orbital character. Indeed, the ^{3}B$_2$ exhibits a strong multi-determinantal character with 57% corresponding to the configuration in which the 4a$_1$/p$_z^{(O)}$ and 2b$_2$/σ_u orbitals are doubly occupied (See Table **??** and Figure 4.7) and the singly occupied orbitals 5b$_1$/Φ_u, 1b$_2$/p$_z^{(O)}$, 3b$_2$/δ_u and 1a$_2$/δ_u and 22% from the electronic configuration in which of the 4a$_1$/p$_z^{(O)}$, 1b$_2$/p$_z^{(O)}$ and 2b$_2$/σ_u orbitals are doubly occupied and the 5b$_1$/Φ and 1a$_2$/δ_u singly occupied. Kovács, however, finds the ground state to be mainly composed of plutonyl orbitals (79%). Such a difference can be explained by the fact that the considered active spaces are different (a CAS(10,16) in his case and CAS(14,13) in our work). Looking closely at the entanglement diagram of PuO$_3$ derived from DMRG calculations [147] (Figure 6a, Full-Valence CAS) there is a strong correlation within the non-bonding plutonyl-like orbitals (5f$_\delta$, 5f$_\phi$) and also between the b$_2$/p$^{(O)}$ and the 5f$_{\delta_u}$ orbitals, in agreement with our analysis of the ^{3}B$_2$ ground-state wave function.

Concerning PuO$_2$(OH)$_2$, the low energy part of the vertical spectrum including SO coupling reported in the Table **??** shows two close-lying states separated by about 323 cm^{-1}, followed by a state at 2222 cm^{-1}. The analysis of the two lowest states shows that they correspond to a fifty-fifty combination of $^3A(1)$ and $^3B(1)$ spin-free states, with a small contribution (6% in each case) of the $^3B(2)$. The next three states also have strong SO-mixings between triplet states but also singlet excited states of $^1A(1)$ and $^1B(1)$ symmetries, placed at the spin-free level at about 5764 and 7444 cm^{-1}, respectively.

TABLE 4.11: Lowest electronic levels in cm^{-1} of PuO$_3$, computed at the SF-CASPT2 and SO-CASPT2 levels with the ANO-RCC-TZVP basis set, and analysis of the various states.

	No.	Term Symbol	ΔE	Character : % [orbital(number of electron)]
SF	1	$^3B_2(1)$	0	36% [4a$_1$/p$^{(O)}$(2), 1b$_1$/Φ_u(1), 1b$_2$/p$^{(O)}$($\bar{1}$), 2b$_2$/σ_u(2), 3b$_2$/δ_u(1), 1a$_2$/δ_u(1)]
				21% [4a$_1$/p$^{(O)}$(2), 1b$_1$/Φ_u(1), 1b$_2$/p$^{(O)}$(1), 2b$_2$/σ_u(2), 3b$_2$/δ_u($\bar{1}$), 1a$_2$/δ_u(1)]
				22% [4a$_1$/p$^{(O)}$(2),1b$_1$/Φ_u(1),1b$_2$/p$^{(O)}$(2),2b$_2$/σ_u(2),1a$_2$/δ_u(1)]
	2	$^3A_2(1)$	3161	43% [4a$_1$/p$^{(O)}$(2), 5a$_1$/Φ_u(1),1b$_2$/p$^{(O)}$($\bar{1}$),2b$_2$/σ_u(2),3b$_2$/δ_u(1),1a$_2$/δ_u(1)]
				23% [4a$_1$/p$^{(O)}$(2), 5a$_1$/Φ_u(1),1b$_2$/p$^{(O)}$(1),2b$_2$/σ_u(2),3b$_2$/δ_u($\bar{1}$),1a$_2$/δ_u(1)]
				17% [4a$_1$/p$^{(O)}$(2), 5a$_1$/Φ_u(1),1b$_2$/p$^{(O)}$(2),2b$_2$/σ_u(2),1a$_2$/δ_u(1)]
	3	$^3B_1(1)$	4663	38% [4a$_1$/p$^{(O)}$(2),5a$_1$/Φ_u(1),1b$_1$/Φ_u(1),1b$_2$/p$^{(O)}$($\bar{1}$),2b$_2$/σ_u(2),3b$_2$/δ_u(1)]
				12% [4a$_1$/p$^{(O)}$(2),5a$_1$/Φ_u(1),2b$_1$/π_u(1),1b$_2$/p$^{(O)}$($\bar{1}$),2b$_2$/σ_u(2),3b$_2$/δ_u(1)]
				12% [4a$_1$/p$^{(O)}$(2), 5a$_1$/Φ_u(1),1b$_1$/Φ_u(1),2b$_1$/π_u(2),1b$_2$/p$^{(O)}$(2)]
	4	$^1A_1(1)$	7239	32% [4a$_1$/p$^{(O)}$(2),1b$_2$/p$^{(O)}$(1),2b$_2$/σ_u(2),3b$_2$/δ_u(1),1a$_2$/δ_u(2)]
				28% [4a$_1$/p$^{(O)}$(2),1b$_2$/p$^{(O)}$(2),2b$_2$/σ_u(2),1a$_2$/δ_u(2)]
				11% [4a$_1$/p$^{(O)}$(1), 5a$_1$/Φ_u($\bar{1}$),1b$_2$/p$^{(O)}$(1),2b$_2$/σ_u(2),1a$_2$/δ_u(2)]
	5	$^3A_2(2)$	7287	20% [4a$_1$/p$^{(O)}$(2),1b$_1$/Φ_u(1),1b$_2$/p$^{(O)}$(1),2b$_2$/σ_u(2),3b$_2$/δ_u(2)]
				18% [4a$_1$/p$^{(O)}$(1),5a$_1$/Φ_u($\bar{1}$),1b$_1$/Φ_u(1),1b$_2$/p$^{(O)}$(2),2b$_2$/σ_u(2),3b$_2$/δ_u(1)]
				17% [4a$_1$/p$^{(O)}$(2),1b$_1$/Φ_u(1),1b$_2$/p$^{(O)}$(2),2b$_2$/σ_u(2),3b$_2$/δ_u(1)]
	6	$^3B_1(2)$	8038	31% [4a$_1$/p$^{(O)}$(1),5a$_1$/Φ_u($\bar{1}$),1b$_2$/p$^{(O)}$(2),2b$_2$/σ_u(2),3b$_2$/δ_u(1),1a$_2$/δ_u(1)]
				11% [4a$_1$/p$^{(O)}$(2),5a$_1$/Φ_u(1),2b$_1$/π_u(1),1b$_2$/p$^{(O)}$($\bar{1}$),2b$_2$/σ_u(2),3b$_2$/δ_u(1)]
				10% [4a$_1$/p$^{(O)}$(2),1b$_2$/p$^{(O)}$(2),2b$_2$/σ_u(2),3b$_2$/δ_u(1),1a$_2$/δ_u(1)]
				10% [4a$_1$/p$^{(O)}$(2),1b$_1$/Φ_u(1),1b$_2$/p$^{(O)}$($\bar{1}$),2b$_2$/σ_u(2),1a$_2$/δ_u(1)]
SO	X		0	47% $^3B_2(1)$ + 24% $^3A_2(1)$ + 14% $^3B_1(1)$
	a		1235	59% $^3B_2(1)$ + 25% $^3A_2(1)$
	b		1783	73% $^3B_2(1)$
	c		3777	51% $^3A_2(1)$
	d		5660	24% $^3B_1(1)$ + 18% $^1A_1(1)$ + 17% $^3A_2(2)$ + 10% $^3B_1(2)$

TABLE 4.12: Lowest electronic levels in cm^{-1} of PuO$_2$(OH)$_2$, computed at the SF-CASPT2 and SO-CASPT2 levels with the ANO-RCC-TZVP basis set, and analysis of the various states.

	State	ΔE	Character : % [orbital(number of electron)]
SF	$^3B(1)$	0	49% [2a/Φ_u(1) ,1b/δ_u(1)]
			48% [1a/δ_u(1) , 2b/Φ_u(1)]
	$^3A(1)$	889	41% [1a/δ_u(1) , 2a/Φ_u(1)]
			59% [1b/δ_u(1), 2b/Φ_u(1)]
	$^3B(2)$	2136	75% [1a/δ_u(1) , 1b/δ_u(1)]
			20% [2a/Φ_u(1) , 2b/Φ_u(1)]
	$^3A(2)$	4698	59% [1a/δ_u(1) , 2a/Φ_u(1)]
			41% [1b/δ_u(1), 2b/Φ_u(1)]
	$^3B(3)$	5351	52% 2a/Φ_u(1), 1b/δ_u(1)
			46% [1a/δ_u(1), 2b/Φ_u(1)]
	$^1A(1)$	5764	[58% 1b/δ_u(1), 2b/Φ_u($\overline{1}$)]
			30% [1a/δ_u(1) , 2a/Φ_u($\overline{1}$)]
			5%[2a/Φ_u(2)]
	$^1B(1)$	7444	50% [1a/δ_u(1), 1b/δ_u($\overline{1}$)]
			28% [2a/Φ_u(1), 2b/Φ_u($\overline{1}$)]
			16%[1a/δ_u(1), 2b/Φ_u($\overline{1}$)]
	$^1A(2)$	9626	39% [1a/δ_u(1), 2a/Φ_u($\overline{1}$)]
			29 % [2a/Φ_u(2)]
			13% [1b/δ_u(1), 2b/Φ_u(2)]
			10% [1a/δ_u(2)]
			7 %[2a/Φ_u(2)]
SO	X	0	46% $^3A(1)$, 41% $^3B(1)$, 6% $^3B(2)$
	a	323	45.% $^3B(1)$, 45% $^3A(1)$, 6% $^3B(2)$
	b	2222	35% $^3B(2)$, 25% $^3B(1)$, 14% $^1A(1)$, 13% $^3A(2)$, 10% $^3B(3)$
	c	3757	40% $^3A(2)$, 25% $^3B(2)$, 19% $^1B(1)$, 7% $^3B(1)$, 6% $^3A(1)$
	d	4158	36% $^3B(3)$, 34% $^3B(2)$, 14% $^1A(2)$, 11% $^3B(1)$,

PuO$_2$ molecule

- PuO$_2$ Geometry

As explained in the section 4.1 La Macchia *et al.* showed that the spin-orbit coupling was of great importance not only to describe the electronic structure but also the geometry of PuO$_2$. In their study, the spin-free results gave a $^5\Sigma_g^+$ as ground state with a Pu-O distance of 1.792 Å. At the spin-orbit level, the ground state was found to be a 1_u composed by 96% of the $^5\Phi_u$ with a bond length of 1.744 Å. At the latter, our SO-CASPT2 calculation predicted a 0_g ground state.

The $^5\Sigma_g^+$ is the lowest at SF level as found in La Macchia's study by the similarities stop here. The equilibrium distance is here longer with 1.804 Å(versus 1.792 Åof La Macchia *et al.*). At this distance, the energy gap to the $^5\phi_u$ state is estimated to 7992 cm^{-1}, while it was equal to 1800 cm^{-1} in La Macchia's study. In spite of this disagreement, the "reduction" of the bond distance while the spin orbit is included might be true and must be tested.

TABLE 4.13: Comparison of CBS extrapolated ^{2}DC^M-EOM-CCSD and SO-CASPT2 PuO$_2$ vertical transition energies in cm^{-1} computed at the 1.744 and 1.808 Å Pu$-$O distances.

| Ω | d(Pu-O)=1.744 Å | | | d(Pu-O)=1.808 Å | |
| | ^{2}DC^M-EOM-CCSD | SO-CASPT2 | | ^{2}DC^M-EOM-CCSD | SO-CASPT2 |
	This work	This work	Ref. [192]	This work	
0_g	0	0	1794	0	0
1_g	2435	1438	2315	2325	2462
2_g	6012	4235	4131	5378	5904
1_u	5721	1778	0	8548	5851
2_u	5926	1805	535	8782	6265
3_u	6622			9882	
4_u	12751			15471	

At the ^{2}DC^M level, the PuO$_2$ ground-state is found to be well-described a closed-shell ($\Omega = 0_g$) determinant, corresponding to occupied f$_{3/2}$ and f$_{5/2}$ spinors. This allowed us to employ accurate single-reference approaches such as CCSD(T) to determine the optimal Pu$-$O bond length, which is equals to 1.808 Å after extrapolation, with a corresponding harmonic vibrational frequency of 793 cm^{-1}. We note that the CBS-^{2}DC^M-CCSD(T) Pu$-$O bond length is longer than the one predicted by La Macchia et al. [192] at the SO-CASPT2 level.

TABLE 4.14: CBS extrapolated Ionization Potentials of PuO_2 in eV computed at the $^2DC^M$-EOM-CCSD level (d(Pu-O)= 1.808 Å) and comparison with experiments.

$^2DC^M$-EOM-CCSD		Exp			
State	IP	[[193]]	[[194]]	[[195]]	[[196]]
		9.4	10.1	7.03	6.6
$3/2_u$	7.65				
$5/2_u$	7.90				
$1/2_u$	9.81				
$3/2_u$	10.81				

Furthermore, our $^2DC^M$-EOM-EE-CCSD calculations (see Table 4.13) confirm that, at the CBS-$^2DC^M$-CCSD(T) equilibrium structure, the $\Omega = 0_g$ state is indeed the ground-state: it is sufficiently well-separated from the lowest-lying states of both g ($\Omega = 1_g$, by over 2000 wavenumbers) and u ($\Omega = 1_u$, by over 5000 wavenumbers), and considering a shorter bond length–namely 1.744 Å, as was proposed by La Macchia et al. [192] for the ground state from SO-CASPT2–does not alter this picture. Thus, our results differ qualitatively from La Macchia et al., since they suggest the PuO_2 ground-state is of $\Omega = 1_u$ symmetry, and corresponding mainly to the occupation of the two $5f_\delta$, one $5f_\phi$ and the 7s orbitals (See Figure 4.6).

From Table 4.13, we observe significant variations for the u states (of nearly 3000 wavenumbers) when the internuclear distance is varied from 1.808 Å to 1.744 Å, while the g states remain more or less at the same energies. With this, at the longer distance, the $\Omega = 2_g$ state becomes lower than the $\Omega = 1_u$ one.

- PuO_2 Electronic Structure

The SO-CASPT2 transition energies computed at the $^2DC^M$ optimal bond length are reported in Table 4.15 (the higher excited states can be found in the Appendix B). The spin-orbit 0_g ground state is composed by the spin-free ground state $^5\Sigma_g^+(1)$ up to 48% and by the $^3\Sigma_g(1)$ up to 22%, which lies 10.308 cm above it. La Macchia *et al.* also found large SO effects this with a SO-value of 8548 cm^{-1}. Note that the vertical transition energies computed at the SO-CASPT2 level are in very good agreement with the $^2DC^M$ ones for the g-states, but the u-states come out about 2300 cm^{-1} lower in energy at the SO-CASPT2 than at the $^2DC^M$-EOM-CCSD level. However, we note that the electronic state spacing within either the g or u symmetries agrees with the SO-CASPT2 calculations. This thus points out to the importance of the choice of the active space to accurately predict the relative energies of g states involving mostly non-bonding 5f Pu atomic-centered orbitals, versus the u states involving the more diffuse plutonium 7s orbital.

TABLE 4.15: Lowest electronic levels in cm^{-1} of PuO_2, computed at the SF-CASPT2 and SO-CASPT2 levels (d(Pu-O)= 1.808 Å) with the ANO-RCC-TZVP basis set, and analysis of the various states.

	State	ΔE	Character : % [orbital(number of electron)]
SF	$^5\Sigma_g^+$	0	84% $[1a_u/\delta_u(1), 2b_{2u}/\Phi_u(1), 2b_{1u}/\delta_u(1), 2b_{3u}/\Phi_u(1)]$
	$^5\Sigma_g$	4798	45% $[1a_u/\delta_u(1), 3b_{2u}/\pi_u(1), 2b_{1u}/\delta_u(1), 2b_{3u}/\Phi_u(1)]$
			45% $[1a_u/\delta_u(1), 2b_{2u}/\Phi_u(1), 2b_{1u}/\delta_u3(1), 3b_{3u}/\pi_u(1)]$
	$^5\Phi_{u(1)}$ ($^5B_{3u}(1)$)	5421	85% $[3a_g(1), 1a_u/\delta_u(1), 2b_{1u}/\delta_u(1), 2b_{3u}/\Phi_u(1)]$
	$^5\Phi_{u(2)}$ ($^5B_{2u}(1)$)	5421	85% $[3a_g(1), 1a_u/\delta_u(1), 2b_{1u}/\delta_u(1), 2b_{3u}/\Phi_u(1)]$
	$^5\Delta_{u(1)}$ ($^5A_u(1)$)	7452	79% $[3a_g(1), 2b_{2u}/\Phi_u(1), 2b_{1u}/\delta_u(1), 2b_{3u}/\Phi_u(1)]$
	$^5\Delta_{u(2)}$ ($^5B_{1u}(1)$)	7462	80% $[3a_g(1), 1a_u/\delta_u(1), 2b_{2u}/\Phi_u0(1), 2b_{3u}/\Phi_u(1)]$
	$^3\Sigma_g^-$	10308	24% $[1a_u/\delta_u(1), 2b_{2u}/\Phi_u(2), 2b_{1u}/\delta_u(1)]$
			24% $[1a_u/\delta_u(1), 2b_{1u}/\delta_u(1), 2b_{3u}/\Phi_u(2)]$
			19% $[2b_{2u}/\Phi_u(1), 2b_{1u}/\delta_u(2), 2b_{3u}/\Phi_u(1)]$
			16% $[1a_u/\delta_u(1), 2b_{2u}/\Phi_u(1), 2b_{3u}/\Phi_u(1)]$
SO	0_g^-	0	48% $^5\Sigma_g^+$, 22% $^3\Sigma_g^-$
	1_g	2462	67% $^5\Sigma_g^+$, 15% $^3\Sigma_g^-$
	1_u	5851	27% $^5\Phi_{u(1)}$, 27% 21% $^5\Phi_{u(2)}$, 13% $^5\Delta_{u(1)}$, 13% $^5\Delta_{u(2)}$
	2_g	5904	85% $^5\Sigma_g^+$
	2_u	6265	21% $^5\Phi_{u(1)}$, 21% $^5\Phi_{u(2)}$, 24% $^5\Delta_{u(1)}$
	3_u	7195	38.85% $^5\Phi_{u(1)}$, 24.97% $^5\Phi_{u(2)}$

Finally, for the computed ionization energies for PuO_2 (IPs, see Table 4.14), our calculations could be grouped into three regions with respect to their energies: one below 8 eV, one between 8 and 10 eV and the last at energies higher than 10 eV. We see that, if one considers only the lowest EOM-IP-CCSD state ($\Omega = 3/2_u$), we observe a good agreement with the results of Rauh et al. [193] (and to a lesser extent, with the results of Capone et al. [194]) but poor agreement with a second measurement of Capone et al. [196] and of Santos et al. [195]. However, if we compare the first $\Omega = 1/2_u$ state to this second measurement of Capone, and the second $\Omega = 3/2_u$ state with that of Santos et al. [195], we see an overall good agreement between the calculated and experimental values. This leads us to suggest that experiments may have measured PuO_2^+ in different electronically excited states, something that would explain the rather different experimental values.

- Spin-free calculations

Beside calculations including spin-orbit coupling, it is informative to discuss the nature of PuO_2 ground-state at the scalar relativistic level (spin free). In our study, CASPT2 and UCCSD(T) calculations give the $^5\Sigma_g$ state ($(5f_\delta)^2(5f_\phi)^2$ occupations) lower in energy than the $^5\Phi_u$ state ($(5f_\delta)^2(5f_\phi)^1(7s)^1$) by 7994 cm^{-1} at the distance Pu-O of 1.804 Å, as found in the previous studies [174, 192]. With the ANO-RCC

AVTZ basis set, the equilibrium Pu−O distance is 1.818 Å and 1.808 Å at UCCSD(T) and CASPT2 levels, respectively, distances that are close to the fully-relativistic ones. These values are also in line with the SF-CASPT2 (CAS(12,14)) of La Macchia (d(Pu-O))= 1.792 Å), but significantly shorter by about 0.4/0.5 Å than the estimations Archibong and Ray [174]. These large discrepancies are probably related to the choice of a large-core RECP (78 electrons), which was proven to yield too long bond distances for actinide molecules [197], while the small-core ECP gives exactly the same distances that the all-electron Douglas-Kroll relativistic approach.

The ground state $^5\Sigma_g^+(1)$ is dominated up to 84% by the configuration that corresponds to the occupation of the two $5f_\delta$ and two $5f_\varphi$ orbitals carrying one electron each. It corresponds to the description of the ground state of Boguslawski *et al* [147]. and also to the $^5\Sigma_g^+(1)$ reported by La Macchia et al. [192]. The former study places the first excited state at 1800 cm^{-1} corresponding to $^5\Phi_u$ state, while in our SO-CASPT2 it appears at higher energy, of 5421 cm^{-1}. We note that in our SF-CASPT2 calculation, the spin-free spectrum is less dense than La Macchia's results [192]. Such differences can be explained by the choice of different active space, the fact that we computed a larger number of spin-free states, and most likely the change in the interatomic Pu−O distance. SO-coupling is not expected to change the energy of the $\Lambda = 0$ $^5\Sigma_g^+$ state, while it lifts the degeneracy of the $^5\Phi_u$ state. Given the small energy gap of 1800 cm^{-1} between the $^5\Sigma_g^+$ and $^5\Phi_u$ state, the 1_u state becomes the ground state in their study, while in our work, it remains a state of *g* symmetry.

TABLE 4.17: Standard enthalpies of formation $\Delta_f H^\ominus$ of PuO_2, $PuO_2(OH)_2$, PuO_3 in kJ mol^{-1} in the gas phase calculated at various level of theory and extrapolated to the CBS-CE limit, and from the average of five reactions listed in Table 4.3, except for $^2DC^M$-CCSD(T). The standard deviations $\Delta\Delta_f H^\ominus$ includes the uncertainty on the average value as well as the experimental error bars.

$\Delta_f H^\ominus$	PuO_2	$PuO_2(OH)_2$	PuO_3
UCCSD + ΔE_{SO}	-348.4 $\pm$ 28.2		
UCCSD(T) + ΔE_{SO}	-404.3 $\pm$ 22.6	-518.8 $\pm$ 32.9	+599.1 $\pm$ 28.3
CASPT2 + ΔE_{SO}	-364.4 $\pm$17.8	-1008.7 $\pm$ 34.3	-539.8 $\pm$ 24.1
Reference	-410 $\pm$ 20 [198] ;	-1018.2 $\pm$3.3[199]	-562.8 $\pm$5[199] ;
	-412 $\pm$ 20 [139] ;		-567.6 $\pm$ 15 [141]
	-440$\pm$ 7 [138];		
	-428.7 $\pm$ 7[138];		
	-428.7 $\pm$ 20 [141];		

4.4.2 Thermodynamic properties

TABLE 4.16: Standard enthalpies of formation $\Delta_f H^\ominus$ of PuO_2, $PuO_2(OH)_2$, PuO_3 in kJ mol^{-1} in the gas phase calculated at various level of theory and extrapolated to the CBS-TE limit, and from the average of five reactions listed in Table 4.3, except for $^2DC^M$-CCSD(T). The standard deviations $\Delta\Delta_f H^\ominus$ includes the uncertainty on the average value as well as the experimental error bars.

$\Delta_f H^\ominus$	PuO_2	$PuO_2(OH)_2$	PuO_3
ΔE_{SO} [1]	34.4	46.9	59.0
B3LYP[1] + ΔE_{SO}	-304.1 $\pm$ 16.4	-787.0 $\pm$ 30.1	-397.3 $\pm$ 21.6
$^2DC^M$-CCSD(T)	-432		
UCCSD + ΔE_{SO}	-347.6$\pm$ 21.1		
UCCSD(T) + ΔE_{SO}	-406.6 $\pm$ 9.3	-260.9 $\pm$ 26.9	+438.0 $\pm$ 8.5
CASPT2 + ΔE_{SO}	-367.3$\pm$17.1	-1009.3 $\pm$ 44.5	-545.0 $\pm$ 23.3
Reference	-410 $\pm$ 20 [198] ;	-1018.2 $\pm$3.3[199]	-562.8 $\pm$5[199] ;
	-412 $\pm$ 20 [139] ;		-567.6 $\pm$ 15 [141]
	-440$\pm$ 7 [138];		
	-428.7 $\pm$ 7[138];		
	-428.7 $\pm$ 20 [141];		

[1] ΔE_{SO} is estimation of the SO contribution.

All the values of enthalpy of formation can be found in the Table 4.16. From our discussion of the electronic structures of the different Pu molecules detailed in section 4.4.1, one will not be surprised to see that the single-reference methods, here DFT and CCSD(T), fail at describing $PuO_2(OH)_2$ and PuO_3 thermodynamic properties,

while they should be in principle usable for PuO_2 molecule. Thus, for this methods, we will focus only on the PuO_2 molecule. One can observe that the enthalpy obtained with the B3LYP functional and the $+\Delta E_{SO}$ correction gives a value about 25% off the experimental one ($100 \, kJ \, mol^{-1}$). A change in the density functional will not ensure a better agreement with experience as observed previously for actinide systems [200] or for transition metal molecules [201]. The $\Delta_f H^\ominus(298.15 \, K)$ computed with $^2DC^M$ approach ($^2DC^M$) is in almost perfect agreement with the available results [138, 141]. Note that the absence of error value is because the calculation was done only for the reaction R_4, as the other reactions involved species with a multideterminantal character. UCCSD+ΔE_{SO} result ($-385.0\pm21.1kJ \, mol^{-1}$) is lower than $^2DC^M$-CCSD(T) one, while the UCCSD(T)+ΔE_{SO} agrees with the best theoretical estimations and the experimental data, thus highlighting the importance of the perturbative triple contributions. For the reaction 4, UCCSD(T) + ΔE_{SO} and CASPT2 + ΔE_{SO} give $-416.22 \, kJ \, mol^{-1}$ and $-387.7 \, kJ \, mol^{-1}$, respectively. The SO-CASPT2 value deviates by about $40 \, kJ \, mol^{-1}$ from both $^2DC^M$-CCSD(T) and experiments, probably because of the incompleteness of the active space. Nevertheless, the SO-CASPT2 results for $PuO_2(OH)_2$ and PuO_3 show great agreement with the experiment values by Krikorian et al. [199].

4.5 Conclusion and Perspectives

Concerning PuO_2, where the static correlation is not important and the wave function can be described by single-reference methods that include the dynamic correlation such as UCCSD(T) the $\Delta_f H^\ominus$ could be reproduced. The distance Pu-O found for the linear PuO_2 is 1.808 Å and the ground state a 0_g mainly composed by the spin-free state ^5A_g.

About $PuO_2(OH)_2$, SO-CASPT2 method is enough to reproduce the only experimental data available but the enthalpy of formation given by this method for PuO_3 is smaller than expected. Since the detection of PuO_3 is complicated one could argue on the validity of the two measurements but we would rather point out the fact that our active space size might not be large enough and could lead to a mistreatment of the static correlation. In order to improve the description, larger active spaces can be handled with the DMRG method recently implemented in Molcas. Exploratory DMRG calculations will be performed in coming weeks.

Our thermodynamics data are about to be implemented by our IRSN colleagues (F. Virot) in the accident simulation code to quantify the amounts of each volatile Pu species released.

Chapter 5

How well are the f-elements described by a Double-Hybrid Functional ?

Contents

Our interest here is to see how double hybrids work for the geometries and thermochemistry of species containing actinides and lanthanides. This project was triggered by two reasons: the first is that we have seen that the B3LYP is not accurate to compute the thermochemistry of PuO_2, thus raising the question of whether other functionals and double hybrids in particular could be more accurate for such f-element complexes. The second, because we are involved in the implementation and benchmarking of double-hybrids four-component-based methods in Dirac in a collaboration with Benjamin Helmich-Paris (Mulheim) and Lucas Visscher (Amsterdam); therefore, we want to investigate if there are significant changes between spin-free (Molpro) and SOC (Dirac) calculations. This chapter presents the first step of the study. It consists in a systematic comparison of structural and thermodynamic properties computed at the spin-free level with the state of the art CCSD(T) method as reference. This is, to the best of our knowledge, the first application of double-hybrid B2-BLYP to actinide chemistry. However, we can refer to recent assessments of double hybrid, in particular B2-PLYP for transition metal thermochemistry [202, 203], leading to average uncertainties of up to 8 kcal.mol^{-1}, which is about 4 kcal.mol^{-1} better than B3LYP. After a brief description of the current development of double-hybrids and the B2-PLYP functional and a review of the available thermodynamic data, we will reach the aim of this chapter and present the first results regarding the f element properties.

5.1 Motivations for double-hybrid functionals

One of the biggest weakness of DFT is not accounting for the dispersion effects as we have seen in the Section 2.3.4. A widely used solution is the Grimme dispersion correction [49–51] which we have used in the Chapter 3. We have seen that even if it lead to good qualitative results, this correction could not be used as quantitative method for such a large system. When the system has a reasonable size, MP2 is a good but expensive solution to include dispersion effects.

The idea of double-hybrids (B2-PLYP) [204] is to add non-locality responsible for dispersive (van der Waals) interactions to hybrid functionals by considering virtuals orbitals and having a well-balanced performance for properties (energetics, etc). It relies on a combination of KS-DFT (Kohn Sham Density Functional Theory) and Perturbation Theory (PT) where the exchange-correlation energy is expressed as:

$$E_{xc} = (1 - a_x)E_x^{GGA} + a_x E_x^{HF} + bE_c^{GGA} + cE_c^{PT2} \qquad (5.1)$$

where

$$E_c^{PT2} = \frac{1}{4} \sum_{ia} \sum_{jb} \frac{[(ia|jb) - (ib|ja)]^2}{\epsilon_i + \epsilon_j - \epsilon_a - \epsilon_b} \tag{5.2}$$

with ϵ_i being the KS eigenvalue of the orbital i, the bracket terms corresponding to the two electrons integrals over the KS orbitals. The parameters a_x, b and c were parametrised to reproduce thermodynamic properties of light elements namely the G2/97 set of heat of formation. During this parametrisation, the relation $b + c = 1$ was found and confirmed [205] and $c \leq a_x$, leading to only two parameters with a value of 0.53 and 0.27 for a_x and c, respectively. The GGA functional used is the BLYP one. Multiple rigorous analysis were done concerning the parametrisation [205–207] and showing that the value of a_x and c are very close to a theoretical optimum.

Even if it is not used in this thesis we can note that it is also possible to perform TDDFT with double hybrid [208, 209] or to add long-range dispersion [210].

During the past 10 years the development of many other double-hybrid functionals was done [207, 211–233] and listed and compared in a review of Grimme *et al* [234]. This work exposes the functional DSD-BLYP-D3 [221] and PWPB95-D3 [203] as the most accurate and robust ones though we have not evaluated them in this thesis.

Most specific performances are also tested such as: spin-state energetics [235], ionisation energies and aqueous redox potentials of organic molecules [236], non-linear optical properties [237] and thermochemistry of 3d transition metals [202]. This last study is particularly interesting since it states that the Mean Average Deviation (MAD) of B2-PLYP is 32.6 kJ.mol^{-1} for the determination of enthalpies of formation. Since the DIRAC implementation concerns only the B2-PLYP functional, it will be compared to HF, CCSD(T), B3LYP hybrid functional, PBE GGA functional and the limiting cases of B2-PLYP, MP2 and BLYP functional.

5.2 Literature review of the available enthalpies of formation $\Delta_{\mathbf{r}} H^{\ominus}$.

The enthalpies of formation theoretical and experimental of the reactions listed in the Table 5.1 are only reported for reaction including UF_6. The enthalpies are extracted from the work of Peterson *et al.* and [184] Privalov *et al*. The former study includes four-component CCSD(T) calculations with a pseudopotential (PP) [179] or all electron basis sets [238]. The latter one includes SCF, MP2, B3LYP and CCSD(T) single point energy using geometries obtained at the HF level with a scalar relativistic pseudopotential or experimental data.

All the reactions were chosen for the fact that they involve close shell species and because the information about the structures are readily accessible.

TABLE 5.1: Reactions used to calculate $\Delta_r H^{\ominus}$ and their previously reported values.

Reactions	$\Delta_r H^{\ominus}$ in kJ.mol^{-1}
R_1: $H_2 + F_2 \longrightarrow 2\,HF$	
R_2: $La^{3+} + H_2O \longrightarrow LaH_2O^{3+}$	
R_3: $CeF_4 + CeO_2 \longrightarrow 2\,CeOF_2$	
R_4: $ThF_4 + ThO_2 \longrightarrow 2\,ThOF_2$	
R_5: $UO_2{}^{2+} + H_2O \longrightarrow UO_2(H_2O)^{2+}$	
R_6: $Ac^{3+} + H_2O \longrightarrow AcH_2O^{3+}$	
R_7: $UF_6 + SO_3 \longrightarrow UO_3 + SF_6$	4C-CCSD(T): 525.5 [1], 527.2 [2][184]
	Exp: 528.9 [184]
R_8: $UF_6 + 3\,H_2O \longrightarrow UO_3 + 6\,HF$	4C-CCSD(T): 481.6 [1], 479.9 [2][184]
	SCF: 539 ; MP2: 487, 534[*]; CCSD(T): 558, 464[*][239]
	B3LYP: 627, 500[*]; Exp: 435 [239]
R_9: $UF_6 + H_2O \longrightarrow UOF_4 + {}_2HF$	
R_{10}: $UF_6 + 2\,H_2O \longrightarrow UO_2F_2 + {}_4HF$	4C-CCSD(T): 204.2[1], 202.1 [2][184]
	SCF: 170; MP2: 232, 263[*]; CCSD(T): 232, 263[*][239]
	B3LYP: 332, 246[*]; Exp: 187 [239]
R_{11}: $UO_2{}^{2+} + 4\,H_2O \longrightarrow UO_2(H_2O)_4{}^{2+}$	
R_{12}: $PaO_2{}^+ + H_2O \longrightarrow PaO_2(H_2O)^+$	

[1] Values FC-CCSD(T)/CBS with pseudo potential.
[2] Values FC-CCSD(T)/CBS with the all electron basis sets.
[*] Corrected values

We aim to reproduce results as close as possible to the experimental ones or to the corresponding method in use.

Concerning the geometries of the molecules, when possible it will be compared to experimental data, otherwise the quantum chemical method used to determined them will be specified.

5.3   Computational details

As in the previous Chapters, the geometry of the molecules under interest is a key information for the description of thermodynamic properties. Therefore the different molecules were first optimised for each of the quantum chemistry methods at the spin-free level with the Molpro2015.1 package [156], followed by an harmonic frequency calculation. The reaction enthalpies are computed as in Chapter 4 in equation 4.3:

$$\Delta_r H^{\ominus} = \sum_i (E_i + ZPE_i + H_{corr,i}) \tag{5.3}$$

The light elements (first and second rows) are described with aug-cc-pVQZ basis sets [cite], for actinides the scalar relativistic effects were included with the relativistic pseudopotential with 60 e- in core, namely ECP60MDF [cite] with the corresponding quadruple-ζ quality basis sets[cite]. For lanthanides,the small-core relativistic pseudo potential with 28 e - in core, namely ECP28WB, [171, 240] and the corresponding quadruple-ζ basis sets were used. Peterson *et al.* [184] reportes that quadruple-ζ basis sets used are close enough from the CBS for us to overcome the need of CBS extrapolations. Since all the molecules involved in the reactions under study (see Table 5.1) are closed-shell, no spin state problem should appear and spin-orbit coupling is expected to be negligible [184].

In most of the reactions the bonding picture changes a lot from the reactants to the products resulting in large differences of dynamical correlation across the reactions making it then relevant for benchmarking correlation methods. A particular attention will be paid to the R_1 since its enthalpy of reaction is computationally challenging because as mentioned in the reference [239], Privalov *et al.* could not reproduce it.

5.4 Results and Discusions

The optimisations of $UO_2(H_2O)_4{}^{2+}$ are still in progress, thus, the results of the reaction R_{11} will not be reported. Table 5.2 presents the reported geometries of molecules with an f-element with the corresponding reference data.

5.4.1 Geometries and total energies

TABLE 5.2: Geometries of the various molecules under study, the distance are given in Å and angles in degree symmetry is given in parenthesis.

Molecule		CCSD(T)	MP2	B2PLYP	B3LYP	BLYP	PBE	HF	Literature
ThF$_4$ (Td)	r(Th-F)	2.112	2.113	2.116	2.117	2.132	2.113	2.116	Exp: 2.124 [241]
	angle(F-Th-F)	109.5	109.5	109.5	109.5	109.4	109.4	109.5	107.2
ThOF$_2$ (Cs)	r(Th-O)	1.890	1.896	1.895	1.888	1.906	1.890	1.870	Exp: 1.886 [242]
	r(Th-F)	2.138	2.136	2.139	2.141	2.152	2.130	2.154	Exp: 2.157
	angle(F-Th-F)	106.9	120.6	106.0	106.1	104.8	103.8	110.6	107
	angle(F-Th-O)	106.9	120.6	106.0	106.1	104.8	103.8	110.6	
ThO$_2$ (C$_{2v}$)	r(Th-O)	1.907	1.912	1.913	1.905	1.923	1.906	1.891	CCSD(T): 1.905 [243]
	angle(O-Th-O)	117.0	114.4	117.8	119.9	119.0	119.2	120.4	117
UF$_6$ (O$_h$)	r(U-F)	2.000	1.999	2.016	2.014	2.041	2.022	1.984	Exp: 1.999 [244]
UO$_3$ (C$_{2v}$)	r(U-O$_{apical}$)	1.8	1.865 [1]	1.871 [1]	1.880	1.880	1.863	1.747	4C-CCSD(T): 1.801[184]
	r(U-O)	1.9	1.865 [1]	1.871 [1]	1.852977	1.854	1.829	1.828	1.852
	angle(O$_{apical}$-U-O)	99.4	119.9 [1]	120 [1]	101.4286	106.5	103.1	97.7	99.5
UO$_2$F$_2$ (C$_{2v}$)	r(U-O)	1.769	1.788	1.798	1.788	1.816	1.816	1.713	4C-CCSD(T): 1.768 [184]
	r(U-F)	2.076	2.073	2.077	2.073	2.093	2.093	2.092	2.075
	angle(O-U-O)	169.1	169.5	166.4	169.5	163.9	163.9	170.2	169.2
	angle(F-U-F)	114.0	112.8	111.7	112.8	118.6	118.6	118.9	114.1
UO$_2$H$_2$O^{2+} (Cs)	r(U-O)	1.713	1.732	1.734	1.716	1.748	1.733	1.660	CCSD(T): 1.789 [243]
	r(U-OH$_2$)	2.324	2.317	2.325	2.330	2.343	2.314	2.373	2.453
	angle(O-U-O)	89.8	88.8	89.5	90.1	90.1	89.4	90.7	90.0
LaF$_3$ (C$_{3v}$)	r(La-F)	2.120	2.120	2.123	2.123	2.134	2.112	2.138	Exp: 2.12 [245]
	angle(F-La-F)	116.2	115.9	115.8	115.8	115.1	114.3	119.5	
CeO$_2$ (C$_{2v}$)	r(Ce-O)	1.821	1.822	1.819	1.835	1.850	1.829	1.790	HF: 1.82 [246]
	angle(O-Ce-O)	121.8	115.4	128.4	139.1	132.6	132.9	116.6	132
CeF$_4$ (Td)	r(Ce-F)	2.028	2.026	2.036	2.042	2.070	2.049	2.031	CISD: 2.04 [247]
CeOF$_2$ (C$_s$)	r(Ce-O)	1.786	1.787	1.804	1.791	1.832	1.811	1.748	B3LYP: 1.794 [248]
	r(Ce-F)	2.082	2.078	2.087	2.090	2.109	2.086	2.098	2.091
	angle(F-Ce-F)	110.5	110.7	109.0	109.6	109.2	108.3	114.9	110.5
AcF$_3$ (C$_{3v}$)	r(Ac-F)	2.195	2.195	2.197	2.197	2.209	2.186	2.210	MP2: 2.272 [249]
	angle(F-Ac-F)	113.4	113.3	113.0	112.7	111.6	110.9	116.7	
PaO$_2$$^+$ (D$_{\infty h}$)	r(Pa-O)	1.773	1.794	1.784	1.775	1.799	1.784	1.738	CCSD(T): 1.776 [243]
PaO$_2$H$_2$O$^+$ (D$_{\infty h}$)	r(Pa-O)	1.789	1.799	1.801	1.791	1.816	1.800	1.754	CCSD(T): 1.788 [243]
	r(Pa-OH$_2$)	2.449	2.441	2.455	2.465	2.475	2.442	2.511	2.447
	angle(O-Pa-OH$_2$)	88.7	88.7	89.1	89.6	88.5	88.8	90.6	98.5

[1] The symmetry is D$_{3h}$

Looking at Table 5.2 the B2-PLYP presents good performances at reproducing the literature data. This is highlighted in Figures 5.1 and 5.2 presenting the bond length and angular deviation with respect to CCSD(T). Unfortunately, B2-PLYP and MP2 predict the wrong symmetry for UO$_3$ giving it as a D$_{3h}$ symmetry for the molecule instead the expected C$_{2v}$.

Concerning the distances, it is the functional B3LYP that is the closest to CCSD(T) with a MAD of 0.006 Å followed by MP2 with 0.012 Å. B2-PLYP functional arrives third with an average error of 0.014 Å. However, while UO$_3$ is taken out of the set, the MAD of MP2 and B2-PLYP are reduced to 0.007 Å and 0.008 Å, respectively.
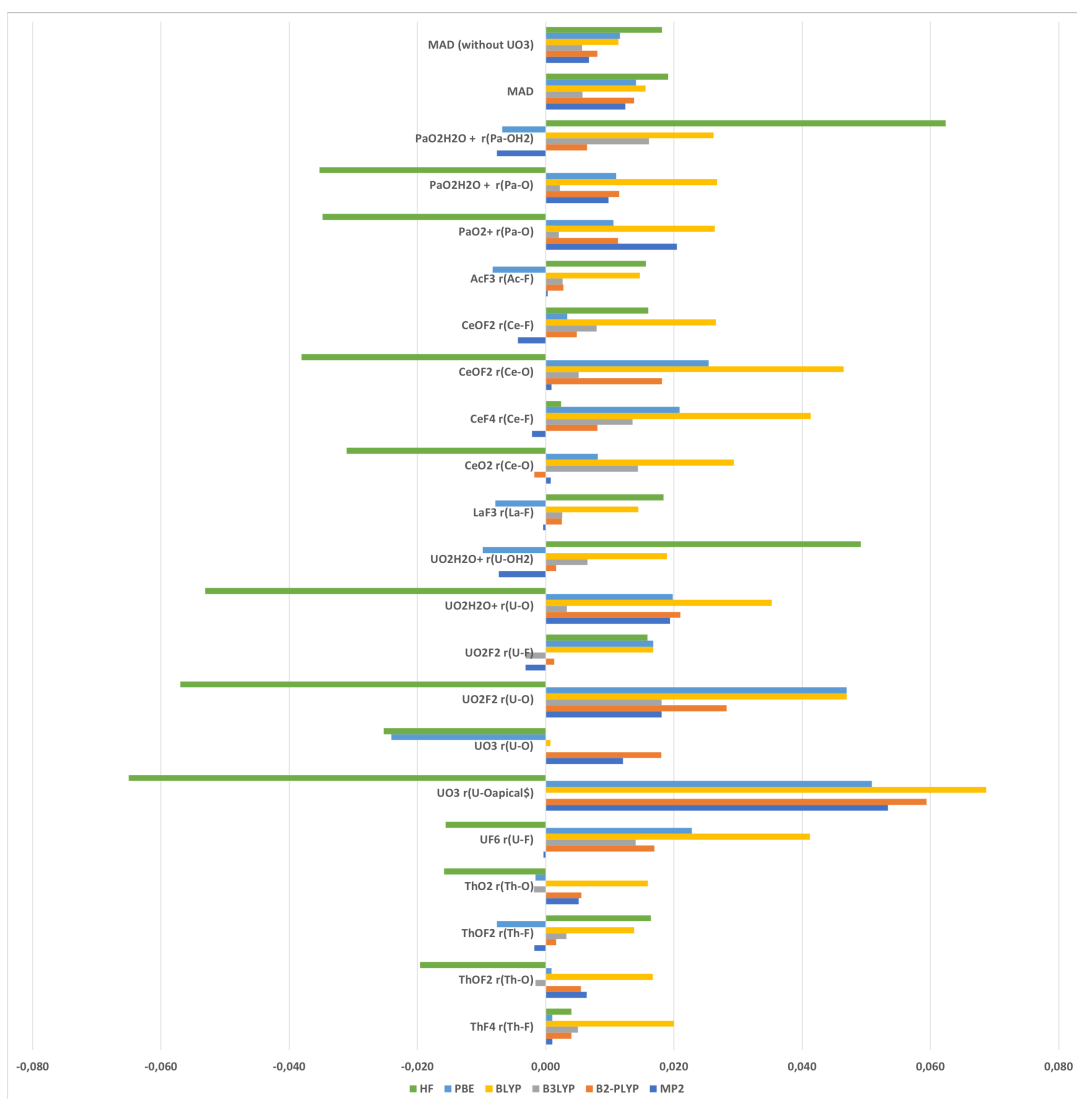
FIGURE 5.1: Error in the bond length in Å with respect to CCSD(T) values and MAD over all complexes
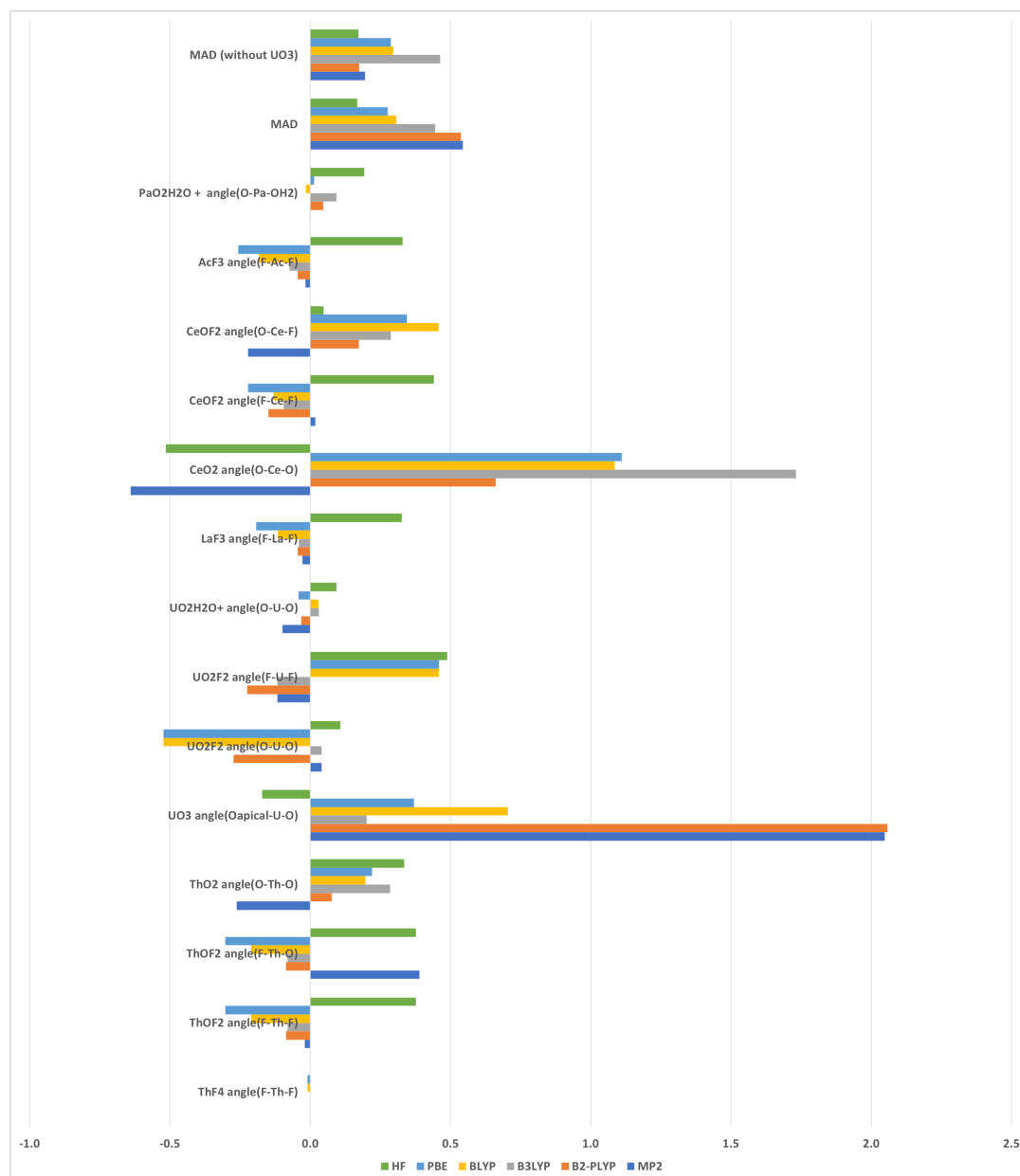
FIGURE 5.2: Differences in the angles (in degrees) with respect to CCSD(T) and the MAD over all complexes

For the intramolecular angles, MP2 and B2-PLYP perform the worst with a MAD of 5.4 due to the bad description of UO_3. While this molecule is taken off the set the MAD of B2-PLYP is the best with 1.7 degrees and MP2 the second best value with MADs of 2.0 degrees. Explanations about the failure of MP2 and B2-PLYP to describe UO_3 are still under investigation.

This small B2-PLYP MAD makes use confident about its capability in giving very accurate geometries while MP2 is performing well.

In Table 5.3, we reported the difference in total energies. One can note that the behaviour of each method/functional depends on the actinide/lanthanide present. Nonetheless, in every cases containing an heavy atom, the B2-PLYP is the closest to CCSD(T) after MP2. MP2 underestimates the total energies while all other methods overestimate it. So far, the smallest MAD is obtained with B2-PLYP attesting its good performance.

5.4.2   Enthalpies of Reactions

As mentioned previously, only scarce experimental values of reaction enthalpies are available for f elements. The only ones to benchmark with are those studying reactions R7, R8, R10 and R12. Thus, we will start the discussion by scrutinize the results obtained for these four reactions. For the reactions R_8 and R_{10} we could see that computed reaction enthalpies were far from the experimental values (see Table 5.3) . This was already noticed in [184] by Peterson *et al.*, thus we decided to correct the results in the same way they did. Peterson *et al.* attributed the error to the description of HF, and because of that they took the difference between the experimental value and theirs for reaction R_{10}. This difference was then divided by 4 (the number of HF molecules in reaction R_{10}) to obtain the correction factor for each HF molecule. This correction was then apply to each reaction involving HF.

Table 5.3 presents the enthalpies of reaction of the chosen reactions. The results obtained on reactions R_8 and R_{10} validate our correction since in reaction R_8 we are closer to the experimental enthalpy of reaction. Figure 5.3 exposes the differences in between the enthalpies of reactions with respect to CCSD(T) values. So far the smallest MAD is HF's with 27.8 $kJ.mol^{-1}$. The second lowest MAD is the one is given by the B2-PLYP functional (with 28.4 $kJ.mol^{-1}$). All the other MADs are above 35 $kJ.mol^{-1}$.
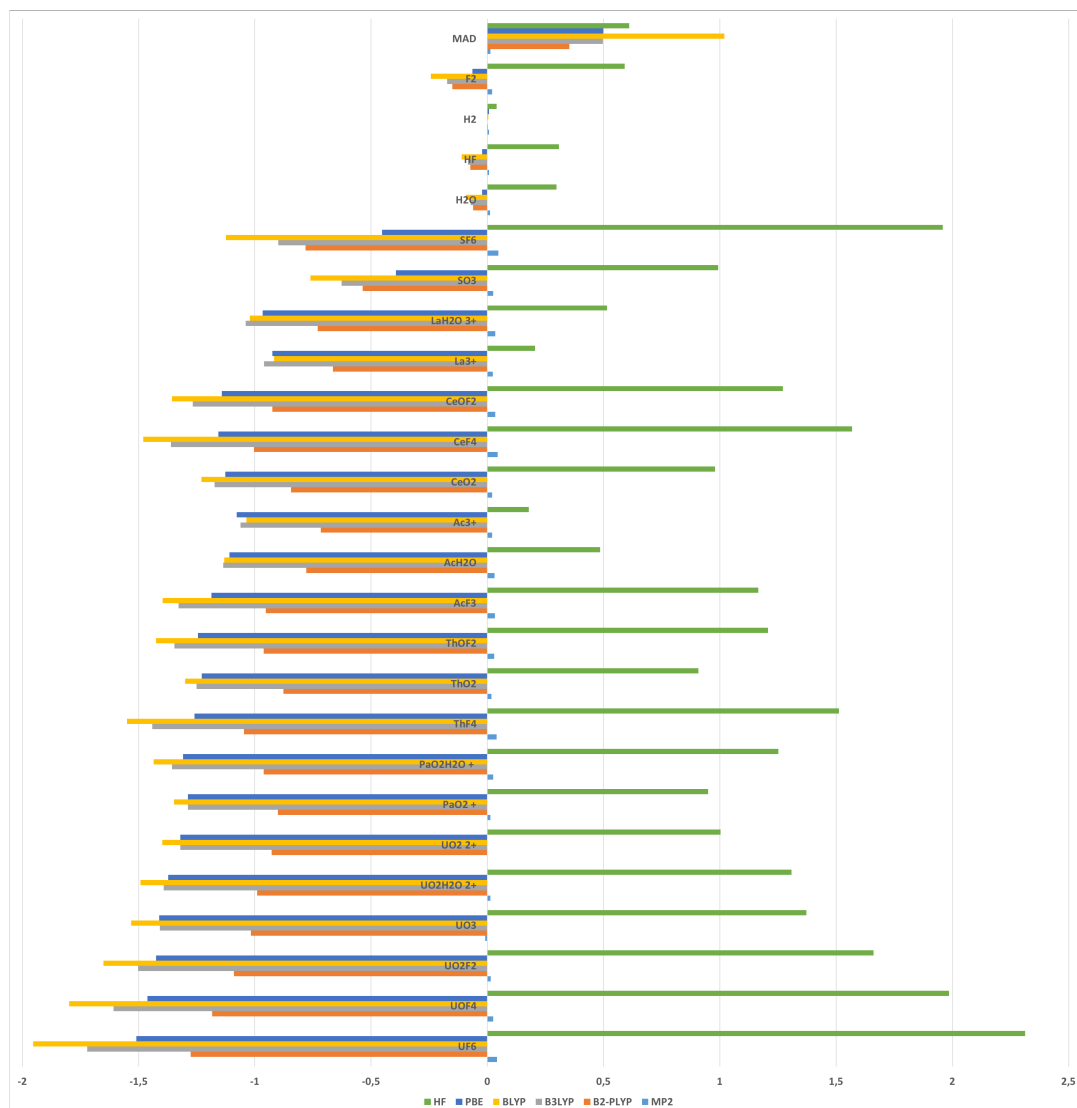
FIGURE 5.3: Difference in energy between the total energy given by
the CCSD(T) and the considered method and functionals in a.u.

TABLE 5.3: $\Delta_r H^{\ominus}$ in kJ.mol^{-1} for the reaction under study.

	CCSD(T)	MP2	B2-PLYP	B3LYP	BLYP	PBE	HF	Exp
R_1	-547.3	-612.6	-578.1	-563.5	-533.0	-544.5	-617.7	
R_2	-381.0	-383.4	-391.7	-401.0	-413.7	-428.5	-345.8	
R_3	-146.0	-136.1	-147.6	-148.0	-162.2	-143.8	-164.5	
R_4	13.3	16.4	13.6	11.0	11.2	11.4	2.8	
R_5	-275.9	-276.8	-276.8	-278.3	-280.5	-356.1	-250.2	
R_6	-338.2	-340.4	-344.6	-347.1	-348.9	-360.9	-310.4	
R_7	539.2	457.1	570.2	643.6	686.7	635.2	604.6	539.3
R_8	468.7	356.0	472.2	545.0	553.2	553.2	527.9	
$R_{8,corrected}$	456.9	424.9	401.6	420.2	553.2	377.9	550.8	435
R_9	43.7	56.4	110.3	140.3	158.6	160.4	75.5	
$R_{9,corrected}$	39.8	79.4	86.8	98.7	99.1	102.0	83.2	
R_{10}	194.9	141.1	234.1	270.2	306.1	303.8	171.7	
$R_{10,corrected}$	187.0	187.0	187.0	187.0	187.0	187.0	187.0	187
R_{12}	-152.4	-155.6	-151.3	-146.8	-117.6	-149.7	-132.8	
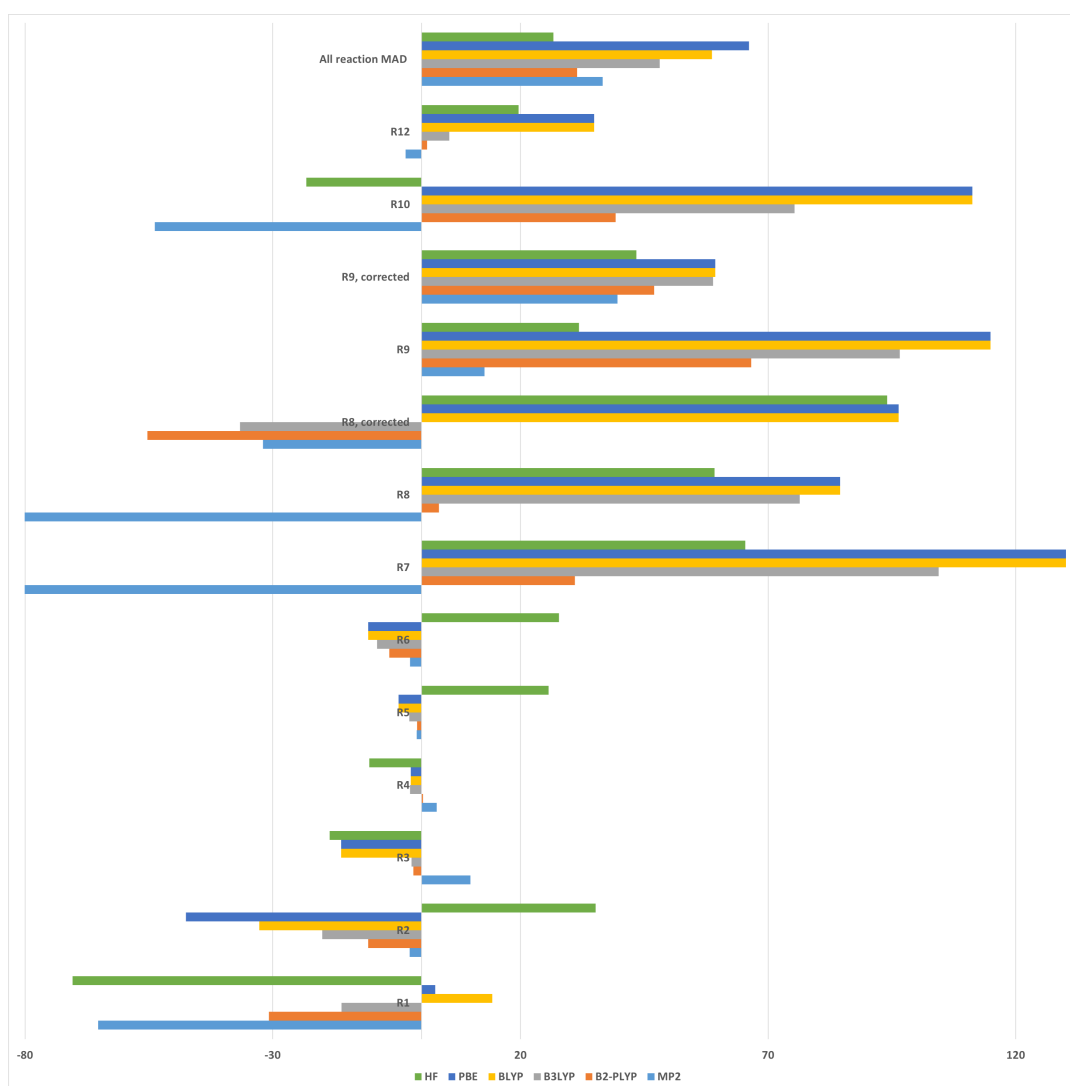
FIGURE 5.4: Differences in the enthalpies of reaction with respect to CCSD(T) values in kJ.mol^{-1}

5.5   Conclusion and Perspectives

Even if we can observe in B2-PLYP some imperfection of MP2, such as the inaccuracies in the description of the geometry of UO_3, it still yields to good results in the description of the geometry. The thermodynamic properties of f-element are even better describe with B2-PLYP than MP2, which is what was desired. The MAD reported for B2-PLYP (28.4 kJ.mol^{-1}) is smaller than the one found in the study of Wilson *et al.* on transition metals (32.6 kJ.mol^{-1}). All of this, demonstrate that this double hybrid is suitable to answer this kind of problems. The follow-up of the current work will be to use the double-hybrid implementation in DIRAC program to assess the importance of SOC to our results.

Chapter 6

Conclusions and perspectives

With respect to the quantum chemical methods used in this thesis to study actinides several conclusions need to be drawn. First, for closed-shell systems or for systems with a dominant single reference character, DFT with hybrid methods, such as semi-empirical dispersion corrections or double hybrid functional, performs well. For large systems it is cheap and efficient. With B2-PLYP, enough correlation can be included to describe properly closed-shell systems. Nonetheless, DFT is still failing for multireference systems. For this type of systems, we chose the CAS method. This method is neither black-box nor cheap. The choice of active space can be tedious and we have seen that in cases, where very accurate results are wanted, this method may fail because of the limited size of active space and probably a lack of accurate dynamic electron correlation treatment.

To the question raised in the introduction about the efficiency of the available tools to describe the structure, the bonding and the thermodynamics of actinide systems, we can not give a simple answer.

First, concerning the geometries, the three studies showed that the structures of actinides and f-elements systems can have their geometries reproduced or unravelled. We have seen that the X-ray structures were well reproduced for the catalysts in Chapter 3 as well as structural experimental values in Chapter 5 with the double-hybrid (B2-BLYP) functional, proving its capability, in most cases, at being as accurate as other quantum chemistry methods but also being predictive. It is worth noticing the failure of the DFT at converging to the expected triplet state for the uranium complexes in Chapter 3. In Chapter 5, only UO_3 structure turned out to be problematic both at MP2 and B2-PLYP levels; and the explanations of this failure are expected soon. Finally, for PuO_2, in Chapter 4 we reported a bond length and a ground state different from what was reported before at spin-orbit level [151].

Chapters 3 and 4 were focusing on the bonding. In the case of closed-shell systems, the exploration of the bonding via the determination of the electronic structure is

rather easy and the ETS-NOCV is a powerful tool to analyse and explore the metal arene chemical bonds and determine the main forces driving them. In particular we have seen that the zirconium-arene bond was mainly covalent while the thorium-arene one was mostly driven by electrostatic forces. In cases of open-shell systems, like in Chapter 4, the electronic wave functions are more difficult to describe. The CAS methods present the main disadvantages to include a limited number of orbitals in the active space thus requiring a thorough analysis of results. For example, in PuO_3, the full valence active space is (34; 26) but we could only compute a active space of (14,14) which might not be large enough.

The third properties we wanted to reproduce were thermodynamics. This part is particularly satisfactory in Chapter 5 where the double hybrid B2-PLYP already exhibits great performances at the spin-free level, compared to either experimental or state-of-the-art CCSD(T) data. In Chapter 4, multireference methods were needed to predict the enthalpies of formation of plutonium oxyhydroxide $PuO_2(OH)_2$ and trioxide PuO_3. The enthalpy of formation of $PuO_2(OH)_2$ was within very good agreement with experimental data but its uniqueness imposes to confirm this value with another method. For PuO_2, the single reference method UCCSD(T) perform very well. Regarding PuO_3 and PuO_2, the results with SO-CASPT2 method are good but not excellent, demonstrating the limit of actual relativistic multireference method accuracy.

As perspectives, the study of the alkyl cation catalysts calls for a further investigation of the possible transition states to have a better comprehension of the catalytic mechanism. Concerning the thermodynamic properties of plutonium oxides and oxyhydroxyde, in the next weeks, we will use the DMRG methods to be able to handle all valence orbitals in the active space to confirm our conclusions on PuO_3 and $PuO_2(OH)_2$. With DMRG we can expect to also be able to predict other thermodynamic values such as the one of uranyl complexes or RuO_2 (also important for nuclear safety) for which it is not easy to properly describe because of a ground and first excited states close to each other in energy [201].

To shed light on the possible formation of PuO_3 we wait for the results of IRSN on accident simulation. At the moment, the double hybrid B2-PLYP is tested on PuO_2 hoping to obtain results as good as the one computed with UCCSD(T) method. In addition we plan to benchmark the implementation of the double hybrid in the DIRAC package to have results in the fully relativistic context.

Finally, the broad range of uses and theoretical challenges to describe actinides makes them a wonderful subject for the development of both experimental and computational chemistry.

Appendix A

Geometries

Contents

A.1   Geometries from the Chapter Coordination of Alkyl cations $[(XA_2)X(CH_2Y)]$ (X = Th, U or Zr; Y = SiMe$_3$, H) with an arene for Ethylene polymerisation: Exploration of the bonding

A.1.1   X-Ray structures of Alkyl cations containing Thorium

X-Ray structure of η^6-2-Th

```
Th   13.572531   10.195293   14.464022          C    15.992251    5.394201   12.387399
Si   13.448412    7.436393   17.277993          H    16.053977    4.497544   12.079063
O    13.505595    7.925594   13.428804          C    13.429707    5.120134   12.400889
N    11.533051    9.429158   13.797651          C    12.203748    6.048476   12.562765
C    10.901366    5.592226   12.256356          C    12.283644    7.315836   13.063811
H    10.792612    4.709827   11.921041          C    14.695748    7.239794   13.098499
N    15.572197    9.327770   13.767395          C    14.706170    5.945503   12.620578
C     9.770801    6.390663   12.427868          C    13.455092    4.557743   10.957491
C     9.943419    7.681786   12.928914          H    14.231605    3.970005   10.849573
H     9.184008    8.241008   13.042613          H    13.515482    5.299149   10.319620
C    11.204383    8.166551   13.264229          H    12.633689    4.050799   10.791760
C    15.830055    8.022389   13.295063          C    13.364508    3.990600   13.406835
C    17.066703    7.444156   13.025269          H    14.146097    3.409198   13.296990
H    17.857644    7.959021   13.135114          H    12.548182    3.469398   13.260375
C    17.163700    6.111844   12.593599          H    13.357828    4.361303   14.314499
```

C	8.348976	5.918571	12.065573
C	7.779819	6.834239	10.992178
H	8.336952	6.780376	10.188578
H	7.767795	7.756243	11.323640
H	6.867297	6.553835	10.776343
C	7.451151	6.026297	13.322042
H	6.543973	5.726883	13.102353
H	7.423094	6.957806	13.624597
H	7.815893	5.462322	14.035069
C	8.306757	4.470612	11.572236
H	8.871372	4.380313	10.776343
H	7.383012	4.228230	11.348692
H	8.638899	3.874953	12.275627
C	18.537694	5.516184	12.265992
C	18.968436	6.042139	10.890042
H	19.001303	7.021174	10.909313
H	18.322590	5.749062	10.211703
H	19.856375	5.690446	10.668426
C	19.586226	5.912234	13.316261
H	19.631919	6.889686	13.381782
H	20.462942	5.562126	13.052248
H	19.332644	5.538363	14.185383
C	18.498147	3.962084	12.196616
H	17.836267	3.681681	11.531766
H	18.253115	3.600887	13.073446
H	19.380741	3.623065	11.938385
C	10.472762	10.428789	13.873193
C	10.172685	11.186036	12.726568
C	9.254284	12.234777	12.826778
H	9.026354	12.740136	12.055938
C	8.673102	12.538943	14.058195
H	8.101807	13.294606	14.133351
C	8.919737	11.759517	15.162423
H	8.481245	11.960710	15.981440
C	9.815959	10.660082	15.104610
C	10.781122	10.877117	11.366036
H	11.297639	10.024818	11.460464
C	9.726444	10.645824	10.302277
H	10.164668	10.450967	9.446644
H	9.173319	11.449013	10.211703
H	9.162631	9.886992	10.562435
C	11.757240	11.941700	10.901605
H	12.117974	11.696149	10.024774
H	12.492068	12.016157	11.547183
H	11.292295	12.803504	10.834156
C	9.943419	9.745998	16.303266
H	10.739170	9.161429	16.151025
C	8.720398	8.835083	16.416965
H	8.582785	8.366160	15.569041
H	7.928121	9.373711	16.627019
H	8.866028	8.179225	17.131919
C	10.164668	10.484236	17.638746
H	10.950266	11.065637	17.563589
H	10.311634	9.828377	18.353700
H	9.376399	11.024448	17.848800
C	16.641839	10.305221	13.803817
C	16.846522	11.122668	12.674537
C	17.778016	12.168240	12.782454
H	17.943151	12.724294	12.030885
C	18.463142	12.405870	13.969548
H	19.054745	13.147276	14.036996
C	18.287585	11.566244	15.052578
H	18.774175	11.726248	15.852325
C	17.389492	10.468394	14.985130
C	16.145630	10.888207	11.350619
H	15.295100	10.403441	11.558746
C	15.757374	12.150814	10.599050
H	15.225626	12.729047	11.184888
H	15.228298	11.910016	9.808939
H	16.567020	12.626074	10.317693
C	16.978523	9.955113	10.454518
H	17.216340	9.148755	10.955564
H	17.793514	10.417699	10.171234
H	16.452120	9.706393	9.666334
C	17.314406	9.490942	16.152952
H	16.553660	8.865183	15.975659
C	18.583654	8.652900	16.289776
H	18.771503	8.199819	15.441852
H	18.458867	7.984368	16.995095
H	19.335316	9.235886	16.522955
C	17.031965	10.205416	17.496141
H	16.991884	9.543221	18.216876
H	16.176893	10.679092	17.442182
H	17.748088	10.848602	17.681143
C	13.547547	9.235886	16.700249
H	14.365210	9.589163	17.131919
H	12.791343	9.684215	17.155044
C	14.955744	6.496804	16.715665
H	14.894285	5.568463	17.020147
H	15.760046	6.911865	17.095304
H	15.009186	6.518983	15.738626
C	11.928254	6.550667	16.636654
H	11.925582	5.627078	16.964261
H	11.938943	6.549083	15.655760
H	11.123952	7.011669	16.952699
C	13.372792	7.379204	19.153447
H	13.320419	6.446110	19.450220
H	12.580247	7.865553	19.463710
H	14.178163	7.795848	19.525377
C	14.776713	12.922319	15.844616
H	15.589031	12.871625	16.334100
C	14.819467	13.261338	14.414708
H	15.634457	13.438769	13.963767
C	13.654431	13.302527	13.796109
H	13.670464	13.348469	12.847976
C	12.434617	13.285101	14.391583
H	11.639668	13.468868	13.904027
C	12.398544	12.980935	15.784876
H	11.562177	12.987272	16.237745
C	13.560908	12.672016	16.503684
H	13.528842	12.315571	17.384369

A.1.2 X-Ray structures of Alkyl cations containing Uranium

X-Ray structure of η^6-2-U

U	26.777247	13.503446	-5.391782
C	25.497402	16.315921	-4.020626
C	27.893793	16.400190	-4.055059
C	25.430473	17.597350	-3.505585
C	26.632399	18.515068	-3.328096
C	27.914952	17.674466	-3.553844
O	26.717354	15.703364	-4.374315
Si	26.631072	16.262875	-8.133831
C	24.096018	18.044889	-3.237884
H	23.961710	18.921763	-2.897945
C	30.257583	16.196670	-4.027539
H	31.048407	15.690409	-4.171598
C	29.183435	18.242011	-3.352548
H	29.244576	19.142671	-3.056607
C	23.158568	15.962366	-3.969999
H	22.400133	15.407714	-4.110156
C	29.007950	15.612476	-4.269500
N	28.754519	14.348168	-4.765203
C	30.354856	17.521319	-3.574698
C	24.403820	15.486983	-4.276868

*A.1. Geometries from the Chapter Coordination of Alkyl cations [(XA₂)X(CH₂Y)]
(X = Th, U or Zr; Y = SiMe₃, H) with an arene for Ethylene polymerisation: 119
Exploration of the bonding*

C	26.755000	14.493941	-7.517706
H	27.582991	14.155731	-7.942175
H	26.014113	14.031340	-7.983711
C	22.984861	17.224017	-3.464068
C	26.656266	19.034331	-1.896880
H	25.852805	19.570197	-1.730358
H	27.452665	19.589755	-1.764128
H	26.678646	18.277243	-1.275016
C	21.507655	19.145925	-2.621513
H	20.581249	19.405101	-2.434346
H	21.882572	19.742619	-3.302546
H	22.038066	19.213498	-1.800228
C	32.136413	17.576864	-1.871746
H	32.160015	16.597673	-1.903774
H	31.477376	17.866163	-1.206623
H	33.021484	17.917039	-1.624046
C	29.814411	13.343790	-4.831172
C	26.579170	19.651369	-4.322192
H	25.768992	20.181213	-4.169628
H	26.565710	19.288665	-5.232495
H	27.368347	20.221366	-4.209327
C	32.773442	17.694354	-4.294861
H	32.799566	16.715508	-4.334237
H	33.655035	18.034497	-4.035020
H	32.532489	18.050408	-5.175523
C	20.679690	17.628652	-4.399922
H	19.773461	17.946297	-4.204289
H	20.641089	16.697617	-4.703401
H	21.076323	18.185034	-5.102414
C	31.739727	18.132602	-3.271332
C	21.540230	17.718094	-3.127766
C	21.880182	11.161747	-5.093721
H	21.309073	10.407725	-5.181944
C	30.161611	13.499830	-8.495930
H	30.124018	14.174566	-9.205638
H	29.294009	13.049366	-8.427158
H	30.855745	12.841255	-8.707738
C	30.028630	12.532901	-3.691824
C	30.498085	14.192065	-7.136667
H	29.750695	14.825877	-6.937473
C	30.568704	13.211348	-5.982792
C	23.382822	12.479164	-3.740216
C	29.288062	12.758400	-2.363339
H	28.420965	13.210892	-2.571568
C	22.127932	11.928080	-6.176361
H	21.683459	11.738521	-6.994313
C	23.479803	13.182263	-8.621181
H	24.294972	12.647655	-8.520836
H	23.601289	13.830272	-9.346231
H	22.726360	12.592456	-8.833046
C	31.705241	19.675266	-3.193034
H	31.461049	20.041413	-4.068639
H	32.589621	20.009073	-2.934462
H	31.043203	19.953795	-2.526301
C	31.661489	11.272571	-4.984758
H	32.262332	10.539710	-5.051257
C	24.012019	12.762677	-2.362468
H	24.560907	13.592982	-2.458987
C	30.954213	11.502818	-3.788722
H	31.113026	10.944549	-3.036663
C	21.928421	14.794371	-7.448177

H	21.753414	15.271735	-6.610376
H	21.165420	14.217298	-7.660837
H	22.059889	15.442003	-8.171844
C	31.745780	15.016128	-7.290026
H	31.958778	15.448323	-6.436657
H	31.602658	15.700958	-7.976267
H	32.489374	14.436399	-7.557159
C	22.448796	11.451407	-3.829330
H	22.198153	10.955051	-3.059089
C	23.048285	13.020830	-6.113177
C	31.476420	12.117041	-6.057834
H	31.962150	11.966677	-6.860292
C	23.189072	13.937936	-7.294136
H	23.957727	14.552269	-7.115890
C	20.956590	16.798913	-2.077153
H	20.050732	17.095963	-1.850022
H	21.518646	16.821537	-1.274675
H	20.922369	15.883851	-2.426315
C	25.101379	17.176726	-7.485641
H	25.116140	17.184210	-6.505788
H	24.291945	16.720178	-7.796677
H	25.105468	18.098108	-7.819462
N	24.756569	14.219735	-4.803727
C	23.685898	13.247855	-4.894962
C	26.550285	16.284225	-9.996505
H	27.327675	15.813040	-10.362619
H	26.551612	17.211739	-10.312920
H	25.729063	15.839122	-10.292976
C	30.108673	13.705849	-1.494609
H	30.289149	14.530998	-1.991562
H	30.956523	13.277097	-1.254409
H	29.607625	13.918315	-0.679593
C	28.969588	11.466217	-1.616584
H	28.468832	10.863644	-2.205283
H	28.430628	11.671200	-0.824164
H	29.804747	11.033975	-1.340758
C	28.129862	17.204837	-7.576894
H	28.938128	16.746716	-7.888707
H	28.139472	17.254471	-6.598197
H	28.103473	18.110796	-7.949675
C	22.932561	13.064852	-1.345834
H	23.345893	13.263844	-0.479850
H	22.342390	12.287750	-1.255243
H	22.410354	13.838636	-1.644066
C	24.938240	11.680020	-1.885629
H	25.315200	11.931837	-1.016786
H	25.663250	11.561272	-2.534237
H	24.440404	10.840785	-1.794868
C	25.637524	10.440018	-5.444645
H	24.825993	10.249767	-4.988849
C	28.009889	10.501915	-5.432921
H	28.839978	10.383985	-4.986235
C	25.574737	10.778353	-6.701535
H	24.732888	10.854368	-7.135190
C	27.995367	10.828474	-6.763773
H	28.812288	10.915857	-7.240763
C	26.776345	11.033079	-7.419501
H	26.751681	11.334091	-8.320222
C	26.829335	10.342762	-4.735580
H	26.831194	10.172242	-3.801014

X-Ray structure of η^6-3-U-endo

U	26.475973	25.967895	3.207091
Si	26.597014	23.130531	0.474077
O	26.538359	23.792852	4.259045
N	24.504125	25.166614	3.840404
N	28.481946	25.255346	3.786880
C	24.048222	21.259237	5.310425
H	23.984236	20.362409	5.620104
C	22.872472	22.003952	5.071475

C	22.987114	23.307995	4.618426
H	22.200615	23.824542	4.480790
C	24.205522	23.867324	4.368006
C	28.855200	24.003590	4.354625
C	30.092271	23.499720	4.627984
H	30.857441	24.030527	4.436824
C	30.273566	22.232120	5.176613
C	29.135141	21.430363	5.409828

H	29.252449	20.549381	5.746270
C	26.607678	20.975611	5.337187
C	25.333282	21.839164	5.094414
C	25.338614	23.081412	4.593575
C	27.751435	23.102010	4.606956
C	27.802091	21.904128	5.149850
C	26.676997	19.864877	4.362271
H	25.906494	19.270689	4.488437
H	26.663666	20.227727	3.452350
H	27.506154	19.357837	4.499906
C	26.610344	20.497092	6.790003
H	26.565020	21.271913	7.388334
H	25.834509	19.918750	6.944843
H	27.434169	19.996390	6.969694
C	21.502097	21.374905	5.390712
C	21.038195	21.912050	6.730744
H	20.166380	21.523848	6.954401
H	21.688724	21.672791	7.422743
H	20.955546	22.888102	6.681042
C	20.462318	21.761523	4.278161
H	20.763587	21.414517	3.414118
H	19.587837	21.374905	4.499906
H	20.385001	22.737575	4.228459
C	21.563417	19.798328	5.425121
H	21.864686	19.465583	4.553431
H	22.189950	19.509949	6.120943
H	20.670273	19.441815	5.618192
C	31.689265	21.763108	5.572314
C	31.739921	20.352902	6.065507
H	31.364000	19.755546	5.384977
H	32.670389	20.100967	6.241374
H	31.217365	20.275262	6.891318
C	32.270474	22.716977	6.616048
H	32.227817	23.635987	6.277694
H	31.750585	22.650427	7.443770
H	33.203609	22.476133	6.793826
C	32.585074	21.896206	4.301100
H	32.555747	22.819969	3.976128
H	33.510211	21.660115	4.528580
H	32.254478	21.292511	3.603366
C	23.429687	26.152173	3.796438
C	23.240394	27.003049	4.897519
C	22.304593	28.069418	4.782823
H	22.149959	28.655683	5.513054
C	21.606074	28.245297	3.557488
H	21.006202	28.974167	3.452350
C	21.792701	27.378576	2.544340
H	21.296807	27.508505	1.745291
C	22.664516	26.313792	2.601688
C	22.768494	25.302881	1.470020
H	23.515002	24.669081	1.678385
C	21.440776	24.478941	1.317092
H	21.536756	23.837218	0.581126
H	21.256815	23.995668	2.148638
H	20.699600	25.087388	1.122109
C	23.080428	26.017490	0.086022
H	23.141748	25.344078	-0.623182
H	22.363247	26.649706	-0.124254
H	23.930914	26.500763	0.152928
C	23.901587	26.768543	6.237551
H	24.760071	26.293193	6.046391
C	23.056433	25.803583	7.147472
H	23.515002	25.675238	8.003869
H	22.171288	26.194954	7.306135

H	22.952455	24.936861	6.700158
C	24.280173	28.048819	7.028953
H	24.701417	27.795299	7.877704
H	24.909372	28.585965	6.501352
H	23.472344	28.573289	7.208644
C	29.564383	26.263088	3.689388
C	29.828327	27.045831	4.811497
C	30.777458	28.126459	4.668127
H	31.009409	28.684204	5.402182
C	31.366667	28.322938	3.337654
H	31.963873	29.047054	3.192372
C	31.070729	27.498998	2.324506
H	31.475977	27.663785	1.481490
C	30.220243	26.435798	2.429644
C	30.084272	25.456577	1.278860
H	29.313769	24.848129	1.468109
C	31.353336	24.612039	1.169899
H	31.265355	23.979823	0.426287
H	32.123839	25.198304	1.009325
H	31.489307	24.116090	2.003357
C	29.806998	26.201292	-0.032497
H	29.721683	25.553232	-0.764640
H	28.975175	26.711501	0.049702
H	30.548174	26.812909	-0.223657
C	29.191129	26.747944	6.164910
H	28.724561	25.863794	6.103739
C	30.278898	26.641783	7.264080
H	30.929426	25.954110	7.015572
H	30.734801	27.505336	7.355837
H	29.860320	26.402524	8.116654
C	28.156682	27.803221	6.505175
H	27.754101	27.598821	7.376864
H	28.585924	28.682619	6.541495
H	27.455498	27.807975	5.818910
C	26.517031	24.898833	1.110640
H	25.714535	25.260099	0.661414
H	27.284867	25.331402	0.655679
C	28.159348	22.157648	1.118286
H	28.156682	22.148141	2.098937
H	28.132687	21.237054	0.781844
H	28.972509	22.598139	0.797137
C	26.655668	23.116271	-1.372529
H	26.695659	22.189338	-1.691766
H	25.853172	23.548839	-1.729998
H	27.450166	23.601128	-1.678385
C	25.066672	22.141803	1.022706
H	25.013350	22.137050	1.999534
H	24.258844	22.558526	0.653767
H	25.135991	21.221208	0.693911
C	26.319739	28.335614	1.288418
H	26.314407	27.849172	0.472165
C	27.476827	28.606563	1.856164
H	28.284655	28.354628	1.422230
C	27.535481	29.267300	3.096792
H	28.367304	29.392475	3.542195
C	26.378393	29.722051	3.664537
C	25.167984	29.420996	3.052825
H	24.354824	29.685608	3.465731
C	25.133325	28.725400	1.825578
H	24.309500	28.538429	1.389733
C	26.429049	30.560252	4.859287
H	25.517243	30.796342	5.128823
H	26.866290	30.067472	5.585695
H	26.935608	31.376269	4.666216

X-Ray structure of η^6-5-U-endo

O	-0.156498	15.730261	3.745891
U	-0.224668	17.934927	4.767428
Si	-0.080636	15.164970	7.520860
N	-2.182485	17.109810	4.142043
N	1.792832	17.216825	4.188683

C	-2.629433	13.191173	2.747389
H	-2.694950	12.297283	2.430165
C	-3.796538	13.913524	2.975866
C	-3.704761	15.241769	3.425267
H	-4.496004	15.750090	3.561221

A.1. *Geometries from the Chapter Coordination of Alkyl cations [(XA₂)X(CH₂Y)]*
(X = Th, U or Zr; Y = SiMe₃, H) with an arene for Ethylene polymerisation: 121
Exploration of the bonding

```
C   -2.457020   15.816188   3.670739        H   -3.177707   16.618800   6.321828
C    2.133414   15.964120   3.655633        C   -5.216161   16.453556   6.669264
C    3.403436   15.499864   3.338408        H   -5.960190   17.064171   6.852423
H    4.159136   16.060119   3.474362        H   -5.124649   15.819335   7.409454
C    3.574522   14.206241   2.819142        H   -5.392553   15.964120   5.838438
C    2.462856   13.408350   2.615212        C   -3.595212   17.951766   7.838084
H    2.586197   12.533345   2.265888        H   -2.793093   18.502579   7.730455
C   -0.069761   12.936225   2.720954        H   -3.437653   17.278201   8.531068
C   -1.349862   13.745133   2.973978        H   -4.347464   18.521464   8.100550
C   -1.328112   15.030886   3.440373        C    2.832615   18.217730   4.301411
C    1.064718   15.108000   3.415826        C    3.138450   18.984146   3.155249
C    1.153046   13.844279   2.907890        C    4.053566   20.035411   3.302532
C   -0.003183   11.777945   3.716056        H    4.283804   20.567339   2.549124
H   -0.029178   12.132039   4.629964        C    4.630221   20.310817   4.539329
H    0.830236   11.279066   3.581991        H    5.204225   21.061496   4.633741
H   -0.769228   11.181494   3.576327        C    4.379029   19.509779   5.621290
C   -0.089655   12.396429   1.282115        H    4.816958   19.689186   6.444563
H   -0.877981   11.829879   1.155603        C    3.484337   18.422318   5.538208
H    0.721483   11.869223   1.119726        C    3.340571   17.484363   6.705140
H   -0.122015   13.147108   0.651443        H    2.567630   16.876895   6.518204
C   -5.172129   13.310778   2.654865        C    4.597861   16.615663   6.867529
C   -6.205282   13.724674   3.716056        H    4.747993   16.102610   6.046144
H   -5.920402   13.395760   4.595976        H    4.474784   16.000316   7.619048
H   -7.076897   13.340679   3.489468        H    5.371333   17.191645   7.039359
H   -6.275839   14.701973   3.740603        C    3.055692   18.224025   8.028796
C   -5.615364   13.841131   1.280227        H    3.822267   18.793723   8.255385
H   -5.625974   14.821578   1.295333        H    2.912456   17.569345   8.744439
H   -6.514565   13.509070   1.076297        H    2.254634   18.777985   7.926832
H   -4.989371   13.531103   0.592907        C    2.522272   18.696150   1.793828
C   -5.141095   11.766929   2.598218        H    2.116703   17.783375   1.833481
H   -4.554360   11.478933   1.867469        C    1.416440   19.670301   1.472827
H   -6.047723   11.426999   2.441494        H    0.681695   19.553844   2.111052
H   -4.801043   11.414409   3.446038        H    1.087529   19.505058   0.564584
C    5.005021   13.753001   2.481147        H    1.758614   20.586224   1.535139
C    5.575576   14.687809   1.425621        C    3.570278   18.680413   0.713755
H    6.517217   14.464336   1.263233        H    3.867360   19.596335   0.532484
H    5.509263   15.614748   1.739069        H    3.190970   18.290122   -0.101965
H    5.068947   14.588663   0.592907        H    4.334201   18.140616   1.008320
C    5.888572   13.850574   3.736827        C   -0.198142   16.931976   6.892076
H    5.572924   13.213205   4.409040        H    0.546417   17.391511   7.356583
H    5.838175   14.760201   4.099369        H   -1.023869   17.275054   7.320706
H    6.816951   13.644413   3.498909        C    1.435008   14.266044   6.886411
C    5.056480   12.308299   1.954328        H    1.432355   14.270765   5.906415
H    4.790433   11.691389   2.668083        H    1.424398   13.339105   7.209300
H    5.968148   12.098990   1.665428        H    2.241371   14.714563   7.213077
H    4.442954   12.213874   1.195256        C    0.005040   15.189835   9.397770
C   -3.244550   18.098125   4.197558        H    0.769228   15.732779   9.682895
C   -4.012452   18.241336   5.364490        H    0.114058   14.273913   9.731989
C   -4.911388   19.330371   5.428690        H   -0.822278   15.573830   9.756536
H   -5.421730   19.470435   6.216086        C   -1.594159   14.203094   6.995929
C   -5.055684   20.186491   4.369387        H   -2.389912   14.602826   7.401901
H   -5.639236   20.932449   4.446805        H   -1.506626   13.273008   7.290495
C   -4.361257   19.983478   3.177908        H   -1.673734   14.231421   6.019709
H   -4.514572   20.554749   2.435830        C   -0.328911   20.403669   6.686258
C   -3.434470   18.930639   3.072166        H   -0.342174   20.025960   7.558625
C   -2.726250   18.678839   1.748510        C   -1.509278   20.693239   6.042368
H   -1.867367   18.205140   1.948664        H   -2.339514   20.527995   6.476663
C   -3.572931   17.753474   0.872367        C   -1.499199   21.225166   4.756477
H   -3.684336   16.889485   1.319880        H   -2.310336   21.404574   4.295746
H   -3.127309   17.619705   0.011329        C   -0.297081   21.483261   4.174899
H   -4.453564   18.159501   0.723196        C    0.901853   21.182675   4.771582
C   -2.385402   19.952003   0.987550        H    1.721479   21.325886   4.316517
H   -3.212190   20.381636   0.683543        C    0.885938   20.664911   6.055586
H   -1.827579   19.728530   0.213371        H    1.705564   20.487078   6.506875
H   -1.896545   20.564191   1.576680        F   -0.272413   22.093876   2.962649
C   -3.917227   17.260890   6.521981
```

A.1.3   X-Ray structures of Alkyl cations containing Zirconium

X-Ray structure of η^6-3′-Zr-exo

Zr	7.285954	8.774163	15.782526
O	8.282123	10.391022	14.632517
N	6.037782	10.513949	15.737937
N	8.621293	7.924604	14.345425
C	7.683726	13.944571	13.954353
H	8.083844	14.707173	13.554143
C	6.413363	14.079126	14.540962
C	5.844292	12.955691	15.147673
H	4.984944	13.030522	15.547883
C	6.501660	11.731730	15.178739
C	9.525022	8.743962	13.625413
C	10.531792	8.332530	12.766515
H	10.671907	7.404743	12.623974
C	11.343474	9.257527	12.106808
C	11.096220	10.627797	12.284070
H	11.640386	11.257814	11.827209
C	9.764440	12.571519	13.303783
C	8.378486	12.736923	13.939733
C	7.752986	11.682390	14.572028
C	9.358702	10.107644	13.766126
C	10.070439	11.091258	13.115556
C	9.834116	13.312058	11.969750
H	9.634537	14.260729	12.110463
H	10.734898	13.220060	11.591469
H	9.179132	12.929556	11.348419
C	10.797486	13.166765	14.268673
H	10.611125	14.119810	14.400249
H	10.744894	12.702701	15.131226
H	11.695268	13.057588	13.892220
C	12.440608	8.749381	11.182122
C	13.324447	7.701830	11.956958
H	13.740545	8.134607	12.731793
H	12.761565	6.958546	12.260313
H	14.023335	7.358586	11.361211
C	11.825687	8.061895	10.014386
H	11.207569	7.370662	10.330534
H	11.335317	8.715614	9.471636
H	12.529310	7.648445	9.471636
C	13.413114	9.838731	10.772775
H	13.789554	10.258385	11.575022
H	14.135691	9.446844	10.239162
H	12.943058	10.511657	10.240989
C	5.689633	15.432942	14.502585
C	6.524951	16.475573	15.222598
H	7.412773	16.524700	14.809596
H	6.085299	17.350191	15.154982
H	6.615473	16.228322	16.165558
C	4.317907	15.369288	15.149500
H	3.771037	14.697344	14.690812
H	4.413528	15.121533	16.094288
H	3.883354	16.243402	15.083712
C	5.517302	15.862992	13.031494
H	4.977773	15.196934	12.558186
H	5.065259	16.732238	12.996773
H	6.396836	15.935524	12.607527
C	4.635503	10.649064	16.114390
C	4.260817	10.961367	17.426494
C	2.913795	11.137363	17.715230
H	2.652761	11.333561	18.608849
C	1.934866	11.036785	16.730238
C	2.325160	10.725841	15.440063
H	1.660592	10.635369	14.767565
C	3.667875	10.537688	15.094677
C	4.020244	10.264885	13.632723
H	5.013773	10.190733	13.552315
C	3.534732	11.429597	12.735448
H	3.766245	11.240789	11.801625
H	2.561892	11.521268	12.819511
H	3.967172	12.261118	13.018702
C	3.391500	8.966358	13.128348
H	3.640094	8.826729	12.190870
H	3.716534	8.215453	13.667444
H	2.416275	9.025349	13.203274
C	5.298783	11.151457	18.550371
H	6.087771	10.578845	18.329250
C	5.793157	12.598983	18.628951
H	6.121621	12.880460	17.749951
H	5.053736	13.180551	18.904895
H	6.518045	12.660645	19.285003
C	4.786192	10.718832	19.930090
H	4.468725	9.792612	19.882577
H	5.512989	10.781503	20.582487
H	4.048384	11.303261	20.202379
C	0.476312	11.367248	17.050041
H	0.375806	11.343025	18.044169
C	0.167541	12.787874	16.595007
H	0.818146	13.405717	16.987907
H	0.220425	12.837202	15.617325
H	-0.735038	13.033770	16.885571
C	-0.505722	10.357198	16.467086
H	-0.273983	9.458964	16.781406
H	-1.414166	10.580861	16.757650
H	-0.458407	10.382440	15.489404
C	8.724414	6.550147	13.901357
C	7.912949	6.118556	12.826820
C	8.096091	4.819031	12.346203
H	7.544826	4.513116	11.635328
C	9.052372	3.957291	12.870679
C	9.808169	4.402191	13.950698
H	10.450845	3.813735	14.330806
C	9.663728	5.672445	14.497103
C	6.864113	7.023863	12.198180
H	6.530177	7.631103	12.918193
C	7.428729	7.903651	11.098060
H	6.714230	8.464996	10.728916
H	8.134606	8.476678	11.465376
H	7.801984	7.342060	10.387184
C	5.647374	6.247618	11.660912
H	5.283776	5.679046	12.371787
H	4.960606	6.881427	11.364866
H	5.924244	5.689371	10.904351
C	10.476433	6.072451	15.719662
H	9.989020	6.820522	16.171041
C	11.869091	6.582939	15.366966
H	12.345549	6.825247	16.187488
H	12.364905	5.883029	14.895486
H	11.790337	7.372226	14.789494
C	10.597018	4.916060	16.741203
H	11.127022	5.215100	17.510556
H	9.703872	4.651283	17.042731
H	11.038640	4.151161	16.317236
C	9.260431	2.545222	12.327929
H	10.246890	2.386918	12.364477
C	8.642170	1.500104	13.241650
H	8.911817	1.676107	14.168163
H	7.666109	1.541500	13.172207
H	8.951510	0.610315	12.974843
C	8.883953	2.312729	10.968311
H	9.290919	2.995402	10.394494
H	9.193640	1.425966	10.690540
H	7.908521	2.357655	10.886076
C	8.775268	9.430622	17.320502
H	8.307558	9.853784	18.069754
H	9.275254	8.652146	17.643959
H	9.398000	10.073301	16.918465
C	6.607178	7.309345	18.119095
C	7.250882	6.408794	17.260196
H	8.069384	6.017177	17.537968
C	6.744188	6.074138	16.035810
H	7.186440	5.422365	15.504024
C	5.590706	6.675344	15.562502
H	5.258827	6.458109	14.698122
C	4.931415	7.581915	16.339165
H	4.138094	7.994394	16.019363
C	5.427308	7.904468	17.607411
H	4.960818	8.539566	18.139196
C	7.083585	7.573345	19.498814
H	6.495514	8.231630	19.926435
H	7.071395	6.740065	20.014153
H	7.998037	7.924672	19.467747

A.1. Geometries from the Chapter Coordination of Alkyl cations $[(XA_2)X(CH_2Y)]$
(X = Th, U or Zr; Y = SiMe$_3$, H) with an arene for Ethylene polymerisation: 123
Exploration of the bonding

A.1.4   Optimised geometries of Alkyl cations containing Thorium

Optimised geometry of η^6-2-Th and the name of the fragment f in the ETS-NOCV in which each atom belongs

Th	13.5411509	10.1377154	14.5509358	f=U	C	10.2305495	10.3306062	10.2068517 f=U
Si	13.4112173	7.5322504	17.4978204	f=U	H	10.8007652	10.0548590	9.3166019 f=U
O	13.4985180	7.8349960	13.6124273	f=U	H	9.5010599	11.0900207	9.9142923 f=U
N	11.5227749	9.3960006	13.7995967	f=U	H	9.6858193	9.4486246	10.5451961 f=U
C	10.9455192	5.5470351	12.3276461	f=U	C	11.9584772	12.0530811	10.7679995 f=U
H	10.8362841	4.5394039	11.9548734	f=U	H	12.5061723	11.7733943	9.8652660 f=U
N	15.5376637	9.3173458	13.8106982	f=U	H	12.6859752	12.4209590	11.4964693 f=U
C	9.8258568	6.3633255	12.4096511	f=U	H	11.3042754	12.8873466	10.5044660 f=U
C	9.9815248	7.6658022	12.8964944	f=U	C	9.6856998	9.7777687	16.0817399 f=U
H	9.1316192	8.3345344	12.9572021	f=U	H	10.5426491	9.1050062	16.0069246 f=U
C	11.2234660	8.1309948	13.3013923	f=U	C	8.4251433	8.9127275	16.1276204 f=U
C	15.7913673	8.0286696	13.3459828	f=U	H	8.3418233	8.2784856	15.2451328 f=U
C	17.0187729	7.5006963	12.9720467	f=U	H	7.5263993	9.5319572	16.1895833 f=U
H	17.8956188	8.1335073	13.0341862	f=U	H	8.4433803	8.2625803	17.0056007 f=U
C	17.1226427	6.1945221	12.4820930	f=U	C	9.8119876	10.5679219	17.3819215 f=U
C	15.9685601	5.4300640	12.3804617	f=U	H	10.7036482	11.1984294	17.3977057 f=U
H	16.0374282	4.4192964	12.0068144	f=U	H	9.8739262	9.8845784	18.2319737 f=U
C	13.4451964	5.0751477	12.6312720	f=U	H	8.9464597	11.2129345	17.5505540 f=U
C	12.2213251	5.9770285	12.7095653	f=U	C	16.6044161	10.2635307	13.8450668 f=U
C	12.3047788	7.2583693	13.1939544	f=U	C	16.7787840	11.1528864	12.7545679 f=U
C	14.6742893	7.2043935	13.2214293	f=U	C	17.7877195	12.1065971	12.8322780 f=U
C	14.7078764	5.9193695	12.7389865	f=U	H	17.9362931	12.7967494	12.0117006 f=U
C	13.4425255	4.2973168	11.3110614	f=U	C	18.6182955	12.1910936	13.9374748 f=U
H	14.3003684	3.6274961	11.2517737	f=U	H	19.4005878	12.9405693	13.9717481 f=U
H	13.4715311	4.9718018	10.4535549	f=U	C	18.4522472	11.3108758	14.9886070 f=U
H	12.5523668	3.6736791	11.2287250	f=U	H	19.1161094	11.3728628	15.8433492 f=U
C	13.4074615	4.0789474	13.8032364	f=U	C	17.4577070	10.3361746	14.9682044 f=U
H	14.2796188	3.4222287	13.7710610	f=U	C	15.9297148	11.0708127	11.4977558 f=U
H	12.5082246	3.4614699	13.7473022	f=U	H	14.9128837	10.7741860	11.7951912 f=U
H	13.4059143	4.5973764	14.7637199	f=U	C	15.8265003	12.3878320	10.7349313 f=U
C	8.4395024	5.8845547	11.9793421	f=U	H	15.5639355	13.2360915	11.3706355 f=U
C	7.9176908	6.7810542	10.8503947	f=U	H	15.0700117	12.3039652	9.9530766 f=U
H	8.5838292	6.7503773	9.9846807	f=U	H	16.7676868	12.6329311	10.2376493 f=U
H	7.8214859	7.8214193	11.1686322	f=U	C	16.4421692	9.9914081	10.5407292 f=U
H	6.9292862	6.4430363	10.5290679	f=U	H	16.4464425	9.0022685	10.9946364 f=U
C	7.4777847	5.9633618	13.1704677	f=U	H	17.4630052	10.2261678	10.2276067 f=U
H	6.4876781	5.6046543	12.8780991	f=U	H	15.8179199	9.9548450	9.6445553 f=U
H	7.3622998	6.9872296	13.5318342	f=U	C	17.3648884	9.3733850	16.1341247 f=U
H	7.8299581	5.3480955	14.0018572	f=U	H	16.4718301	8.7616463	15.9910548 f=U
C	8.4539888	4.4440075	11.4745932	f=U	C	18.5702046	8.4333869	16.1724097 f=U
H	9.0968831	4.3240268	10.5991082	f=U	H	18.6555576	7.8490821	15.2572107 f=U
H	7.4433857	4.1532997	11.1803993	f=U	H	18.4762324	7.7339345	17.0065442 f=U
H	8.7837445	3.7442284	12.2464610	f=U	H	19.4997500	8.9918326	16.3103739 f=U
C	18.4863186	5.6656603	12.0377325	f=U	C	17.2415441	10.0901175	17.4769903 f=U
C	18.9881421	6.5088337	10.8587986	f=U	H	17.1033516	9.3630039	18.2805042 f=U
H	19.0965641	7.5610272	11.1309185	f=U	H	16.3937546	10.7770891	17.5005999 f=U
H	18.2996336	6.4479457	10.0124772	f=U	H	18.1402206	10.6649430	17.7121421 f=U
H	19.9653575	6.1483343	10.5274803	f=U	C	13.4931435	9.2830186	16.8053328 f=U
C	19.4892647	5.7671788	13.1915918	f=U	H	14.3816515	9.7454179	17.2697837 f=U
H	19.6540149	6.8018053	13.4986825	f=U	H	12.6316977	9.8147787	17.2471611 f=U
H	20.4560660	5.3615223	12.8833908	f=U	C	14.9126528	6.5317840	16.9803795 f=U
H	19.1473189	5.2033597	14.0628291	f=U	H	14.8187365	5.5078077	17.3538912 f=U
C	18.4249925	4.2074922	11.5900877	f=U	H	15.8303965	6.9446519	17.4074739 f=U
H	17.7678338	4.0709094	10.7278683	f=U	H	15.0428410	6.4776692	15.8967079 f=U
H	18.0861434	3.5483540	12.3932988	f=U	C	11.8474905	6.6589310	16.9367496 f=U
H	19.4228595	3.8776437	11.2937161	f=U	H	11.8420964	5.6339427	17.3191504 f=U
C	10.5226752	10.4095246	13.7394240	f=U	H	11.7489874	6.6064370	15.8496706 f=U
C	10.3924842	11.1763814	12.5587559	f=U	H	10.9543500	7.1515076	17.3302000 f=U
C	9.4745988	12.2211291	12.5401612	f=U	C	13.3884479	7.6116642	19.3749136 f=U
H	9.3631736	12.8172040	11.6410803	f=U	H	13.3422745	6.6090710	19.8097699 f=U
C	8.6829065	12.5007577	13.6402780	f=U	H	12.5222756	8.1700561	19.7406040 f=U
H	7.9697568	13.3162732	13.6040570	f=U	H	14.2860040	8.0995391	19.7649674 f=U
C	8.7817089	11.7146781	14.7742515	f=U	C	14.9635327	13.0048072	15.1370528 f=B
H	8.1297067	11.9162214	15.6167982	f=U	H	16.0276938	13.0028906	14.9293386 f=B
C	9.6845539	10.6577207	14.8487296	f=U	C	14.0518998	13.2555576	14.1108529 f=B
C	11.1667063	10.8589817	11.2945455	f=U	H	14.4129924	13.4643714	13.1114026 f=B
H	11.8752658	10.0584404	11.5264475	f=U	C	12.6851956	13.2744506	14.3762951 f=B

```
H    11.9749179   13.4871561   13.5868063  f=B        H    12.7760406   12.5675868   17.6921270  f=B
C    12.2238385   13.0253003   15.6668106  f=B        C    14.4981855   12.7588473   16.4235351  f=B
H    11.1596929   13.0395968   15.8654698  f=B        H    15.2011788   12.5782390   17.2268758  f=B
C    13.1300729   12.7600194   16.6864401  f=B
```

Optimised geometry of η^6-2′-Th and the name of the fragment f in the ETS-NOCV in which each atom belongs

```
C     6.448660    8.349540   15.663848  f=B        C     8.059835   16.032898   16.559612  f=U
C     7.300386    9.148847   14.911264  f=B        C     2.373532   14.098188   13.786825  f=U
C     6.925039   10.448375   14.570928  f=B        H    10.152131   10.330023   23.888875  f=U
C     5.699877   10.954523   14.987350  f=B        H     8.450525    7.308436   21.378778  f=U
C     4.845149   10.153568   15.744930  f=B        H     6.221636   15.391464   19.216544  f=U
C     5.217007    8.854583   16.079916  f=B        H     8.801289   15.121396   22.622734  f=U
H     8.256217    8.763558   14.578559  f=B        H    10.459639   12.330648   24.238107  f=U
Th    7.164431   10.644975   17.851354  f=U        H    10.002900   13.958665   23.806240  f=U
C     9.379337   10.971753   16.902655  f=U        H     8.744294   12.767600   24.174469  f=U
O     8.269407   11.505852   19.921606  f=U        H    11.824988   12.142624   22.141416  f=U
C     8.688510   10.620761   20.908436  f=U        H    11.103007   12.465198   20.558827  f=U
C     9.324873   11.041861   22.054830  f=U        H    11.358488   13.796020   21.696255  f=U
C     9.682854   12.512835   22.223304  f=U        H     8.428081   17.782964   19.900585  f=U
C     8.678455   13.348153   21.439599  f=U        H     6.782925   17.546487   19.293858  f=U
C     8.078501   12.823486   20.321152  f=U        H     7.112413   18.826152   20.456160  f=U
C     8.365939    9.300966   20.626994  f=U        H     4.984813   16.574685   20.818948  f=U
C     8.713481    8.339491   21.572384  f=U        H     5.357082   16.227597   22.511691  f=U
C     9.353649    8.701681   22.755722  f=U        H     5.286129   17.901841   21.943617  f=U
C     9.650656   10.046886   22.973504  f=U        H     8.933574   17.373606   22.393645  f=U
C     8.355137   14.672802   21.748207  f=U        H     7.546741   18.388853   22.782707  f=U
C     7.480591   15.423653   20.971475  f=U        H     7.650387   16.766923   23.457643  f=U
C     6.917940   14.836237   19.833472  f=U        H    11.640703    8.634550   24.297409  f=U
C     7.203610   13.520925   19.493551  f=U        H    11.550679    6.930088   24.745862  f=U
C     9.736427    7.670919   23.817652  f=U        H    11.756464    7.390254   23.049753  f=U
C     9.081644    8.043433   25.153185  f=U        H     8.200520    6.195917   23.330624  f=U
N     7.699676    9.092247   19.423501  f=U        H     9.755592    5.905573   22.528094  f=U
C     7.296067    7.779314   19.050671  f=U        H     9.569888    5.568591   24.244652  f=U
C     8.212604    6.884735   18.461359  f=U        H     7.992544    8.059968   25.064985  f=U
C     7.754086    5.636466   18.050225  f=U        H     9.348778    7.310570   25.918811  f=U
C     6.433287    5.239485   18.194469  f=U        H     9.404244    9.024079   25.507326  f=U
C     5.549754    6.133385   18.792223  f=U        H     8.457690    4.940785   17.603033  f=U
C     5.948273    7.386616   19.238601  f=U        H     4.518457    5.831085   18.931744  f=U
N     6.689588   12.792345   18.424627  f=U        H     5.219483    9.316942   19.783169  f=U
C     5.804834   13.415369   17.499156  f=U        H     4.397689    8.719048   22.029836  f=U
C     4.411124   13.178389   17.596127  f=U        H     4.869599    7.036302   21.762049  f=U
C     3.571541   13.739065   16.642895  f=U        H     6.105086    8.298043   21.846915  f=U
C     4.046292   14.544896   15.611789  f=U        H     2.880197    8.812384   20.072817  f=U
C     5.411699   14.775050   15.549290  f=U        H     3.345861    8.153629   18.502933  f=U
C     6.308386   14.229095   16.463696  f=U        H     3.132745    7.088407   19.893355  f=U
C     7.088977   16.853075   21.347217  f=U        H     9.832313    8.249140   18.605377  f=U
C     7.854314   17.363808   22.565489  f=U        H    10.302822    6.411946   20.214725  f=U
C     9.714309   12.913093   23.695877  f=U        H    10.466955    5.272560   18.873125  f=U
C    11.079816   12.742952   21.614541  f=U        H    11.611734    6.604369   19.047000  f=U
C     9.681194    7.215740   18.284940  f=U        H     9.526918    7.732119   16.168719  f=U
C    10.126998    7.102465   16.828350  f=U        H    11.169676    7.411654   16.726623  f=U
C     5.978854    3.873659   17.737045  f=U        H    10.053588    6.074735   16.464599  f=U
C     4.915656    3.964707   16.644952  f=U        H     6.854906    3.374881   17.308324  f=U
C     4.961000    8.267096   19.984546  f=U        H     6.253572    2.933285   19.681652  f=U
C     3.505638    8.065806   19.579893  f=U        H     4.597109    3.460537   19.367043  f=U
C     3.819112   12.378437   18.744211  f=U        H     5.227143    2.020410   18.567851  f=U
C     2.457881   11.761962   18.444061  f=U        H     5.272237    4.536188   15.784462  f=U
C     3.108121   15.160683   14.601050  f=U        H     4.641388    2.967195   16.294703  f=U
C     2.122265   16.121320   15.262480  f=U        H     4.005624    4.444141   17.016024  f=U
C     7.782213   14.549984   16.314864  f=U        H     2.505624   13.557923   16.711566  f=U
C     8.319906   14.149930   14.942119  f=U        H     5.794312   15.410401   14.756373  f=U
C     7.371238   17.801557   20.177554  f=U        H     4.509890   11.552580   18.975309  f=U
C     5.590301   16.887479   21.672558  f=U        H     3.298689   12.635573   20.832968  f=U
C    11.260601    7.659871   23.985513  f=U        H     4.681936   13.614883   20.330078  f=U
C     9.285294    6.260050   23.448736  f=U        H     3.048178   14.075460   19.840086  f=U
C     5.098534    8.071927   21.496682  f=U        H     2.443194   11.181806   17.518788  f=U
C    10.562128    6.323028   19.159695  f=U        H     2.166043   11.098397   19.259802  f=U
C     5.488537    3.024870   18.908129  f=U        H     1.681735   12.526691   18.367518  f=U
C     3.715116   13.226717   20.013531  f=U        H     8.328201   13.979937   17.070267  f=U
```

```
H    9.130050   16.234179   16.471880 f=U         H    1.498399   16.605965   14.508211 f=U
H    7.543497   16.656840   15.825489 f=U         H    1.457184   15.594541   15.951904 f=U
H    7.742040   16.343841   17.554241 f=U         H    9.871404   10.025805   16.646618 f=U
H    9.397846   14.319703   14.894657 f=U         H    9.413709   11.606802   16.011060 f=U
H    8.138224   13.095654   14.726289 f=U         H   10.003158   11.456396   17.663952 f=U
H    7.860456   14.737197   14.143512 f=U         H    7.590831   11.058690   13.973750 f=B
H    3.726010   15.742515   13.908517 f=U         H    5.407176   11.967868   14.736753 f=B
H    3.071820   13.431188   13.275369 f=U         H    3.884992   10.544719   16.056569 f=B
H    1.726274   13.487868   14.422540 f=U         H    4.550204    8.224420   16.654750 f=B
H    1.741605   14.566840   13.029173 f=U         H    6.736682    7.341461   15.938480 f=B
H    2.640904   16.899829   15.825484 f=U
```

Optimised geometry of η^6-3-Th-endo and the name of the fragment f in the ETS-NOCV in which each atom belongs

```
Th   26.469113   25.919467   3.054570 f=Th        C    23.437643   26.045708   3.736822 f=Th
Si   26.498129   23.187135   0.209239 f=Th        C    23.193232   26.811633   4.899734 f=Th
O    26.545771   23.688876   4.136458 f=Th        C    22.251709   27.832567   4.840704 f=Th
N    24.479648   25.075114   3.757777 f=Th        H    22.052590   28.425707   5.726678 f=Th
N    28.517924   25.221841   3.760973 f=Th        C    21.550486   28.094794   3.676630 f=Th
C    24.105598   21.278497   5.415433 f=Th        C    20.820296   28.895638   3.649621 f=Th
H    24.052209   20.284913   5.836461 f=Th        C    21.758117   27.308521   2.557807 f=Th
C    22.935505   22.003301   5.237570 f=Th        H    21.170142   27.492155   1.666019 f=Th
C    23.021269   23.288249   4.689001 f=Th        C    22.679653   26.264577   2.564402 f=Th
H    22.129472   23.886926   4.549660 f=Th        C    22.752016   25.336264   1.369209 f=Th
C    24.244585   23.822236   4.316302 f=Th        H    23.644763   24.718343   1.483349 f=Th
C    28.834930   23.976126   4.298954 f=Th        C    21.543678   24.396568   1.366107 f=Th
C    30.095976   23.511931   4.639610 f=Th        H    21.603724   23.704147   0.522898 f=Th
H    30.946854   24.165120   4.489640 f=Th        H    21.492525   23.805016   2.280166 f=Th
C    30.271912   22.231574   5.176165 f=Th        H    20.611991   24.960193   1.271014 f=Th
C    29.152555   21.435039   5.371738 f=Th        C    22.833622   26.056432   0.026414 f=Th
H    29.274497   20.444078   5.784788 f=Th        H    22.931493   25.326972  -0.780787 f=Th
C    26.640519   20.976713   5.274151 f=Th        H    21.934328   26.641345  -0.179127 f=Th
C    25.365650   21.783038   5.072275 f=Th        H    23.689098   26.732023  -0.040362 f=Th
C    25.380943   23.041064   4.525425 f=Th        C    23.882047   26.522059   6.217689 f=Th
C    27.754998   23.120629   4.514888 f=Th        H    24.563594   25.682679   6.062735 f=Th
C    27.858350   21.862623   5.053187 f=Th        C    22.873655   26.093737   7.283140 f=Th
C    26.668153   19.821188   4.259757 f=Th        H    23.391056   25.834750   8.209990 f=Th
H    25.803826   19.169318   4.401271 f=Th        H    22.169142   26.897423   7.509556 f=Th
H    26.648363   20.196642   3.234743 f=Th        H    22.301963   25.222208   6.962220 f=Th
H    27.572801   19.223325   4.386791 f=Th        C    24.703823   27.707821   6.711773 f=Th
C    26.670432   20.405166   6.697648 f=Th        H    25.221499   27.453694   7.639612 f=Th
H    26.651614   21.203516   7.441974 f=Th        H    25.456603   28.016314   5.981290 f=Th
H    25.815150   19.752300   6.873370 f=Th        H    24.071507   28.575248   6.916668 f=Th
H    27.568157   19.807784   6.858219 f=Th        C    29.534589   26.220856   3.708390 f=Th
C    21.565837   21.440444   5.616069 f=Th        C    29.742928   27.052520   4.833574 f=Th
C    20.892009   22.367916   6.633781 f=Th        C    30.701983   28.055733   4.751219 f=Th
H    19.915904   21.967019   6.917791 f=Th        H    30.877429   28.696796   5.607479 f=Th
H    21.495885   22.461869   7.539534 f=Th        C    31.453602   28.241287   3.604421 f=Th
H    20.728952   23.368796   6.228016 f=Th        H    32.200623   29.025774   3.564420 f=Th
C    20.690088   21.347737   4.361113 f=Th        C    31.264721   27.406359   2.519459 f=Th
H    21.148432   20.701537   3.608780 f=Th        H    31.876719   27.539654   1.634518 f=Th
H    19.711579   20.932108   4.615291 f=Th        C    30.319452   26.384784   2.546155 f=Th
H    20.524517   22.327814   3.909266 f=Th        C    30.216109   25.460988   1.351702 f=Th
C    21.661712              6.233881 f=Th        H    29.349086   24.815817   1.506254 f=Th
H    22.092698   19.321863   5.540052 f=Th        C    31.446241   24.558303   1.250698 f=Th
H    22.256036   20.047567   7.150917 f=Th        H    31.355726   23.889038   0.391749 f=Th
H    20.660483   19.696860   6.492125 f=Th        H    32.356540   25.148614   1.117881 f=Th
C    31.679939   21.758846   5.537326 f=Th        H    31.566469   23.942200   2.141915 f=Th
C    31.690734   20.333640   6.084065 f=Th        C    30.025468   26.218907   0.039455 f=Th
H    31.307353   19.614486   5.356066 f=Th        H    29.851268   25.518546  -0.780545 f=Th
H    32.716728   20.044169   6.320659 f=Th        H    29.177639   26.906995   0.078308 f=Th
H    31.106100   20.243909   7.002891 f=Th        H    30.910057   26.805036  -0.220261 f=Th
C    32.268408   22.686666   6.606896 f=Th        C    29.008315   26.849444   6.143433 f=Th
H    32.339373   23.718410   6.255516 f=Th        H    28.164802   26.176540   5.954794 f=Th
H    31.657825   22.678132   7.513038 f=Th        C    29.909590   26.164717   7.172527 f=Th
H    33.276153   22.359312   6.874867 f=Th        H    30.266565   25.198930   6.815215 f=Th
C    32.571260   21.798332   4.290836 f=Th        H    30.778685   26.788618   7.397685 f=Th
H    32.672828   22.810963   3.895951 f=Th        H    29.364612   26.001022   8.105411 f=Th
H    33.574293   21.439714   4.535737 f=Th        C    28.457855   28.149350   6.722713 f=Th
H    32.168149   21.163421   3.498296 f=Th        H    27.861080   27.941690   7.613142 f=Th
```

```
H   29.258894   28.827417    7.024926 f=Th        H   25.048904   21.204938    0.430768 f=Th
H   27.826359   28.679312    6.006731 f=Th        C   26.827615   28.441463    1.316750 f=A
C   26.484300   24.957442    0.858341 f=Th        H   27.085837   27.949098    0.386075 f=A
H   25.609820   25.448510    0.394133 f=Th        C   27.820063   28.983913    2.131822 f=A
H   27.365781   25.442901    0.403947 f=Th        H   28.865567   28.874316    1.869306 f=A
C   28.047737   22.290222    0.770925 f=Th        C   27.470234   29.689727    3.274113 f=A
H   28.154622   22.260180    1.858087 f=Th        H   28.253011   30.128912    3.882477 f=A
H   28.022145   21.257050    0.412318 f=Th        C   26.133457   29.867310    3.638993 f=A
H   28.950212   22.749567    0.359284 f=Th        C   25.150973   29.272326    2.846033 f=A
C   26.484766   23.216983   -1.668929 f=Th        H   24.105505   29.373111    3.116053 f=A
H   26.497324   22.202336   -2.077350 f=Th        C   25.490418   28.582979    1.686483 f=A
H   25.591738   23.716558   -2.054552 f=Th        H   24.702520   28.189350    1.055050 f=A
H   27.356506   23.743600   -2.067007 f=Th        C   25.764723   30.726492    4.805827 f=A
C   24.987683   22.236778    0.789041 f=Th        H   24.755135   30.515800    5.157193 f=A
H   24.893503   22.203574    1.877209 f=Th        H   26.459298   30.603577    5.638495 f=A
H   24.064604   22.661076    0.385989 f=Th        H   25.799387   31.780010    4.512007 f=A
```

Optimised geometry of η^6-4-Th-endo and the name of the fragment f in the ETS-NOCV in which each atom belongs

```
C   -0.405504   20.474935    6.472660 f=B         C   -5.051963   11.934404    1.913275 f=Th
H   -0.451964   19.897584    7.391840 f=B         H   -4.461375   11.881833    0.995315 f=Th
C   -1.580961   20.887258    5.843236 f=B         H   -6.056915   11.579727    1.675306 f=Th
H   -2.548584   20.589392    6.230125 f=B         H   -4.624376   11.241402    2.642110 f=Th
C   -1.525375   21.714859    4.730646 f=B         C    4.991460   13.666076    2.472793 f=Th
H   -2.437800   22.049040    4.254497 f=B         C    5.605641   14.606920    1.429624 f=Th
C   -0.289387   22.128361    4.248432 f=B         H    6.611113   14.269476    1.165878 f=Th
C    0.890761   21.705107    4.846807 f=B         H    5.689967   15.629811    1.802986 f=Th
H    1.848502   22.028407    4.460721 f=B         H    5.005237   14.626711    0.516798 f=Th
C    0.828943   20.882566    5.963866 f=B         C    5.863277   13.672319    3.733919 f=Th
H    1.751910   20.590332    6.451028 f=B         H    5.445883   13.018721    4.503511 f=Th
Br  -0.214734   23.294165    2.778681 f=B         H    5.958830   14.674531    4.156801 f=Th
O   -0.137029   15.618435    3.854669 f=Th        H    6.869528   13.318038    3.496458 f=Th
Th  -0.207254   17.846730    4.922957 f=Th        C    4.995106   12.251723    1.898777 f=Th
Si  -0.118522   15.157580    7.798293 f=Th        H    4.601785   11.521239    2.610039 f=Th
N   -2.193952   17.020068    4.221336 f=Th        H    6.020457   11.958932    1.663655 f=Th
N    1.830457   17.131702    4.248284 f=Th        H    4.415627   12.184283    0.974691 f=Th
C   -2.590922   13.195811    2.629948 f=Th        C   -3.237475   17.989542    4.256989 f=Th
H   -2.649661   12.196827    2.222161 f=Th        C   -4.030672   18.149565    5.415555 f=Th
C   -3.759238   13.920821    2.819720 f=Th        C   -5.001467   19.147346    5.425738 f=Th
C   -3.667255   15.213281    3.349689 f=Th        H   -5.621181   19.275276    6.305987 f=Th
H   -4.558044   15.812622    3.494180 f=Th        C   -5.207280   19.962933    4.328997 f=Th
C   -2.438551   15.756988    3.687913 f=Th        H   -5.976300   20.726544    4.355224 f=Th
C    2.153015   15.892179    3.702890 f=Th        C   -4.442450   19.787016    3.189331 f=Th
C    3.412718   15.428971    3.359864 f=Th        H   -4.626331   20.416672    2.326806 f=Th
H    4.264951   16.080615    3.510567 f=Th        C   -3.455403   18.810081    3.123461 f=Th
C    3.584121   14.146308    2.825456 f=Th        C   -2.699432   18.621235    1.823636 f=Th
C    2.462686   13.351421    2.632720 f=Th        H   -1.814047   18.009960    2.034213 f=Th
H    2.583210   12.359043    2.222378 f=Th        C   -3.546606   17.848541    0.810246 f=Th
C   -0.052978   12.900052    2.731413 f=Th        H   -3.840670   16.870516    1.190998 f=Th
C   -1.326425   13.706023    2.946988 f=Th        H   -2.986463   17.698609   -0.115853 f=Th
C   -1.306004   14.970620    3.477839 f=Th        H   -4.453714   18.407897    0.566263 f=Th
C    1.070082   15.041016    3.483720 f=Th        C   -2.233279   19.937665    1.209300 f=Th
C    1.168536   13.781983    2.949052 f=Th        H   -3.075021   20.541094    0.863108 f=Th
C   -0.017853   11.736482    3.735730 f=Th        H   -1.603845   19.742514    0.338989 f=Th
H   -0.029700   12.103119    4.763913 f=Th        H   -1.658794   20.545727    1.911388 f=Th
H    0.885644   11.139244    3.596541 f=Th        C   -3.908763   17.243891    6.622137 f=Th
H   -0.882813   11.084915    3.595519 f=Th        H   -3.024594   16.619234    6.479860 f=Th
C   -0.034995   12.340189    1.302920 f=Th        C   -5.115906   16.310986    6.727848 f=Th
H   -0.892939   11.689904    1.129312 f=Th        H   -6.041430   16.878823    6.853081 f=Th
H    0.861273   11.743464    1.130502 f=Th        H   -5.010901   15.650904    7.592229 f=Th
H   -0.059071   13.144276    0.565289 f=Th        H   -5.217683   15.685165    5.840912 f=Th
C   -5.133420   13.357466    2.459291 f=Th        C   -3.743717   18.023576    7.925264 f=Th
C   -6.023893   13.339843    3.706953 f=Th        H   -2.909258   18.729106    7.886016 f=Th
H   -5.581815   12.728508    4.497247 f=Th        H   -3.560794   17.337950    8.755902 f=Th
H   -7.003768   12.922166    3.462486 f=Th        H   -4.642262   18.594119    8.171093 f=Th
H   -6.185632   14.343492    4.105414 f=Th        C    2.801737   18.172617    4.277836 f=Th
C   -5.780717   14.244655    1.389207 f=Th        C    2.987104   18.971199    3.124594 f=Th
H   -5.918110   15.270121    1.739052 f=Th        C    3.880039   20.034852    3.186067 f=Th
H   -6.765218   13.852638    1.121674 f=Th        H    4.035063   20.650536    2.307169 f=Th
H   -5.170988   14.274494    0.482843 f=Th        C    4.586737   20.313735    4.342532 f=Th
```

A.1. Geometries from the Chapter Coordination of Alkyl cations [(XA₂)X(CH₂Y)]
(X = Th, U or Zr; Y = SiMe₃, H) with an arene for Ethylene polymerisation: 127
Exploration of the bonding

Atom	X	Y	Z	Frag
H	5.281749	21.145330	4.368413	f=Th
C	4.424848	19.510406	5.456396	f=Th
H	5.008658	19.715130	6.346571	f=Th
C	3.550639	18.426862	5.449285	f=Th
C	3.499367	17.521187	6.661331	f=Th
H	2.662577	16.833095	6.525282	f=Th
C	4.772863	16.678442	6.753621	f=Th
H	4.912909	16.065453	5.862802	f=Th
H	4.723898	16.009073	7.615874	f=Th
H	5.654796	17.312999	6.873193	f=Th
C	3.289628	18.282035	7.968393	f=Th
H	4.139740	18.926328	8.203837	f=Th
H	3.179184	17.580687	8.798633	f=Th
H	2.396106	18.911775	7.947592	f=Th
C	2.292167	18.676893	1.811438	f=Th
H	1.574111	17.869313	1.983082	f=Th
C	1.528826	19.884834	1.276874	f=Th
H	0.798356	20.263812	1.996235	f=Th
H	0.994162	19.621003	0.361992	f=Th
H	2.200758	20.710783	1.033392	f=Th
C	3.290381	18.176866	0.766672	f=Th
H	4.036423	18.942970	0.540609	f=Th
H	2.773134	17.930509	-0.163594	f=Th
H	3.813374	17.283323	1.109274	f=Th
C	-0.186655	16.922252	7.134223	f=Th
H	0.666802	17.451565	7.594321	f=Th
H	-1.089616	17.373716	7.581814	f=Th
C	1.445115	14.287914	7.233342	f=Th
H	1.548189	14.256041	6.145824	f=Th
H	1.438215	13.255484	7.595246	f=Th
H	2.341017	14.763455	7.640635	f=Th
C	-0.122014	15.200019	9.675767	f=Th
H	0.740214	15.748334	10.065100	f=Th
H	-0.084483	14.188510	10.090308	f=Th
H	-1.023474	15.682360	10.063522	f=Th
C	-1.613888	14.177721	7.228798	f=Th
C	-2.542246	14.587068	7.635410	f=Th
H	-1.533799	13.147503	7.588106	f=Th
H	-1.712607	14.141432	6.140946	f=Th

Optimised geometry of η^6-5-Th-endo and the name of the fragment f in the ETS-NOCV in which each atom belongs

Atom	X	Y	Z	Frag
O	-0.113290	15.647010	3.880077	f=Th
Th	-0.166280	17.900891	4.905746	f=Th
Si	-0.087969	15.235443	7.805776	f=Th
N	-2.165704	17.090403	4.182502	f=Th
N	1.866667	17.148530	4.243142	f=Th
C	-2.582531	13.236490	2.659033	f=Th
H	-2.647753	12.231946	2.266731	f=Th
C	-3.744286	13.977853	2.822147	f=Th
C	-3.642578	15.277400	3.331435	f=Th
H	-4.527883	15.890055	3.450659	f=Th
C	-2.411730	15.815317	3.675216	f=Th
C	2.177651	15.904927	3.703822	f=Th
C	3.429527	15.439816	3.335895	f=Th
H	4.284286	16.093500	3.460955	f=Th
C	3.589099	14.153768	2.806751	f=Th
C	2.463456	13.358168	2.644887	f=Th
H	2.575219	12.362194	2.241297	f=Th
C	-0.051179	12.912731	2.797166	f=Th
C	-1.316937	13.737753	2.983853	f=Th
C	-1.287019	15.010633	3.495873	f=Th
C	1.087975	15.057754	3.505926	f=Th
C	1.175797	13.793946	2.980461	f=Th
C	-0.022519	11.789710	3.847225	f=Th
H	-0.029347	12.196750	4.860118	f=Th
H	0.876608	11.181124	3.729836	f=Th
H	-0.893001	11.140054	3.734421	f=Th
C	-0.040024	12.295266	1.392980	f=Th
H	-0.902325	11.644219	1.247149	f=Th
H	0.850499	11.684131	1.243645	f=Th
H	-0.059345	13.068393	0.622849	f=Th
C	-5.119217	13.426088	2.446149	f=Th
C	-6.039502	13.454456	3.671479	f=Th
H	-5.623928	12.862134	4.490162	f=Th
H	-7.017604	13.039826	3.415047	f=Th
H	-6.200833	14.471030	4.035639	f=Th
C	-5.727284	14.295041	1.338655	f=Th
H	-5.854070	15.331563	1.658642	f=Th
H	-6.712233	13.912474	1.059194	f=Th
H	-5.097090	14.290747	0.445920	f=Th
C	-5.047940	11.988066	1.939097	f=Th
H	-4.440792	11.902783	1.034528	f=Th
H	-6.053188	11.641543	1.690572	f=Th
H	-4.644479	11.308689	2.694082	f=Th
C	4.988060	13.671321	2.425766	f=Th
C	5.581391	14.610664	1.369169	f=Th
H	6.580098	14.271050	1.083497	f=Th
H	5.675937	15.633130	1.741149	f=Th
H	4.960728	14.632329	0.470099	f=Th
C	5.885668	13.677860	3.668690	f=Th
H	5.484188	13.024211	4.446653	f=Th
H	5.989379	14.680056	4.089744	f=Th
H	6.886933	13.323698	3.410802	f=Th
C	4.978106	12.256545	1.852919	f=Th
H	4.600553	11.526823	2.573438	f=Th
H	5.997753	11.962887	1.595146	f=Th
H	4.377755	12.188769	0.942284	f=Th
C	-3.232968	18.037255	4.205087	f=Th
C	-4.047439	18.169601	5.351552	f=Th
C	-5.047945	19.137940	5.350668	f=Th
H	-5.683965	19.244069	6.222313	f=Th
C	-5.262442	19.950175	4.253546	f=Th
H	-6.053750	20.690938	4.270148	f=Th
C	-4.477767	19.797994	3.123648	f=Th
H	-4.670010	20.423302	2.259974	f=Th
C	-3.461474	18.850414	3.068484	f=Th
C	-2.686820	18.683362	1.775485	f=Th
H	-1.760730	18.142998	2.005339	f=Th
C	-3.470813	17.825691	0.779073	f=Th
H	-3.694297	16.837867	1.180846	f=Th
H	-2.897702	17.696742	-0.142317	f=Th
H	-4.415323	18.311951	0.520501	f=Th
C	-2.312948	20.009436	1.119460	f=Th
H	-3.194104	20.538000	0.749816	f=Th
H	-1.669647	19.828636	0.256191	f=Th
H	-1.782123	20.680727	1.796939	f=Th
C	-3.918135	17.263826	6.558240	f=Th
H	-3.021209	16.656145	6.422648	f=Th
C	-5.108788	16.309217	6.655917	f=Th
H	-6.045253	16.859893	6.776672	f=Th
H	-4.996685	15.650719	7.520671	f=Th
H	-5.194104	15.681975	5.768721	f=Th
C	-3.777868	18.042059	7.864942	f=Th
H	-2.946677	18.750839	7.837847	f=Th
H	-3.603172	17.355608	8.696696	f=Th
H	-4.683927	18.606127	8.098320	f=Th
C	2.840200	18.187015	4.265407	f=Th
C	3.047763	18.953298	3.095430	f=Th
C	3.896610	20.052422	3.158550	f=Th
H	4.059220	20.652462	2.270186	f=Th
C	4.546634	20.388381	4.333813	f=Th
H	5.202499	21.250933	4.365176	f=Th
C	4.386708	19.598153	5.458293	f=Th
H	4.940889	19.840506	6.357663	f=Th
C	3.556916	18.479574	5.448482	f=Th

```
C    3.541588   17.557385    6.650437 f=Th      H    1.590072   14.320769    6.170590 f=Th
H    2.690467   16.882410    6.539847 f=Th      H    1.464248   13.327870    7.623986 f=Th
C    4.807905   16.696664    6.659002 f=Th      H    2.371390   14.832884    7.669985 f=Th
H    4.896362   16.103399    5.748857 f=Th      C   -0.097001   15.293656    9.683222 f=Th
H    4.792615   16.007682    7.506909 f=Th      H    0.763556   15.846266   10.070285 f=Th
H    5.701321   17.320076    6.749304 f=Th      H   -0.059517   14.285856   10.106740 f=Th
C    3.412374   18.278769    7.988585 f=Th      H   -1.000217   15.778226   10.064110 f=Th
H    4.275761   18.914900    8.195622 f=Th      C   -1.582102   14.249737    7.242728 f=Th
H    3.352749   17.549112    8.799206 f=Th      H   -2.510253   14.662636    7.646296 f=Th
H    2.518608   18.904182    8.048089 f=Th      H   -1.502411   13.222293    7.609940 f=Th
C    2.400678   18.593323    1.773874 f=Th      H   -1.681352   14.205223    6.155251 f=Th
H    1.888765   17.637203    1.900539 f=Th      C   -0.653737   20.458107    6.769763 f=F
C    1.363050   19.627863    1.350755 f=Th      H   -0.802646   20.044086    7.759425 f=F
H    0.560101   19.731821    2.088269 f=Th      C   -1.744219   20.879930    6.011475 f=F
H    0.901674   19.343836    0.402473 f=Th      H   -2.752289   20.766436    6.389852 f=F
H    1.808500   20.617403    1.223588 f=Th      C   -1.551659   21.460755    4.766006 f=F
C    3.442791   18.400287    0.673786 f=Th      H   -2.387660   21.804933    4.170855 f=F
H    3.967942   19.330621    0.445382 f=Th      C   -0.257589   21.607648    4.291723 f=F
H    2.959241   18.061882   -0.245333 f=Th      C    0.846552   21.174993    5.010291 f=F
H    4.185743   17.653395    0.957927 f=Th      H    1.845147   21.305425    4.609919 f=F
C   -0.160675   16.994646    7.128982 f=Th      C    0.637143   20.613982    6.267054 f=F
H    0.680462   17.537292    7.596724 f=Th      H    1.496325   20.321749    6.858551 f=F
H   -1.072379   17.438398    7.565636 f=Th      F   -0.068418   22.190126    3.114084 f=F
C    1.477541   14.358441    7.256920 f=Th
```

Optimised geometry of η^1-5-Th-vertical and the name of the fragment f in the ETS-NOCV in which each atom belongs

```
F    3.119340   -0.636733    0.186344 f=F       C   11.521915   -2.305854    3.182466 f=Th
C    2.014853   -0.687149    1.035935 f=F       C   11.251282   -3.813960    3.113269 f=Th
C    1.700597    0.445550    1.745456 f=F       C    9.457161    2.164247   -5.645014 f=Th
C    0.593352    0.379012    2.581655 f=F       C    8.740421    3.508102   -5.823638 f=Th
C   -0.145619   -0.791110    2.675385 f=F       C    6.373052    0.122556    4.013963 f=Th
C    0.212898   -1.907548    1.933512 f=F       C    7.475555    0.022295    5.068638 f=Th
C    1.315831   -1.867080    1.090968 f=F       C    6.161005   -3.775823    0.668605 f=Th
H   -1.008557   -0.832425    3.328262 f=F       C    7.457071   -4.571961    0.836244 f=Th
H    0.310538    1.251594    3.157492 f=F       C    6.039514   -1.958288   -3.692289 f=Th
H    2.291261    1.348372    1.649296 f=F       C    5.447996   -3.309395   -3.300225 f=Th
H    1.616679   -2.720310    0.496932 f=F       C    4.234459    2.718295   -2.590626 f=Th
H   -0.367118   -2.819419    2.004548 f=F       C    4.590786    3.765419   -3.646902 f=Th
C    4.109276    1.348825   -3.220747 f=Th      C    5.380478    2.084610    0.936174 f=Th
C    5.101309    0.353378   -3.075817 f=Th      Si   6.586760    3.519221    1.137846 f=Th
C    4.981896   -0.877438   -3.766851 f=Th      C    5.733265    4.944052    2.014684 f=Th
C    3.868138   -1.085298   -4.570686 f=Th      C    8.068775    2.997617    2.165803 f=Th
C    2.884339   -0.121193   -4.700504 f=Th      C    7.185553    4.128737   -0.532651 f=Th
C    3.009147    1.080217   -4.030536 f=Th      C   13.006470   -2.074558    2.913146 f=Th
N    6.200583    0.550602   -2.193367 f=Th      C   11.209640   -1.801578    4.595647 f=Th
C    7.470551    0.855122   -2.671320 f=Th      C   10.952872    2.391555   -5.846906 f=Th
C    8.509243    0.643006   -1.763948 f=Th      C    8.972531    1.185563   -6.721003 f=Th
C    9.836814    0.844015   -2.042634 f=Th      C    5.227287    0.979348    4.552066 f=Th
C   10.123126    1.343938   -3.319057 f=Th      C    5.067161   -4.677179    0.106418 f=Th
C    9.135744    1.602238   -4.260843 f=Th      C    6.802168   -2.077842   -5.011726 f=Th
C    7.802587    1.338081   -3.925835 f=Th      C    2.973444    3.136102   -1.837771 f=Th
O    8.054338    0.176101   -0.536288 f=Th      H   12.224542   -0.790430    0.997994 f=Th
C    8.991264   -0.369642    0.333479 f=Th      H    8.797646   -2.244560    3.114224 f=Th
C   10.344190   -0.245064    0.146417 f=Th      H    7.009004    1.505719   -4.644286 f=Th
C   10.923629    0.553459   -1.015309 f=Th      H   11.155768    1.536107   -3.572384 f=Th
C   11.152432   -0.871807    1.102749 f=Th      H   10.691904    2.475491   -0.003748 f=Th
C   10.628904   -1.591390    2.168493 f=Th      H   11.903692    2.474509   -1.292638 f=Th
C    9.237881   -1.679481    2.302074 f=Th      H   12.260406    1.700796    0.259655 f=Th
C    8.397146   -1.065383    1.387935 f=Th      H   12.861150   -0.435421   -0.963686 f=Th
Th   5.638157   -0.067164   -0.105750 f=Th      H   12.497338    0.325262   -2.499861 f=Th
N    7.006346   -1.067641    1.375915 f=Th      H   11.700636   -1.192661   -2.063707 f=Th
C    6.241745   -1.808171    2.321446 f=Th      H   11.371860   -0.723895    4.674046 f=Th
C    5.901495   -1.245931    3.574189 f=Th      H   11.859943   -2.295894    5.321670 f=Th
C    5.120501   -1.993551    4.449196 f=Th      H   10.178051   -2.011493    4.885263 f=Th
C    4.665589   -3.253578    4.113293 f=Th      H   10.210704   -4.050631    3.345842 f=Th
C    4.984336   -3.792908    2.881007 f=Th      H   11.880578   -4.342493    3.833882 f=Th
C    5.771922   -3.098067    1.968828 f=Th      H   11.473106   -4.206509    2.117891 f=Th
C   11.477026    1.884262   -0.478818 f=Th      H   13.309291   -2.456498    1.935134 f=Th
C   12.059239   -0.237780   -1.675428 f=Th      H   13.597312   -2.600926    3.665640 f=Th
```

A.1. Geometries from the Chapter Coordination of Alkyl cations [(XA₂)X(CH₂Y)]
(X = Th, U or Zr; Y = SiMe₃, H) with an arene for Ethylene polymerisation: 129
Exploration of the bonding

H	13.271260	-1.015787	2.970150	f=Th	H	2.023116	-0.304910	-5.332371 f=Th
H	9.199021	1.578924	-7.715184	f=Th	H	2.243110	1.837275	-4.151726 f=Th
H	7.893633	1.023996	-6.669715	f=Th	H	5.063609	2.682650	-1.880322 f=Th
H	9.466364	0.215883	-6.620761	f=Th	H	5.530565	3.525093	-4.146533 f=Th
H	9.062271	4.227903	-5.067339	f=Th	H	4.697625	4.751023	-3.187300 f=Th
H	7.655977	3.403263	-5.749219	f=Th	H	3.809476	3.834332	-4.408152 f=Th
H	8.965376	3.925969	-6.808159	f=Th	H	2.134978	3.306497	-2.516800 f=Th
H	11.356882	3.110821	-5.130232	f=Th	H	3.146004	4.070953	-1.299125 f=Th
H	11.126408	2.794355	-6.846933	f=Th	H	2.654951	2.379898	-1.114592 f=Th
H	11.522107	1.462210	-5.765337	f=Th	H	6.764722	-1.670735	-2.924705 f=Th
H	4.864216	-1.577139	5.416301	f=Th	H	4.858407	-3.246758	-2.382183 f=Th
H	4.059349	-3.818053	4.812273	f=Th	H	6.244384	-4.041422	-3.146204 f=Th
H	4.622356	-4.781875	2.630661	f=Th	H	4.792273	-3.702770	-4.080098 f=Th
H	6.371557	-2.996093	-0.078895	f=Th	H	6.129983	-2.365536	-5.824199 f=Th
H	8.282693	-3.938901	1.161342	f=Th	H	7.578559	-2.842665	-4.933536 f=Th
H	7.739590	-5.044894	-0.107411	f=Th	H	7.280938	-1.136547	-5.283185 f=Th
H	7.318435	-5.360952	1.580171	f=Th	H	4.495565	2.496989	0.419390 f=Th
H	4.910659	-5.557293	0.732995	f=Th	H	5.041364	1.824459	1.953486 f=Th
H	5.353072	-5.041284	-0.881110	f=Th	H	7.682408	3.350048	-1.117148 f=Th
H	4.108492	-4.159270	0.015172	f=Th	H	7.903993	4.941016	-0.388200 f=Th
H	6.796481	0.623345	3.140931	f=Th	H	6.366284	4.528934	-1.135367 f=Th
H	7.115790	-0.498071	5.960250	f=Th	H	4.873490	5.305651	1.443879 f=Th
H	7.798398	1.020792	5.373451	f=Th	H	6.416696	5.787062	2.151182 f=Th
H	8.348981	-0.508823	4.691395	f=Th	H	5.373528	4.646483	3.003464 f=Th
H	4.368458	0.995917	3.876609	f=Th	H	7.785475	2.771763	3.196918 f=Th
H	5.564066	2.007833	4.701832	f=Th	H	8.793504	3.816215	2.204449 f=Th
H	4.873618	0.614392	5.519097	f=Th	H	8.582200	2.121517	1.760960 f=Th
H	3.769718	-2.019910	-5.111020	f=Th				

Optimised geometry of η¹-6-Th-vertical and the name of the fragment f in the ETS-NOCV in which each atom belongs

C	4.078764	1.565437	-3.050514	f=Th	C	5.852038	-1.814352	-3.616612 f=Th
C	5.030930	0.527165	-2.946449	f=Th	C	5.228428	-3.148810	-3.215350 f=Th
C	4.836050	-0.691409	-3.642015	f=Th	C	4.293886	2.930944	-2.434616 f=Th
C	3.684864	-0.846600	-4.403004	f=Th	C	4.639183	3.956515	-3.515604 f=Th
C	2.734396	0.156473	-4.485450	f=Th	C	5.620042	2.325287	1.011215 f=Th
C	2.934893	1.347033	-3.815138	f=Th	Si	6.938723	3.661012	1.147061 f=Th
N	6.162369	0.670264	-2.095322	f=Th	C	6.222560	5.169963	2.007215 f=Th
C	7.430896	0.913081	-2.610829	f=Th	C	8.392545	3.044094	2.163031 f=Th
C	8.483694	0.653722	-1.732622	f=Th	C	7.541505	4.189147	-0.550068 f=Th
C	9.810616	0.795029	-2.047467	f=Th	C	12.987905	-2.087212	2.931452 f=Th
C	10.084329	1.280235	-3.332383	f=Th	C	11.232233	-1.700966	4.634799 f=Th
C	9.084245	1.583530	-4.246690	f=Th	C	10.891620	2.283058	-5.885091 f=Th
C	7.749982	1.380733	-3.874439	f=Th	C	8.824362	1.189687	-6.703267 f=Th
O	8.040745	0.213266	-0.491716	f=Th	C	5.280708	1.189373	4.600252 f=Th
C	8.977886	-0.343145	0.370068	f=Th	C	5.014271	-4.569271	0.268321 f=Th
C	10.329551	-0.273421	0.150201	f=Th	C	6.557403	-1.948440	-4.966379 f=Th
C	10.913483	0.456930	-1.052797	f=Th	C	3.093561	3.407109	-1.620197 f=Th
C	11.136795	-0.894597	1.111143	f=Th	H	12.208586	-0.853680	0.980892 f=Th
C	10.612384	-1.557060	2.212713	f=Th	H	8.780525	-2.116841	3.216411 f=Th
C	9.222070	-1.594250	2.376417	f=Th	H	6.945245	1.587587	-4.569907 f=Th
C	8.383198	-0.984963	1.457557	f=Th	H	11.117635	1.425217	-3.613421 f=Th
Th	5.636555	0.132242	0.028979	f=Th	H	10.853809	2.414681	-0.087310 f=Th
N	6.993453	-0.939845	1.471774	f=Th	H	12.011851	2.297453	-1.419600 f=Th
C	6.220227	-1.657165	2.427791	f=Th	H	12.375117	1.540513	0.138528 f=Th
C	5.896511	-1.074947	3.675143	f=Th	H	12.777492	-0.666422	-1.048109 f=Th
C	5.097548	-1.794245	4.558420	f=Th	H	12.406044	0.081888	-2.590747 f=Th
C	4.613341	-3.046480	4.235518	f=Th	H	11.523895	-1.364632	-2.082675 f=Th
C	4.921946	-3.608331	3.009891	f=Th	H	11.427004	-0.626483	4.671786 f=Th
C	5.725620	-2.942906	2.090410	f=Th	H	11.881587	-2.188819	5.366067 f=Th
C	11.577514	1.758740	-0.574766	f=Th	H	10.200708	-1.869758	4.950247 f=Th
C	11.964343	-0.428668	-1.734546	f=Th	H	10.142049	-3.960210	3.481174 f=Th
C	11.502358	-2.263437	3.234948	f=Th	H	11.810755	-4.286365	3.951852 f=Th
C	11.185153	-3.763964	3.223550	f=Th	H	11.377434	-4.197386	2.239015 f=Th
C	9.392734	2.134550	-5.638229	f=Th	H	13.261049	-2.512648	1.962659 f=Th
C	8.743624	3.515727	-5.788870	f=Th	H	13.576756	-2.604336	3.691920 f=Th
C	6.407116	0.283407	4.103825	f=Th	H	13.284984	-1.035580	2.945536 f=Th
C	7.480844	0.158208	5.185059	f=Th	H	9.043208	1.575581	-7.702110 f=Th
C	6.103149	-3.642394	0.798155	f=Th	H	7.740150	1.087110	-6.621436 f=Th
C	7.408332	-4.425175	0.961629	f=Th	H	9.267039	0.193917	-6.621330 f=Th

H	9.127029	4.212860	-5.040090	f=Th	H	2.794779	2.680269	-0.859331 f=Th
H	7.658080	3.468032	-5.680088	f=Th	H	6.615762	-1.562552	-2.874836 f=Th
H	8.959433	3.926795	-6.778373	f=Th	H	4.691691	-3.081667	-2.266555 f=Th
H	11.354732	2.977804	-5.180085	f=Th	H	6.004046	-3.911970	-3.115653 f=Th
H	11.056027	2.679185	-6.889378	f=Th	H	4.521149	-3.503737	-3.968456 f=Th
H	11.412924	1.324563	-5.821879	f=Th	H	5.844227	-2.205432	-5.753937 f=Th
H	4.853451	-1.362474	5.522080	f=Th	H	7.308716	-2.740665	-4.924660 f=Th
H	3.993886	-3.589217	4.940224	f=Th	H	7.058284	-1.022465	-5.249815 f=Th
H	4.537993	-4.591784	2.770733	f=Th	H	4.747326	2.800377	0.530224 f=Th
H	6.292596	-2.874550	0.033839	f=Th	H	5.297204	2.117033	2.045484 f=Th
H	8.235989	-3.781799	1.258826	f=Th	H	7.979068	3.367171	-1.122148 f=Th
H	7.677063	-4.916187	0.023104	f=Th	H	8.307811	4.962700	-0.444202 f=Th
H	7.287128	-5.199781	1.723594	f=Th	H	6.732680	4.618500	-1.147378 f=Th
H	4.897848	-5.451873	0.900632	f=Th	H	5.381798	5.586728	1.445801 f=Th
H	5.283562	-4.928152	-0.726187	f=Th	H	6.974278	5.957904	2.109915 f=Th
H	4.042611	-4.074482	0.202487	f=Th	H	5.861564	4.923797	3.009556 f=Th
H	6.869724	0.754782	3.234024	f=Th	H	8.099523	2.844076	3.197231 f=Th
H	7.081457	-0.328732	6.078620	f=Th	H	9.175338	3.807654	2.193349 f=Th
H	7.839505	1.148091	5.477433	f=Th	H	8.837228	2.130146	1.760861 f=Th
H	8.338687	-0.417041	4.837217	f=Th	F	3.345025	-1.481475	-0.490926 f=F
H	4.450282	1.244452	3.892156	f=Th	C	2.119049	-1.320570	0.075798 f=F
H	5.655793	2.202610	4.762568	f=Th	C	1.980962	-0.294753	0.983390 f=F
H	4.876331	0.840262	5.553245	f=Th	C	0.784881	-0.050183	1.611934 f=F
H	3.529299	-1.770865	-4.947950	f=Th	C	-0.288853	-0.875503	1.301136 f=F
H	1.842714	0.012878	-5.084808	f=Th	C	-0.149713	-1.908246	0.384984 f=F
H	2.198488	2.137326	-3.904363	f=Th	C	1.067182	-2.143236	-0.243382 f=F
H	5.157083	2.863906	-1.768336	f=Th	H	-1.243297	-0.704784	1.782551 f=F
H	5.536758	3.669606	-4.065705	f=Th	H	0.701750	0.763088	2.321850 f=F
H	4.818721	4.936989	-3.067869	f=Th	F	3.078675	0.469421	1.224273 f=F
H	3.820816	4.060831	-4.232634	f=Th	H	1.200370	-2.939922	-0.964282 f=F
H	2.222873	3.591417	-2.253632	f=Th	H	-0.996023	-2.541678	0.151729 f=F
H	3.327995	4.346190	-1.113450	f=Th				

Optimised geometry of η^6-6-Th-exo and the name of the fragment f in the ETS-NOCV in which each atom belongs

Th	-0.281113	17.831764	4.911994	f=Th	C	5.026606	12.343647	1.875173 f=Th
C	-0.248155	16.989317	7.160963	f=Th	C	0.02478 11.756221	3.883116	f=Th
Si	-0.24196	15.23722	7.860108	f=Th	C	0.017556	12.207192	1.419024 f=Th
C	-1.754947	14.280659	7.296585	f=Th	C	-3.951601	17.358069	6.598062 f=Th
O	-0.164173	15.574553	3.903963	f=Th	C	-3.92761	18.122359	7.918485 f=Th
C	-1.318106	14.91378	3.501055	f=Th	C	-2.748502	18.370494	1.721278 f=Th
C	-1.312083	13.649344	2.969776	f=Th	C	-1.914368	19.539057	1.205064 f=Th
C	-0.022972	12.855171	2.808123	f=Th	C	2.075338	18.957791	1.92197 f=Th
C	1.179131	13.774005	2.984742	f=Th	C	2.849176	18.099312	0.918023 f=Th
C	1.054975	15.034538	3.512378	f=Th	C	3.497213	17.389482	6.607388 f=Th
C	-2.464197	15.689364	3.676764	f=Th	C	3.326807	18.101479	7.948185 f=Th
C	-3.676546	15.142323	3.290531	f=Th	C	1.303546	14.318728	7.321671 f=Th
C	-3.741652	13.848166	2.76099 f=Th	C	-0.260035	15.312201	9.736378 f=Th
C	-2.562585	13.130362	2.612753	f=Th	C	-6.001784	13.209024	3.609237 f=Th
C	2.47734 13.379133	2.641788	f=Th	C	-5.75538	14.166961	1.313112 f=Th
C	3.57822 14.209343	2.802916	f=Th	C	5.493951	14.7054 1.283616	f=Th
C	3.380938	15.488882	3.334663	f=Th	C	5.927876	13.874592	3.600798 f=Th
C	2.115015	15.92237	3.69658 f=Th	C	-3.751143	17.921202	0.658789 f=Th
C	-5.100945	13.269596	2.369604	f=Th	C	-5.146988	16.401185	6.586023 f=Th
C	-4.988055	11.860749	1.793468	f=Th	C	4.750558	16.514524	6.649415 f=Th
N	-2.241223	16.948176	4.2235 f=Th	C	1.699775	20.283493	1.26817 f=Th
C	-3.245783	17.954284	4.205437	f=Th	H	-2.602629	12.130476	2.205642 f=Th
C	-3.991708	18.246676	5.372253	f=Th	H	-4.575276	15.736566	3.404082 f=Th
C	-4.865779	19.330257	5.345308	f=Th	H	4.215594	16.169515	3.451285 f=Th
C	-5.040672	20.088579	4.20115 f=Th	H	2.619199	12.38852	2.234932 f=Th
C	-4.347868	19.763923	3.048091	f=Th	H	-0.004211	12.18446	4.886884 f=Th
C	-3.44775	18.704281	3.022264	f=Th	H	0.941742	11.170719	3.788102 f=Th
N	1.76643 17.166117	4.218433	f=Th	H	-0.826733	11.08009	3.775273 f=Th
C	2.732905	18.210672	4.294504	f=Th	H	-0.826217	11.530886	1.280256 f=Th
C	2.856484	19.118901	3.212685	f=Th	H	0.923554	11.614261	1.292158 f=Th
C	3.778295	20.154575	3.317757	f=Th	H	-0.012956	12.961481	0.630822 f=Th
C	4.572619	20.301384	4.440955	f=Th	H	-5.559367	12.580722	4.385874 f=Th
C	4.452285	19.408963	5.488504	f=Th	H	-6.975508	12.7884 3.345799	f=Th
C	3.542185	18.356762	5.444033	f=Th	H	-6.174942	14.199875	4.034494 f=Th
C	4.986747	13.778283	2.395037	f=Th	H	-5.927582	15.178463	1.687297 f=Th

A.1. *Geometries from the Chapter Coordination of Alkyl cations [(XA₂)X(CH₂Y)]*
(X = Th, U or Zr; Y = SiMe₃, H) with an arene for Ethylene polymerisation: 131
Exploration of the bonding

H	-6.724998	13.756196	1.020849	f=Th	H	4.698659	15.819438	7.490939	f=Th
H	-5.133574	14.236883	0.41727	f=Th	H	5.649484	17.123481	6.775975	f=Th
H	-4.378992	11.838134	0.886366	f=Th	H	4.211344	18.687144	8.208871	f=Th
H	-5.982982	11.496944	1.52869	f=Th	H	3.177128	17.372161	8.74767	f=Th
H	-4.564572	11.157096	2.514345	f=Th	H	2.471649	18.781537	7.948544	f=Th
H	6.502625	14.412677	0.981197	f=Th	H	1.146756	18.416474	2.151127	f=Th
H	5.535299	15.746676	1.61056	f=Th	H	1.201931	20.969888	1.955569	f=Th
H	4.848104	14.652528	0.403747	f=Th	H	1.030363	20.104885	0.425196	f=Th
H	5.581759	13.242885	4.422376	f=Th	H	2.577412	20.795753	0.868861	f=Th
H	6.012054	14.898128	3.971398	f=Th	H	3.796011	18.582884	0.6631	f=Th
H	6.931326	13.545533	3.319558	f=Th	H	2.273597	17.98332	-0.003543	f=Th
H	4.695699	11.626595	2.630632	f=Th	H	3.068113	17.106852	1.310168	f=Th
H	6.052482	12.084893	1.605048	f=Th	H	0.643776	17.48359	7.584048	f=Th
H	4.412005	12.215142	0.980827	f=Th	H	-1.114091	17.499365	7.62023	f=Th
H	-5.44129	19.570313	6.231481	f=Th	H	1.42187	14.278972	6.235756	f=Th
H	-5.734165	20.921685	4.202689	f=Th	H	1.26273	13.288474	7.687351	f=Th
H	-4.512585	20.344411	2.147274	f=Th	H	2.206297	14.771139	7.740047	f=Th
H	-2.075264	17.529096	1.904839	f=Th	H	0.612141	15.845947	10.123696	f=Th
H	-4.329667	17.060317	0.996199	f=Th	H	-0.251521	14.307574	10.168866	f=Th
H	-3.228245	17.638182	-0.257597	f=Th	H	-1.152619	15.823456	10.107362	f=Th
H	-4.449483	18.723644	0.408664	f=Th	H	-2.677746	14.715474	7.688992	f=Th
H	-2.535591	20.406589	0.971254	f=Th	H	-1.698561	13.255714	7.675054	f=Th
H	-1.388597	19.255214	0.29084	f=Th	H	-1.84645	14.226011	6.208844	f=Th
H	-1.166225	19.866104	1.933001	f=Th	H	0.595273	20.216477	7.644759	f=F
H	-3.04863	16.747082	6.536484	f=Th	H	-1.724150	19.942888	6.795392	f=F
H	-6.088161	16.956609	6.613188	f=Th	H	-2.381456	20.956813	4.618841	f=F
H	-5.118174	15.746689	7.460443	f=Th	F	1.674463	22.764851	4.116384	f=F
H	-5.147701	15.77017	5.697109	f=Th	H	2.239873	21.564320	6.332672	f=F
H	-3.117166	18.853664	7.974199	f=Th	C	1.226557	21.414600	5.981901	f=F
H	-3.797397	17.424474	8.748503	f=Th	C	0.310571	20.648822	6.693492	f=F
H	-4.862626	18.657729	8.09746	f=Th	C	-0.983923	20.477976	6.209266	f=F
H	3.886251	20.857989	2.502037	f=Th	C	-1.370641	21.058694	4.999987	f=F
H	5.29168	21.110866	4.493911	f=Th	C	-0.455906	21.828848	4.306887	f=F
H	5.088496	19.52232	6.358975	f=Th	C	0.834873	22.010228	4.799450	f=F
H	2.640493	16.729379	6.457757	f=Th	F	-0.797031	22.418000	3.173317	f=F
H	4.861795	15.92641	5.738864	f=Th					

Optimised geometry of η^6-6-Th-side and the name of the fragment f in the ETS-NOCV in which each atom belongs

C	3.5195	18.3662	5.4188	f=Th	C	-5.1084	13.2624	2.3482	f=Th
C	2.7095	18.2118	4.2703	f=Th	C	-5.7586	14.1606	1.2894	f=Th
C	2.8311	19.1136	3.1830	f=Th	C	4.9781	13.7740	2.3931	f=Th
C	3.7529	20.1500	3.2812	f=Th	C	5.9169	13.8740	3.6005	f=Th
C	4.5473	20.3045	4.4031	f=Th	C	-3.9619	17.3294	6.5874	f=Th
C	4.4278	19.4196	5.4563	f=Th	C	-5.1780	16.3993	6.5659	f=Th
N	1.7483	17.1617	4.2002	f=Th	C	-2.7521	18.3861	1.7234	f=Th
C	2.1015	15.9165	3.6854	f=Th	C	-3.7733	17.9355	0.6788	f=Th
C	1.0439	15.0252	3.5055	f=Th	C	2.0465	18.9466	1.8950	f=Th
C	1.1700	13.7640	2.9799	f=Th	C	1.6891	20.2710	1.2282	f=Th
C	2.4691	13.3710	2.6379	f=Th	C	3.4768	17.4061	6.5883	f=Th
C	3.5684	14.2038	2.7982	f=Th	C	4.7386	16.5444	6.6435	f=Th
C	3.3687	15.4847	3.3259	f=Th	C	-0.2605	16.9679	7.1552	f=Th
O	-0.1754	15.5628	3.8986	f=Th	Si	-0.2301	15.2151	7.8508	f=Th
C	-1.3279	14.9029	3.4919	f=Th	C	-0.2439	15.2851	9.7273	f=Th
C	-1.3210	13.6386	2.9604	f=Th	C	-1.7380	14.2495	7.2880	f=Th
C	-0.0314	12.8436	2.8055	f=Th	C	1.3214	14.3103	7.3068	f=Th
C	-2.5709	13.1211	2.5989	f=Th	C	-4.9949	11.8536	1.7718	f=Th
C	-3.7499	13.8398	2.7440	f=Th	C	-6.0135	13.2023	3.5845	f=Th
C	-3.6857	15.1336	3.2747	f=Th	C	5.0210	12.3385	1.8760	f=Th
C	-2.4739	15.6793	3.6644	f=Th	C	5.4858	14.6999	1.2809	f=Th
Th	-0.2921	17.8204	4.9105	f=Th	C	-3.9160	18.0764	7.9167	f=Th
N	-2.2490	16.9363	4.2129	f=Th	C	-1.9251	19.5511	1.1880	f=Th
C	-3.2448	17.9495	4.2049	f=Th	C	2.8050	18.0674	0.8976	f=Th
C	-3.9851	18.2377	5.3762	f=Th	C	3.2900	18.1265	7.9222	f=Th
C	-4.8335	19.3418	5.3692	f=Th	H	-2.6107	12.1214	2.1914	f=Th
C	-4.9881	20.1259	4.2400	f=Th	H	-4.5845	15.7280	3.3870	f=Th
C	-4.3056	19.8036	3.0799	f=Th	H	4.2016	16.1677	3.4402	f=Th
C	-3.4329	18.7221	3.0337	f=Th	H	2.6132	12.3799	2.2330	f=Th
C	0.0141	11.7507	3.8868	f=Th	H	-0.0171	12.1846	4.8881	f=Th
C	0.0124	12.1876	1.4204	f=Th	H	0.9315	11.1650	3.7971	f=Th

```
H   -0.8370   11.0745    3.7809 f=Th        H    5.2607   21.1187    4.4541 f=Th
H   -0.8307   11.5099    1.2838 f=Th        H    5.0586   19.5444    6.3287 f=Th
H    0.9189   11.5942    1.2991 f=Th        H    2.6277   16.7359    6.4386 f=Th
H   -0.0167   12.9370    0.6276 f=Th        H    4.8622   15.9527    5.7367 f=Th
H   -5.5740   12.5737    4.3626 f=Th        H    4.6885   15.8534    7.4885 f=Th
H   -6.9866   12.7823    3.3178 f=Th        H    5.6304   17.1633    6.7727 f=Th
H   -6.1875   14.1932    4.0093 f=Th        H    4.1622   18.7316    8.1793 f=Th
H   -5.9312   15.1721    1.6633 f=Th        H    3.1508   17.4015    8.7276 f=Th
H   -6.7276   13.7508    0.9939 f=Th        H    2.4232   18.7914    7.9122 f=Th
H   -5.1337   14.2303    0.3957 f=Th        H    1.1103   18.4218    2.1321 f=Th
H   -4.3829   11.8306    0.8667 f=Th        H    1.2185   20.9737    1.9187 f=Th
H   -5.9893   11.4907    1.5037 f=Th        H    1.0044   20.0966    0.3965 f=Th
H   -4.5744   11.1494    2.4939 f=Th        H    2.5718   20.7599    0.8112 f=Th
H    6.4953   14.4079    0.9806 f=Th        H    3.7592   18.5336    0.6379 f=Th
H    5.5253   15.7418    1.6060 f=Th        H    2.2269   17.9526   -0.0226 f=Th
H    4.8413   14.6446    0.4001 f=Th        H    3.0088   17.0751    1.2979 f=Th
H    5.5705   13.2427    4.4223 f=Th        H    0.6127   17.4848    7.5906 f=Th
H    5.9981   14.8982    3.9699 f=Th        H   -1.1450   17.4551    7.6034 f=Th
H    6.9216   13.5467    3.3216 f=Th        H    1.4371   14.2727    6.2205 f=Th
H    4.6902   11.6223    2.6323 f=Th        H    1.2899   13.2794    7.6716 f=Th
H    6.0478   12.0809    1.6080 f=Th        H    2.2214   14.7699    7.7231 f=Th
H    4.4080   12.2073    0.9810 f=Th        H    0.6247   15.8256   10.1133 f=Th
H   -5.4020   19.5802    6.2602 f=Th        H   -0.2251   14.2796   10.1573 f=Th
H   -5.6589   20.9772    4.2577 f=Th        H   -1.1399   15.7876   10.1021 f=Th
H   -4.4601   20.4018    2.1888 f=Th        H   -2.6624   14.6777    7.6842 f=Th
H   -2.0765   17.5446    1.8987 f=Th        H   -1.6749   13.2235    7.6626 f=Th
H   -4.3453   17.0747    1.0272 f=Th        H   -1.8319   14.1982    6.2003 f=Th
H   -3.2672   17.6520   -0.2468 f=Th        H    0.7754   20.6094    7.8893 f=F
H   -4.4764   18.7380    0.4422 f=Th        H   -1.4835   19.9474    7.0719 f=F
H   -2.5505   20.4168    0.9573 f=Th        H   -2.2297   20.6287    4.7985 f=F
H   -1.4146   19.2622    0.2668 f=Th        F    2.4289   22.0678    6.5455 f=F
H   -1.1636   19.8763    1.9027 f=Th        F    1.6304   22.8049    4.0976 f=F
H   -3.0725   16.7000    6.5137 f=Th        C    0.8392   22.0435    4.8297 f=F
H   -6.1068   16.9744    6.6065 f=Th        C    1.2567   21.6582    6.1014 f=F
H   -5.1589   15.7307    7.4298 f=Th        C    0.4416   20.8740    6.8934 f=F
H   -5.1966   15.7825    5.6673 f=Th        C   -0.8098   20.4888    6.4165 f=F
H   -3.0985   18.7999    7.9661 f=Th        C   -1.2303   20.8749    5.1448 f=F
H   -3.7823   17.3685    8.7376 f=Th        C   -0.3931   21.6493    4.3456 f=F
H   -4.8436   18.6188    8.1124 f=Th        H   -0.7026   21.9890    3.3647 f=F
H    3.8599   20.8493    2.4619 f=Th
```

Optimised geometry of η^6-6-Th-endo and the name of the fragment f in the ETS-NOCV in which each atom belongs

```
C    3.477468   20.142211   3.344767 f=Th    C   -3.998495   15.106810   3.446703 f=Th
C    2.559315   19.088440   3.248252 f=Th    C   -2.768903   15.653939   3.822391 f=Th
C    2.482665   18.150969   4.324976 f=Th    C    4.665638   13.622946   2.401651 f=Th
C    3.333864   18.289348   5.460652 f=Th    C    5.123397   14.525285   1.234421 f=Th
C    4.236242   19.361504   5.493746 f=Th    C   -0.305112   11.726233   4.290288 f=Th
C    4.311560   20.280776   4.452927 f=Th    C   -0.342346   11.923168   1.778110 f=Th
C    3.333017   17.302216   6.618655 f=Th    C   -5.456847   13.221585   2.555470 f=Th
C    3.195237   17.995976   7.984193 f=Th    C   -6.400777   13.241116   3.777006 f=Th
N    1.507918   17.101124   4.268571 f=Th    N   -2.524870   16.943124   4.311358 f=Th
Th  -0.533459   17.819405   4.989196 f=Th    C   -3.538014   17.954380   4.283612 f=Th
C   -0.494988   17.083987   7.276719 f=Th    C   -4.366001   18.182676   5.421733 f=Th
Si  -0.482609   15.376207   8.107996 f=Th    C   -5.277176   19.246833   5.381445 f=Th
C    1.053759   14.398616   7.607217 f=Th    C   -5.396175   20.061272   4.258568 f=Th
C    1.723698   18.942337   1.979396 f=Th    C   -4.606308   19.814617   3.137509 f=Th
C    2.406115   18.000503   0.967958 f=Th    C   -3.674510   18.768702   3.118195 f=Th
C    1.839100   15.830115   3.779553 f=Th    C   -4.347827   17.272961   6.641699 f=Th
C    0.764358   14.932286   3.667148 f=Th    C   -4.218406   18.042000   7.965791 f=Th
C    0.862964   13.644140   3.174496 f=Th    C   -2.895131   18.496221   1.837869 f=Th
C    2.153385   13.234344   2.784401 f=Th    C   -2.320864   19.768224   1.198120 f=Th
C    3.270364   14.073159   2.868375 f=Th    C   -6.060843   14.091922   1.431800 f=Th
C    3.097551   15.377150   3.372513 f=Th    C   -5.366143   11.775274   2.044181 f=Th
C   -0.357375   12.718472   3.099807 f=Th    C    5.671972   13.748004   3.565123 f=Th
C   -1.643475   13.546403   3.203586 f=Th    C    4.678044   12.165473   1.914569 f=Th
C   -1.631659   14.839892   3.690900 f=Th    C   -5.608046   16.387822   6.677836 f=Th
O   -0.453344   15.498655   4.083853 f=Th    C   -3.770275   17.744425   0.816452 f=Th
C   -2.908630   13.037519   2.847794 f=Th    C    1.404077   20.277556   1.293683 f=Th
C   -4.084463   13.788390   2.958177 f=Th    C    4.604262   16.433185   6.610385 f=Th
```

A.1. Geometries from the Chapter Coordination of Alkyl cations [(XA$_2$)X(CH$_2$Y)]
(X = Th, U or Zr; Y = SiMe$_3$, H) with an arene for Ethylene polymerisation: 133
Exploration of the bonding

```
C   -0.471427  15.585210   9.985197 f=Th      H   -3.333090  18.693837   7.984412 f=Th
C   -2.017073  14.385438   7.627230 f=Th      H   -4.131997  17.337331   8.805462 f=Th
H   -2.965340  12.018332   2.472338 f=Th      H   -5.100231  18.669656   8.161716 f=Th
H   -4.892167  15.726996   3.527480 f=Th      H    3.552629  20.866310   2.533384 f=Th
H    3.942490  16.064544   3.428851 f=Th      H    5.023729  21.106360   4.500254 f=Th
H    2.277808  12.224434   2.400483 f=Th      H    4.896917  19.474033   6.355028 f=Th
H   -0.316346  12.256778   5.252441 f=Th      H    2.471925  16.631763   6.484291 f=Th
H    0.611233  11.120656   4.242804 f=Th      H    4.703074  15.863125   5.678533 f=Th
H   -1.170897  11.049255   4.261408 f=Th      H    4.576344  15.713996   7.442063 f=Th
H   -1.198757  11.239206   1.722583 f=Th      H    5.505725  17.052042   6.733456 f=Th
H    0.560458  11.303783   1.703258 f=Th      H    4.085104  18.594790   8.226879 f=Th
H   -0.376553  12.593115   0.908300 f=Th      H    3.085498  17.244483   8.779482 f=Th
H   -5.993828  12.638059   4.601693 f=Th      H    2.327291  18.668415   8.030274 f=Th
H   -7.382474  12.827017   3.503170 f=Th      H    0.762601  18.463715   2.257426 f=Th
H   -6.565281  14.261486   4.151325 f=Th      H    0.978739  21.022373   1.982710 f=Th
H   -6.206624  15.133379   1.752528 f=Th      H    0.685747  20.118055   0.478692 f=Th
H   -7.043305  13.696531   1.133970 f=Th      H    2.301666  20.722697   0.841236 f=Th
H   -5.412471  14.096060   0.543285 f=Th      H    3.378129  18.416970   0.663404 f=Th
H   -4.733420  11.693771   1.148039 f=Th      H    1.786247  17.895722   0.065420 f=Th
H   -6.370083  11.421296   1.770411 f=Th      H    2.577976  17.000976   1.384641 f=Th
H   -4.974774  11.091044   2.811444 f=Th      H    0.392815  17.627078   7.669152 f=Th
H    6.122432  14.220084   0.889252 f=Th      H   -1.378263  17.622782   7.686297 f=Th
H    5.182168  15.581774   1.532878 f=Th      H    1.156048  14.285857   6.517678 f=Th
H    4.431354  14.450383   0.382782 f=Th      H    1.002177  13.388115   8.041568 f=Th
H    5.364892  13.132712   4.423394 f=Th      H    1.974959  14.864700   7.986421 f=Th
H    5.774933  14.786671   3.909533 f=Th      H    0.415108  16.143120  10.322337 f=Th
H    6.667068  13.408945   3.241206 f=Th      H   -0.461987  14.607667  10.491441 f=Th
H    4.383026  11.463745   2.708743 f=Th      H   -1.360338  16.131884  10.334409 f=Th
H    5.695385  11.895208   1.598171 f=Th      H   -2.938335  14.847574   8.011473 f=Th
H    4.015051  12.013435   1.050113 f=Th      H   -1.954808  13.378425   8.068246 f=Th
H   -5.921687  19.429277   6.243422 f=Th      H   -2.127379  14.263890   6.539381 f=Th
H   -6.118018  20.879785   4.249134 f=Th      C   -0.440917  20.878248   4.959267 f=F
H   -4.726458  20.442717   2.253369 f=Th      C    0.686687  20.974758   5.795315 f=F
H   -2.051979  17.829057   2.091184 f=Th      C    0.499284  21.108800   7.167083 f=F
H   -4.140740  16.794486   1.221944 f=Th      C   -0.795351  21.136173   7.709972 f=F
H   -3.192679  17.525278  -0.093460 f=Th      C   -1.910581  21.033135   6.885139 f=F
H   -4.637390  18.357142   0.527336 f=Th      C   -1.736120  20.905798   5.501965 f=F
H   -3.113966  20.430876   0.823727 f=Th      H    1.701367  20.979875   5.391659 f=F
H   -1.691045  19.505138   0.336729 f=Th      F    1.549265  21.222137   7.989030 f=F
H   -1.708584  20.351708   1.901867 f=Th      H   -0.298818  20.869337   3.875138 f=F
H   -3.478377  16.606637   6.545334 f=Th      F   -0.939957  21.259180   9.032545 f=F
H   -6.517675  16.999610   6.772797 f=Th      H   -2.904213  21.072415   7.331658 f=F
H   -5.569561  15.706669   7.540479 f=Th      H   -2.612225  20.862404   4.852201 f=F
H   -5.700417  15.775681   5.771744 f=Th
```

Optimised geometry of η^2-E-Th and the name of the fragment f in the ETS-NOCV in which each atom belongs

```
C   21.847110  13.218075   0.029437 f=Th      C   20.293051  16.664835  -4.434125  f=Th
C   22.243178  14.460897  -0.521528 f=Th      C   21.190648  15.893936  -3.741004  f=Th
C   22.901704  15.420206   0.287493 f=Th      O   22.379862  15.435881  -4.295372  f=Th
C   23.187838  15.096854   1.609350  f=Th     C   19.143598  17.044362  -3.730178  f=Th
C   22.835709  13.868886   2.140739  f=Th     C   18.922276  16.683373  -2.407646  f=Th
C   22.165940  12.947590   1.356963  f=Th     C   19.886205  15.908000  -1.752104  f=Th
N   22.070791  14.724384  -1.905604  f=Th     C   21.032539  15.497390  -2.411557  f=Th
Th  23.908423  14.003799  -2.987916  f=Th     C   24.479529  17.580554  -9.093641  f=Th
C   23.084229  11.927646  -3.860379  f=Th     C   25.658547  18.491474  -8.730240  f=Th
Si  21.697883  11.549284  -5.081391  f=Th     C   20.194110  18.526593  -6.103935  f=Th
C   20.052949  12.186872  -4.439322  f=Th     C   19.611404  16.186171  -6.780334  f=Th
C   23.247791  16.804657  -0.217781  f=Th     C   17.663067  17.102832  -1.650041  f=Th
C   24.701966  17.176531   0.052609  f=Th     C   16.725998  17.950498  -2.506254  f=Th
C   21.020343  12.216908  -0.746789  f=Th     C   26.189652  14.692150  -4.883797  f=Th
C   19.548569  12.316697  -0.339403  f=Th     C   26.690753  13.547550  -5.549312  f=Th
N   24.791161  14.944346  -4.836444  f=Th     C   28.059350  13.297847  -5.510715  f=Th
C   24.132397  15.719102  -5.786060  f=Th     C   28.925987  14.138571  -4.840708  f=Th
C   22.797790  16.006050  -5.492148  f=Th     C   28.434409  15.256543  -4.190849  f=Th
C   21.977409  16.778136  -6.274645  f=Th     C   27.077603  15.560784  -4.195965  f=Th
C   22.546441  17.274150  -7.453608  f=Th     C   25.807251  12.610126  -6.342315  f=Th
C   23.863218  17.019077  -7.812680  f=Th     C   25.981023  12.834353  -7.845391  f=Th
C   24.651912  16.234930  -6.962407  f=Th     C   26.608574  16.837360  -3.524103  f=Th
C   20.526660  17.045459  -5.891159  f=Th     C   27.441588  17.220654  -2.305338  f=Th
```

C	21.556337	9.693661	-5.327932	f=Th	H	23.969559	18.773129	-10.809929	f=Th
C	22.046343	12.342433	-6.747187	f=Th	H	23.110702	19.262915	-9.353352	f=Th
C	16.899678	15.851437	-1.200520	f=Th	H	29.988937	13.926889	-4.827043	f=Th
C	18.057876	17.924322	-0.417095	f=Th	H	23.086883	16.821504	-1.300458	f=Th
C	22.313323	17.851305	0.391058	f=Th	H	29.126347	15.909962	-3.675236	f=Th
C	21.505198	10.778902	-0.582707	f=Th	H	19.148036	13.314623	-0.520607	f=Th
C	24.982946	16.428185	-9.970074	f=Th	H	19.422387	12.085167	0.721474	f=Th
C	23.480451	18.397508	-9.908823	f=Th	H	18.947403	11.606121	-0.911614	f=Th
C	26.593957	18.005753	-4.513307	f=Th	H	25.724413	13.853382	-8.134541	f=Th
C	26.067152	11.141571	-6.010772	f=Th	H	25.334249	12.155574	-8.406482	f=Th
H	18.403131	17.640124	-4.243753	f=Th	H	27.012710	12.640642	-8.150600	f=Th
H	25.689493	16.036231	-7.202942	f=Th	H	23.686132	15.824214	2.239806	f=Th
H	21.930287	17.876857	-8.104671	f=Th	H	28.453622	12.429123	-6.024642	f=Th
H	19.750293	15.620154	-0.716474	f=Th	H	21.083964	12.484010	-1.803559	f=Th
H	23.993529	11.452306	-4.266859	f=Th	H	17.163515	18.234697	0.128871	f=Th
H	22.845056	11.369858	-2.937494	f=Th	H	18.608267	18.823708	-0.703960	f=Th
H	19.153008	18.731197	-5.853497	f=Th	H	18.680543	17.350762	0.272926	f=Th
H	20.329780	18.810298	-7.147745	f=Th	H	20.066910	13.256462	-4.213680	f=Th
H	20.828381	19.166539	-5.488042	f=Th	H	19.737427	11.657622	-3.536595	f=Th
H	15.846936	18.224247	-1.919149	f=Th	H	19.279202	12.019808	-5.194489	f=Th
H	16.374447	17.407263	-3.386815	f=Th	H	22.484145	9.270753	-5.722601	f=Th
H	17.201168	18.877693	-2.836083	f=Th	H	20.756016	9.451336	-6.033046	f=Th
H	26.437082	17.952507	-8.185970	f=Th	H	21.334188	9.182422	-4.387272	f=Th
H	25.330448	19.329205	-8.109954	f=Th	H	25.940680	17.813661	-5.363341	f=Th
H	26.111410	18.899364	-9.637442	f=Th	H	27.603240	18.189088	-4.891442	f=Th
H	18.563102	16.361530	-6.529147	f=Th	H	26.250345	18.917060	-4.017965	f=Th
H	19.820358	15.122552	-6.649563	f=Th	H	27.553807	16.398692	-1.593680	f=Th
H	19.759717	16.436451	-7.832991	f=Th	H	26.974557	18.057049	-1.783747	f=Th
H	25.760654	15.846775	-9.470707	f=Th	H	28.442603	17.549106	-2.592028	f=Th
H	25.410792	16.820870	-10.895857	f=Th	H	22.925911	11.905868	-7.227014	f=Th
H	24.168582	15.749217	-10.233900	f=Th	H	22.201166	13.422959	-6.683780	f=Th
H	15.991836	16.137915	-0.663641	f=Th	H	21.198410	12.170292	-7.416715	f=Th
H	17.496537	15.229778	-0.529840	f=Th	H	22.547077	18.843158	-0.002793	f=Th
H	16.608551	15.239948	-2.057803	f=Th	H	22.425484	17.886803	1.477719	f=Th
H	23.068753	13.636711	3.173546	f=Th	H	21.269054	17.635469	0.163155	f=Th
H	25.312561	10.509711	-6.484817	f=Th	H	24.933030	18.145381	-0.394781	f=Th
H	26.043652	10.945384	-4.935711	f=Th	H	25.399094	16.440821	-0.357896	f=Th
H	27.039597	10.810052	-6.381602	f=Th	H	24.906711	17.257959	1.122191	f=Th
H	24.769399	12.841190	-6.093934	f=Th	C	26.471504	12.963033	-1.559296	f=F
H	25.570389	16.689314	-3.194245	f=Th	C	25.496519	12.651090	-0.702519	f=F
H	21.868676	12.000128	1.790645	f=Th	H	25.203156	13.312913	0.108506	f=F
H	22.572295	10.671456	-0.794024	f=Th	H	24.991800	11.689823	-0.748135	f=F
H	20.961852	10.120369	-1.263992	f=Th	H	26.798991	12.274123	-2.333134	f=F
H	21.331968	10.403863	0.428502	f=Th	H	27.024737	13.894649	-1.485349	f=F
H	22.624717	17.796978	-10.227329	f=Th					

A.1.5   Optimised geometries of Alkyl cations containing Uranium

Optimised geometry of η^6-2-U

U	26.800801	13.592814	-5.510886		H	27.657731	14.009038	-8.081075
C	25.491564	16.354392	-4.125418		H	25.897664	14.000468	-8.066364
C	27.859184	16.450443	-4.100940		C	22.962081	17.231350	-3.514712
C	25.374046	17.619561	-3.607720		C	26.545780	19.064114	-1.941638
C	26.584983	18.512217	-3.372946		H	25.642966	19.653100	-1.776663
C	27.866905	17.717483	-3.576799		H	27.397400	19.719182	-1.754472
O	26.704269	15.785651	-4.471938		H	26.566917	18.256036	-1.208279
Si	26.748725	16.263684	-8.357543		C	21.519420	19.128052	-2.641993
C	24.072324	18.040990	-3.315238		H	20.489393	19.409663	-2.413867
H	23.936071	19.035812	-2.915692		H	21.897596	19.839603	-3.380282
C	30.220188	16.219437	-3.954170		H	22.099150	19.239253	-1.722441
H	31.115029	15.624078	-4.087968		C	32.345398	17.198517	-2.025562
C	29.126541	18.236029	-3.254768		H	32.506732	16.185276	-2.399907
H	29.177043	19.237272	-2.851155		H	31.744232	17.133317	-1.115349
C	23.154197	15.944873	-4.031913		H	33.322367	17.608172	-1.757125
H	22.310559	15.281382	-4.176239		C	29.805556	13.442668	-4.839113
C	28.996215	15.672194	-4.305170		C	26.552193	19.680812	-4.371123
N	28.755425	14.406473	-4.835895		H	25.642392	20.270138	-4.239342
C	30.300529	17.515419	-3.430218		H	26.579185	19.320344	-5.401177
C	24.425166	15.485274	-4.344659		H	27.409759	20.339120	-4.217147
C	26.778469	14.516861	-7.642928		C	32.544149	18.151328	-4.327783

A.1. Geometries from the Chapter Coordination of Alkyl cations [(XA$_2$)X(CH$_2$Y)]
(X = Th, U or Zr; Y = SiMe$_3$, H) with an arene for Ethylene polymerisation: 135
Exploration of the bonding

H	32.714518	17.158779	-4.749780	H	32.100533	11.991274	-6.874219
H	33.520806	18.578219	-4.086297	C	23.020567	13.949256	-7.211135
H	32.083187	18.772426	-5.099434	H	23.864406	14.626238	-7.063852
C	20.657882	17.624523	-4.411195	C	20.969504	16.776983	-2.080826
H	19.651565	17.978086	-4.173094	H	19.956329	17.094454	-1.821588
H	20.564615	16.604010	-4.787757	H	21.577117	16.810911	-1.173131
H	21.055466	18.248659	-5.215074	H	20.915606	15.738034	-2.413315
C	31.669022	18.093653	-3.070331	C	25.184386	17.157574	-7.836846
C	21.547648	17.694299	-3.165275	H	25.071592	17.224607	-6.752064
C	21.808269	11.226944	-4.874431	H	24.291556	16.669657	-8.236224
H	21.050588	10.451720	-4.879614	H	25.197361	18.177318	-8.232864
C	30.412511	13.398266	-8.542697	N	24.768544	14.225881	-4.841291
H	30.335210	14.119434	-9.359476	C	23.752146	13.222525	-4.857619
H	29.540937	12.743199	-8.604023	C	26.772624	16.154835	-10.232090
H	31.297555	12.788620	-8.737350	H	27.672651	15.648994	-10.592301
C	30.049640	12.697456	-3.662349	H	26.752358	17.151948	-10.681267
C	30.510203	14.133732	-7.209000	H	25.907894	15.604016	-10.612132
H	29.627020	14.765887	-7.098002	C	30.341608	13.507969	-1.308866
C	30.576414	13.219479	-6.001855	H	30.864947	14.397379	-1.661677
C	23.567820	12.412978	-3.712184	H	31.088627	12.748095	-1.066251
C	29.348920	12.993585	-2.351449	H	29.819117	13.767429	-0.385121
H	28.623463	13.791967	-2.528938	C	28.592478	11.784703	-1.807714
C	21.980390	12.037195	-5.980298	H	27.835621	11.426989	-2.509936
H	21.345209	11.894524	-6.847401	H	28.086699	12.042829	-0.874627
C	23.250793	13.168848	-8.503801	H	29.266299	10.951369	-1.594781
H	24.144407	12.542989	-8.454812	C	28.248346	17.245122	-7.805123
H	23.369329	13.856229	-9.344718	H	29.176377	16.814151	-8.189238
H	22.404839	12.517532	-8.736037	H	28.336417	17.315384	-6.718361
C	31.569684	19.504055	-2.494917	H	28.180909	18.263558	-8.199184
H	31.131538	20.206564	-3.208142	C	23.549502	13.464920	-1.433089
H	32.570526	19.867326	-2.252717	H	24.129666	13.627673	-0.521457
H	30.980681	19.529486	-1.574720	H	22.627970	12.946131	-1.155389
C	31.712367	11.412966	-4.857821	H	23.281318	14.437698	-1.844433
H	32.446786	10.615850	-4.869923	C	24.782199	11.321412	-1.764336
C	24.350617	12.624722	-2.430434	H	25.438511	11.534204	-0.918324
H	25.254524	13.194362	-2.679122	H	25.317446	10.663177	-2.451053
C	31.003709	11.687375	-3.700574	H	23.927313	10.767982	-1.370276
H	31.202326	11.107937	-2.805781	C	25.594100	9.997042	-5.377091
C	21.762270	14.806669	-7.349048	H	24.761453	9.589362	-4.817891
H	21.603122	15.430853	-6.469947	C	27.942134	10.519101	-5.548983
H	20.874611	14.185137	-7.491402	H	28.943723	10.506546	-5.135160
H	21.846915	15.466632	-8.215871	C	25.379494	10.515147	-6.646812
C	31.732670	15.055063	-7.232214	H	24.382527	10.508200	-7.068628
H	31.802451	15.653685	-6.324210	C	27.728898	11.028977	-6.828773
H	31.674671	15.740739	-8.080969	H	28.572872	11.381829	-7.408480
H	32.654880	14.476800	-7.331643	C	26.446421	11.034485	-7.375398
C	22.592172	11.423751	-3.750368	H	26.290706	11.407912	-8.380757
H	22.432412	10.798651	-2.879927	C	26.871514	10.003360	-4.827268
C	22.937241	13.048575	-5.996127	H	27.039543	9.581841	-3.843284
C	31.505942	12.182604	-5.988417				

A.1.6 Optimised geometries of Alkyl cations containing Zirconium

Optimised geometry of η^6-2′-Zr and the name of the fragment f in the ETS-NOCV in which each atom belongs

C	6.765617	8.543203	16.019925	f=B	C	8.051034	12.749072	20.103447 f=Z
C	7.594672	9.346129	15.246965	f=B	C	8.280057	9.255044	20.402336 f=Z
C	7.196142	10.639722	14.906181	f=B	C	8.560596	8.286726	21.368180 f=Z
C	5.972804	11.130791	15.343249	f=B	C	9.515616	8.635298	22.577247 f=Z
C	5.154178	10.338319	16.152808	f=B	C	9.478542	9.973302	22.811748 f=Z
C	5.548108	9.046473	16.486256	f=B	C	8.253111	14.586079	21.549236 f=Z
H	8.549431	8.971886	14.901321	f=B	C	7.383513	15.319339	20.747801 f=Z
Zr	7.388531	10.680855	17.780436	f=Z	C	6.858483	14.724108	19.597930 f=Z
C	9.476823	11.030952	17.040068	f=Z	C	7.181169	13.414049	19.256415 f=Z
O	8.269054	11.440735	19.704398	f=Z	C	9.461558	7.595019	23.654881 f=Z
C	8.628986	10.555301	20.706789	f=Z	C	8.743402	7.979213	24.954065 f=Z
C	9.220970	10.971548	21.878665	f=Z	N	7.666527	9.057113	19.160128 f=Z
C	9.596177	12.436971	22.049428	f=Z	C	7.320155	7.685229	18.917442 f=Z
C	8.610252	13.271948	21.243984	f=Z	C	8.292561	6.787389	18.441989 f=Z

```
C     7.924372     5.462894    18.219243 f=Z          H     5.172311     9.157319    19.494083 f=Z
C     6.643436     4.992255    18.459809 f=Z          H     4.263650     8.778327    21.763931 f=Z
C     5.709381     5.895833    18.955297 f=Z          H     4.844233     7.109950    21.721998 f=Z
C     6.015533     7.228151    19.204871 f=Z          H     5.999277     8.447249    21.711694 f=Z
N     6.709354    12.678854    18.161878 f=Z          H     2.848548     8.577403    19.718800 f=Z
C     5.793790    13.422420    17.343529 f=Z          H     3.416166     7.685328    18.303492 f=Z
C     4.404791    13.321505    17.575246 f=Z          H     3.185581     6.861806    19.839551 f=Z
C     3.544369    14.075971    16.786534 f=Z          H     9.805655     8.271329    18.334010 f=Z
C     3.998873    14.939301    15.795797 f=Z          H    10.463436     6.757366    20.182720 f=Z
C     5.368096    15.023748    15.598507 f=Z          H    10.664756     5.426295    19.035438 f=Z
C     6.282390    14.286679    16.346818 f=Z          H    11.720952     6.837195    18.946788 f=Z
C     6.966115    16.747203    21.102858 f=Z          H     9.493775     7.335754    16.002418 f=Z
C     7.652049    17.254159    22.368855 f=Z          H    11.168315     7.277577    16.559820 f=Z
C     9.607344    12.844484    23.519379 f=Z          H    10.188352     5.815982    16.549550 f=Z
C    11.005365    12.649569    21.462693 f=Z          H     7.184001     3.061091    17.813897 f=Z
C     9.729930     7.193328    18.175972 f=Z          H     6.703419     2.902632    20.248589 f=Z
C    10.162820     6.891034    16.741693 f=Z          H     5.000618     3.260531    19.943677 f=Z
C     6.285478     3.546344    18.210695 f=Z          H     5.711505     1.773855    19.315796 f=Z
C     5.181821     3.405791    17.165219 f=Z          H     5.459866     3.884216    16.223342 f=Z
C     4.956975     8.131120    19.814740 f=Z          H     4.980056     2.351711    16.961921 f=Z
C     3.531246     7.793075    19.385413 f=Z          H     4.248396     3.858345    17.510703 f=Z
C     3.825036    12.445980    18.672675 f=Z          H     2.477136    13.996342    16.958363 f=Z
C     2.467497    11.840098    18.322728 f=Z          H     5.739936    15.694090    14.829888 f=Z
C     3.041172    15.761244    14.966304 f=Z          H     4.528812    11.622897    18.844284 f=Z
C     2.250963    16.743154    15.828516 f=Z          H     3.282134    12.555753    20.767863 f=Z
C     7.760670    14.445703    16.047375 f=Z          H     4.659292    13.580684    20.346768 f=Z
C     8.070690    14.297339    14.557208 f=Z          H     3.025055    14.059450    19.876922 f=Z
C     7.326302    17.694915    19.953681 f=Z          H     2.442099    11.371183    17.335437 f=Z
C     5.450141    16.785160    21.331705 f=Z          H     2.196899    11.083883    19.062567 f=Z
C    10.974200     7.554671    23.903527 f=Z          H     1.676357    12.592999    18.339442 f=Z
C     9.003939     6.193832    23.258062 f=Z          H     8.292559    13.658651    16.586978 f=Z
H     8.284576     7.261235    21.171217 f=Z          H     9.365763    15.875988    16.298718 f=Z
H     6.168539    15.273180    18.970894 f=Z          H     7.783310    16.618070    16.050233 f=Z
H     8.665378    15.040704    22.437342 f=Z          H     8.190092    15.901656    17.615256 f=Z
H    10.337666    12.256421    24.076020 f=Z          H     9.150252    14.237740    14.400297 f=Z
H     9.905766    13.887622    23.627945 f=Z          H     7.611651    13.408930    14.117843 f=Z
H     8.628259    12.712520    23.983202 f=Z          H     7.711329    15.156260    13.986028 f=Z
H    11.735101    12.043939    22.004695 f=Z          H     3.648979    16.346516    14.267533 f=Z
H    11.044661    12.367011    20.408760 f=Z          H     2.662673    14.200154    13.495038 f=Z
H    11.293617    13.699933    21.544630 f=Z          H     1.457407    14.279404    14.785979 f=Z
H     8.401770    17.687980    19.759981 f=Z          H     1.460087    15.495549    13.509926 f=Z
H     6.813361    17.427730    19.027610 f=Z          H     2.914448    17.396077    16.399301 f=Z
H     7.035820    18.717484    20.207501 f=Z          H     1.611544    17.370887    15.203804 f=Z
H     4.897447    16.481220    20.440229 f=Z          H     1.605797    16.217401    16.537449 f=Z
H     5.160581    16.122475    22.150918 f=Z          H     9.985759    10.086449    16.820017 f=Z
H     5.134555    17.799495    21.588964 f=Z          H     9.526360    11.652714    16.141655 f=Z
H     8.739628    17.275510    22.263279 f=Z          H    10.043300    11.537249    17.825413 f=Z
H     7.323190    18.274893    22.574635 f=Z          C     5.027882     8.119345    21.344000 f=Z
H     7.399525    16.647924    23.242254 f=Z          C    10.696641     6.513226    19.146332 f=Z
H    11.356428     8.520654    24.239192 f=Z          C     5.906079     2.831771    19.505962 f=Z
H    11.208964     6.817641    24.675722 f=Z          C     3.698954    13.206581    19.994957 f=Z
H    11.514543     7.277311    22.995038 f=Z          C     8.302917    15.788679    16.537731 f=Z
H     7.925012     6.149437    23.088775 f=Z          C     2.104801    14.880875    14.142108 f=Z
H     9.510072     5.835066    22.358283 f=Z          H     9.943884    10.244620    23.749566 f=Z
H     9.238419     5.494863    24.063640 f=Z          H     7.845085    11.258052    14.300136 f=B
H     7.661076     8.015551    24.807948 f=Z          H     5.659133    12.132494    15.081835 f=B
H     8.955785     7.241210    25.731701 f=Z          H     4.209622    10.729768    16.504973 f=B
H     9.064587     8.953571    25.326710 f=Z          H     4.914149     8.421604    17.099425 f=B
H     8.671252     4.766910    17.849489 f=Z          H     7.065048     7.538292    16.286669 f=B
H     4.706281     5.543943    19.166778 f=Z
```

Optimised geometry of η^6-2-Zr and the name of the fragment f in the ETS-NOCV in which each atom belongs

```
;lkjhgfdsdrftghjklp;
```

Optimised geometry of η^6-3′-Zr-exo and the name of the fragment f in the ETS-NOCV in which each atom belongs
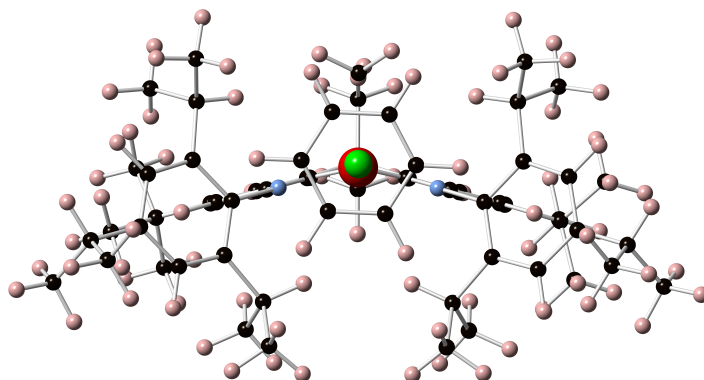
FIGURE A.1: **2'-Zr-a** molecule. Green: Pu; red: O; blue: N; black: C; pink: H

```
Zr  7.241484   8.778722   15.728818   f=Z        C   4.449933   15.454959   15.065231   f=Z
O   8.37604    10.43795   14.725539   f=Z        H   3.796974   14.761958   14.528403   f=Z
N   6.041734   10.575997  15.687056   f=Z        H   4.45103    15.179758   16.12301    f=Z
N   8.580454   7.966974   14.257685   f=Z        H   4.006296   16.449677   14.986067   f=Z
C   7.847188   13.982576  14.065712   f=Z        C   5.76314    15.919013   13.014691   f=Z
H   8.340867   14.845178  13.639288   f=Z        H   5.176693   15.205728   12.430227   f=Z
C   6.548546   14.119205  14.559059   f=Z        H   5.276267   16.895079   12.945114   f=Z
C   5.915737   13.007942  15.107004   f=Z        H   6.74679    16.005144   12.549168   f=Z
H   4.908206   13.088679  15.487045   f=Z        C   4.660025   10.709227   16.060997   f=Z
C   6.560912   11.770446  15.170919   f=Z        C   4.300172   11.057838   17.376605   f=Z
C   9.457686   8.790449   13.542351   f=Z        C   2.948951   11.216177   17.674901   f=Z
C   10.396445  8.399063   12.592137   f=Z        H   2.66217    11.480989   18.686918   f=Z
H   10.488642  7.34834    12.351078   f=Z        C   1.946728   11.061465   16.728534   f=Z
C   11.196338  9.338666   11.937741   f=Z        C   2.332178   10.732959   15.4356     f=Z
C   11.05044   10.685071  12.256195   f=Z        H   1.569189   10.618426   14.672579   f=Z
H   11.667627  11.41714   11.757684   f=Z        C   3.662998   10.560343   15.074594   f=Z
C   9.964387   12.575135  13.6375     f=Z        C   3.983874   10.251212   13.623686   f=Z
C   8.529419   12.771957  14.104719   f=Z        H   5.052405   10.026627   13.558602   f=Z
C   7.843191   11.714965  14.662143   f=Z        C   3.714556   11.460192   12.726124   f=Z
C   9.369295   10.147382  13.80374    f=Z        H   3.984213   11.233569   11.691628   f=Z
C   10.125937  11.125106  13.204583   f=Z        H   2.654716   11.7277     12.743193   f=Z
C   10.323614  13.539776  12.511312   f=Z        H   4.290299   12.330043   13.043208   f=Z
H   10.230982  14.57351   12.845571   f=Z        C   3.214969   9.042157    13.093204   f=Z
H   11.362163  13.407536  12.206714   f=Z        H   3.522626   8.822293    12.068282   f=Z
H   9.684256   13.397917  11.638253   f=Z        H   3.37927    8.142452    13.691201   f=Z
C   10.903549  12.832114  14.832205   f=Z        H   2.13874    9.22657     13.073153   f=Z
H   10.79525   13.860951  15.182735   f=Z        C   5.328534   11.294083   18.46876    f=Z
H   10.678964  12.163515  15.665722   f=Z        H   6.224168   10.726947   18.197704   f=Z
H   11.942768  12.671409  14.536719   f=Z        C   5.738926   12.766197   18.558806   f=Z
C   12.1962    8.858842   10.88479    f=Z        H   6.185356   13.124851   17.63257    f=Z
C   13.185709  7.877959   11.52368    f=Z        H   4.868977   13.389582   18.783206   f=Z
H   13.742256  8.35351    12.335036   f=Z        H   6.466102   12.906057   19.362746   f=Z
H   12.682995  6.997693   11.929344   f=Z        C   4.866663   10.833415   19.850879   f=Z
H   13.905614  7.533028   10.77715    f=Z        H   4.443631   9.825299    19.853821   f=Z
C   11.440193  8.149451   9.754941    f=Z        H   5.707009   10.851923   20.549002   f=Z
H   10.888694  7.279704   10.118005   f=Z        H   4.105157   11.499925   20.261716   f=Z
H   10.727811  8.825013   9.275063    f=Z        C   0.49476    11.25608    17.095625   f=Z
H   12.143268  7.802524   8.993403    f=Z        H   0.467841   11.506463   18.16191    f=Z
C   12.993337  10.009111  10.27525    f=Z        C   -0.127385  12.421453   16.329699   f=Z
H   13.583338  10.540351  11.026303   f=Z        H   0.430775   13.346411   16.488697   f=Z
H   13.68955   9.613599   9.532765    f=Z        H   -0.148137  12.222629   15.25485    f=Z
H   12.348039  10.729747  9.766824    f=Z        H   -1.15738   12.585655   16.654351   f=Z
C   5.86003    15.481822  14.481236   f=Z        C   -0.31574   9.977254    16.898486   f=Z
C   6.682208   16.512038  15.264871   f=Z        H   0.102675   9.146664    17.471432   f=Z
H   7.691833   16.618366  14.863564   f=Z        H   -1.348565  10.125093   17.221968   f=Z
H   6.201045   17.49216   15.215714   f=Z        H   -0.339518  9.682131    15.845967   f=Z
H   6.76683    16.228464  16.316794   f=Z        C   8.723797   6.578796    13.92012    f=Z
```

C	7.933199	6.024248	12.890256	f=Z	H	10.030744	2.030424	13.44568	f=Z
C	8.114705	4.686552	12.560278	f=Z	C	7.974383	1.609377	13.067519	f=Z
H	7.505573	4.258712	11.772254	f=Z	H	7.66456	1.673585	14.113085	f=Z
C	9.050226	3.878302	13.195526	f=Z	H	7.142472	1.954414	12.447563	f=Z
C	9.811753	4.450824	14.202076	f=Z	H	8.147306	0.557217	12.83032	f=Z
H	10.54556	3.832723	14.709134	f=Z	C	9.68957	2.29021	11.356487	f=Z
C	9.67749	5.783626	14.583113	f=Z	H	10.606795	2.852447	11.169614	f=Z
C	6.901207	6.83332	12.125691	f=Z	H	9.878672	1.241744	11.115352	f=Z
H	6.596811	7.667998	12.76726	f=Z	H	8.925386	2.65484	10.664915	f=Z
C	7.484733	7.440819	10.84804	f=Z	C	8.68459	9.195491	17.393953	f=Z
H	6.719476	8.012559	10.316729	f=Z	H	8.219318	9.763178	18.20611	f=Z
H	8.322596	8.105118	11.055649	f=Z	H	9.140681	8.301301	17.826483	f=Z
H	7.835466	6.650299	10.178958	f=Z	H	9.489988	9.810183	16.983148	f=Z
C	5.65189	6.030165	11.767412	f=Z	C	6.399183	7.241748	18.048942	f=t
H	5.258706	5.453637	12.608836	f=Z	C	7.042913	6.322772	17.208383	f=t
H	4.865322	6.699292	11.412636	f=Z	H	7.925389	5.808493	17.567453	f=t
H	5.84912	5.321333	10.960095	f=Z	C	6.563710	6.045666	15.934283	f=t
C	10.571936	6.31737	15.685831	f=Z	H	7.070384	5.316600	15.317068	f=t
H	10.126239	7.246935	16.047122	f=Z	C	5.443818	6.721495	15.442507	f=t
C	11.974768	6.651486	15.173733	f=Z	H	5.069741	6.508599	14.449781	f=t
H	12.597962	7.01566	15.994496	f=Z	C	4.796711	7.643354	16.260262	f=t
H	12.454898	5.759762	14.761196	f=Z	H	3.923633	8.176336	15.908099	f=t
H	11.955385	7.417182	14.399607	f=Z	C	5.277655	7.904809	17.543025	f=t
C	10.700352	5.354788	16.866994	f=Z	H	4.761421	8.632196	18.154469	f=t
H	11.163343	5.863011	17.716054	f=Z	C	6.846925	7.436240	19.457397	f=t
H	9.740565	4.947067	17.192041	f=Z	H	6.599208	8.430215	19.827540	f=t
H	11.338864	4.502893	16.622291	f=Z	H	6.335326	6.708595	20.095550	f=t
C	9.235178	2.430524	12.807497	f=Z	H	7.918576	7.273051	19.566346	f=t
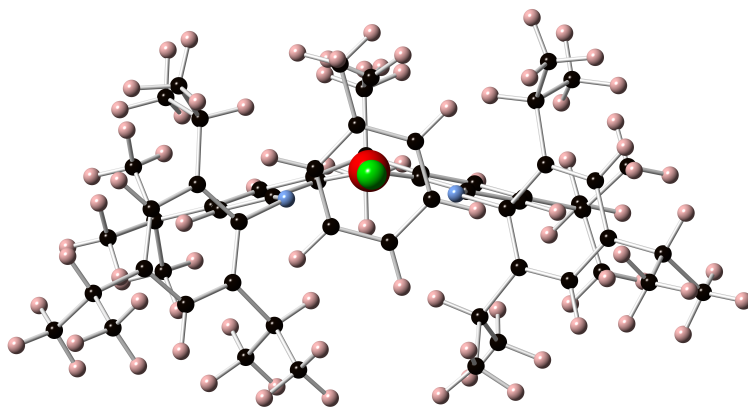
FIGURE A.2: **3′-Zr-a** molecule. Green: Pu; red: O; blue: N; black: C; pink: H

A.1. *Geometries from the Chapter Coordination of Alkyl cations [(XA₂)X(CH₂Y)]*
(X = Th, U or Zr; Y = SiMe₃, H) with an arene for Ethylene polymerisation: 139
Exploration of the bonding

Optimised geometry of η^6-4′-Zr-exo and the name of the fragment f in the ETS-NOCV in which each atom belongs

Zr	7.199815	10.734381	18.139199	f=Z	H	5.078085	16.678940	20.703242 f=Z
C	9.010617	10.914767	16.901978	f=Z	H	5.353573	16.328814	22.414726 f=Z
N	6.732466	12.730258	18.505216	f=Z	H	5.389765	17.997863	21.830443 f=Z
C	7.237468	13.496107	19.551206	f=Z	H	8.978854	17.347302	22.450513 f=Z
C	8.127030	12.821728	20.372407	f=Z	H	7.605515	18.403378	22.766366 f=Z
C	8.721761	13.342691	21.493135	f=Z	H	7.634193	16.787180	23.463695 f=Z
C	8.396184	14.670369	21.785527	f=Z	H	11.481180	8.547794	24.412880 f=Z
C	7.524385	15.414368	20.995482	f=Z	H	11.336491	6.842235	24.839879 f=Z
C	6.946060	14.813874	19.871378	f=Z	H	11.599238	7.313721	23.155124 f=Z
C	9.704397	12.492366	22.289867	f=Z	H	8.008385	6.200588	23.340154 f=Z
C	9.311673	11.029192	22.120943	f=Z	H	9.571459	5.886366	22.562140 f=Z
C	8.686371	10.623636	20.964629	f=Z	H	9.346346	5.533664	24.271503 f=Z
O	8.317457	11.509324	19.963324	f=Z	H	7.799523	8.057223	25.076170 f=Z
C	9.579950	10.018531	23.040570	f=Z	H	9.115235	7.271574	25.959908 f=Z
C	9.237008	8.684177	22.809422	f=Z	H	9.220736	8.985946	25.562437 f=Z
C	8.598960	8.345833	21.617138	f=Z	H	8.642841	5.106947	17.584314 f=Z
C	8.306896	9.327319	20.674377	f=Z	H	4.626910	5.794792	18.793041 f=Z
C	7.167156	16.862897	21.330599	f=Z	H	5.112218	9.310802	19.632402 f=Z
C	7.546677	17.770764	20.155282	f=Z	H	4.198509	8.703377	21.840827 f=Z
C	9.727690	12.896902	23.760780	f=Z	H	4.778847	7.046900	21.632469 f=Z
C	11.111337	12.689274	21.693133	f=Z	H	5.934886	8.377892	21.760609 f=Z
C	9.566489	7.636205	23.872515	f=Z	H	2.790275	8.686098	19.768697 f=Z
C	11.085089	7.586506	24.080001	f=Z	H	3.400996	7.992781	18.260272 f=Z
N	7.644696	9.178804	19.459128	f=Z	H	3.146781	6.973663	19.676032 f=Z
C	7.301602	7.866091	19.023120	f=Z	H	9.817991	8.479446	18.595735 f=Z
C	8.278702	7.025886	18.452638	f=Z	H	10.369122	6.720232	20.257812 f=Z
C	7.894025	5.760398	18.020840	f=Z	H	10.596780	5.547755	18.953528 f=Z
C	6.592132	5.296211	18.127032	f=Z	H	11.678799	6.934698	19.093796 f=Z
C	5.647580	6.144083	18.697171	f=Z	H	9.557871	7.853322	16.157331 f=Z
C	5.968379	7.413734	19.158565	f=Z	H	11.216259	7.708092	16.749054 f=Z
C	9.729745	7.432499	18.297428	f=Z	H	10.232977	6.266238	16.526185 f=Z
C	10.204199	7.309467	16.849433	f=Z	H	7.128336	3.464428	17.235543 f=Z
C	6.219295	3.912676	17.651095	f=Z	H	6.509414	2.972740	19.594376 f=Z
C	5.172435	3.956146	16.540569	f=Z	H	4.833399	3.416440	19.254391 f=Z
C	4.900485	8.250931	19.839466	f=Z	H	5.550776	2.017132	18.456356 f=Z
C	3.486824	7.958775	19.349525	f=Z	H	5.511448	4.556798	15.693363 f=Z
C	5.818481	13.331859	17.592169	f=Z	H	4.961723	2.948284	16.176307 f=Z
C	6.296126	14.043585	16.472427	f=Z	H	4.230448	4.379850	16.898827 f=Z
C	5.368049	14.582774	15.588096	f=Z	H	2.487351	13.695155	17.075037 f=Z
C	3.997794	14.463192	15.772887	f=Z	H	5.727005	15.132477	14.723720 f=Z
C	3.554159	13.780257	16.900238	f=Z	H	4.661308	11.961003	19.520064 f=Z
C	4.428366	13.215366	17.819975	f=Z	H	3.029932	13.102346	20.980549 f=Z
C	7.770942	14.284981	16.222082	f=Z	H	4.244706	14.234883	20.382954 f=Z
C	8.199296	13.914005	14.804881	f=Z	H	2.626260	14.221795	19.674087 f=Z
C	3.860042	12.547012	19.056172	f=Z	H	2.962441	10.853683	17.994139 f=Z
C	2.702071	11.603131	18.746028	f=Z	H	2.393472	11.080161	19.653509 f=Z
C	3.026833	15.075727	14.791992	f=Z	H	1.827210	12.143424	18.378647 f=Z
C	2.190181	16.173872	15.445218	f=Z	H	8.332240	13.659450	16.919845 f=Z
C	9.091935	6.239915	23.478514	f=Z	H	9.208527	15.898556	16.339156 f=Z
C	8.885200	8.015287	25.192833	f=Z	H	7.596570	16.419022	15.841223 f=Z
C	5.658166	16.967870	21.582322	f=Z	H	7.916864	16.023364	17.535131 f=Z
C	7.893314	17.367613	22.574818	f=Z	H	9.283159	14.004305	14.706426 f=Z
C	10.641991	6.609766	19.208002	f=Z	H	7.923962	12.890358	14.544636 f=Z
C	5.753994	3.030976	18.808193	f=Z	H	7.751567	14.578374	14.061905 f=Z
C	4.963593	8.089279	21.359540	f=Z	H	3.625286	15.539494	14.000316 f=Z
C	3.419369	13.590835	20.084049	f=Z	H	2.723240	13.248947	13.642200 f=Z
C	2.133956	14.020750	14.143082	f=Z	H	1.496131	13.530410	14.883314 f=Z
C	8.140054	15.742239	16.505820	f=Z	H	1.480029	14.480297	13.398746 f=Z
H	10.071961	10.277875	23.968308	f=Z	H	2.821821	16.947082	15.887089 f=Z
H	8.301516	7.325759	21.416671	f=Z	H	1.540080	16.647416	14.706258 f=Z
H	6.249845	15.363208	19.249527	f=Z	H	1.552126	15.768846	16.235125 f=Z
H	8.838922	15.129311	22.656782	f=Z	H	9.538701	9.964884	16.794549 f=Z
H	10.454037	12.299617	24.312854	f=Z	H	8.710989	11.257021	15.903437 f=Z
H	10.037240	13.936769	23.869874	f=Z	H	9.711156	11.650599	17.307009 f=Z
H	8.749465	12.774499	24.228994	f=Z	C	5.335433	10.773110	15.476623 f=t
H	11.837963	12.074331	22.228760	f=Z	C	5.525781	9.667681	16.313699 f=t
H	11.138670	12.408082	20.638483	f=Z	C	6.337495	8.606945	15.891653 f=t
H	11.412788	13.735928	21.774913	f=Z	C	6.980050	8.669311	14.667198 f=t
H	8.616436	17.710773	19.940983	f=Z	C	6.796046	9.782767	13.856071 f=t
H	7.003500	17.507786	19.245230	f=Z	C	5.974804	10.831879	14.249578 f=t
H	7.306609	18.810306	20.392142	f=Z	Br	7.661406	9.865988	12.196192 f=t

H	7.603622	7.850533	14.332358 f=t	H	4.901991	9.545096	17.202458 f=t
H	5.824671	11.681194	13.596222 f=t	H	6.442404	7.722144	16.508373 f=t
H	4.670173	11.577534	15.768395 f=t				

Optimised geometry of η^6-4′-Zr-horizontal and the name of the fragment f in the ETS-NOCV in which each atom belongs

C	1.148781	9.601211	14.619544 f=Z	H	-3.481685	8.002451	20.725676 f=Z
C	0.673990	10.683643	15.398187 f=Z	H	-2.721743	11.308468	22.317984 f=Z
C	0.555205	11.967135	14.828107 f=Z	H	-1.884428	12.019301	20.931235 f=Z
C	0.877636	12.126313	13.484817 f=Z	H	-3.630742	11.745886	20.858792 f=Z
C	1.327173	11.081041	12.694370 f=Z	H	-4.814205	12.222189	15.792557 f=Z
C	1.468641	9.831507	13.288947 f=Z	H	-3.856136	11.467314	14.511872 f=Z
N	0.323648	10.458942	16.760571 f=Z	H	-5.608424	11.293276	14.514456 f=Z
C	-1.008264	10.342883	17.141844 f=Z	H	-3.591101	8.922962	14.445997 f=Z
C	-1.188772	10.200101	18.510549 f=Z	H	-4.421655	7.921366	15.642244 f=Z
C	-2.393944	10.021929	19.139171 f=Z	H	-5.349713	8.781375	14.405696 f=Z
C	-3.509981	9.995356	18.296186 f=Z	H	-6.104176	10.751811	17.455766 f=Z
C	-3.405406	10.133943	16.915083 f=Z	H	-6.769737	9.868012	16.084993 f=Z
C	-2.140558	10.314812	16.342525 f=Z	H	-5.951323	8.986084	17.369386 f=Z
C	-2.457356	9.925330	20.660457 f=Z	H	-1.091241	8.920483	25.153255 f=Z
C	-1.117508	9.409622	21.175998 f=Z	H	0.029522	8.159731	26.282824 f=Z
C	0.025033	9.602267	20.435973 f=Z	H	0.551367	9.547839	25.317974 f=Z
O	0.018714	10.206175	19.189549 f=Z	H	2.279856	6.559147	23.817026 f=Z
C	1.293988	9.186109	20.798453 f=Z	H	2.544634	8.139139	24.579362 f=Z
C	1.438173	8.561830	22.032834 f=Z	H	1.905476	6.795820	25.521025 f=Z
C	0.325322	8.354522	22.847404 f=Z	H	-0.093701	5.700011	23.458299 f=Z
C	-0.930438	8.773471	22.401611 f=Z	H	-0.347239	5.912075	25.196225 f=Z
C	-4.628998	10.060579	16.001102 f=Z	H	-1.475559	6.629163	24.046163 f=Z
C	-5.931041	9.908045	16.783116 f=Z	H	6.581655	9.877803	21.384232 f=Z
C	-3.601916	9.017999	21.106840 f=Z	H	5.502852	6.211410	19.515345 f=Z
C	-2.686008	11.339441	21.226728 f=Z	H	2.039379	7.291088	18.762551 f=Z
Zr	1.952082	10.409557	18.036020 f=Z	H	1.760770	4.985668	19.592276 f=Z
C	0.441767	7.673773	24.211278 f=Z	H	3.368241	5.036358	20.324017 f=Z
C	-0.421839	6.406751	24.224502 f=Z	H	2.086880	6.095926	20.927566 f=Z
N	2.273716	9.444370	19.846307 f=Z	H	2.647700	5.450121	17.288330 f=Z
C	3.601394	8.966923	20.053222 f=Z	H	3.785214	6.776571	17.002139 f=Z
C	4.557828	9.769887	20.707707 f=Z	H	4.274163	5.369710	17.944581 f=Z
C	5.842125	9.265130	20.878495 f=Z	H	3.218604	11.391398	20.957663 f=Z
C	6.211278	7.996550	20.455108 f=Z	H	3.475617	10.342469	23.183313 f=Z
C	5.244122	7.216088	19.832223 f=Z	H	5.182185	10.804157	23.217997 f=Z
C	3.946550	7.664689	19.622511 f=Z	H	3.929394	12.048709	23.226782 f=Z
C	4.223933	11.126257	21.290369 f=Z	H	5.264702	12.251528	19.730738 f=Z
C	4.200484	11.071998	22.818928 f=Z	H	4.852313	13.192887	21.171175 f=Z
C	7.607960	7.475617	20.699160 f=Z	H	6.193719	12.056591	21.214065 f=Z
C	7.598198	6.285850	21.656917 f=Z	H	8.169420	8.284706	21.178501 f=Z
C	2.934903	6.713715	19.015303 f=Z	H	7.113650	6.539612	22.601786 f=Z
C	2.511977	5.648498	20.028610 f=Z	H	7.065800	5.434335	21.224844 f=Z
C	0.088374	13.177657	15.608518 f=Z	H	8.618643	5.962380	21.874307 f=Z
C	-1.290949	13.651900	15.151491 f=Z	H	8.377564	7.982089	18.725182 f=Z
C	1.650904	11.297224	11.235080 f=Z	H	9.345603	6.793343	19.601906 f=Z
C	3.129182	11.053835	10.939911 f=Z	H	7.815359	6.307713	18.875731 f=Z
C	1.255845	8.195331	15.184761 f=Z	H	1.828258	9.006228	12.687072 f=Z
C	-0.107129	7.502395	15.213686 f=Z	H	0.773115	13.108742	13.035497 f=Z
C	2.117158	12.537237	18.628359 f=Z	H	1.592295	8.269404	16.233328 f=Z
C	-4.726407	11.336766	15.158261 f=Z	H	-0.015899	6.498803	15.636409 f=Z
C	-4.484491	8.850128	15.070011 f=Z	H	-0.840265	8.054894	15.800117 f=Z
C	-0.048212	8.634482	25.301440 f=Z	H	-0.493622	7.403323	14.195809 f=Z
C	1.877829	7.273990	24.539736 f=Z	H	3.245736	7.783301	14.375911 f=Z
C	5.187094	12.214211	20.819768 f=Z	H	2.377135	6.368399	14.985307 f=Z
C	8.324365	7.122831	19.398196 f=Z	H	1.919015	7.071413	13.447875 f=Z
C	3.442650	6.047997	17.740087 f=Z	H	0.009751	12.888008	16.658622 f=Z
C	1.088070	14.330447	15.505460 f=Z	H	-1.598901	14.525375	15.731253 f=Z
C	2.262699	7.314899	14.455771 f=Z	H	-1.276771	13.941344	14.097250 f=Z
C	0.765447	10.444159	10.329609 f=Z	H	-2.048440	12.879259	15.282607 f=Z
H	-1.791650	8.600673	23.033093 f=Z	H	0.811792	15.132069	16.194099 f=Z
H	2.421050	8.229484	22.337577 f=Z	H	2.107569	14.015674	15.739302 f=Z
H	-2.027091	10.404964	15.269053 f=Z	H	1.101130	14.757085	14.499797 f=Z
H	-4.485716	9.858622	18.738007 f=Z	H	1.437713	12.348742	11.014946 f=Z
H	-3.658924	8.975175	22.194838 f=Z	H	3.767928	11.702558	11.544443 f=Z
H	-4.560578	9.406600	20.762172 f=Z	H	3.405091	10.014849	11.141816 f=Z

A.1. Geometries from the Chapter Coordination of Alkyl cations [(XA₂)X(CH₂Y)]
(X = Th, U or Zr; Y = SiMe₃, H) with an arene for Ethylene polymerisation: 141
Exploration of the bonding

```
 H    3.347912   11.254404    9.888684 f=Z          C    6.668704    7.903664   15.667402 f=t
 H   -0.293501   10.631874   10.517600 f=Z          C    6.662601    7.965837   14.281666 f=t
 H    0.968350   10.665448    9.279369 f=Z          C    5.963600    8.971677   13.630088 f=t
 H    0.949810    9.377701   10.484074 f=Z          C    5.262890    9.923889   14.357237 f=t
 H    3.036382   12.746366   19.183090 f=Z          H    5.960261    9.024021   12.547885 f=t
 H    2.073659   13.210702   17.768137 f=Z          H    7.208921    7.228521   13.706043 f=t
 H    1.275731   12.787666   19.283410 f=Z          H    4.709335   10.709690   13.860260 f=t
Br    4.407454   11.206023   16.741043 f=t          H    5.988764    8.812140   17.500800 f=t
 C    5.293763    9.833134   15.735801 f=t          H    7.217446    7.121333   16.177889 f=t
 C    5.981724    8.848467   16.418211 f=t
```

Optimised geometry of η^6-5′-Zr-exo and the name of the fragment f in the ETS-NOCV in which each atom belongs

```
 C    5.537644    9.678384   16.311264 f=t          C    7.776121   14.289557   16.220646 f=Z
 C    6.329164    8.599653   15.891837 f=t          C    8.144154   15.746347   16.507494 f=Z
 C    6.959412    8.638335   14.661669 f=t          C    9.006617   10.913195   16.891880 f=Z
 C    6.770844    9.748100   13.854006 f=t          C    8.880950    8.010272   25.188540 f=Z
 C    5.973807   10.816795   14.229568 f=t          C   11.084494    7.588027   24.080407 f=Z
 C    5.348104   10.777171   15.462709 f=t          C    7.893123   17.369939   22.573133 f=Z
 H    7.571843    7.817650   14.310294 f=t          C    7.552894   17.772942   20.152692 f=Z
 F    7.367646    9.784202   12.673467 f=t          C   10.205503    7.310334   16.839624 f=Z
 H    5.839430   11.651137   13.553299 f=t          C    5.172468    3.955187   16.543854 f=Z
 H    4.693620   11.589993   15.755161 f=t          C    3.492982    7.962947   19.345178 f=Z
 H    4.912054    9.567614   17.200501 f=t          C    2.701033   11.606301   18.737014 f=Z
 H    6.426936    7.721394   16.518662 f=t          C    2.198950   16.179353   15.443691 f=Z
 C    6.301309   14.046565   16.468613 f=Z          C    8.205701   13.923379   14.801733 f=Z
 C    5.823385   13.333500   17.587476 f=Z          H   10.067514   10.277122   23.969450 f=Z
 C    4.432990   13.214396   17.813007 f=Z          H    8.305760    7.325812   21.411116 f=Z
 C    3.559163   13.779248   16.892915 f=Z          H    6.254774   15.366510   19.244677 f=Z
 C    4.003208   14.465242   15.767567 f=Z          H    8.835735   15.130606   22.657789 f=Z
 C    5.373509   14.586207   15.584190 f=Z          H   10.438410   12.298455   24.321038 f=Z
 N    6.736627   12.732991   18.501777 f=Z          H   10.022798   13.935857   23.878013 f=Z
 C    7.240378   13.498687   19.548519 f=Z          H    8.733977   12.772169   24.228646 f=Z
 C    8.127616   12.823494   20.371745 f=Z          H   11.833525   12.077313   22.243597 f=Z
 C    8.719851   13.343995   21.494008 f=Z          H   11.142146   12.412485   20.650162 f=Z
 C    8.394694   14.672015   21.785492 f=Z          H   11.409181   13.739091   21.789734 f=Z
 C    7.525627   15.416832   20.993315 f=Z          H    8.622978   17.710981   19.940590 f=Z
 C    6.949279   14.816662   19.867997 f=Z          H    7.011054   17.510916   19.241567 f=Z
 O    8.318138   11.511676   19.962765 f=Z          H    7.314248   18.812943   20.388970 f=Z
 C    8.686274   10.624969   20.963944 f=Z          H    5.081491   16.683658   20.695175 f=Z
 C    9.308959   11.029850   22.121915 f=Z          H    5.352531   16.335012   22.407664 f=Z
 C    9.699312   12.493265   22.294236 f=Z          H    5.392095   18.003396   21.821754 f=Z
 C    9.577314   10.018302   23.040606 f=Z          H    8.978940   17.347873   22.451581 f=Z
 C    9.236923    8.683736   22.807174 f=Z          H    7.606483   18.406241   22.763508 f=Z
 C    8.601174    8.346100   21.613473 f=Z          H    7.630845   16.790308   23.461608 f=Z
 C    8.309031    9.328402   20.671661 f=Z          H   11.477744    8.549562   24.415918 f=Z
Zr    7.200536   10.736097   18.137230 f=Z          H   11.335605    6.843003   24.839637 f=Z
 N    7.648668    9.180079   19.455337 f=Z          H   11.601518    7.317890   23.156354 f=Z
 C    7.305780    7.867236   19.019609 f=Z          H    8.012671    6.196405   23.331187 f=Z
 C    8.282386    7.028363   18.446250 f=Z          H    9.578092    5.887344   22.555793 f=Z
 C    7.898096    5.762522   18.015136 f=Z          H    9.350275    5.531005   24.264075 f=Z
 C    6.597061    5.296615   18.124920 f=Z          H    7.795475    8.050015   25.069251 f=Z
 C    5.653105    6.143085   18.698077 f=Z          H    9.110716    7.265899   25.955056 f=Z
 C    5.973519    7.413241   19.158489 f=Z          H    9.213449    8.981120   25.560398 f=Z
 C    9.714604   12.895924   23.765852 f=Z          H    8.646520    5.110020   17.576524 f=Z
 C   11.109096   12.692277   21.705024 f=Z          H    4.633080    5.792613   18.796756 f=Z
 C    9.566310    7.634770   23.869297 f=Z          H    5.120969    9.309471   19.640278 f=Z
 C    9.095842    6.238076   23.471827 f=Z          H    4.199801    8.692424   21.843070 f=Z
 C    7.169310   16.865846   21.327293 f=Z          H    4.776612    7.035665   21.627247 f=Z
 C    5.659852   16.972833   21.575316 f=Z          H    5.935612    8.363186   21.765294 f=Z
 C    9.732527    7.436883   18.287811 f=Z          H    2.796710    8.689492   19.766203 f=Z
 C   10.647309    6.618527   19.199803 f=Z          H    3.410948    8.003339   18.255863 f=Z
 C    6.224645    3.912821   17.649377 f=Z          H    3.149482    6.976848   19.664960 f=Z
 C    5.766506    3.029187   18.807865 f=Z          H    9.819225    8.484878   18.582882 f=Z
 C    4.905830    8.249180   19.841030 f=Z          H   10.376230    6.732724   20.249673 f=Z
 C    4.964562    8.079041   21.360366 f=Z          H   10.602694    5.555521   18.949375 f=Z
 C    3.864048   12.543749   19.047736 f=Z          H   11.683557    6.944138   19.082454 f=Z
 C    3.430556   13.585624   20.080671 f=Z          H    9.555955    7.849040   16.146453 f=Z
 C    3.032499   15.080256   14.787970 f=Z          H   11.215834    7.712571   16.736349 f=Z
 C    2.136596   14.028098   14.138760 f=Z          H   10.238110    6.266049   16.520170 f=Z
```

H	7.132587	3.466715	17.229142 f=Z		H	9.212542	15.903925	16.341530 f=Z
H	6.525946	2.971328	19.590185 f=Z		H	7.600308	16.424500	15.844586 f=Z
H	4.847569	3.412804	19.259047 f=Z		H	7.920571	16.024505	17.537478 f=Z
H	5.563128	2.015392	18.455984 f=Z		H	9.289211	14.018285	14.703534 f=Z
H	5.506041	4.557714	15.695795 f=Z		H	7.934759	12.899217	14.538856 f=Z
H	4.962473	2.947307	16.179249 f=Z		H	7.755577	14.587825	14.060289 f=Z
H	4.231125	4.376134	16.906999 f=Z		H	3.631026	15.543844	13.996236 f=Z
H	2.492292	13.692200	17.066114 f=Z		H	2.723559	13.255896	13.635752 f=Z
H	5.732714	15.137895	14.721184 f=Z		H	1.498770	13.537821	14.879016 f=Z
H	4.663630	11.952345	19.507924 f=Z		H	1.482549	14.490207	13.396134 f=Z
H	3.040624	13.095507	20.976064 f=Z		H	2.832812	16.950538	15.885919 f=Z
H	4.261410	14.224740	20.380348 f=Z		H	1.548995	16.655395	14.706215 f=Z
H	2.639533	14.221750	19.674652 f=Z		H	1.561048	15.774498	16.233811 f=Z
H	2.955123	10.859998	17.979873 f=Z		H	9.529982	9.961519	16.777541 f=Z
H	2.394102	11.079667	19.642905 f=Z		H	8.702572	11.261323	15.896745 f=Z
H	1.826796	12.152215	18.376552 f=Z		H	9.712619	11.644496	17.295639 f=Z
H	8.337490	13.662454	16.916066 f=Z					

Optimised geometry of η^6-5′-Zr-horizontal and the name of the fragment f in the ETS-NOCV in which each atom belongs

C	4.956835	9.670408	15.943967 f=t		C	0.880813	11.904527	13.405515 f=Z
C	6.074845	9.090378	16.485056 f=t		C	1.247849	10.824287	12.618656 f=Z
C	7.174465	8.969835	15.644581 f=t		C	1.330568	9.576793	13.227951 f=Z
C	7.111237	9.424195	14.334801 f=t		C	1.033743	9.384055	14.570482 f=Z
C	5.948883	10.003554	13.846154 f=t		C	0.190685	13.027025	15.528276 f=Z
C	4.831654	10.137945	14.661571 f=t		C	1.189759	14.166133	15.321952 f=Z
H	5.901550	10.355603	12.822990 f=t		C	1.082086	7.981728	15.150044 f=Z
H	7.975236	9.326106	13.689307 f=t		C	2.095292	7.071836	14.465544 f=Z
H	3.905863	10.575787	14.308477 f=t		C	1.563285	11.007138	11.152977 f=Z
F	3.840492	9.798254	16.789883 f=t		C	0.697886	10.117671	10.264513 f=Z
H	6.086304	8.748216	17.513100 f=t		C	1.835201	7.353448	24.602246 f=Z
H	8.082719	8.517133	16.023156 f=t		C	-0.507519	6.590262	24.338905 f=Z
Zr	1.957971	10.200814	17.974402 f=Z		C	-4.579021	8.838280	15.177185 f=Z
C	2.450817	12.321618	18.285107 f=Z		C	-5.952936	10.016339	16.871308 f=Z
N	0.315954	10.318194	16.720485 f=Z		C	4.146719	11.063438	22.780140 f=Z
C	-1.011543	10.271017	17.131581 f=Z		C	7.604667	6.117442	21.585506 f=Z
C	-1.171727	10.201249	18.508356 f=Z		C	2.492683	5.577057	20.061481 f=Z
C	-2.372519	10.104767	19.162902 f=Z		C	-0.300668	7.328617	15.131634 f=Z
C	-3.503793	10.083021	18.340215 f=Z		C	3.048064	10.783840	10.871098 f=Z
C	-3.418946	10.150087	16.952844 f=Z		C	-1.210755	13.506898	15.148438 f=Z
C	-2.158107	10.250734	16.353050 f=Z		H	-1.784182	8.809318	23.093551 f=Z
C	-2.414460	10.086404	20.687169 f=Z		H	2.398468	8.220895	22.368177 f=Z
C	-1.094992	9.523728	21.203745 f=Z		H	-2.060312	10.288158	15.274929 f=Z
C	0.045315	9.636727	20.444364 f=Z		H	-4.475842	10.007903	18.804166 f=Z
O	0.049582	10.193124	19.171042 f=Z		H	-3.637572	9.284335	22.286909 f=Z
C	-0.923093	8.920918	22.448425 f=Z		H	-4.540647	9.693696	20.849303 f=Z
C	0.316192	8.456899	22.894700 f=Z		H	-3.543061	8.230137	20.867002 f=Z
C	1.428025	8.588118	22.063395 f=Z		H	-2.569304	11.561846	22.277407 f=Z
C	1.298852	9.180478	20.811920 f=Z		H	-1.721569	12.156096	20.843054 f=Z
C	-4.660352	10.088124	16.062613 f=Z		H	-3.481472	11.977436	20.813764 f=Z
C	-4.723246	11.334359	15.172732 f=Z		H	-4.771581	12.245514	15.773948 f=Z
C	-3.598816	9.268753	21.197396 f=Z		H	-3.856965	11.409659	14.512300 f=Z
C	-2.553448	11.537445	21.185548 f=Z		H	-5.614584	11.298342	14.541448 f=Z
C	0.416176	7.812628	24.277364 f=Z		H	-3.696604	8.853189	14.533858 f=Z
C	-0.013382	8.828766	25.342488 f=Z		H	-4.539262	7.930397	15.783949 f=Z
N	2.279183	9.365119	19.844578 f=Z		H	-5.459315	8.776705	14.532308 f=Z
C	3.602887	8.884245	20.073960 f=Z		H	-6.083436	10.892918	17.510817 f=Z
C	4.559056	9.695379	20.717595 f=Z		H	-6.804828	9.978996	16.189225 f=Z
C	5.838225	9.184165	20.910376 f=Z		H	-5.996068	9.120695	17.495837 f=Z
C	6.205662	7.909449	20.505403 f=Z		H	-1.043128	9.160480	25.196734 f=Z
C	5.241759	7.127195	19.879657 f=Z		H	0.053360	8.380801	26.337169 f=Z
C	3.947203	7.578453	19.657898 f=Z		H	0.629775	9.711947	25.324439 f=Z
C	4.236476	11.073988	21.253058 f=Z		H	2.193092	6.598726	23.897115 f=Z
C	5.250411	12.123041	20.799128 f=Z		H	2.543733	8.185712	24.608442 f=Z
C	7.604569	7.393801	20.748203 f=Z		H	1.851726	6.903954	25.597245 f=Z
C	8.361292	7.188359	19.437332 f=Z		H	-0.223123	5.845359	23.591642 f=Z
C	2.938576	6.628517	19.043934 f=Z		H	-0.445128	6.122409	25.324658 f=Z
C	3.457552	5.950739	17.779368 f=Z		H	-1.551308	6.858166	24.164962 f=Z
C	0.642687	10.501407	15.345133 f=Z		H	6.577157	9.800951	21.411715 f=Z
C	0.582503	11.782891	14.758700 f=Z		H	5.501027	6.120475	19.570066 f=Z

A.1. Geometries from the Chapter Coordination of Alkyl cations [(XA₂)X(CH₂Y)]
(X = Th, U or Zr; Y = SiMe₃, H) with an arene for Ethylene polymerisation: 143
Exploration of the bonding

H	2.048391	7.208580	18.775639 f=Z	H	-0.255199	6.325269	15.562157 f=Z
H	1.741317	4.915783	19.623133 f=Z	H	-1.034834	7.907335	15.691802 f=Z
H	3.340064	4.961611	20.374783 f=Z	H	-0.655608	7.236020	14.101757 f=Z
H	2.060793	6.038582	20.950412 f=Z	H	3.087826	7.524191	14.405501 f=Z
H	2.667536	5.347381	17.326643 f=Z	H	2.181156	6.133199	15.014659 f=Z
H	3.804223	6.672452	17.035804 f=Z	H	1.780248	6.815210	13.451781 f=Z
H	4.288866	5.276447	17.995905 f=Z	H	0.180323	12.771817	16.590235 f=Z
H	3.254720	11.357955	20.868128 f=Z	H	-1.465301	14.406413	15.714133 f=Z
H	3.380245	10.372287	23.133446 f=Z	H	-1.261269	13.757330	14.085456 f=Z
H	5.100957	10.770871	23.225949 f=Z	H	-1.969342	12.753304	15.358050 f=Z
H	3.897163	12.060816	23.150004 f=Z	H	0.976357	14.981680	16.016172 f=Z
H	5.400559	12.111028	19.716994 f=Z	H	2.222481	13.848661	15.479827 f=Z
H	4.912857	13.121865	21.084551 f=Z	H	1.123783	14.577055	14.311841 f=Z
H	6.225484	11.966685	21.266337 f=Z	H	1.332488	12.049227	10.906964 f=Z
H	8.132546	8.165908	21.318123 f=Z	H	3.669203	11.463874	11.459654 f=Z
H	7.080004	6.262356	22.531896 f=Z	H	3.343392	9.757665	11.107987 f=Z
H	7.121261	5.292248	21.056099 f=Z	H	3.268400	10.956848	9.815282 f=Z
H	8.628428	5.809061	21.808642 f=Z	H	-0.365186	10.282906	10.450359 f=Z
H	8.421725	8.117606	18.865025 f=Z	H	0.894563	10.327083	9.210776 f=Z
H	9.380852	6.848170	19.632193 f=Z	H	0.908182	9.058313	10.433046 f=Z
H	7.873536	6.433073	18.814542 f=Z	H	3.378294	12.432557	18.853548 f=Z
H	1.627538	8.723499	12.630716 f=Z	H	2.581884	12.812227	17.314974 f=Z
H	0.821798	12.885097	12.944358 f=Z	H	1.660679	12.854688	18.822414 f=Z
H	1.376605	8.056921	16.208835 f=Z				

Optimised geometry of η^2-E′-Zr-horizontal and the name of the fragment f in the ETS-NOCV in which each atom belongs

C	7.558282	8.854639	16.089291 f=Z	C	14.890901	11.374616	16.931186 f=Z
C	8.153290	9.648401	15.078342 f=Z	C	12.093599	5.792469	16.850034 f=Z
C	7.667009	10.948369	14.824314 f=Z	C	11.071509	5.339423	17.887842 f=Z
C	6.595211	11.412500	15.579647 f=Z	C	15.049059	7.523058	20.529803 f=Z
C	5.996834	10.658307	16.576170 f=Z	C	15.873489	6.243283	20.655511 f=Z
C	6.502170	9.383756	16.816629 f=Z	C	5.490044	8.228339	10.911512 f=Z
N	9.263475	9.130158	14.357418 f=Z	C	6.642649	6.379226	9.734524 f=Z
Zr	11.046520	9.240895	15.415755 f=Z	C	16.115175	4.337158	13.529685 f=Z
C	11.761421	11.267041	14.913923 f=Z	C	16.371435	5.037955	11.167085 f=Z
C	8.251683	11.859960	13.765859 f=Z	C	7.297567	12.033327	12.582954 f=Z
C	8.608811	13.234999	14.332718 f=Z	C	3.568930	10.375914	17.146084 f=Z
C	4.833615	11.202755	17.369227 f=Z	C	7.469596	6.462294	15.319809 f=Z
C	5.162448	11.310860	18.856453 f=Z	C	12.891823	4.584485	16.354046 f=Z
C	8.021682	7.434911	16.362634 f=Z	C	13.963181	7.583101	21.601655 f=Z
C	7.684915	6.937324	17.762502 f=Z	C	16.315403	9.728787	15.700392 f=Z
N	12.807960	8.160428	15.283434 f=Z	H	9.300203	7.312590	9.451316 f=Z
C	13.331354	7.589170	14.131490 f=Z	H	7.014344	8.789188	12.761740 f=Z
C	12.535474	7.769066	13.008069 f=Z	H	15.143495	6.712897	14.837603 f=Z
C	12.792276	7.252753	11.764618 f=Z	H	14.241837	6.108341	10.691156 f=Z
C	13.984352	6.528825	11.651876 f=Z	H	11.121463	6.537547	8.811728 f=Z
C	14.845998	6.335662	12.727576 f=Z	H	12.767650	6.128993	9.230043 f=Z
C	14.505337	6.869671	13.976416 f=Z	H	11.431404	5.428841	10.157404 f=Z
C	11.836420	7.522869	10.606950 f=Z	H	11.664110	8.989793	9.010334 f=Z
C	10.453085	7.833021	11.170998 f=Z	H	12.387851	9.636361	10.489558 f=Z
C	10.322002	8.335418	12.444128 f=Z	H	13.335656	8.577165	9.436234 f=Z
O	11.397449	8.502465	13.300421 f=Z	H	17.378093	7.326077	12.316590 f=Z
C	9.261147	7.697449	10.461613 f=Z	H	17.267394	6.793030	13.998486 f=Z
C	8.019357	8.037219	11.003266 f=Z	H	18.269786	5.897727	12.858675 f=Z
C	7.961072	8.536759	12.304033 f=Z	H	16.019334	4.636078	14.575743 f=Z
C	9.127244	8.691326	13.045804 f=Z	H	15.280057	3.675013	13.288308 f=Z
C	16.148550	5.547313	12.588662 f=Z	H	17.040300	3.762981	13.435112 f=Z
C	17.331273	6.447567	12.964526 f=Z	H	16.438687	5.856158	10.445809 f=Z
C	11.783222	6.330474	9.653169 f=Z	H	17.312842	4.486385	11.123910 f=Z
C	12.337245	8.760653	9.839429 f=Z	H	15.578884	4.356799	10.847533 f=Z
C	6.760947	7.848753	10.155921 f=Z	H	7.723304	8.473041	8.292195 f=Z
C	6.857185	8.730396	8.904859 f=Z	H	5.964159	8.605085	8.287268 f=Z
C	13.411749	7.977729	16.555700 f=Z	H	6.937805	9.786527	9.173617 f=Z
C	14.365857	8.901124	17.037096 f=Z	H	5.348799	7.616794	11.806337 f=Z
C	14.863913	8.727117	18.323159 f=Z	H	5.485975	9.280829	11.206290 f=Z
C	14.475519	7.675444	19.141992 f=Z	H	4.623708	8.068808	10.266280 f=Z
C	13.560933	6.770006	18.632358 f=Z	H	6.570689	5.725488	10.607146 f=Z
C	13.022924	6.876392	17.358909 f=Z	H	5.745205	6.234887	9.127837 f=Z
C	14.899885	10.037793	16.191982 f=Z	H	7.498702	6.053457	9.140850 f=Z

```
H    6.211869    12.408856    15.384529 f=Z          H   13.472425     4.149515    17.171953 f=Z
H    6.045477     8.783068    17.593069 f=Z          H   10.526037     6.176114    18.329495 f=Z
H    9.120999     7.403883    16.264222 f=Z          H   10.345594     4.666380    17.426089 f=Z
H    7.825124     5.447897    15.516291 f=Z          H   11.541648     4.786226    18.703527 f=Z
H    6.377479     6.450296    15.365866 f=Z          H   14.258463    10.128337    15.313193 f=Z
H    7.762023     6.737305    14.306907 f=Z          H   16.686876    10.548867    15.081445 f=Z
H    8.152145     5.967058    17.934455 f=Z          H   17.002729     9.605699    16.541405 f=Z
H    8.020314     7.623258    18.544698 f=Z          H   16.344102     8.818135    15.101172 f=Z
H    6.609110     6.794469    17.885221 f=Z          H   15.145093    12.185008    16.244738 f=Z
H    9.167373    11.395839    13.392369 f=Z          H   13.916206    11.599404    17.371727 f=Z
H    7.071788    11.081971    12.101429 f=Z          H   15.626395    11.394079    17.738594 f=Z
H    6.356118    12.486056    12.904716 f=Z          H   15.723516     8.371150    20.690010 f=Z
H    7.744535    12.691525    11.834239 f=Z          H   13.390397     8.511226    21.539646 f=Z
H    9.210494    13.167229    15.241638 f=Z          H   13.264611     6.747531    21.506611 f=Z
H    9.172013    13.810845    13.595138 f=Z          H   14.408551     7.527417    22.597292 f=Z
H    7.713058    13.810680    14.576578 f=Z          H   16.669865     6.206345    19.909492 f=Z
H    4.640890    12.214298    16.995999 f=Z          H   16.331861     6.182525    21.644996 f=Z
H    3.311987    10.317290    16.086547 f=Z          H   15.249334     5.355276    20.525444 f=Z
H    3.691240     9.355654    17.519418 f=Z          H   10.939087    11.982021    14.833614 f=Z
H    2.724733    10.822073    17.676332 f=Z          H   12.458811    11.627763    15.678074 f=Z
H    6.046331    11.929730    19.026742 f=Z          H   12.296647    11.265589    13.958929 f=Z
H    4.327298    11.759011    19.399157 f=Z          C   10.924368     9.553377    18.192012 f=t
H    5.348561    10.326569    19.294609 f=Z          C   10.128037    10.543560    17.768890 f=t
H   13.264375     5.918623    19.248369 f=Z          H   10.525372    11.530788    17.554392 f=t
H   15.595102     9.433720    18.701999 f=Z          H    9.054213    10.413600    17.672924 f=t
H   11.548122     6.192245    15.987721 f=Z          H   10.518402     8.584812    18.471925 f=t
H   12.216789     3.813811    15.974068 f=Z          H   11.988135     9.695550    18.360094 f=t
H   13.579450     4.855213    15.553094 f=Z
```

A.2   Geometries from the Chapter Thermodynamic properties and electronic structures of Plutonium Oxides in Angstrom

A.2.1   Molecules containing Plutonium

PuO$_2$(OH)$_2$ coordinates in Å

Label	x	y	z
Pu	0.000000	0.967853	0.000000
O	-0.017474	0.880968	1.740764
O	0.017474	0.880968	-1.740764
O	1.676305	2.238293	0.001209
O	-1.676305	2.238293	-0.001209
H	2.063158	2.697914	0.750904
H	-2.063158	2.697914	-0.750904

PuO$_3$ coordinates in Å

Label	x	y	z
Pu	0.000000	0.000000	0.000000
O	1.934000	0.000000	0.000000
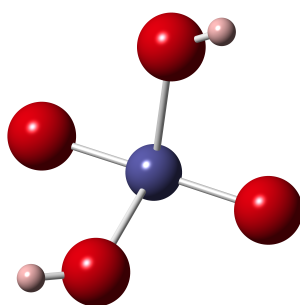
FIGURE A.3: $PuO_2(OH)_2$ molecule.Blue: Pu; red: O: pink; H.

```
O                      -0.118952      0.000000      1.762992
O                      -0.118952      0.000000      -1.762992
```
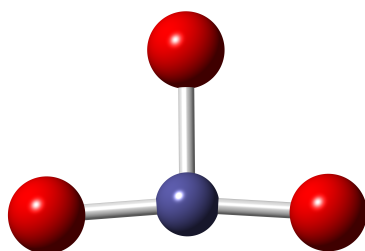

FIGURE A.4: PuO_3 molecule. Blue: Pu; red: O.

PuO_2 coordinates in Å

Label	x	y	z
Pu	0.000000	0.000000	0.000000
O	0.000000	0.000000	1.808000
O	0.000000	0.000000	-1.808000
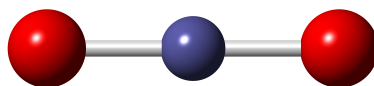
FIGURE A.5: PuO$_2$ molecule. Blue: Pu; red: O.

A.2.2   Organic Molecules

H$_2$O$_2$ coordinates in Å

Label	x	y	z
O	-0.275341	-0.185870	0.687291
O	-0.213172	0.301727	-0.678278
H	0.365257	0.397493	1.116183
H	0.173256	-0.463349	-1.125197

H$_2$O coordinates in Å

Label	x	y	z
O	0.000000	0.000000	0.000000
H	0.521742	0.000000	0.823124
H	0.521742	0.000000	-0.823124

O$_2$ coordinates in Å

Label	x	y	z
O	0.000000	0.000000	0.603760
O	0.000000	0.000000	-0.603760

OH coordinates in Å

Label	x	y	z
O	0.000000	0.000000	0.975370
H	0.000000	0.000000	0.000000

H_2 coordinates in Å

Label	x	y	z
H	0.000000	0.000000	0.372000
H	0.000000	0.000000	-0.372000

Appendix B

Electronic levels of Plutonium and Plutonium oxydes

TABLE B.1: Electronic levels (cm-1) of the plutonium atom and analysis of the various states obtained with the ano-cc-TZVP.

J-value	E (cm-1)	Character
0	0	54% ^7F , 38% ^5D , 7% ^3P
1	1806	64% ^7F , 32% ^5D
2	4208	82% ^7F , 17% ^5D
3	6353	88% ^7F , 10% ^5D
4	8091	93% ^7F
5	9552	90% ^7F
6	11010	85% ^7F , 10% ^5G
0	12499	44% ^7F , 21% ^5D , 8% ^3P
1	13612	66% ^9H , 9% ^7F , 7% ^7G
2	14399	82% ^9H , 14% ^7G
1	14845	38% ^5D, 20% ^7F , 9% ^9G
3	15551	89% ^9H , 8% ^7G
4	17026	86% ^9H , 6% ^7G
1	17032	66% ^9D , 29% ^7P

TABLE B.2: Energy electronic states (E < 16 000 cm^{-1}) of PuO$_2$(OH)$_2$ at SF-CASPT2 and SO-CASPT2 levels obtained with the ano-cc-TZVP.

	Term Symbol	Character : % [orbital(number of electron)]	E (cm^{-1})
SF	$^3B(1)$	49% 2a/Φ_u(1), 1b/δ_u(1)	0
		48% 1a/δ_u(1), 2b/Φ_u(1)	
	$^3A(1)$	41% 1a/δ_u(1) , 2a/Φ_u(1)	889
		59% 1b/δ_u(1) , 2b/Φ_u(1)	
	$^3B(2)$	75% 1a/δ_u(1), 1b/δ_u(1)	2136
		20% 2a/Φ_u(1), 2b/Φ_u(1)	
	$^3A(2)$	59% 1a/δ_u(1) , 2a/Φ_u(1)	4698
		41% 1b/δ_u(1) , 2b/Φ_u(1)	
	$^3B(3)$	52% 2a/Φ_u(1), 1b/δ_u(1)	5351
		46% 1a/δ_u(1), 2b/Φ_u(1)	
	$^1A(1)$	58% 1b/δ_u(1) , 2b/Φ_u($\bar{1}$)	5764
		30% 1a/δ_u(1) , 2a/Φ_u($\bar{1}$)	
		5% 2a/Φ_u(2)	
	$^1B(1)$	50% 1a/δ_u(1), 1b/δ_u($\bar{1}$)	7444
		28% 2a/Φ_u(1), 2b/Φ_u($\bar{1}$)	
		16% 1a/δ_u(1), 2b/Φ_u($\bar{1}$)	
	$^1A(2)$	39% 1a/δ_u(1) , 2a/Φ_u($\bar{1}$)	9626
		29 % 2a/Φ_u(2)	
		13% 1b/δ_u(1) , 2b/Φ_u($\bar{1}$)	
		10% 1a/δ_u(2)	
		7 % 2a/Φ_u(2)	
	$^1A(3)$	44% 1b/δ_u(2)	10184
		33% 2a/Φ_u(2)	
		12% 2b/Φ_u(2)	
		9% 1a/δ_u(2)	
	$^1B(2)$	66% 2a/Φ_u(1), 2b/Φ_u($\bar{1}$)	10287
		26% 1a/δ_u(1), 2b/Φ_u($\bar{1}$)	
		8% 1a/δ_u(1), 1b/δ_u($\bar{1}$)	
SO	X	46.1% $^3A(1)$, 41.4% $^3B(1)$, 6.4% $^3B(2)$	0
	a	45.3% $^3B(1)$, 44.8% $^3A(1)$, 6.3% $^3B(2)$	323
	b	34.9% $^3B(2)$, 24.7% $^3B(1)$, 14.4% $^1A(1)$, 12.5% $^3A(2)$, 10.1% $^3B(3)$	2222
	c	40.3% $^3A(2)$, 25.4% $^3B(2)$, 18.8% $^1B(1)$, 7.1% $^3B(1)$, 6.1% $^3A(1)$	3757
	d	35.5% $^3B(3)$, 34.3% $^3B(2)$, 14.3% $^1A(2)$, 11.1% $^3B(1)$,	4158
	e	63.5% $^3B(1)$, 30.1% $^3B(2)$	7268
	f	92.8% $^3A(1)$	7575
	g	32.4% $^1A(1)$, 28.1% $^3B(3)$, 27.8% $^3A(2)$, 6.3% $^3B(2)$,	10041
	h	41.1% $^3A(2)$, 24.1% $^3B(3)$, 15.3% $^3B(2)$, 10.5% $^3B(1)$, 6.1% $^1B(1)$	10142
	i	33.5% $^3A(2)$, 26.3% $^3B(2)$, 13.8% $^3B(3)$, 13.1% $^1B(1)$, 8.2% $^3B(1)$	10343
	j	29.3% $^3B(2)$, 25.6% $^3B(3)$, 22.0% $^3B(1)$, 16.6% $^1A(2)$	11089
	k	26.3% $^3B(3)$, 22.9% $^3A(1)$, 17.0% $^3B(1)$, 16.6% $^3A(2)$, 13.0% $^3B(2)$	12269
	l	26.1% $^3A(2)$, 23.6% $^3A(1)$, 21.3% $^3B(3)$, 15.4% $^3B(2)$, 9.6% $^3B(1)$	12311
	m	27.5% $^3B(3)$, 24.6% $^3A(2)$, 22.2% $^3A(1)$, 12.1% $^3B(1)$, 9.7% $^3B(2)$	13782
	n	34.8% $^3B(3)$, 21.8% $^3A(2)$, 17.7% $^3A(1)$, 13.0% $^3B(1)$, 8.5% $^3B(2)$	13783
	o	40.9% $^1A(1)$, 19.7% $^1A(3)$, 15.4% $^3B(2)$, 7.3% $^3B(4)$,	15696

TABLE B.3: Vertical transitions in cm^{-1} of the low-energy (E < 16 000 cm^{-1}) electronic states of PuO$_3$ at SF-CASPT2 and SO-CASPT2 levels obtained with the ANO-RCC-TZVP. Orbitals 1a$_1$, 2a$_1$/π_u, 3a$_1$ always doubly occupied and do not appear in the following table.

	Term Symbol	Character : % [orbital(number of electron)]	E (cm^{-1})
SF	$^3B_2(1)$	36% [4a$_1$/p$^{(O)}$(2), 1b$_1$/Φ_u(1), 1b$_2$/p$^{(O)}$($\bar{1}$), 2b$_2$/σ_u(2), 3b$_2$/δ_u(1), 1a$_2$/δ_u(1)]	0
		21% [4a$_1$/p$^{(O)}$(2), 1b$_1$/Φ_u(1), 1b$_2$/p$^{(O)}$(1), 2b$_2$/σ_u(2), 3b$_2$/δ_u($\bar{1}$), 1a$_2$/δ_u(1)]	
		22% [4a$_1$/p$^{(O)}$(2),1b$_1$/Φ_u(1),1b$_2$/p$^{(O)}$(2),2b$_2$/σ_u(2),1a$_2$/δ_u(1)]	
	$^3A_2(1)$	43% [4a$_1$/p$^{(O)}$(2), 5a$_1$/Φ_u(1),1b$_2$/p$^{(O)}$($\bar{1}$),2b$_2$/σ_u(2),3b$_2$/δ_u(1),1a$_2$/δ_u(1)]	3161
		23% [4a$_1$/p$^{(O)}$(2), 5a$_1$/Φ_u(1),1b$_2$/p$^{(O)}$(1),2b$_2$/σ_u(2),3b$_2$/δ_u($\bar{1}$),1a$_2$/δ_u(1)]	
		17% [4a$_1$/p$^{(O)}$(2), 5a$_1$/Φ_u(1),1b$_2$/p$^{(O)}$(2),2b$_2$/σ_u(2),1a$_2$/δ_u(1)]	
	$^3B_1(1)$	38% [4a$_1$/p$^{(O)}$(2),5a$_1$/Φ_u(1),1b$_1$/Φ_u(1),1b$_2$/p$^{(O)}$($\bar{1}$),2b$_2$/σ_u(2),3b$_2$/δ_u(1)]	4663
		12% [4a$_1$/p$^{(O)}$(2), 5a$_1$/Φ_u(1), 2b$_1$/π_u(1),1b$_2$/p$^{(O)}$(1),2b$_2$/σ_u(2),3b$_2$/δ_u(1)]	
		12% [4a$_1$/p$^{(O)}$(2), 5a$_1$/Φ_u(1),1b$_1$/Φ_u(1),2b$_1$/π_u(2),1b$_2$/p$^{(O)}$(2)]	
	$^1A_1(1)$	32% [4a$_1$/p$^{(O)}$(2),1b$_2$/p$^{(O)}$(1),2b$_2$/σ_u(2),3b$_2$/δ_u($\bar{1}$),1a$_2$/δ_u(2)]	7239
		28% [4a$_1$/p$^{(O)}$(2),1b$_2$/p$^{(O)}$(2),2b$_2$/σ_u(2),1a$_2$/δ_u(2)]	
		11% [4a$_1$/p$^{(O)}$(1),5a$_1$/Φ_u($\bar{1}$),1b$_2$/p$^{(O)}$(1),2b$_2$/σ_u(2),1a$_2$/δ_u(2)]	
	$^3A_2(2)$	20% [4a$_1$/p$^{(O)}$(2),1b$_1$/Φ_u(1),1b$_2$/p$^{(O)}$(1),2b$_2$/σ_u(2),3b$_2$/δ_u(2)]	7287
		18% [4a$_1$/p$^{(O)}$(1),5a$_1$/Φ_u($\bar{1}$),1b$_1$/Φ_u(1),1b$_2$/p$^{(O)}$(2),2b$_2$/σ_u(2),3b$_2$/δ_u(1)]	
		17% [4a$_1$/p$^{(O)}$(2),1b$_1$/Φ_u(1),1b$_2$/p$^{(O)}$(2),2b$_2$/σ_u(2),3b$_2$/δ_u(1)]	
	$^3B_1(2)$	31% [4a$_1$/p$^{(O)}$(1),5a$_1$/Φ_u($\bar{1}$),1b$_2$/p$^{(O)}$(2),2b$_2$/σ_u(2),3b$_2$/δ_u(1),1a$_2$/δ_u(1)]	8038
		11% [4a$_1$/p$^{(O)}$(2),5a$_1$/Φ_u(1),2b$_1$/π_u(1),1b$_2$/p$^{(O)}$($\bar{1}$),2b$_2$/σ_u(2),3b$_2$/δ_u(1)]	
		10% [4a$_1$/p$^{(O)}$(2),1b$_2$/p$^{(O)}$(2),2b$_2$/σ_u(2),3b$_2$/δ_u(1),1a$_2$/δ_u(1)]	
		10% [4a$_1$/p$^{(O)}$(2),1b$_1$/Φ_u(1),2b$_1$/π_u(1),1b$_2$/p$^{(O)}$($\bar{1}$),2b$_2$/σ_u(2),1a$_2$/δ_u(1)]	
	$^5B_2(1)$	47% [4a$_1$/p$^{(O)}$(2), 1b$_1$/Φ_u($\bar{1}$)(1), 1b$_2$/p$^{(O)}$(2), 2b$_2$/σ_u(1), 3b$_2$/δ_u(1), 1a$_2$/δ_u(1)]	8962

Table B.3 – *Continued from previous page*

Term Symbol	Character : % [orbital(number of electron)]	E (cm^{-1})
$^3A_1(1)$	41% [$4a_1/p^{(O)}(2), 5a_1/\Phi_u(1), 1b_1/\Phi_u(\bar{1})(1), 1b_2/p^{(O)}(1), 2b_2/\sigma_u(2), 1a_2/\delta_u(1)$] 39% [$4a_1/p^{(O)}(2), 1b_1/\Phi_u(\bar{1})(1), 2b_1/\tau_u(1), 1b_2/p^{(O)}(\bar{1}), 2b_2/\sigma_u(2), 3b_2/\delta_u(1)$] 11% [$4(2), 1b_1/\Phi_u(\bar{1})(1), 8(1), 1b_2/p^{(O)}(\bar{1}), 2b_2/\sigma_u(2), 3b_2/\delta_u(1)$]	9645
$^3B_2(2)$	15% [$4a_1/p^{(O)}(2), 2b_1/\tau_u(1), 1b_2/p^{(O)}(2), 2b_2/\sigma_u(2), 1a_2/\delta_u(1)$]] 15% [$4a_1/p^{(O)}(1), 5a_1/\Phi_u(\bar{1}), 2b_1/\tau_u(1), 1b_2/p^{(O)}(2), 2b_2/\sigma_u(2), 1a_2/\delta_u(1)$] 12% [$4a_1/p^{(O)}(2), 2b_1/\tau_u(1), 1b_2/p^{(O)}(\bar{1}), 2b_2/\sigma_u(2), 3b_2/\delta_u(1), 1a_2/\delta_u(1)$]	9731
$^1A_2(1)$	26% [$4a_1/p^{(O)}(2), 5a_1/\Phi_u(1), 1b_2/p^{(O)}(1), 2b_2/\sigma_u(2), 11(\bar{1}), 1a_2/\delta_u(\bar{1})$] 24% [$4a_1/p^{(O)}(2), 5a_1/\Phi_u(1), 1b_2/p^{(O)}(\bar{1}), 2b_2/\sigma_u(2), 3b_2/\delta_u(1), 1a_2/\delta_u(\bar{1})$] 18% [$4a_1/p^{(O)}(2), 1b_1/\Phi_u(1), 1b_2/p^{(O)}(1), 2b_2/\sigma_u(2), 1a_2/\delta_u(2)$] 16% [$4a_1/p^{(O)}(2), 5a_1/\Phi_u(1), 1b_2/p^{(O)}(2), 2b_2/\sigma_u(2), 1a_2/\delta_u(\bar{1})$]	10293
$^1B_2(1)$	30% [$4a_1/p^{(O)}(2), 1b_1/\Phi_u(1), 1b_2/p^{(O)}(\bar{1}), 2b_2/\sigma_u(2), 3b_2/\delta_u(1), 1a_2/\delta_u(\bar{1})$] 22% [$4a_1/p^{(O)}(2), 1b_1/\Phi_u(1), 1b_2/p^{(O)}(1), 2b_2/\sigma_u(2), 3b_2/\delta_u(\bar{1}), 1a_2/\delta_u(\bar{1})$] 16% [$4a_1/p^{(O)}(2), 1b_1/\Phi_u(1), 1b_2/p^{(O)}(1), 2b_2/\sigma_u(2), 1a_2/\delta_u(\bar{1})$] 15% [$4a_1/p^{(O)}(2), 5a_1/\Phi_u(1), 1b_2/p^{(O)}(\bar{1}), 2b_2/\sigma_u(2), 1a_2/\delta_u(2)$]	10604
$^5A_1(1)$	27% [$4a_1/p^{(O)}(2), 5a_1/\Phi_u(1), 1b_1/\Phi_u(1), 1b_2/p^{(O)}(2), 2b_2/\sigma_u(1), 1a_2/\delta_u(1)$] 15% [$4a_1/p^{(O)}(2), 2b_1/\tau_u^*(1), 1b_1/\Phi_u(1), 1b_2/p^{(O)}(2), 2b_2/\sigma_u(1), 1a_2/\delta_u(1)$] 12% [$4a_1/p^{(O)}(2), 5a_1/\Phi_u(1), 1b_1/\Phi_u(1), 1b_2/p^{(O)}(1), 2b_2/\sigma_u(2), 1a_2/\delta_u(1)$]	10662
$^3B_1(3)$	26% [$4a_1/p^{(O)}(2), 1b_1/\Phi_u(1), 2b_1/\tau_u(1), 1b_2/p^{(O)}(\bar{1}), 2b_2/\sigma_u(2), 1a_2/\delta_u(1)$] 17% [$4a_1/p^{(O)}(1), 5a_1/\Phi_u(\bar{1}), 1b_2/p^{(O)}(2), 2b_2/\sigma_u(2), 3b_2/\delta_u(1), 1a_2/\delta_u(1)$]	11567
$^1B_1(1)$	34% [$4a_1/p^{(O)}(2), 1b_2/p^{(O)}(1), 2b_2/\sigma_u(2), 3b_2/\delta_u(2), 1a_2/\delta_u(\bar{1})$] 18% [$4a_1/p^{(O)}(1), 5a_1/\Phi_u(\bar{1}), 1b_2/p^{(O)}(2), 2b_2/\sigma_u(2), 3b_2/\delta_u(1), 1a_2/\delta_u(\bar{1})$] 17% [$4a_1/p^{(O)}(2), 1b_2/p^{(O)}(2), 2b_2/\sigma_u(2), 3b_2/\delta_u(1), 1a_2/\delta_u(\bar{1})$]	11632
$^5B_1(1)$	36% [$4a_1/p^{(O)}(2), 1b_1/\Phi_u(1), 2b_1/\tau_u(1), 1b_2/p^{(O)}(2), 2b_2/\sigma_u(1), 1a_2/\delta_u(1)$]	12017

Table B.3 – *Continued from previous page*

Term Symbol	Character : % [orbital(number of electron)]	E (cm^{-1})
$^5A_2(1)$	15% [4a$_1$/p$^{(O)}$(2), 1b$_1$/Φ_u(1), 2b$_1$/τ_u(1), 1b$_2$/p$^{(O)}$(1), 2b$_2$/σ_u(2), 1a$_2$/δ_u(1)]	12017
	36% [4a$_1$/p$^{(O)}$(2), 1b$_1$/Φ_u(1), 2b$_1$/τ_u(1), 1b$_2$/p$^{(O)}$(2), 2b$_2$/σ_u(1), 1a$_2$/δ_u(1)]	
	15% [4a$_1$/p$^{(O)}$(2), 1b$_1$/Φ_u(1), 2b$_1$/τ_u(1), 1b$_2$/p$^{(O)}$(1), 2b$_2$/σ_u(2), 1a$_2$/δ_u(1)]	
$^3B_2(3)$	24% [4a$_1$/p$^{(O)}$(2), 1b$_1$/Φ_u(1), 1b$_2$/p$^{(O)}$(1), 2b$_2$/σ_u(2), 3b$_2$/δ_u(1), 1a$_2$/δ_u($\overline{1}$)]	12023
	11% [4a$_1$/p$^{(O)}$(2), 5a$_1$/Φ_u(1), 1b$_2$/p$^{(O)}$(1), 2b$_2$/σ_u(2), 3b$_2$/δ_u(2)]	
$^3A_2(3)$	17% [4a$_1$/p$^{(O)}$(2), 1b$_1$/Φ_u(1), 1b$_2$/p$^{(O)}$(1), 2b$_2$/σ_u(2), 1a$_2$/δ_u(2)]	12940
	15% [4a$_1$/p$^{(O)}$(2), 5a$_1$/Φ_u(1), 1b$_2$/p$^{(O)}$(1), 2b$_2$/σ_u(2), 3b$_2$/δ_u(1), 1a$_2$/δ_u($\overline{1}$)]	
$^1A_1(2)$	21% [4a$_1$/p$^{(O)}$(2), 5a$_1$/Φ_u(2), 1b$_2$/p$^{(O)}$(1), 2b$_2$/σ_u(2), 3b$_2$/δ_u($\overline{1}$)]	13213
	10% [4a$_1$/p$^{(O)}$(1), 5a$_1$/Φ_u($\overline{1}$), 1b$_2$/p$^{(O)}$(2), 2b$_2$/σ_u(2), 3b$_2$/δ_u(2)]	
	10% [4a$_1$/p$^{(O)}$(2), 5a$_1$/Φ_u(2), 1b$_2$/p$^{(O)}$(2), 2b$_2$/σ_u(2)]	
$^3A_1(2)$	44% [4a$_1$/p$^{(O)}$(2), 5a$_1$/Φ_u(1), 1b$_1$/Φ_u(1), 1b$_2$/p$^{(O)}$($\overline{1}$), 2b$_2$/σ_u(2), 1a$_2$/δ_u(1)]	13421
	29% [4a$_1$/p$^{(O)}$(2), 5a$_1$/Φ_u(1), 1b$_1$/Φ_u(1), 1b$_2$/p$^{(O)}$($\overline{1}$), 2b$_2$/σ_u(2), 1a$_2$/δ_u(1)]	
$^3B_1(4)$	29% [4a$_1$/p$^{(O)}$(2), 2b$_1$/τ^*_u(1), 1b$_1$/Φ_u(1), 1b$_2$/p$^{(O)}$($\overline{1}$), 2b$_2$/σ_u(2), 3b$_2$/δ_u(1)]	13518
	15% [4a$_1$/p$^{(O)}$(2), 5a$_1$/Φ_u(1), 2b$_1$/τ_u(1), 1b$_2$/p$^{(O)}$($\overline{1}$), 2b$_2$/σ_u(2), 3b$_2$/δ_u(1)]	
	13% [4a$_1$/p$^{(O)}$(2), 2b$_1$/τ^*_u(1), 1b$_1$/Φ_u(1), 1b$_2$/p$^{(O)}$($\overline{1}$), 2b$_2$/σ_u(2), 2b$_2$/σ_u(2)]	
	11% [4a$_1$/p$^{(O)}$(2), 5a$_1$/Φ_u(1), 2b$_1$/τ^*_u(1), 1b$_2$/p$^{(O)}$($\overline{1}$), 2b$_2$/σ_u(2), 1a$_2$/δ_u(1)]	
$^5A_1(2)$	29% [4a$_1$/p$^{(O)}$(2), 1b$_1$/Φ_u(1), 2b$_1$/τ_u(1), 1b$_2$/p$^{(O)}$(2), 2b$_2$/σ_u(1), 3b$_2$/δ_u(1)]	13575
	14% [4a$_1$/p$^{(O)}$(2), 5a$_1$/Φ_u(1), 1b$_1$/Φ_u(1), 1b$_2$/p$^{(O)}$(2), 2b$_2$/σ_u(1), 1a$_2$/δ_u(1)]	
	13% [4a$_1$/p$^{(O)}$(2), 1b$_1$/Φ_u(1), 2b$_1$/τ_u(1), 1b$_2$/p$^{(O)}$(1), 2b$_2$/σ_u(2), 3b$_2$/δ_u(1)]	
	12% [4a$_1$/p$^{(O)}$(2), 5a$_1$/Φ_u(1), 2b$_1$/τ_u(1), 1b$_2$/p$^{(O)}$(2), 2b$_2$/σ_u(1), 1a$_2$/δ_u(1)]	
$^5B_1(2)$	30% [4a$_1$/p$^{(O)}$(2), 5a$_1$/Φ_u(1), 1b$_1$/Φ_u(1), 1b$_2$/p$^{(O)}$(2), 2b$_2$/σ_u(1), 3b$_2$/δ_u(1)]	13970
	20% [4a$_1$/p$^{(O)}$(2), 5a$_1$/Φ_u(1), 1b$_1$/Φ_u(1), 1b$_2$/p$^{(O)}$(1), 2b$_2$/σ_u(2), 3b$_2$/δ_u(1)]	
	16% [4a$_1$/p$^{(O)}$(2), 5a$_1$/Φ_u(1), 2b$_1$/τ_u(1), 1b$_2$/p$^{(O)}$(2), 2b$_2$/σ_u(1), 3b$_2$/δ_u(1)]	

Table B.3 – *Continued from previous page*

Term Symbol	Character : % [orbital(number of electron)]	E (cm^{-1})
$^5A_2(2)$	10 % [$4a_1/p^{(O)}(2)$, $5a_1/\Phi_u(1)$, $2b_1/\tau_u(1)$, $1b_2/p^{(O)}(1)$, $2b_2/\sigma_u(2)$, $3b_2/\delta_u(1)$] 30% [$4a_1/p^{(O)}(2)$, $5a_1/\Phi_u(1)$, $1b_1/\Phi_u(1)$, $1b_2/p^{(O)}(2)$, $2b_2/\sigma_u(1)$, $3b_2/\delta_u(1)$] 20% [$4a_1/p^{(O)}(2)$, $5a_1/\Phi_u(1)$, $1b_1/\Phi_u(1)$, $1b_2/p^{(O)}(1)$, $2b_2/\sigma_u(2)$, $3b_2/\delta_u(1)$] 16% [$4a_1/p^{(O)}(2)$, $5a_1/\Phi_u(1)$, $2b_1/\tau_u(1)$, $1b_2/p^{(O)}(2)$, $2b_2/\sigma_u(1)$, $3b_2/\delta_u(1)$] 10% [$4a_1/p^{(O)}(2)$, $5a_1/\Phi_u(1)$, $2b_1/\tau_u(1)$, $1b_2/p^{(O)}(1)$, $2b_2/\sigma_u(2)$, $3b_2/\delta_u(1)$]	13971
$^5B_1(3)$	86% [$4a_1/p^{(O)}(1)$, $5a_1/\Phi_u(1)$, $1b_2/p^{(O)}(2)$, $2b_2/\sigma_u(2)$, $3b_2/\delta_u(1)$, $1a_2/\delta_u(1)$]	14055
$^5A_2(3)$	86% [$4a_1/p^{(O)}(1)$, $5a_1/\Phi_u(1)$, $1b_2/p^{(O)}(2)$, $2b_2/\sigma_u(2)$, $3b_2/\delta_u(1)$, $1a_2/\delta_u(1)$]	14056
$^5A_1(3)$	80% [$4a_1/p^{(O)}(1)$, $1b_1/\Phi_u(1)$, $1b_2/p^{(O)}(2)$, $2b_2/\sigma_u(2)$, $3b_2/\delta_u(1)$, $1a_2/\delta_u(1)$]	14139
$^3A_1(3)$	58% [$4a_1/p^{(O)}(1)$, $1b_1/\Phi_u(\bar{1})$, $1b_2/p^{(O)}(2)$, $2b_2/\sigma_u(2)$, $3b_2/\delta_u(1)$, $1a_2/\delta_u(1)$] 20% [$4a_1/p^{(O)}(1)$, $1b_1/\Phi_u(1)$, $1b_2/p^{(O)}(2)$, $2b_2/\sigma_u(2)$, $3b_2/\delta_u(\bar{1})$, $1a_2/\delta_u(1)$] 10% [$4a_1/p^{(O)}(1)$, $1b_1/\Phi_u(1)$, $1b_2/p^{(O)}(2)$, $2b_2/\sigma_u(2)$, $3b_2/\delta_u(1)$, $1a_2/\delta_u(\bar{1})$]	14236
$^3B_2(4)$	19% [$4a_1/p^{(O)}(1)$, $5a_1/\Phi_u(\bar{1})$, $1b_1/\Phi_u(1)$, $1b_2/p^{(O)}(2)$, $2b_2/\sigma_u(2)$, $1a_2/\delta_u(1)$] 18% [$4a_1/p^{(O)}(2)$, $5a_1/\Phi_u(1)$, $1b_2/p^{(O)}(1)$, $2b_2/\sigma_u(2)$, $3b_2/\delta_u(2)$]	14843
$^1A_1(3)$	27% [$4a_1/p^{(O)}(2)$, $1b_1/\Phi_u(2)$, $1b_2/p^{(O)}(1)$, $2b_2/\sigma_u(2)$, $3b_2/\delta_u(\bar{1})$] 13% [$4a_1/p^{(O)}(2)$, $1b_1/\Phi_u(2)$, $1b_2/p^{(O)}(2)$, $2b_2/\sigma_u(2)$]	14889
$^1A_2(2)$	47% [$4a_1/p^{(O)}(2)$, $1b_1/\Phi_u(1)$, $1b_2/p^{(O)}(\bar{1})$, $2b_2/\sigma_u(2)$, $3b_2/\delta_u(2)$] 10% [$4a_1/p^{(O)}(2)$, $5a_1/\Phi_u(1)$, $1b_2/p^{(O)}(\bar{1})$, $2b_2/\sigma_u(2)$, $3b_2/\delta_u(1)$, $1a_2/\delta_u(\bar{1})$] 9% [$4a_1/p^{(O)}(2)$, $5a_1/\Phi_u(1)$, $1b_2/p^{(O)}(1)$, $2b_2/\sigma_u(2)$, $3b_2/\delta_u(\bar{1})$, $1a_2/\delta_u(\bar{1})$]	14984
$^5B_2(2)$	64% [$4a_1/p^{(O)}(1)$, $5a_1/\Phi_u(1)$, $1b_1/\Phi_u(1)$, $1b_2/p^{(O)}(2)$, $2b_2/\sigma_u(2)$, $1a_2/\delta_u(1)$] 10% [$4a_1/p^{(O)}(1)$, $6(1)$, $1b_1/\Phi_u(1)$, $1b_2/p^{(O)}(2)$, $2b_2/\sigma_u(2)$, $1a_2/\delta_u(1)$]	15035
$^1B_1(2)$	33% [$4a_1/p^{(O)}(2)$, $5a_1/\Phi_u(1)$, $1b_1/\Phi_u(\bar{1})$, $1b_2/p^{(O)}(1)$, $2b_2/\sigma_u(2)$, $3b_2/\delta_u(\bar{1})$] 13% [$4a_1/p^{(O)}(2)$, $5a_1/\Phi_u(1)$, $1b_1/\Phi_u(\bar{1})$, $1b_2/p^{(O)}(2)$, $2b_2/\sigma_u(2)$,] 12% [$4a_1/p^{(O)}(2)$, $1b_2/p^{(O)}(1)$, $2b_2/\sigma_u(2)$, $3b_2/\delta_u(2)$, $1a_2/\delta_u(\bar{1})$]	15593

Table B.3 – *Continued from previous page*

Term Symbol	Character : % [orbital(number of electron)] 11% [$4a_1/p^{(O)}(2)$, $5a_1/\Phi_u(2)$, $1b_2/p^{(O)}(1)$, $2b_2/\sigma_u(2)$, $1a_2/\delta_u(\bar{1})$]	E (cm^{-1})
SO X	47.15% $^3B_2(1)$, 24.15% $^3A_2(1)$, 14.14% $^3B_1(1)$	0
a	58.72% $^3B_2(1)$, 24.89% $^3A_2(1)$	1235
b	73.37% $^3B_2(1)$	1783
c	51.22% $^3A_2(1)$	3777
d	23.54% $^3B_1(1)$, 18.35% $^1A_1(1)$, 16.73% $^3A_2(2)$, 10.23% $^3B_1(2)$	5660
e	49.43% $^3B_1(1)$, 22.12% $^3A_1(1)$	6658
f	43.87% $^3B_1(1)$, 19.21% $^3A_1(1)$, 11.3% $^3B_1(2)$	7062
g	23.47% $^3B_2(1)$, 17.68% $^3A_2(1)$, 17.17% $^3B_1(2)$	7929
h	26.14% $^3A_2(1)$, 21.08% $^5B_2(1)$, 18.73% $^3A_2(2)$	7973
i	32.2% $^3A_2(2)$, 24.4% $^3A_2(1)$, 15% $^5B_2(1)$	8675
j	28.2% $^3A_2(1)$, 22.38% $^3B_1(1)$, 11.46% $^5B_2(1)$	9096
k	28.45% $^3A_2(1)$, 26.41% $^3B_2(1)$	9345
l	30.77% $^3B_1(2)$, 19% $^3B_1(1)$	9399
m	16.69% $^3B_2(1)$, 14.81% $^5B_2(1)$	9690
n	28.51% $^3B_1(2)$, 11.78% $^3A_1(2)$, 10.3% $^3B_1(1)$	9879
o	24.08% $^3A_2(2)$, 15.86% $^5B_1(1)$, 13.35% $^3B_2(2)$	10224
p	25.31% $^3A_2(2)$, 14.83% $^3B_2(2)$, 9.57% $^5B_1(1)$	10235
q	23.29% $^5B_2(1)$, 13.35% $^5B_1(3)$	10342
r	29.37% $^5B_1(1)$, 24.74% $^5A_1(1)$, 10.19% $^5B_2(1)$, 10.05% $^5A_1(2)$	10686
s	23.12% $^3B_2(2)$, 20.68% $^3B_1(3)$, 15.13% $^3B_1(2)$	10749

Table B.3 – *Continued from previous page*

Term Symbol	Character : % [orbital(number of electron)]	E (cm^{-1})
t	25.96% $^5B_1$(1) , 20.75% $^5A_1$(1) , 15.44% $^5B_2$(1)	10768
u	23.74% $^5B_2$(1) , 11.62% $^3B_1$(3) , 10.37% $^5A_1$(1)	11022
v	24.63% $^5B_2$(1) , 21.07% $^5A_1$(1) , 12.44% $^3B_1$(1)	11207
w	14.48% $^3A_1$(1) , 10.17% $^3A_1$(2)	11616
x	36.43% $^5A_1$(1) , 12.09% $^3B_1$(2)	12429
y	20.5% $^3A_2$(2)	12567
z	11.52% $^1A_1$(1) , 10.25% $^3B_1$(3) , 10.04% $^3B_2$(3)	12693
aa	14.11% $^1A_2$(1)	12794
ab	29.09% $^3B_2$(2) , 24.21% $^3A_2$(3)	12873
ac	16.43% $^3A_1$(3) , 15.09% $^5B_1$(2) , 14.7% $^3A_1$(1) , 10.89% $^5B_1$(1)	13058
ad	30.37% $^3A_2$(3) , 13.89% $^1A_1$(1) ,	13309
ae	20.38% $^5B_1$(2) , 13.23% $^5A_1$(3) , 9.98% $^5B_2$(2)	13341
af	34.08% $^3B_2$(3) , 16.97% $^1A_2$(1) , 11.74% $^1A_2$(2)	13488
ag	24.73% $^3A_1$(1) , 12.48% $^5B_1$(2) , 11.36% $^5B_1$(1)	13582
ah	18.48% $^5B_1$(2) , 15.12% $^5A_1$(3)	13814
ai	27.31% $^5B_2$(1) , 14.88% $^1B_2$(1) , 12.3% $^3A_1$(1)	13936
aj	28.12% $^5B_2$(1) , 19.38% $^5A_1$(1) , 10% $^5B_1$(2)	13996
ak	17.59% $^5B_1$(2) , 14.15% $^5B_1$(3) , 11.94% $^5A_1$(2) , 11.41% $^5A_1$(1)	14024
al	53.19% $^1B_1$(1) , 12.49% $^3A_2$(3)	14216
am	22.79% $^5A_1$(2) , 12.86% $^5B_1$(3) , 10.57% $^3B_1$(3)	14257
an	31.62% $^5B_2$(1) , 10.41% $^3A_1$(2)	14680
ao	19.07% $^5B_1$(1) , 17.32% $^5B_1$(2) , 16.76% $^5A_1$(3)	14724
ap	21.09% $^5A_1$(1) , 10.26% $^5A_1$(2) , 10% $^5B_1$(3)	14750

Table B.3 – *Continued from previous page*

Term Symbol	Character : % [orbital(number of electron)]	E (cm^{-1})
aq	16.59% $^5B_1(3)$, 13.06% $^5B_1(2)$, 9.69% $^5A_1(2)$	14874
ar	16.33% $^5B_1(1)$	15129
as	20.39% $^5A_1(2)$, 20.07% $^5B_1(1)$, 12.66% $^5B_1(3)$, 10.85% $^3B_1(3)$, 9.82% $^5A_1(1)$	15141
at	28.7% $^3B_2(2)$, 12.63% $^5B_2(1)$	15375
au	15.53% $^3A_1(2)$, 12.26% $^5B_1(3)$, 10.67% $^5B_1(1)$, 9.55% $^3B_2(2)$	15439
av	25.7% $^3B_2(3)$, 10.77% $^3B_2(2)$, 10.04% $^5A_1(2)$	15494
aw	23.7% $^5B_1(3)$, 12.34% $^3A_1(2)$, 11.09% $^3B_1(3)$	15616
ay	12.56% $^5A_1(3)$, 11.67% $^3B_1(2)$, 10.58% $^3A_1(3)$, 10.25% $^3A_2(3)$	15708
az	15.14% $^5B_1(3)$, 10.79% $^3B_1(3)$	15906
ba	18.56% $^3B_2(3)$, 16.95% $^5B_1(3)$	15948

TABLE B.4: Vertical transitions in cm^{-1} of the low-energy (E $< 16\,000$ cm^{-1}) electronic states of PuO$_3$ at SF-CASPT2 and SO-CASPT2 levels obtained with the ANO-RCC-TZVP. Orbitals 1a$_1$, 2a$_1/\tau_u$, 3a$_1$ always doubly occupied and do not appear in the following table.

	Term Symbol	Character : % [orbital(number of electron)]	E (cm^{-1})
SF	$^5A_g(1)$	84% [1a$_u/\delta_u$(1), 2b$_{2u}/\Phi_u$(1), 2b$_{1u}/\delta_u$(1), 2b$_{3u}/\Phi_u$(1)]	0
	$^5A_g(2)$	45% [1a$_u/\delta_u$(1), 3b$_{2u}/\tau_u$(1), 2b$_{1u}/\delta_u$(1), 2b$_{3u}/\Phi_u$(1)]	4798
		45% [1a$_u/\delta_u$(1), 2b$_{2u}/\Phi_u$(1), 2b$_{1u}/\delta_u$3(1), 3b$_{3u}/\tau_u$(1)]	
	$^5B_{3u}(1)$	85% [3a$_g$(1), 1a$_u/\delta_u$(1), 2b$_{1u}/\delta_u$(1), 2b$_{3u}/\Phi_u$(1)]	5421
	$^5B_{2u}?(1)$	85% [3a$_g$(1), 1a$_u/\delta_u$(1), 2b$_{1u}/\delta_u$(1), 2b$_{3u}/\Phi_u$(1)]	5421
	$^5B_{3g}(1)$	44% [2b$_{2u}/\Phi_u$(1), 3b$_{2u}/\tau_u$1(1), 2b$_{1u}/\delta_u$(1), 2b$_{3u}/\Phi_u$(1)]	6019
		44% [1a$_u/\delta_u$(1), 2b$_{2u}/\Phi_u$(1), 2b$_{3u}/\Phi_u$(1), 3b$_{3u}/\tau_u$(1)]	
	$^5B_{2g}(1)$	44% [2b$_{2u}/\Phi_u$(1), 3b$_{2u}/\tau_u$(1), 2b$_{1u}/\delta_u$(1), 2b$_{3u}/\Phi_u$(1)]	6019
		44% [1a$_u/\delta_u$(1), 2b$_{2u}/\Phi_u$(1), 2b$_{3u}/\Phi_u$(1), 3b$_{3u}/\tau_u$(1)]	
	$^5A_g(3)$	45% [1a$_u/\delta_u$(1), 3b$_{2u}/\tau_u$(1), 2b$_{1u}/\delta_u$(1), 2b$_{3u}/\Phi_u$(1)]	6067
		45% [1a$_u/\delta_u$(1), 2b$_{2u}/\Phi_u$(1), 2b$_{1u}/\delta_u$(1), 3b$_{3u}/\tau_u$(1)]	
	$^5B_{1g}(1)$	44% [1a$_u/\delta_u$(1), 2b$_{2u}/\Phi_u$(1), 3b$_{2u}/\tau_u$(1), 2b$_{1u}/\delta_u$(1)]	6158
		44% [1a$_u/\delta_u$(1), 2b$_{1u}/\delta_u$(1), 2b$_{3u}/\Phi_u$(1), 3b$_{3u}/\tau_u$(1)]	
	$^3B_{3u}(1)$	59% [3a$_g$(1),1a$_u/\delta_u(\bar{1})$, 2b$_{2u}/\Phi_u$(1), 2b$_{1u}/\delta_u$(1)]	6855
		19% [3a$_g$(1),1a$_u/\delta_u$(1), 2b$_{2u}/\Phi_u(\bar{1})$, 2b$_{1u}/\delta_u$(1)]	
		10% [3a$_g$(1),1a$_u/\delta_u$(1), 2b$_{2u}/\Phi_u$(1), 2b$_{1u}/\delta_u(\bar{1})$]	
	$^3B_{2u}(1)$	59% [3a$_g$(1), 1a$_u/\delta_u(\bar{1})$, 2b$_{1u}/\delta_u$(1), 2b$_{3u}/\Phi_u$(1)]	6855
		20% [3a$_g$(1), 1a$_u/\delta_u$(1), 2b$_{1u}/\delta_u(\bar{1})$, 2b$_{3u}/\Phi_u$(1)]	
	$^5B_{1g}(2)$	44% [1a$_u/\delta_u$(1), 2b$_{1u}/\delta_u$(1), 2b$_{3u}/\Phi_u$(1), 3b$_{3u}/\tau_u$(1)]	7293
		44% [1a$_u/\delta_u$(1), 2b$_{2u}/\Phi_u$(1), 3b$_{2u}/\tau_u$(1), 2b$_{1u}/\delta_u$(1)]	

Table B.4 – *Continued from previous page*

Term Symbol	Character : % [orbital(number of electron)]	E (cm^{-1})
$^5A_u(1)$	79% [$3a_g(1)$, $2b_{2u}/\Phi_u(1)$, $2b_{1u}/\delta_u(1)$, $2b_{3u}/\Phi_u(1)$]	7452
$^5B_{1u}(1)$	80% [$3a_g(1)$, $1a_u/\delta_u(1)$, $2b_{2u}/\Phi_u0(1)$, $2b_{3u}/\Phi_u(1)$]	7462
$^5B_{3g}(2)$	37% [$1a_u/\delta_u(1)$, $2b_{2u}/\Phi_u(1)$, $2b_{3u}/\Phi_u(1)$, $3b_{3u}/\pi_u(1)$]	7637
	33%[$2b_{2u}/\Phi_u(1)$, $3b_{2u}/\tau_u(1)$, $2b_{1u}/\delta_u3(1)$, $2b_{3u}/\Phi_u(1)$]	
	12% [$2b_{2u}/\Phi_u(1)$, $3b_{2u}/\tau_u(1)$, $2b_{1u}/\delta_u(1)$, $3b_{3u}/\tau_u(1)$]	
$^5B_{2g}(2)$	37% [$1a_u/\delta_u(1)$, $2b_{2u}/\Phi_u(1)$, $2b_{3u}/\Phi_u6(1)$, $3b_{3u}/\tau_u(1)$]	7637
	33%[$2b_{2u}/\Phi_u(1)$, $3b_{2u}/\tau_u(1)$, $2b_{1u}/\delta_u(1)$, $2b_{3u}/\Phi_u(1)$]	
	12% [$2b_{2u}/\Phi_u(1)$, $3b_{2u}/\tau_u(1)$, $2b_{1u}/\delta_u(1)$, $3b_{3u}/\tau_u(1)$]	
$^3B_{1u}(1)$	51%[$3a_g(1)$, $1a_u/\delta_u(1)$, $2b_{2u}/\Phi_u(\bar{1})$, $2b_{3u}/\Phi_u(1)$]	9586
	68%[$3a_g(1)$, $1a_u/\delta_u(1)$, $2b_{2u}/\Phi_u(\bar{1})$, $2b_{3u}/\Phi_u(1)$]	
$^3A_u(1)$	51% [$3a_g(1)$, $2b_{2u}/\Phi_u(\bar{1})$, $2b_{1u}/\delta_u(1)$, $2b_{3u}/\Phi_u(1)$]	9614
	17% [$3a_g(1)$, $2b_{2u}/\Phi_u(1)$, $2b_{1u}/\delta_u(\bar{1})$, $2b_{3u}/\Phi_u(1)$]	
$^3B_{3g}(1)$	38% [$1a_u/\delta_u(1)$, $2b_{2u}/\Phi_u(1)$, $2b_{1u}/\delta_u(2)$]	10101
	36% [$1a_u/\delta_u(2)$, $2b_{1u}/\delta_u(1)$, $2b_{3u}/\Phi_u(1)$]	
$^3B_{2g}(1)$	38% [$1a_u/\delta_u(1)$, $2b_{2u}/\Phi_u(1)$, $2b_{1u}/\delta_u(2)$]	10101
	36% [$1a_u/\delta_u(2)$, $2b_{1u}/\delta_u(1)$, $2b_{3u}/\Phi_u(1)$]	
$^3B_{1g}(1)$	24% [$1a_u/\delta_u(1)$, $2b_{2u}/\Phi_u(2)$, $2b_{1u}/\delta_u(1)$]	10308
	24% [$1a_u/\delta_u(1)$, $2b_{1u}/\delta_u(1)$, $2b_{3u}/\Phi_u(2)$]	
	19% [$2b_{2u}/\Phi_u(1)$, $2b_{1u}/\delta_u(2)$, $2b_{3u}/\Phi_u(1)$]	
	16% [$1a_u/\delta_u(1)$, $2b_{2u}/\Phi_u(1)$, $2b_{3u}/\Phi_u(1)$]	
$^5A_u(2)$	23% [$3a_g(1)$, $1a_u/\delta_u(1)$, $2b_{2u}/\Phi_u(1)$, $3b_{2u}/\tau_u(1)$]	11344
	23% [$3a_g(1)$, $1a_u/\delta_u(1)$, $2b_{3u}/\Phi_u(1)$, $3b_{3u}/\tau_u(1)$]	
	20% [$3a_g(1)$, $3b_{2u}/\tau_u(1)$, $2b_{1u}/\delta_u(1)$, $2b_{3u}/\Phi_u(1)$]	

Table B.4 – Continued from previous page

Term Symbol	Character : % [orbital(number of electron)]	E (cm^{-1})
$^5B_{1u}(2)$	20% [3a$_g$(1), 2b$_{2u}$/Φ_u(1), 2b$_{1u}$/δ_u(1), 3b$_{3u}$/π_u(1)]	11347
	23% [3a$_g$(1), 2b$_{1u}$/δ_u(1), 2b$_{3u}$/Φ_u(1), 3b$_{3u}$/π_u(1)]	
	23% [3a$_g$(1), 2b$_{2u}$/Φ_u(1), 3b$_{2u}$/π_u(1), 2b$_{1u}$/δ_u(1)]	
	19% [3a$_g$(1), 1a$_u$/δ_u(1), 2b$_{2u}$/Φ_u(1), 3b$_{3u}$/π_u(1)]	
	19% [3a$_g$(1), 1a$_u$/δ_u(1), 11(1), 2b$_{3u}$/Φ_u(1)]	
$^3B_{3g}(2)$	35%[1a$_u$/δ_u(2), 2b$_{1u}$/δ_u(1), 2b$_{3u}$/Φ_u(1)]	11467
	33% [1a$_u$/δ_u(1), 3b$_{2u}$/π_u(1), 2b$_{1u}$/δ_u(2)]	
$^3B_{2g}(2)$	35%[1a$_u$/δ_u(2), 2b$_{1u}$/δ_u(1), 2b$_{3u}$/Φ_u(1)]	11467
	33% [1a$_u$/δ_u(1), 3b$_{2u}$/π_u(1), 2b$_{1u}$/δ_u(2)]	
$^3B_{1g}(2)$	34% [1a$_u$/δ_u(2), 3b$_{2u}$/π_u(1), 2b$_{3u}$/Φ_u(1)]	12812
	33% [3b$_{2u}$/π_u(1), 2b$_{1u}$/δ_u(2), 2b$_{3u}$/Φ_u(1)]	
$^3A_g(1)$	51% [1a$_u$/δ_u(1), 2b$_{2u}$/Φ_u(1), 2b$_{1u}$/δ_u($\overline{1}$), 2b$_{3u}$/Φ_u(1)]	12815
	17% [1a$_u$/δ_u(1), 2b$_{2u}$/Φ_u($\overline{1}$), 2b$_{1u}$/δ_u(1), 2b$_{3u}$/Φ_u(1)]	
$^3B_{1u}(2)$	20%[3a$_g$(1), 2b$_{2u}$/Φ_u($\overline{1}$), 3b$_{2u}$/π_u(1), 2b$_{1u}$/δ_u(1)]	13398
	20%[3a$_g$(1), 2b$_{1u}$/δ_u($\overline{1}$), 2b$_{3u}$/Φ_u(1), 3b$_{3u}$/π_u(1)]	
	15%[3a$_g$(1), 3b$_{2u}$/π_u(1), 2b$_{3u}$/τ_u(1), 2b$_{3u}$/Φ_u(1)]	
	15%[3a$_g$(1), 1a$_u$/δ_u($\overline{1}$), 2b$_{2u}$/Φ_u(1), 3b$_{3u}$/π_u(1)]	
$^3A_u(2)$	15% [3a$_g$(1), 1a$_u$/δ_u($\overline{1}$), 2b$_{2u}$/Φ_u(1), 3b$_{2u}$/π_u(1)]	13402
	15% [3a$_g$(1), 1a$_u$/δ_u($\overline{1}$), 2b$_{3u}$/Φ_u(1), 3b$_{3u}$/π_u(1)]	
	14% [3a$_g$(1), 3b$_{2u}$/π_u($\overline{1}$), 2b$_{1u}$/δ_u(1), 2b$_{3u}$/Φ_u(1)]	
	14% [3a$_g$(1), 2b$_{2u}$/π_u($\overline{1}$), 2b$_{1u}$/δ_u(1), 3b$_{3u}$/π_u(1)]	
$^5B_{3g}(3)$	46% [2b$_{2u}$/Φ_u(1), 3b$_{2u}$/π_u(1), 2b$_{1u}$/δ_u(1), 3b$_{3u}$/π_u(1)]	13460
	45% [1a$_u$/δ_u(1), 3b$_{2u}$/π_u(1), 2b$_{3u}$/Φ_u(1), 3b$_{3u}$/π_u(1)]	

Table B.4 – *Continued from previous page*

Term Symbol	Character : % [orbital(number of electron)]	E (cm^{-1})
$^5B_{2g}(3)$	46% [$2b_{2u}/\Phi_u(1)$, $3b_{2u}/\tau_u(1)$, $2b_{1u}/\delta_u(1)$, $3b_{3u}/\tau_u(1)$] 45% [$1a_u/\delta_u(1)$, $3b_{2u}/\tau_u(1)$, $2b_{3u}/\Phi_u(1)$, $3b_{3u}/\tau_u(1)$]	13460
$^3B_{1g}(3)$	34% [$1a_u/\delta_u(1)$, $2b_{1u}/\delta_u(1)$, $2b_{3u}/\Phi_u(2)$] 34% [$1a_u/\delta_u(1)$, $3b_{2u}/\tau_u(2)$, $2b_{1u}/\delta_u(1)$]	13638
$^3A_g(2)$	47% [$1a_u/\delta_u(1)$, $2b_{2u}/\Phi_u(1)$, $2b_{1u}/\delta_u(1)$, $2b_{3u}/\Phi_u(\bar{1})$] 17% [$1a_u/\delta_u(1)$, $2b_{2u}/\Phi_u(\bar{1})$, $2b_{1u}/\delta_u(1)$, $2b_{3u}/\Phi_u(1)$]	13659
$^5B_{3u}(2)$	45% [$2a_g/\delta_u(1)$, $1a_u/\delta_u(1)$, $2b_{1u}/\delta_u(1)$, $2b_{3u}/\Phi_u6(1)$] 42% [$1b_{1g}/\delta_u(1)$, $1a_u/\delta_u(1)$, $2b_{2u}/\Phi_u0(1)$, $2b_{1u}/\delta_u(1)$]	14688
$^5B_{2u}(2)$	45% [$2a_g/\delta_u(1)$, $1a_u/\delta_u(1)$, $2b_{1u}/\delta_u(1)$, $2b_{3u}/\Phi_u(1)$] 42% [$1b_{1g}/\delta_u(1)$, $1a_u/\delta_u(1)$, $2b_{2u}/\Phi_u(1)$, $2b_{1u}/\delta_u(1)$]	14688
$^3B_{3u}(2)$	30% [$3a_g(1)$, $1a_u/\delta_u(1)$, $2b_{2u}/\Phi_u(1)$, $2b_{1u}/\delta_u(\bar{1})$] 22% [$3a_g(1)$, $1a_u/\delta_u(2)$, $2b_{3u}/\Phi_u(1)$] 22% [$3a_g(1)$, $2b_{1u}/\delta_u(2)$, $2b_{3u}/\Phi_u(1)$] 11% [$3a_g(1)$, $1a_u/\delta_u(\bar{1})$, $2b_{2u}/\Phi_u(1)$, $2b_{1u}/\delta_u(1)$]	15060
$^3B_{2u}(2)$	34% [$3a_g(1)$, $1a_u/\delta_u(1)$, $2b_{1u}/\delta_u(\bar{1})$, $2b_{3u}/\Phi_u(1)$] 22% [$3a_g(1)$, $1a_u/\delta_u(2)$, $2b_{2u}/\Phi_u(1)$] 22% [$3a_g(1)$, $2b_{2u}/\Phi_u(1)$, $2b_{1u}/\delta_u(3)$] 11% [$3a_g(1)$, $1a_u/\delta_u(\bar{1})$, $2b_{1u}/\delta_u(1)$, $2b_{3u}/\Phi_u(1)$]	15062
$^1B_{3u}(1)$	32% [$3a_g(1)$, $1a_u/\delta_u(1)$, $2b_{1u}/\delta_u(1)$, $2b_{3u}/\Phi_u(1)$] 21% [$3a_g(1)$, $3b_{2u}/\tau_u(1)$, $2b_{1u}/\delta_u(2)$] 21% [$3a_g(1)$, $1a_u/\delta_u(2)$, $3b_{2u}/\tau_u(1)$]	15336
$^1B_{2u}(1)$	32% [$3a_g(1)$, $1a_u/\delta_u(1)$, $2b_{1u}/\delta_u(1)$, $2b_{3u}/\Phi_u(1)$] 21% [$3a_g(1)$, $3b_{2u}/\tau_u(1)$, $2b_{1u}/\delta_u(2)$]	15336

Table B.4 – *Continued from previous page*

Term Symbol	Character : % [orbital(number of electron)]	E (cm^{-1})
	21% [3a$_g$(1), 1a$_u$/δ_u(2), 3b$_{2u}$/π_u(1)]	
$^3B_{3u}$(3)	29% [3a$_g$(1), 1a$_u$/δ_u(1), 2b$_{2u}$/Φ_u($\overline{1}$), 2b$_{1u}$/δ_u(1)]	15370
	24% [3a$_g$(1), 2b$_{1u}$/δ_u(2), 2b$_{3u}$/Φ_u(1)]	
	23% [3a$_g$(1), 1a$_u$/δ_u(2), 2b$_{3u}$/Φ_u(1)]	
$^3B_{2u}$(3)	37% [3a$_g$(1), 1a$_u$/δ_u(1), 2b$_{1u}$/δ_u(1), 2b$_{3u}$/Φ_u($\overline{1}$)]	15382
	24% [3a$_g$(1), 2b$_{2u}$/Φ_u(1), 2b$_{1u}$/δ_u(3)]	
	23% [3a$_g$(1), 1a$_u$/δ_u(2), 2b$_{2u}$/Φ_u(1)]	
^5A_g(4)	64% [2b$_{2u}$/Φ_u(1), 3b$_{2u}$/π_u(1), 2b$_{3u}$/Φ_u(1), 3b$_{3u}$/π_u(1)]	15800
	20% [2b$_{2u}$/Φ_u(1), 3b$_{2u}$/π_u(1), 2b$_{1u}$/δ_u(1), 2b$_{3u}$/Φ_u(1)]	
	23% [1a$_u$/δ_u(1), 3b$_{2u}$/π_u(1), 2b$_{1u}$/δ_u(1), 3b$_{3u}$/π_u(1)]	
	14% [2b$_{2u}$/Φ_u(2), 2b$_{1u}$/δ_u(1), 3b$_{3u}$/π_u(1)]	
	10% [2b$_{1u}$/δ_u(1), 2b$_{3u}$/Φ_u(2), 3b$_{3u}$/π_u(1)]	
$^1B_{3u}$(2)	41% [3a$_g$(1), 1a$_u$/δ_u(1), 13(1), 2b$_{3u}$/Φ_u(1)]	15850
	23% [3a$_g$(1), 2b$_{2u}$/Φ_u(1), 2b$_{1u}$/δ_u(2)]	
	23% [3a$_g$(1), 1a$_u$/δ_u(2), 2b$_{2u}$/Φ_u(1)]	
$^1B_{2u}$(2)	41% [3a$_g$(1), 1a$_u$/δ_u(1), 2b$_{1u}$/δ_u(1), 2b$_{3u}$/Φ_u(1)]	15850
	23% [3a$_g$(1), 2b$_{2u}$/Φ_u(1), 2b$_{1u}$/δ_u(2)]	
	23% [3a$_g$(1), 1a$_u$/δ_u(2), 2b$_{2u}$/Φ_u(1)]	
SO 0$_g^-$	48% ^5A_g(1) , 22.45% $^3B_{1g}$(1)	0
1$_g$	67% ^5A_g(1) , 14.59% $^3B_{1g}$(1)	2462
1$_u$	27% $^5B_{2u}$(1), 26.81% $^5B_{3u}$(1) , 13.24% ^5A_u(1) , 12.77% $^5B_{1u}$(1)	5851
2$_g$	85.58% ^5A_g(1)	5904

Table B.4 – *Continued from previous page*

Term Symbol	Character : % [orbital(number of electron)]	E (cm^{-1})
2_u	24.14% $^5A_u(1)$, 21.34% $^5B_{2u}(1)$, 21.31% $^5B_{3u}(1)$	6266
3_u	38.85% $^5B_{3u}(1)$, 24.97% $^3B_{2u}(1)$	7197
a_g	49.54% $^5A_g(2)$, 36.86% $^5B_{1g}(1)$	7240
b_g	31.53% $^5A_g(3)$, 23.96% $^5B_{1g}(2)$, 18.11% $^3B_{3g}(2)$, 18.11% $^3B_{2g}(2)$	7595
c_u	22.24% $^3B_{2u}(1)$, 21.61% $^3B_{3u}(1)$, 12.23% $^3A_u(1)$, 10.77% $^5B_{2u}(1)$, 10.68% $^5B_{3u}(1)$	7911
d_g	47.71% $^5A_g(2)$, 28.33% $^5B_{1g}(1)$, 15.29% $^5B_{2g}(1)$	8738
e_g	32.7% $^5A_g(3)$, 23.46% $^5B_{1g}(2)$, 18.02% $^5A_g(1)$, 12.56% $^3B_{2g}(2)$, 12.56% $^3B_{3g}(2)$	8971
f_g	49.36% $^5B_{2g}(1)$, 49.3% $^5B_{3g}(1)$	9610
g_g	72.76% $^5A_g(2)$	10193
h_g	44.58% $^5A_g(3)$, 22.96% $^5B_{1g}(2)$, 17.34% $^5B_{3g}(2)$	10763
i_g	63.19% $^5B_{1g}(1)$, 10.62% $^5B_{2g}(1)$, 10.62% $^5B_{3g}(1)$	11038
j_u	44.22% $^5A_u(2)$, 43.57% $^5B_{1u}(2)$	11105
k_u	48.86% $^5A_u(1)$, 43.03% $^5B_{1u}(1)$	11239
l_u	29.76% $^5B_{3u}(1)$, 29.64% $^5B_{2u}(1)$	11362
m_u	21.94% $^5A_u(1)$, 21.78% $^5B_{1u}(1)$, 18.43% $^5B_{3u}(1)$, 18.4% $^5B_{2u}(1)$	11700
n_g	19.12% $^5B_{2g}(2)$, 19.07% $^5B_{3g}(2)$, 17.44% $^3B_{1g}(1)$, 14.82% $^1A_g(1)$	11817
o_u	42.88% $^3B_{2u}(1)$, 31.88% $^5B_{3u}(1)$	11850
p_g	36.81% $^5B_{2g}(1)$, 36.81% $^5B_{3g}(1)$, 9.67% $^5A_g(3)$	12253
q_g	30.81% $^5B_{1g}(1)$, 23.75% $^5A_g(2)$, 17.24% $^3B_{2g}(1)$, 10.5% $^5B_{3g}(1)$	12345
r_u	36.84% $^5B_{1u}(1)$, 14.5% $^3B_{3u}(1)$, 14.32% $^3B_{2u}(1)$, 9.93% $^3A_u(3)$	12539
s_u	26.69% $^3A_u(2)$, 26.67% $^3B_{1u}(2)$, 21.97% $^5A_u(2)$, 21.84% $^5B_{1u}(2)$	12545
t_g	53.19% $^5B_{1g}(2)$, 14.79% $^5B_{2g}(2)$, 14.79% $^5B_{3g}(2)$	12687
u_u	25.54% $^5A_u(1)$, 19.8% $^3B_{1u}(1)$, 19.02% $^5B_{1u}(1)$	13216

Table B.4 – *Continued from previous page*

Term Symbol	Character : % [orbital(number of electron)]	E (cm^{-1})
v_u	43.47% $^3A_u(1)$, 24.48% $^3B_{1u}(1)$	13241
w_g	28.83% $^5B_{1g}(2)$, 20.15% $^5B_{2g}(2)$, 19.79% $^5A_g(3)$, 12.91% $^5B_{3g}(2)$, 12.71% $^5B_{2g}(1)$	13394
x_g	58.26% $^5B_{2g}(1)$	13728
y_g	34.24% $^5B_{1g}(1)$, 21.57% $^3B_{3g}(1)$, 21.56% $^3B_{2g}(1)$, 20.21% $^5A_g(2)$	14074
z_g	45.19% $^5B_{3g}(2)$, 38.99% $^5B_{2g}(2)$	14162
aa_u	47.44% $^3B_{1u}(1)$, 14.08% $^1A_u(1)$, 12.08% $^5A_u(1)$	14253
ab_g	32.6% $^5B_{3g}(1)$, 32.6% $^5B_{2g}(1)$, 17.93% $^3B_{1g}(2)$, 10.46% $^5A_g(2)$	14698
ac_g	35.2% $^5B_{3g}(2)$, 35.19% $^5B_{2g}(2)$, 11.61% $^3B_{3g}(2)$, 11.61% $^3B_{2g}(2)$	14747
ad_g	27.69% $^5B_{3g}(1)$, 27.69% $^5B_{2g}(1)$, 16.03% $^3A_g(1)$, 13.05% $^5B_{1g}(1)$	14862
ae_u	48.62% $^5A_u(3)$, 48.07% $^5B_{1u}(3)$	14968
af_g	24.6% $^5B_{2g}(1)$, 24.55% $^5B_{3g}(1)$, 14.87% $^3B_{1g}(2)$, 12.76% $^3A_g(1)$	15217
ag_g	57.87% $^5B_{3g}(2)$, 12.24% $^3B_{2g}(2)$	15786
ah_u	32.7% $^5B_{3u}(2)$, 32.65% $^5B_{2u}(2)$, 15.35% $^5B_{3u}(1)$, 14.96% $^5B_{2u}(1)$	15843
ai_g	35.75% $^5B_{2g}(3)$, 35.52% $^5B_{3g}(3)$, 12.29% $^5B_{1g}(1)$	15851

Appendix C

Additional ETS-NOCV Results

NOCV orbitals

NOCV deformation densities

-9.5 kcal/mol
- 39.7 kJ/mol

π donation form $2p_y$ of toluene
to 7s and 5f of Th

-5.0 kcal/mol
-20.9 kJ/mol

π donation form $2p_y$ of toluene
to 6d and 5f of Th

-2.5 kcal/mol
-10.5kJ/mol

σ donation form $2p_y$ of toluene
to 7s and 5f of Th

Sum of the smaller
contributions

ΔE = - 8.2 kcal/mol
= - 34.3 kJ/mol

Left: Antibonding
Right: Bonding

Yellow: Depletion of electron density
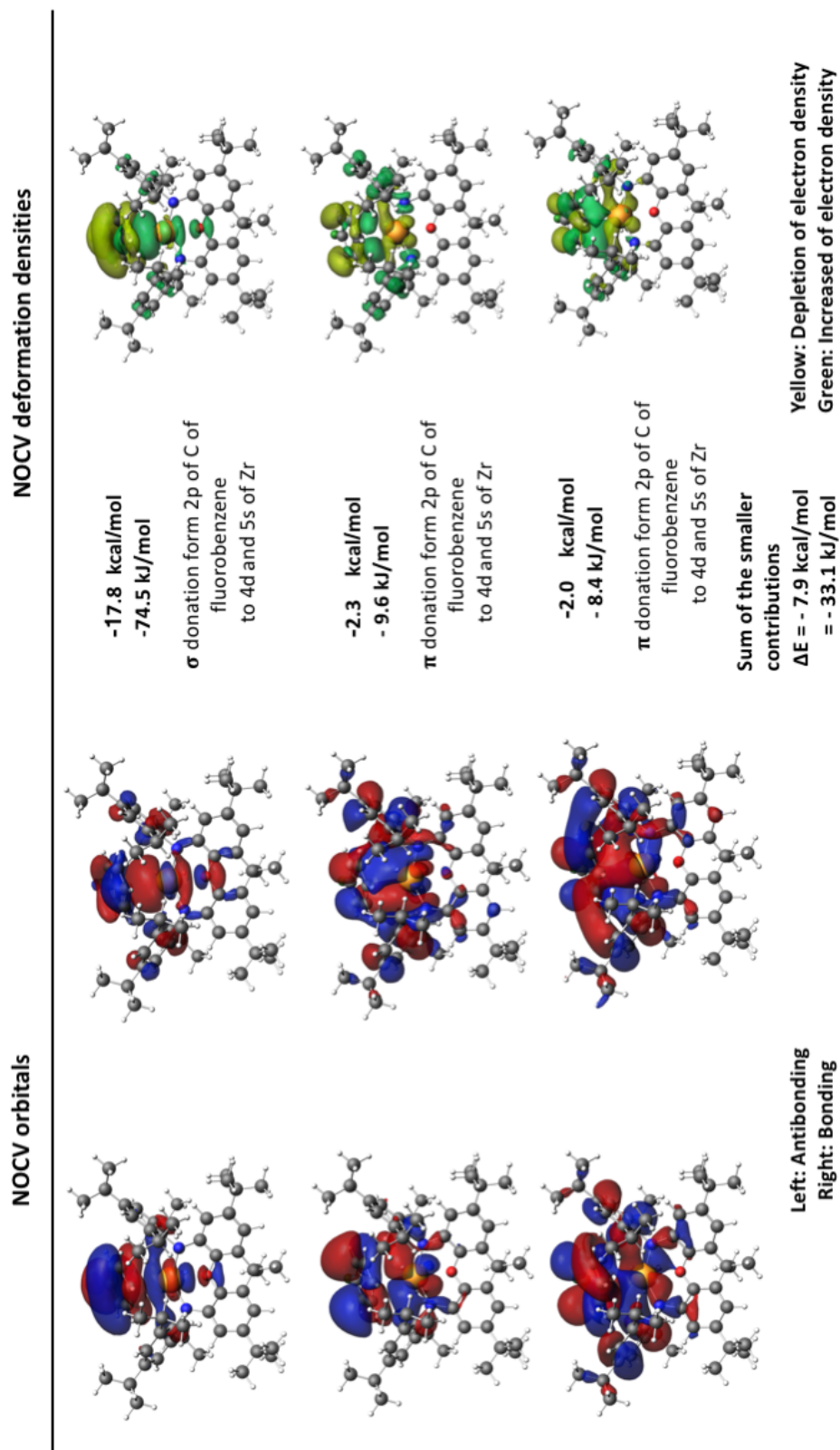**Green: Increased of electron density**
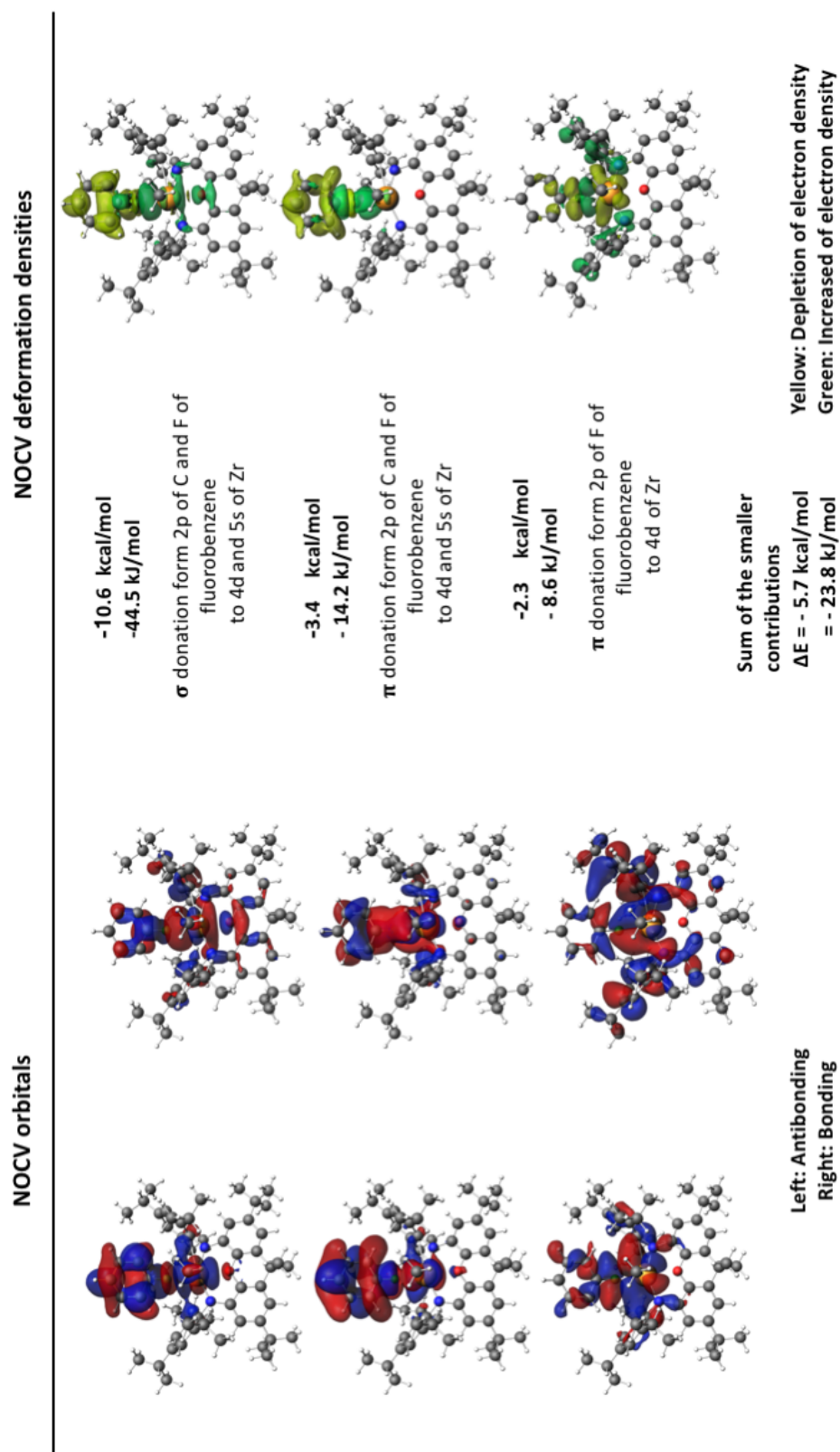
FIGURE C.1: On the left hand side: the NOCV Orbitals (with isosurfaces set to 0.01) and on the right hand side ETS-NOCV deformation density contributions, Increased (green) and decreased (yellow) electron density is presented relative to that in the isolated fragments (isosurfaces are set to 0.0001) for the molecule η^6-**3-Th-down**.

NOCV deformation densities

NOCV orbitals

-8.0 kcal/mol
-33.5 kJ/mol

π donation form $2p_y$ of benzene
to 6d and 5f of Th

-5.1 kcal/mol
- 21.3 kJ/mol

π donation form $2p_y$ of benzene
to 6d and 5f of Th

-2.8 kcal/mol
- 11.7 kJ/mol

σ donation form $2p_y$ of benzene
to 6d and 5f of Th

Sum of the smaller
contributions

ΔE = - 7,7 kcal/mol
= - 32.1 kJ/mol

Yellow: Depletion of electron density
Green: Increased of electron density

Left: Antibonding
Right: Bonding
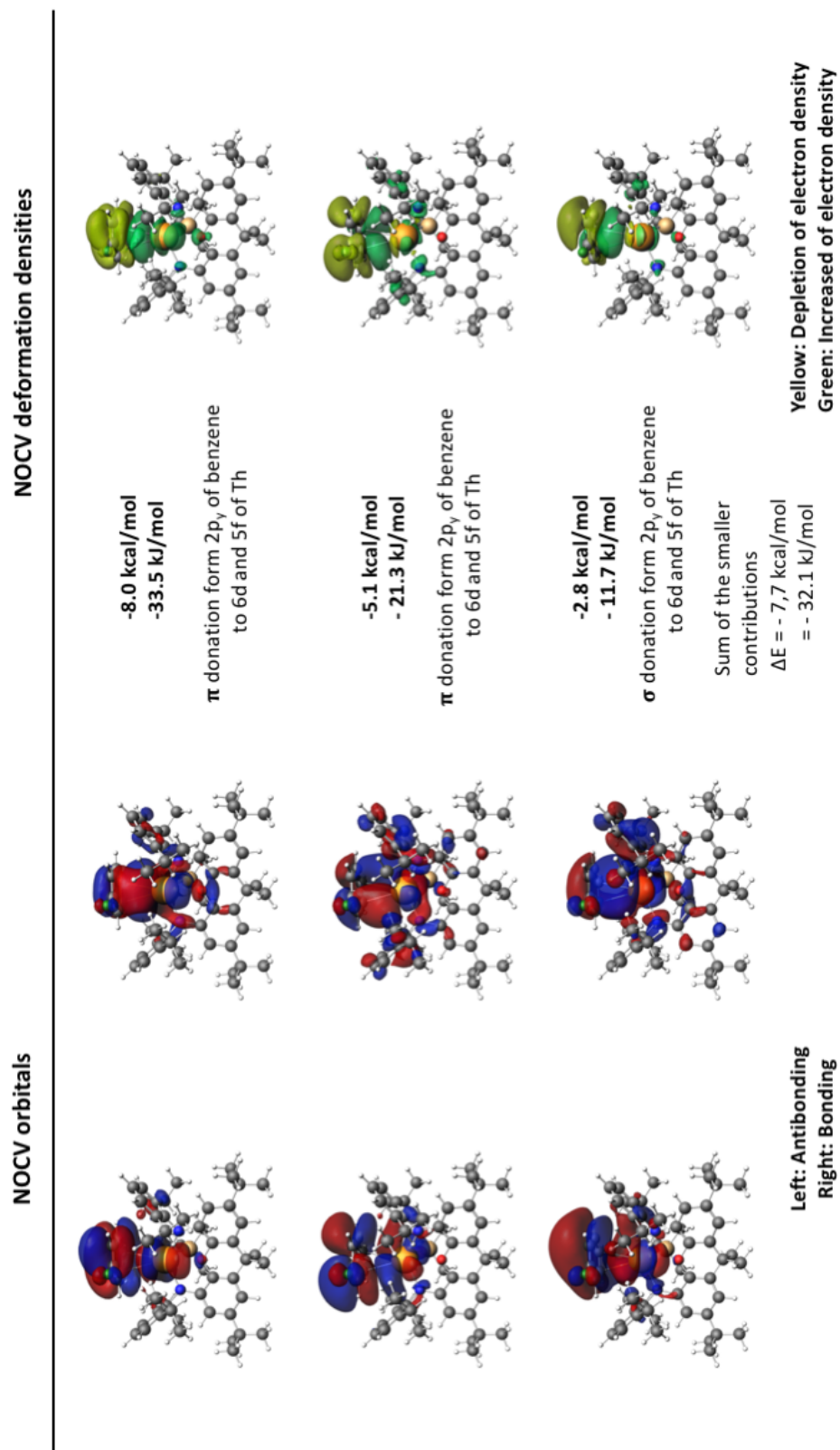
FIGURE C.2: On the left hand side: the NOCV Orbitals (with isosurfaces set to 0.01) and on the right hand side ETS-NOCV deformation density contributions, Increased (green) and decreased (yellow) electron density is presented relative to that in the isolated fragments (isosurfaces are set to 0.0001) for the molecule η^6-**5-Th-endo**.

NOCV deformation densities

NOCV orbitals

-9.5 kcal/mol
- 39.7 kJ/mol

π donation form 2p$_y$ of difluorobenzene
to 7s and 6d of Th

-3.7 kcal/mol
-15.5 kJ/mol

σ donation form 2p$_y$ of difluorobenzene
to 6d and 5f of Th

Sum of the smaller
contributions
ΔE = - 7.7 kcal/mol
= - 32.2 kJ/mol

Left: Antibonding
Right: Bonding

Yellow: Depletion of electron density
Green: Increased of electron density
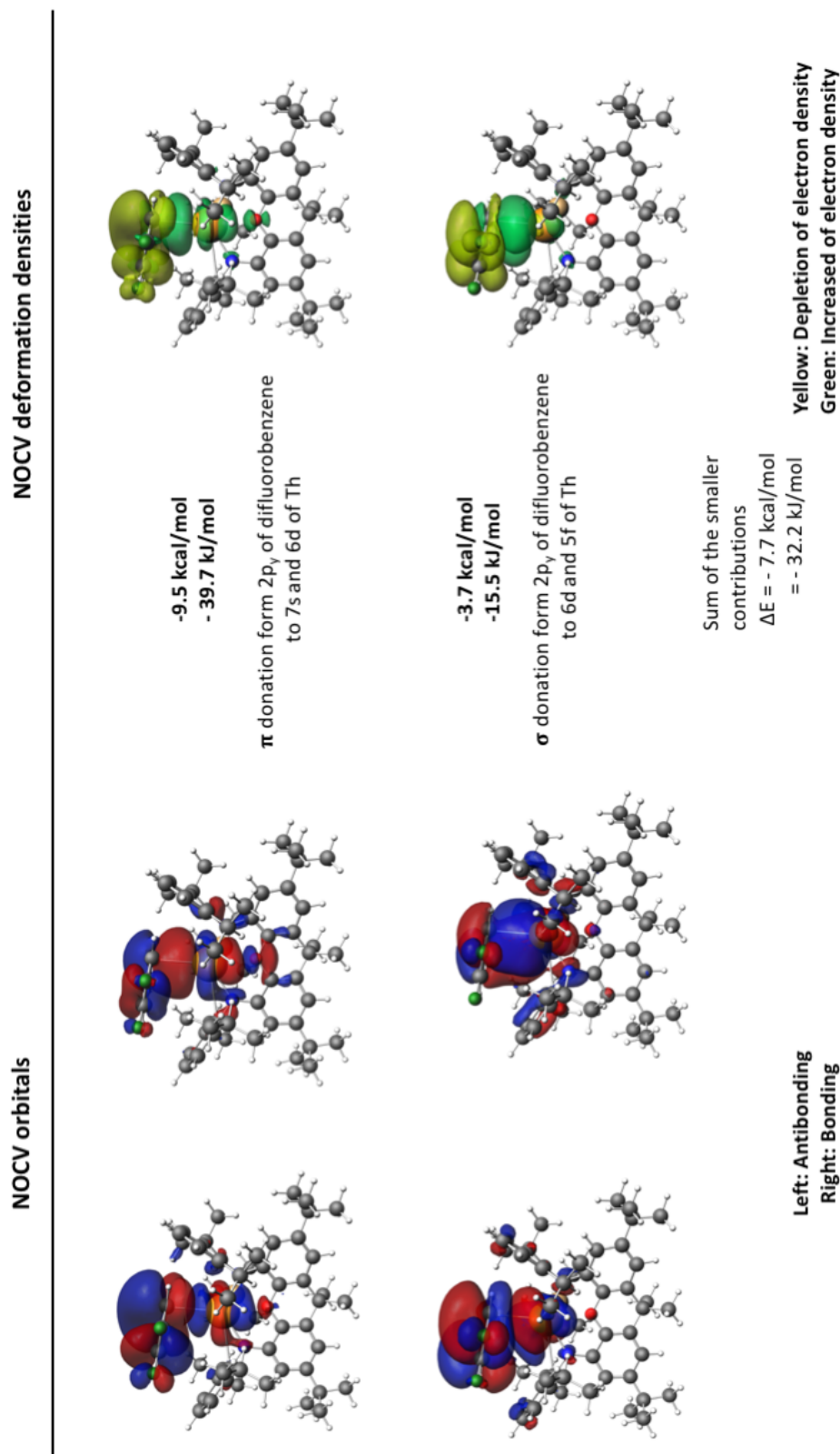
FIGURE C.3: On the left hand side: the NOCV Orbitals (with isosurfaces set to 0.01) and on the right hand side ETS-NOCV deformation density contributions, Increased (green) and decreased (yellow) electron density is presented relative to that in the isolated fragments (isosurfaces are set to 0.0001) for the molecule η^6-**6-Th-exo** .

NOCV deformation densities

NOCV orbitals

-9.1 kcal/mol
- 38.1 kJ/mol

π donation form 2p$_y$ of difluorobenzene
to 7s and 6d of Th

-3.9 kcal/mol
-16.2 kJ/mol

σ donation form 2p$_y$ of difluorobenzene
to 6d and 5f of Th

Sum of the smaller
contributions
ΔE = - 6.9 kcal/mol
= - 28.9 kJ/mol

Yellow: Depletion of electron density
Green: Increased of electron density

Left: Antibonding
Right: Bonding
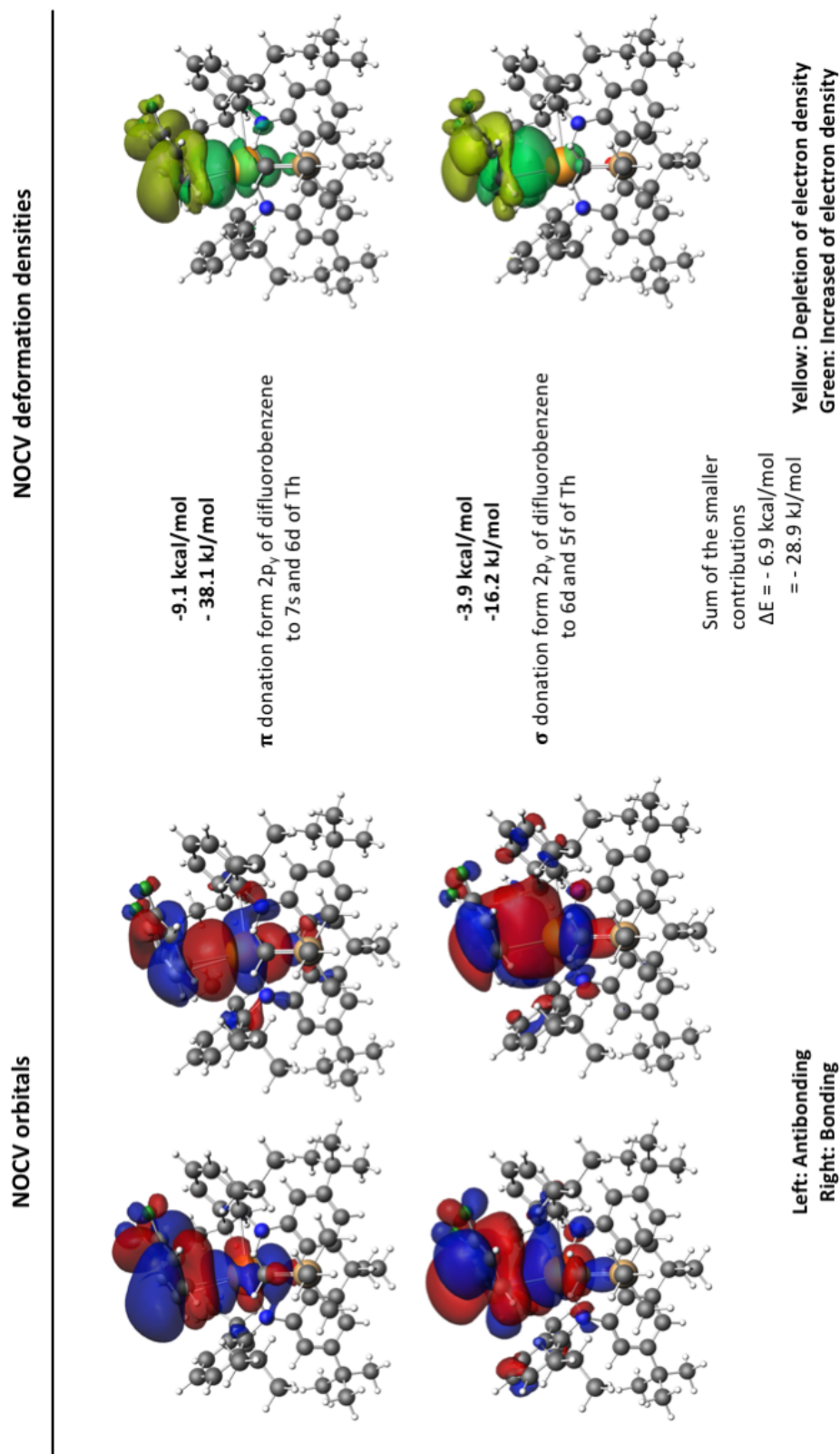
FIGURE C.4: On the left hand side: the NOCV Orbitals (with isosurfaces set to 0.01) and on the right hand side ETS-NOCV deformation density contributions, Increased (green) and decreased (yellow) electron density is presented relative to that in the isolated fragments (isosurfaces are set to 0.0001) for the molecule η^6-**6-Th-side.**

NOCV deformation densities

NOCV orbitals

-9.1 kcal/mol
- 38.1 kJ/mol

π donation form 2p$_y$ of difluorobenzene
to 7s and 6d of Th

-3.9 kcal/mol
-16.2 kJ/mol

σ donation form 2p$_y$ of difluorobenzene
to 6d and 5f of Th

Sum of the smaller
contributions
ΔE = - 6.9 kcal/mol
= - 28.9 kJ/mol

Yellow: Depletion of electron density
Green: Increased of electron density

Left: Antibonding
Right: Bonding
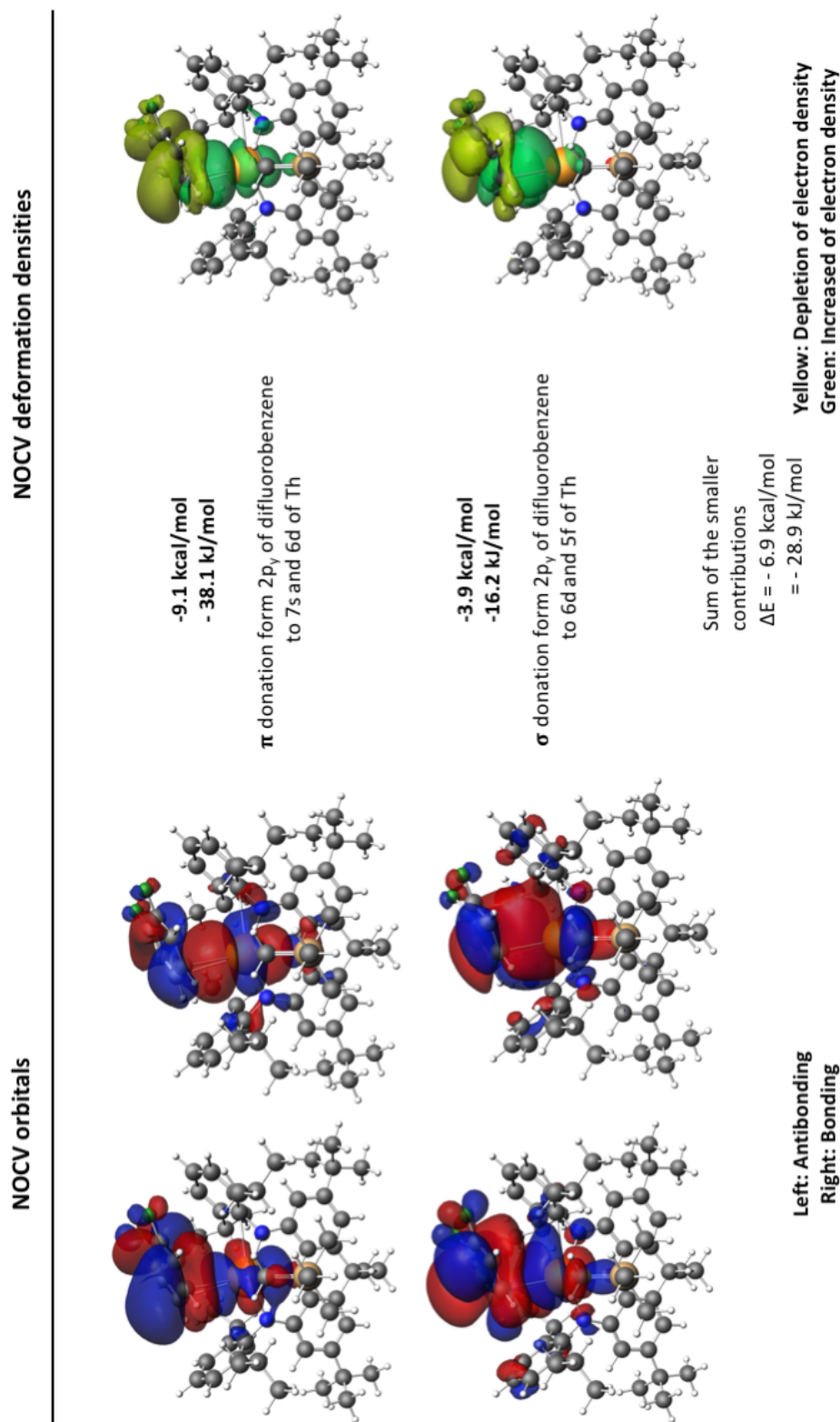
FIGURE C.5: On the left hand side: the NOCV Orbitals (with isosurfaces set to 0.01) and on the right hand side ETS-NOCV deformation density contributions, Increased (green) and decreased (yellow) electron density is presented relative to that in the isolated fragments (isosurfaces are set to 0.0001) for the molecule η^6-**6-Th-endo**.

NOCV orbitals

NOCV deformation densities

-15.8 kcal/mol
-66.1 kJ/mol

π donation form 2p of toluene
to 4d of Zr

-16.0   kcal/mol
- 66.9 kJ/mol

π donation form 2p of toluene
to 4d and 5s of Zr

-11.2   kcal/mol
-46.0 kJ/mol

σ donation form 2p of toluene
to 4d and 5s of Zr

**Sum of the smaller
contributions**
ΔE = - 20.1 kcal/mol
= - 84.1 kJ/mol

**Left: Antibonding
Right: Bonding**

**Yellow: Depletion of electron density
Green: Increased of electron density**
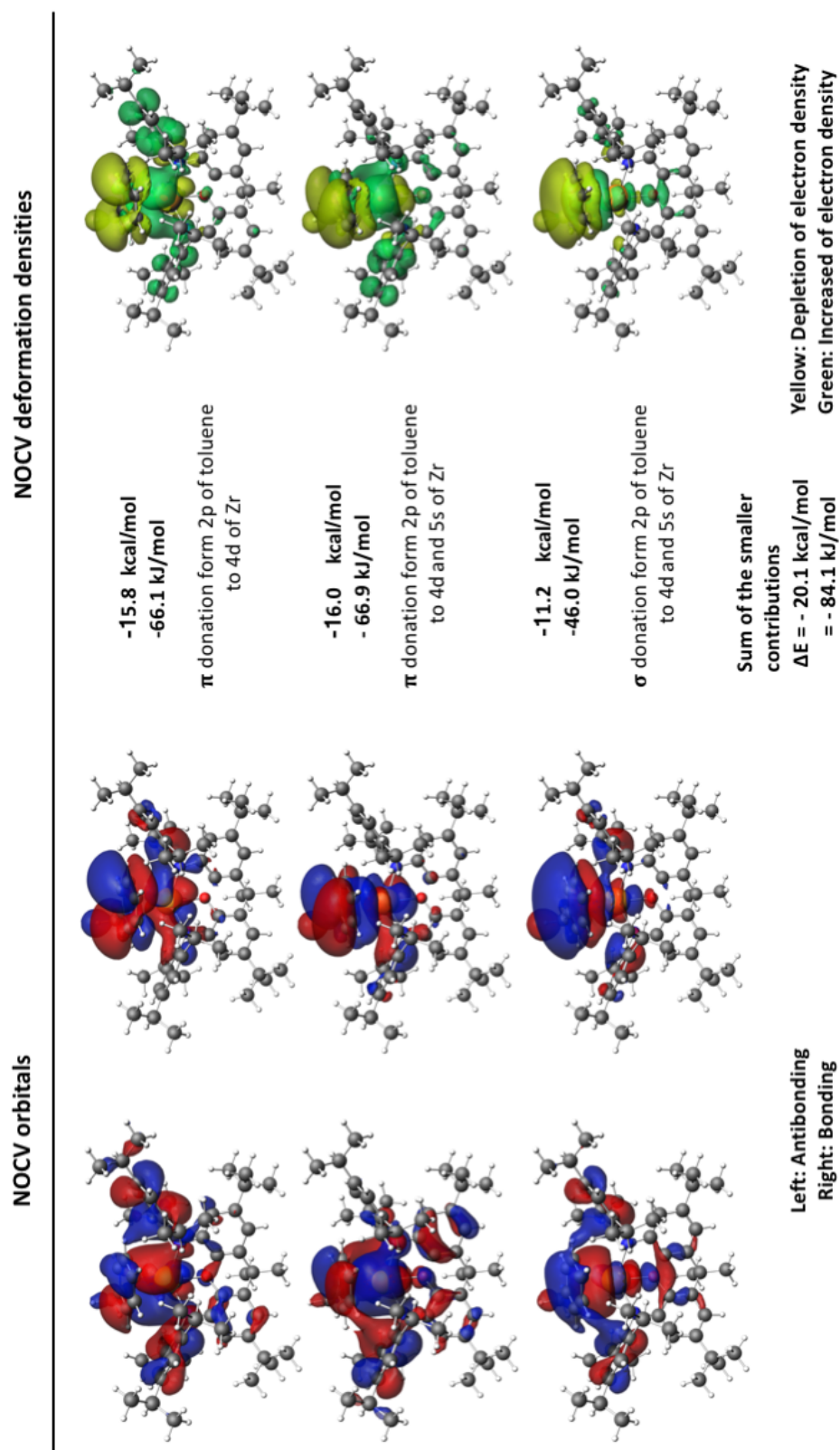
FIGURE C.6: On the left hand side: the NOCV Orbitals (with isosurfaces set to 0.01) and on the right hand side ETS-NOCV deformation density contributions, Increased (green) and decreased (yellow) electron density is presented relative to that in the isolated fragments (isosurfaces are set to 0.0001) for the molecule η^2-**E′-Zr.**

NOCV deformation densities

-17.6 kcal/mol
-73.6 kJ/mol

σ donation form 2p of Br and 2p of C
of bromobenzene
to 4d of Zr

-2.5 kcal/mol
-10.5 kJ/mol

π donation form 2p of C
bromobenzen
to 4d and 5s of Zr

-2.0 kcal/mol
-8.4 kJ/mol

σ donation form 2p of Br and 2p of C
of bromobenzene
to 4d and 5s of Zr

**Sum of the smaller
contributions**

ΔE = - 8.2 kcal/mol
= - 33.4 kJ/mol

Yellow: Depletion of electron density
Green: Increased of electron density

NOCV orbitals

Left: Antibonding
Right: Bonding
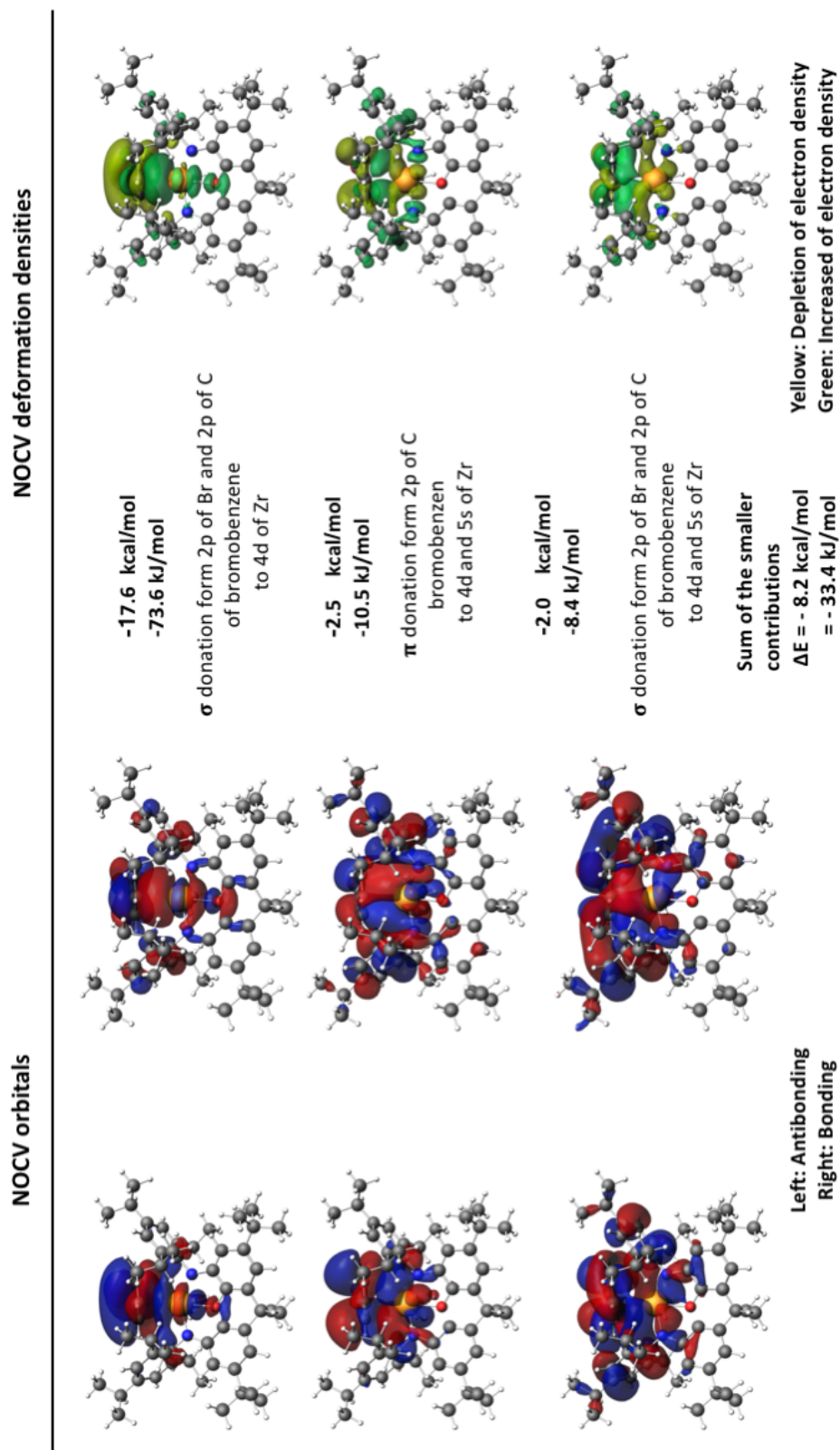
FIGURE C.7: On the left hand side: the NOCV Orbitals (with isosurfaces set to 0.01) and on the right hand side ETS-NOCV deformation density contributions, Increased (green) and decreased (yellow) electron density is presented relative to that in the isolated fragments (isosurfaces are set to 0.0001) for the molecule η^6-**4'-Zr-exo**.

NOCV deformation densities

NOCV orbitals

-15.7 kcal/mol
-65.5 kJ/mol

σ donation form 2p of Br of
bromobenzene
to 4d and 5s of Zr

-2.6 kcal/mol
- 10.8 kJ/mol

π donation form 2p of Br of
bromobenzene
to 4d of Zr

Sum of the smaller
contributions
ΔE = - 7.2 kcal/mol
= - 30.2 kJ/mol

Left: Antibonding
Right: Bonding

Yellow: Depletion of electron density
Green: Increased of electron density
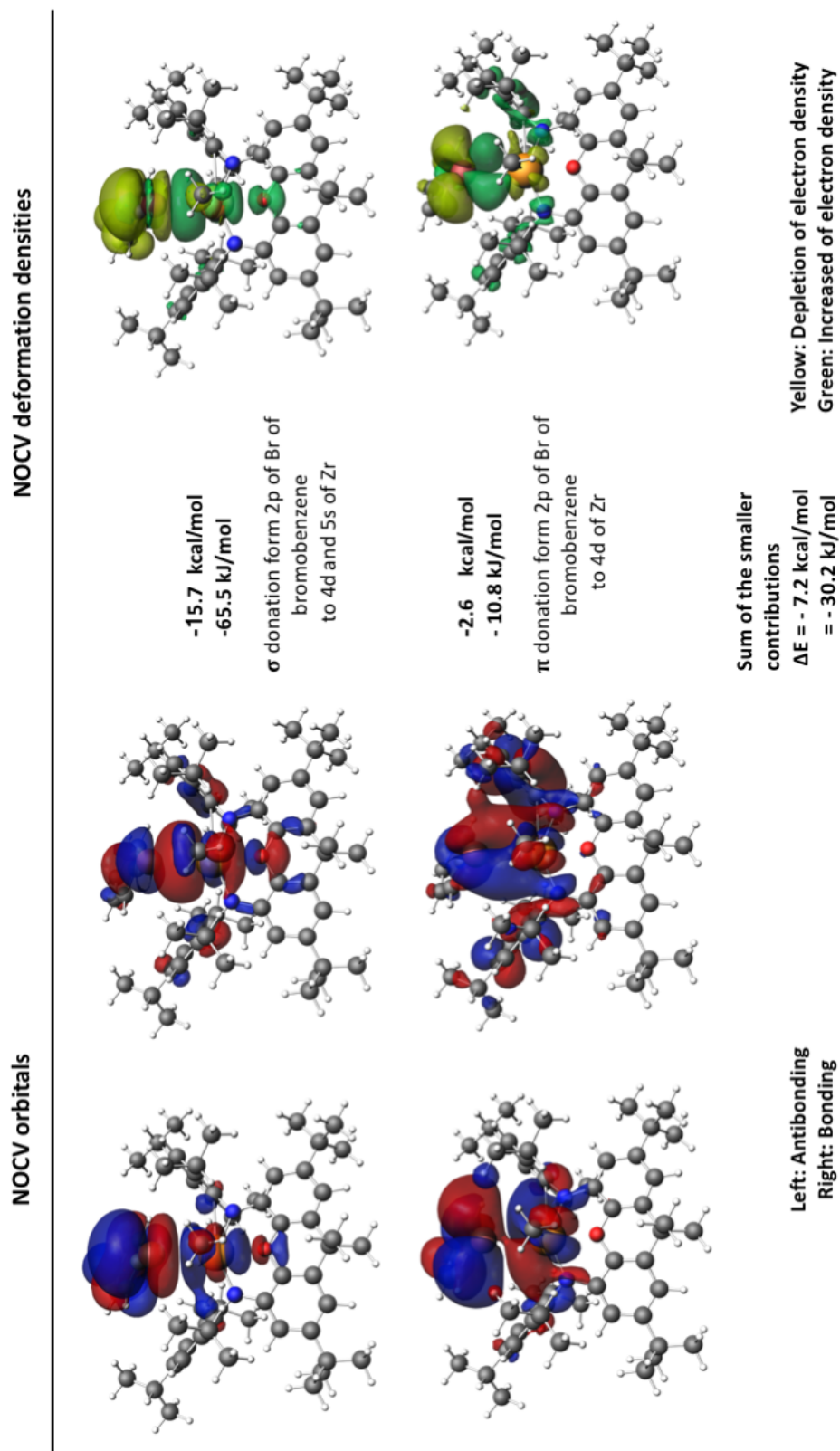
FIGURE C.8: On the left hand side: the NOCV Orbitals (with isosurfaces set to 0.01) and on the right hand side ETS-NOCV deformation density contributions, Increased (green) and decreased (yellow) electron density is presented relative to that in the isolated fragments (isosurfaces are set to 0.0001) for the molecule η^6-**4'-Zr-exo**.

NOCV deformation densities

-17.8 kcal/mol
-74.5 kJ/mol

σ donation form 2p of C of fluorobenzene to 4d and 5s of Zr

-2.3 kcal/mol
-9.6 kJ/mol

π donation form 2p of C of fluorobenzene to 4d and 5s of Zr

-2.0 kcal/mol
-8.4 kJ/mol

π donation form 2p of C of fluorobenzene to 4d and 5s of Zr

Sum of the smaller contributions

ΔE = -7.9 kcal/mol
= -33.1 kJ/mol

Yellow: Depletion of electron density
Green: Increased of electron density

NOCV orbitals

Left: Antibonding
Right: Bonding

FIGURE C.9: On the left hand side: the NOCV Orbitals (with isosurfaces set to 0.01) and on the right hand side ETS-NOCV deformation density contributions, Increased (green) and decreased (yellow) electron density is presented relative to that in the isolated fragments (isosurfaces are set to 0.0001) for the molecule η^6-**5'-Zr-exo**.

FIGURE C.10: On the left hand side: the NOCV Orbitals (with isosurfaces set to 0.01) and on the right hand side ETS-NOCV deformation density contributions, Increased (green) and decreased (yellow) electron density is presented relative to that in the isolated fragments (isosurfaces are set to 0.0001) for the molecule η^1-**5'-Zr-horizontal**.

Bibliography

[1] Bernd F. Straub. Organotransition Metal Chemistry. From Bonding to Catalysis. Edited by John?F. H Vol. 49. 42. WILEY-VCH Verlag, 2010, pp. 7622–7622. DOI: 10.1002/anie. 201004890.

[2] Ataf Ali Altaf et al. "Zirconium complexes in homogeneous ethylene polymerization". In: Journal of Coordination Chemistry 64.10 (2011), pp. 1815–1836. DOI: 10.1080/00958972.2011.568616.

[3] Andrew J. Peacock and Allison Calhoun. "Polymer Chemistry". In: Polymer Chemistry. Carl Hanser Verlag GmbH & Co. KG, 2006, pp. I–XIX. ISBN: 978-3-446-22283-0. DOI: doi:10.3139/9783446433434.fm.

[4] M Salvatores. "Physics and Safety of transmutation Systems". In: NEA Nuclear Science Report 6090 (2006).

[5] R. P. Feynman. Quantum Electrodynamics. New York: WA. Benjamin, 1961.

[6] Attila Szabo and Neil S. Ostlund. Modern Quantum Chemistry: Introduction to Advanced Electroni First. Mineola: Dover Publications, Inc., 1996.

[7] Lev Davidovich Landau and Evgenii Mikhailovich Lifshitz. Quantum Mechanics: Non-Relativistic T Vol. 3. Elsevier, 2013.

[8] W. Pauli. "Uber den Zusammenhang des Abschlusses der Elektronengruppen im Atom mit der Komplexstruktur der Spektren". In: Zeitschrift fur Physik 31.1 (1925), pp. 765–783. DOI: 10.1007/BF02980631.

[9] J. C. Slater. "A Simplification of the Hartree-Fock Method". In: Phys. Rev. 81 (3 1951), pp. 385–390. DOI: 10.1103/PhysRev.81.385.

[10] Frank Jensen. Introduction to Computational Chemistry. John Wiley & Sons, 2006. ISBN: 0470011874.

[11] Per-Olov L owdin. "Quantum Theory of Many-Particle Systems. III. Extension of the Hartree-Fock Scheme to Include Degenerate Systems and Correlation Effects". In: Phys. Rev. 97 (6 1955), pp. 1509–1520. DOI: 10.1103/PhysRev.97.1509.

[12] L. González, D. Escudero, and L. Serrano-Andrés. "Progress and Challenges in the Calculation of Electronic Excited States". In: ChemPhysChem 13 (2012), pp. 28–51. ISSN: 1439-7641. DOI: 10.1002/cphc.201100200.

[13] Chr. Møller and M. S. Plesset. "Note on an Approximation Treatment for Many-Electron Systems". In: Phys. Rev. 46 (7 1934), pp. 618–622. DOI: 10.1103/PhysRev.46.618.

[14] Bernard Levy and Gaston Berthier. "Generalized brillouin theorem for multi-configurational SCF theories". In: International Journal of Quantum Chemistry 2.2 (), pp. 307–319. DOI: 10.1002/qua.560020210.

[15] T Koopmans. "Über die Zuordnung von Wellenfunktionen und Eigenwerten zu den Einzelnen Elektronen Eines Atoms". In: Physica 1.1 (1934), pp. 104–113. DOI: https://doi.org/10.1016/S0031-8914(34)90011-2.

[16] R J Bartlett. "Many-Body Perturbation Theory and Coupled Cluster Theory for Electron Correlation in Molecules". In: Annual Review of Physical Chemistry 32.1 (1981), pp. 359–401. DOI: 10.1146/annurev.pc.32.100181.002043.

[17] A. Szabo and N. S. Ostlund. Modern Quantum Chemistry: Introduction to Advanced Electronic New York: McGraw-Hill, 1989.

[18] Jiří Čížek. In: The Journal of Chemical Physics 45.11 (1966), pp. 4256–4266. DOI: 10.1063/1.1727484.

[19] Čižek J. and Paldus J. In: International Journal of Quantum Chemistry 5.4 (), pp. 359–379. DOI: 10.1002/qua.560050402.

[20] "Coupled cluster theory for high spin, open shell reference wave functions". In: The Journal of Chemical Physics 99.7 (1993), pp. 5219–5227. DOI: 10.1063/1.465990.

[21] Peter J. Knowles, Claudia Hampel, and Hans-Joachim Werner. "Erratum: "Coupled cluster theory for high spin, open shell reference wave functions" [J. Chem. Phys. 99, 5219 (1993)]". In: The Journal of Chemical Physics 112.6 (2000), pp. 3106–3107. DOI: 10.1063/1.480886.

[22] R. J. Bartlett and M. Musiał. "Coupled-Cluster Theory In Quantum Chemistry". In: Reviews of Modern Physics 79 (2007), pp. 291–350.

[23] George D. Purvis and Rodney J. Bartlett. In: The Journal of Chemical Physics 76.4 (1982), pp. 1910–1918. DOI: 10.1063/1.443164.

[24] Watts John D. and Bartlett Rodney J. In: International Journal of Quantum Chemistry 48.27 (), pp. 51–66. DOI: 10.1002/qua.560480809.

[25] Krishnan Raghavachari et al. "A fifth-order perturbation comparison of electron correlation theories". In: Chemical Physics Letters 157.6 (1989), pp. 479–483. ISSN: 0009-2614. DOI: https://doi.org/10.1016/S0009-2614(89)87395-6.

[26] Miles J.O. Deegan and Peter J. Knowles. "Perturbative corrections to account for triple excitations in closed and open shell coupled cluster theories". In: Chemical Physics Letters 227.3 (1994), pp. 321–326. ISSN: 0009-2614. DOI: https://doi.org/10.1016/0009-2614(94)00815-9.

[27] Rodney J. Bartlett. "Coupled-cluster approach to molecular structure and spectra: a step toward predictive quantum chemistry". In: The Journal of Physical Chemistry 93.5 (1989), pp. 1697–1708. DOI: 10.1021/j100342a008.

[28] Peter M. W. Gill et al. In: The Journal of Chemical Physics 89.12 (1988), pp. 7307–7314. DOI: 10.1063/1.455312.

[29] Martin Rosenberg et al. "Excited State Aromaticity and Antiaromaticity: Opportunities for Photophysical and Photochemical Rationalizations". In: Chemical Reviews 114.10 (2014), pp. 5379–5425. DOI: 10.1021/cr300471v.

[30] Gustavo E. Scuseria. "The open-shell restricted Hartree—Fock singles and doubles coupled-cluster method including triple excitations CCSD (T): application to C+3". In: Chemical Physics Letters 176.1 (1991), pp. 27 –35. ISSN: 0009-2614. DOI: https://doi.org/10.1016/0009-2614(91)90005-T.

[31] Lee Timothy J. and Taylor Peter R. In: International Journal of Quantum Chemistry 36.S23 (), pp. 199–207. DOI: 10.1002/qua.560360824.

[32] Timothy J. Lee. "Comparison of the T1 and D1 diagnostics for electronic structure theory: a new definition for the open-shell D1 diagnostic". In: Chemical Physics Letters 372 (2003), pp. 362–367.

[33] Curtis L Janssen and Ida M B Nielsen. "New diagnostics for coupled-cluster and Møller-Plesset perturbation theory". In: Chem. Phys. Lett. 290 (1998), pp. 423–430.

[34] Timothy J Lee. "Comparison of the T1 and D1 diagnostics for electronic structure theory: a new definition for the open-shell D1 diagnostic". In: Chemical Physics Letters 372.3 (2003), pp. 362 –367. ISSN: 0009-2614. DOI: https://doi.org/10.1016/S0009-2614(03)00435-4.

[35] Matthew L. Leininger et al. "A new diagnostic for open-shell coupled-cluster theory". In: Chemical Physics Letters 328.4 (2000), pp. 431 –436. ISSN: 0009-2614. DOI: https://doi.org/10.1016/S0009-2614(00)00966-0.

[36] Wanyi Jiang, Nathan J. DeYonker, and Angela K. Wilson. "Multireference Character for 3d Transition-Metal-Containing Molecules". In: J. Chem. Theory Comput. 8 (2012), pp. 460–468.

[37] P. Tecmer et al. "Electronic spectroscopy of UO_2^{2+}, NUO^+ and NUN: An Evaluation of Time-Dependent Density Functional Theory for Actinides". In: Phys. Chem. Chem. Phys. 13 (2011), pp. 6249–6259.

[38] P. Hohenberg and W. Kohn. "Inhomogeneous Electron Gas". In: Phys. Rev. 136 (1964), B864–B871. DOI: 10.1103/PhysRev.136.B864.

[39] W. Kohn and L. J. Sham. In: Phys. Rev. 140 (1965), A1133–A1138.

[40] J. P. Perdew and Y. Wang. "Accurate and simple analytic representation of the electron-gas correlation energy". In: Phys. Rev. B 45 (1992), pp. 13244–13249. DOI: 10.1103/PhysRevB.45.13244.

[41]   S. H. Vosko, L. Wilk, and M. Nusair. "Accurate spin-dependent electron liq-
       uid correlation energies for local spin-density calculations - A critical analy-
       sis". In: Can. J. Phys. 58 (1980), pp. 1200–1211. DOI: 10.1139/p80-159.

[42]   J. P. Perdew et al. "Atoms, molecules, solids, and surfaces: Applications of
       the generalized gradient approximation for exchange and correlation". In:
       Phys. Rev. B 46 (1992), pp. 6671–6687. DOI: 10.1103/PhysRevB.46.6671.

[43]   J. P. Perdew, K. Burke, and M. Ernzerhof. "Generalized gradient approxima-
       tion made simple". In: Phys. Rev. Lett. 77 (1996), pp. 3865–3868.

[44]   P. J. Stephens et al. "Ab Initio Calculation of Vibrational Absorption and Cir-
       cular Dichroism Spectra Using Density Functional Force Fields". In: The Journal of Physical Che
       98.45 (1994), pp. 11623–11627. DOI: 10.1021/j100096a001.

[45]   Carlo Adamo and Vincenzo Barone. "Toward reliable density functional meth-
       ods without adjustable parameters: The PBE0 model". In: The Journal of Chemical Physics
       110.13 (1999), pp. 6158–6170. DOI: 10.1063/1.478522.

[46]   John P. Perdew, Matthias Ernzerhof, and Kieron Burke. "Rationale for mixing
       exact exchange with density functional approximations". In: The Journal of Chemical Physics
       105.22 (1996), pp. 9982–9985. DOI: 10.1063/1.472933.

[47]   Christos P. Constantinides, Panayiotis A. Koutentis, and Jürgen Schatz. "A
       DFT Study of the Ground State Multiplicities of Linear vs Angular Poly-
       heteroacenes". In: Journal of the American Chemical Society 126.49 (2004), pp. 16232–
       16241. DOI: 10.1021/ja045006t.

[48]   Marcel Swart et al. "Validation of Exchange-Correlation Functionals for Spin
       States of Iron Complexes". In: The Journal of Physical Chemistry A 108.25 (2004),
       pp. 5479–5483. DOI: 10.1021/jp049043i.

[49]   Stefan Grimme. "Semiempirical GGA-type density functional constructed with
       a long-range dispersion correction". In: Journal of Computational Chemistry
       27.15 (), pp. 1787–1799. DOI: 10.1002/jcc.20495.

[50]   Stefan Grimme et al. "A consistent and accurate ab initio parametrization of
       density functional dispersion correction (DFT-D) for the 94 elements H-Pu".
       In: The Journal of Chemical Physics 132.15 (2010), p. 154104. DOI: 10.1063/
       1.3382344.

[51]   Stefan Grimme. "Accurate description of van der Waals complexes by density
       functional theory including empirical corrections". In: Journal of Computational Chemistry
       25.12 (), pp. 1463–1473. DOI: 10.1002/jcc.20078.

[52]   Pekka Pyykkö. "Relativistic effects in structural chemistry". EN. In: Chem. Rev.
       88.3 (1988), pp. 563–594. ISSN: 0009-2665. DOI: 10.1021/cr00085a006.

[53]   Albert A Michelson and Edward W Morley. In: Am. J. Sci. 134 (1887), p. 33.

[54]   P. A. M. Dirac. "The quantum theory of the electron". In: Proc. R. Soc. London
       117 (1928), p. 610.

[55] "A theory of electrons and protons". In: Proceedings of the Royal Society of London A: Mathematica
126.801 (1930), pp. 360–365. ISSN: 0950-1207. DOI: 10.1098/rspa.1930.0013.
eprint: http://rspa.royalsocietypublishing.org/content/126/801/360.
full.pdf.

[56] "IV. The triplets of helium". In: Philosophical Transactions of the Royal Society of London A: Mathe
228.659-669 (1929), pp. 151–196. ISSN: 0264-3952. DOI: 10.1098/rsta.1929.
0004. eprint: http://rsta.royalsocietypublishing.org/content/228/
659-669/151.full.pdf.

[57] G. Breit. "The Effect of Retardation on the Interaction of Two Electrons". In:
Phys. Rev. 34 (4 1929), pp. 553–573. DOI: 10.1103/PhysRev.34.553.

[58] H. B. G. Casimir and D. Polder. "The Influence of Retardation on the London-
van der Waals Forces". In: Phys. Rev. 73 (4 1948), pp. 360–372. DOI: 10.1103/
PhysRev.73.360.

[59] Kenneth G Dyall and Knut Faegri Jr. Introduction to relativistic quantum chemistry.
Oxford University Press, 2007.

[60] Markus Reiher and Alexander Wolf. Relativistic quantum chemistry: the fundamental theory of mo
John Wiley Sons, 2014.

[61] Christoph van Wüllen. "Molecular density functional calculations in the reg-
ular relativistic approximation: Method, application to coinage metal diatomics,
hydrides, fluorides and chlorides, and comparison with first-order relativis-
tic calculations". In: The Journal of Chemical Physics 109.2 (1998), pp. 392–
399. DOI: 10.1063/1.476576.

[62] Alexander Wolf, Markus Reiher, and Bernd Artur Hess. "The generalized
Douglas–Kroll transformation". In: The Journal of Chemical Physics 117.20
(2002), pp. 9215–9226. DOI: 10.1063/1.1515314.

[63] Markus Reiher and Alexander Wolf. "Exact decoupling of the Dirac Hamilto-
nian. II. The generalized Douglas–Kroll–Hess transformation up to arbitrary
order". In: The Journal of Chemical Physics 121.22 (2004), pp. 10945–10956.
DOI: 10.1063/1.1818681.

[64] L. L. Foldy and S. A. Wouthuysen. "On the Dirac Theory of Spin 1/2 Particles
and Its Non-Relativistic Limit". In: Physical Review 78 (1950), p. 29.

[65] Bernd Artur Hess et al. "A mean-field spin-orbit method applicable to corre-
lated wavefunctions". In: Chem. Phys. Lett. 251 (1996), pp. 365–371.

[66] M Krauss and W J Stevens. "Effective potentials in molecular quantum chem-
istry". In: Annual Review of Physical Chemistry 35.1 (1984), pp. 357–385.

[67] M. Dolg and X. Cao. "Relativistic Pseudopotentials: Their Development And
Scope Of Applications". In: Chem. Rev. 112 (2012), pp. 403–480.

[68] Helmut Eschrig. Optimized LCAO Method and Electronic Structure of Extended Systems, Berlin.
Jan. 1989.

[69]   J. C. Slater. "Atomic Shielding Constants". In: Phys. Rev. 36 (1 1930), pp. 57–
       64. DOI: 10.1103/PhysRev.36.57.

[70]   "Electronic wave functions - I. A general method of calculation for the sta-
       tionary states of any molecular system". In: Proceedings of the Royal Society of London A: Mat
       200.1063 (1950), pp. 542–554. DOI: 10.1098/rspa.1950.0036.

[71]   T. H. Dunning Jr. "Gaussian basis sets for use in correlated molecular calcu-
       lations. I. The atoms boron through neon and hydrogen". In: J. Chem. Phys.
       90 (1989), pp. 1007–1023. DOI: 10.1063/1.456153.

[72]   J. M. L. Martin and A. Sundermann. "Correlation consistent valence basis sets
       for use with the Stuttgart-Dresden-Bonn relativistic effective core potentials:
       The atoms Ga-Kr and In-Xe". In: J. Chem. Phys. 114 (2001), pp. 3408–3420.
       DOI: 10.1063/1.1337864.

[73]   Florian Weigend and Reinhart Ahlrichs. "Balanced basis sets of split valence,
       triple zeta valence and quadruple zeta valence quality for H to Rn: Design
       and assessment of accuracy". In: Phys. Chem. Chem. Phys. 7 (18 2005), pp. 3297–
       3305. DOI: 10.1039/B508541A.

[74]   Florian Weigend. "Accurate Coulomb-fitting basis sets for H to Rn". In: Phys. Chem. Chem. Phy
       8 (9 2006), pp. 1057–1065. DOI: 10.1039/B515623H.

[75]   Per-Olof Widmark, B. Joakim Persson, and Björn O. Roos. "Density matrix
       averaged atomic natural orbital (ANO) basis sets for correlated molecular
       wave functions". In: Theoretica chimica acta 79.6 (1991), pp. 419–432. ISSN:
       1432-2234. DOI: 10.1007/BF01112569.

[76]   Jan Almlöf and Peter R Taylor. "Atomic natural orbital (ANO) basis sets
       for quantum chemical calculations". In: Advances in Quantum Chemistry 22
       (1991), pp. 301–373. DOI: 10.1016/S0065-3276(08)60366-4.

[77]   B. O. Roos et al. "Main group atoms and dimers studied with a new rela-
       tivistic ANO basis set". In: J. Phys. Chem. A 108 (2004), pp. 2851–2858. DOI:
       10.1021/jp031064+.

[78]   B. O. Roos et al. "New relativistic ANO basis sets for actinide atoms". In:
       Chem. Phys. Lett. 409 (2005), pp. 295–299. DOI: 10.1016/j.cplett.2005.05.
       011.

[79]   M. Gutowski et al. "The basis set superposition error in correlated electronic
       structure calculations". In: Chemical Physics Letters 124.4 (1986), pp. 370 –
       375. ISSN: 0009-2614. DOI: https://doi.org/10.1016/0009-2614(86)85036-
       9.

[80]   T. Helgaker, P. Jørgensen, and J. Olsen. Molecular Electronic-Structure Theory.
       New York: Wiley, 2000.

[81] David H. Bross and Kirk A. Peterson. "Theoretical spectroscopy study of the low-lying electronic states of UX and UX+, X = F and Cl". In: The Journal of Chemical Physics 143.18 (2015), p. 184313. DOI: 10.1063/1.4935492.

[82] Hans H. Brintzinger et al. "Stereospecific Olefin Polymerization with Chiral Metallocene Catalysts". In: Angewandte Chemie International Edition in English 34.11 (), pp. 1143–1170. DOI: 10.1002/anie.199511431.

[83] Raymond J. Butcher et al. In: Organometallics 15.5 (1996), pp. 1488–1496. DOI: 10.1021/om9508694.

[84] Li Jia et al. "Cationic d0/f0 metallocene catalysts. properties of binuclear organoborane Lewis acid cocatalysts and weakly coordinating counteranions derived therefrom". In: Organometallics 13.10 (1994), pp. 3755–3757. DOI: 10.1021/om00022a003.

[85] Xinmin. Yang, Charlotte. Stern, and Tobin J. Marks. "Models for organometallic molecule-support complexes. Very large counterion modulation of cationic actinide alkyl reactivity". In: Organometallics 10.4 (1991), pp. 840–842. DOI: 10.1021/om00050a008.

[86] Zerong Lin et al. "Models for organometallic molecule-support complexes. Synthesis and properties of cationic organoactinides". In: Journal of the American Chemical Society 109.13 (1987), pp. 4127–4129. DOI: 10.1021/ja00247a056.

[87] Ming Yuan He et al. "Supported organoactinides. Surface chemistry and catalytic properties of alumina-bound cyclopentadienyl and pentamethylcyclopentadienyl thorium and uranium hydrocarbyls and hydrides". In: Journal of the American Chemical Society 107.3 (1985), pp. 641–652. DOI: 10.1021/ja00289a016.

[88] Paul J. Toscano and Tobin J. Marks. "Supported organoactinides. High-resolution solid-state carbon-13 NMR studies of catalytically active, alumina-bound pentamethylcyclopentadienyl)thorium methyl and hydride complexes". In: Journal of the American Chemical Society 107.3 (1985), pp. 653–659. DOI: 10.1021/ja00289a017.

[89] William C. Finch et al. "Organometallic molecule-inorganic surface coordination and catalytic chemistry. In situ CPMAS NMR delineation of organoactinide adsorbate structure, dynamics, and reactivity". In: Journal of the American Chemical Society 112.17 (1990), pp. 6221–6232. DOI: 10.1021/ja00173a009.

[90] David. Hedden and Tobin J. Marks. "[(CH3)5C5]2Th(CH3)2 surface chemistry and catalysis. Direct NMR spectroscopic observation of surface alkylation and ethylene insertion/polymerization on MgCl2". In: Journal of the American Chemical Society 110.5 (1988), pp. 1647–1649. DOI: 10.1021/ja00213a061.

[91] Tobin J. Marks. "Surface-bound metal hydrocarbyls. Organometallic connections between heterogeneous and homogeneous catalysis". In: Accounts of Chemical Research 25.2 (1992), pp. 57–65. DOI: 10.1021/ar00014a001.

[92] Li Jia et al. "Cationic Metallocene Polymerization Catalysts Based on Tetrakis(pentafluoropheny and Its Derivatives. Probing the Limits of Anion "Noncoordination" via a Synthetic, Solution Dynamic, Structural, and Catalytic Olefin Polymerization Study". In: Organometallics 16.5 (1997), pp. 842–857. DOI: 10.1021/om960880j.

[93] Jayachandran Jayakumar et al. "One-Pot Synthesis of Highly Substituted Poly-heteroaromatic Compounds by Rhodium(III)-Catalyzed Multiple C-H Activation and Annulation". In: Angewandte Chemie International Edition 53.37 (), pp. 9889–9892. DOI: 10.1002/anie.201405183.

[94] Dennis B Malpass. Introduction to industrial polyethylene: properties, catalysts, and processes Vol. 45. John Wiley & Sons, 2010.

[95] Paul G. Hayes, Warren E. Piers, and Masood Parvez. In: Journal of the American Chemical Socie 125.19 (2003). PMID: 12733887, pp. 5622–5623. DOI: 10.1021/ja034680s.

[96] Paul G. Hayes, Warren E. Piers, and Masood Parvez. "Arene Complexes of Diketiminato Supported Organoscandium Cations: Mechanism of Arene Exchange and Alkyne Insertion in Solvent Separated Ion Pairs". In: Chemistry – A European Journ 13.9 (2007), pp. 2632–2640. DOI: 10.1002/chem.200601087.

[97] Renato P. Orenha et al. "Nature of the Ru–àíNO Coordination Bond: Kohn–Sham Molecular Orbital and Energy Decomposition Analysis". In: ChemistryOpen 6.3 (), pp. 410–416. DOI: 10.1002/open.201700028.

[98] R. D. Shannon. "Revised effective ionic radii and systematic studies of inter-atomic distances in halides and chalcogenides". In: Acta Crystallographica Section A 32.5 (1976), pp. 751–767. DOI: 10.1107/S0567739476001551.

[99] Carlos A. Cruz et al. "Extremely Stable Thorium(IV) Dialkyl Complexes Supported by Rigid Tridentate 4,5-Bis(anilido)xanthene and 2,6-Bis(anilidomethyl)pyridine Ligands". In: Organometallics 26.3 (2007), pp. 692–701. DOI: 10.1021/om060914f.

[100] Carlos A. Cruz et al. In: Organometallics 28.6 (2009), pp. 1891–1899. DOI: 10.1021/om800624t.

[101] Carlos A. Cruz et al. "Single and Double Alkyl Abstraction from a Bis(anilido)xanthene Thorium(IV) Dibenzyl Complex: Isolation of an Organothorium Cation and a Thorium Dication". In: Organometallics 27.1 (2008), pp. 15–17. DOI: 10.1021/om7011503.

[102] Cassandra E. Hayes and Daniel B. Leznoff. "Diamido-Ether Uranium(IV) Alkyl Complexes as Single-Component Ethylene Polymerization Catalysts". In: Organometallics 29.4 (2010), pp. 767–774. DOI: 10.1021/om900546p.

[103] Paul J. Fagan et al. "Synthesis and properties of bis(pentamethylcyclopentadienyl) actinide hydrocarbyls and hydrides. A new class of highly reactive f-element organometallic compounds". In: Journal of the American Chemical Society 103.22 (1981), pp. 6650–6667. DOI: 10.1021/ja00412a021.

[104]   Tobin J. Marks and William A. Wachter. "Tris(.eta.5-cyclopentadienyl)alkyl and -alkenyl compounds of thorium(IV)". In: Journal of the American Chemical Society 98.3 (1976), pp. 703–710. DOI: 10.1021/ja00419a011.

[105]   Andrew Streitwieser and Norio Yoshida. "Di-.pi.-cyclooctatetraenethorium". In: Journal of the American Chemical Society 91.26 (1969), pp. 7528–7528. DOI: 10.1021/ja01054a061.

[106]   Andrew Streitwieser and Ulrich Mueller-Westerhoff. "Bis(cyclooctatetraenyl)uranium (uranocene). A new class of sandwich complexes that utilize atomic f orbitals". In: Journal of the American Chemical Society 90.26 (1968), pp. 7364–7364. DOI: 10.1021/ja01028a044.

[107]   F.T. Edelmann and W.A. Herrmann. Synthetic Methods of Organometallic and Inorganic Chemistry. Thieme, 2014. ISBN: 9783131792211.

[108]   Nicholas R. Andreychuk. "NON-DONOR LIGANDS IN ORGANOACTINIDE CHEMISTRY". PhD thesis. McMaster Univerity, 2017.

[109]   Kelly S. A. Motolko et al. "Zirconium Complexes of a Rigid, Dianionic Pincer Ligand: Alkyl Cations, Arene Coordination, and Ethylene Polymerization". In: Organometallics 36.16 (2017), pp. 3084–3093. DOI: 10.1021/acs.organomet.7b00424.

[110]   Benedict M. Gardner et al. "The role of 5f-orbital participation in unexpected inversion of the [sigma]-bond metathesis reactivity trend of triamidoamine thorium(iv) and uranium(iv) alkyls". In: Chem. Sci. 5 (6 2014), pp. 2489–2497. DOI: 10.1039/C4SC00182F.

[111]   Elena Domeshek et al. "Organoactinides in the polymerization of ethylene: is TIBA a better cocatalyst than MAO?" In: Dalton Trans. 42 (25 2013), pp. 9069–9078. DOI: 10.1039/C3DT00032J. URL: http://dx.doi.org/10.1039/C3DT00032J.

[112]   Tobin J. Marks and Victor W. Day. "Actinide Hydrocarbyl and Hydride Chemistry". In: Fundamental and Technological Aspects of Organo-f-Element Chemistry. Ed. by Tobin J. Marks and Ignazio L. Fragalà. Dordrecht: Springer Netherlands, 1985, pp. 115–157. ISBN: 978-94-009-5406-9. DOI: 10.1007/978-94-009-5406-9_4.

[113]   Axel D. Becke. In: The Journal of Chemical Physics 98.7 (1993), pp. 5648–5652. DOI: 10.1063/1.464913.

[114]   John P. Perdew, Kieron Burke, and Matthias Ernzerhof. "Generalized Gradient Approximation Made Simple". In: Phys. Rev. Lett. 77 (18 1996), pp. 3865–3868. DOI: 10.1103/PhysRevLett.77.3865.

[115]   Xiaoyan Cao, Michael Dolg, and Hermann Stoll. "Valence basis sets for relativistic energy-consistent small-core actinide pseudopotentials". In: The Journal of Chemical Physics 118.2 (2003), pp. 487–496. DOI: 10.1063/1.1521431.

[116] Xiaoyan Cao and Michael Dolg. "Segmented contraction scheme for small-core actinide pseudopotential basis sets". In: Journal of Molecular Structure: THEOCHEM 673.1 (2004), pp. 203 –209. ISSN: 0166-1280. DOI: https://doi.org/10.1016/j.theochem.2003.12.015.

[117] Paula L. Diaconescu et al. In: Journal of the American Chemical Society 122.25 (2000), pp. 6108–6109. DOI: 10.1021/ja994484e.

[118] "Applications of the ETS-NOCV method in descriptions of chemical reactions". In: Journal of Molecular Modeling 17.9 (2011), p. 2337. ISSN: 0948-5023. DOI: 10.1007/s00894-011-1023-6.

[119] Mariusz P. Mitoraj, Artur Michalak, and Tom Ziegler. "On the Nature of the Agostic Bond between Metal Centers and Hydrogen Atoms in Alkyl Complexes. An Analysis Based on the Extended Transition State Method and the Natural Orbitals for Chemical Valence Scheme (ETS-NOCV)". In: Organometallics 28.13 (2009), pp. 3727–3733. DOI: 10.1021/om900203m.

[120] Sung-Kwan Kim et al. In: Journal of the American Chemical Society 132.29 (2010). PMID: 20597488, pp. 9954–9955. DOI: 10.1021/ja101685u.

[121] E. Broclawik et al. "Formaldehyde activation by Cu(I) and Ag(I) sites in ZSM-5: ETS-NOCV analysis of charge transfer processes". In: Catalysis Today 169.1 (2011), pp. 45 –51. ISSN: 0920-5861. DOI: https://doi.org/10.1016/j.cattod.2010.08.020.

[122] Sylvester Ndambuki and Tom Ziegler. In: Inorganic Chemistry 51.14 (2012). PMID: 22731692, pp. 7794–7800. DOI: 10.1021/ic300824u.

[123] Mariusz P. Mitoraj and Artur Michalak. "On the asymmetry in molybdenum–oxygen bonding in the MoO3 structure: ETS–NOCV analysis". In: Structural Chemistry 23.5 (2012), pp. 1369–1375. ISSN: 1572-9001. DOI: 10.1007/s11224-012-0056-5.

[124] Holger Braunschweig et al. "Bond-strengthening backdonation in a transition-metal diborene complex". In: Nature Chemistry 5 (Dec. 2012), 115 EP –.

[125] Paul G. Hayes et al. "The Osmium–Silicon Triple Bond: Synthesis, Characterization, and Reactivity of an Osmium Silylyne Complex". In: Journal of the American Chemical S 135.32 (2013), pp. 11780–11783. DOI: 10.1021/ja406799y.

[126] Ignacy Cukrowski, Jurgens H. de Lange, and Mariusz Mitoraj. In: The Journal of Physical Chem 118.3 (2014), pp. 623–637. DOI: 10.1021/jp410744x.

[127] Estefania Fernandez Villanueva, Otilia Mo, and Manuel Yanez. "On the existence and characteristics of [small pi]-beryllium bonds". In: Phys. Chem. Chem. Phys. 16 (33 2014), pp. 17531–17536. DOI: 10.1039/C4CP01992J.

[128] Wan-Lu Li et al. "Electronic Structure and Bonding Situation in M2O2 (M = Be, Mg, Ca) Rhombic Clusters". In: The Journal of Physical Chemistry A 122.10 (2018), pp. 2816–2822. DOI: 10.1021/acs.jpca.8b01335.

[129] Ndambuki Sylvester and Ziegler Tom. "An analysis of unsupported triple and quadruple metal–metal bonds between two homonuclear group 6 transition elements based on the combined natural orbitals for chemical valence and extended transition state method". In: International Journal of Quantum Chemistry 113.6 (), pp. 753–761. DOI: 10.1002/qua.24068.

[130] TURBOMOLE V5.10 2008, a development of University of Karlsruhe and Forschungszentrum Karls

[131] K. Eichkorn et al. "Auxiliary basis sets for main row atoms and transition metals and their use to approximate Coulomb potentials". In: Theoretical Chemistry Accounts 97 (1997), p. 119.

[132] Martin ulka, L. Cantrel, and V. Vallet. "Theoretical Study of Plutonium(IV) Complexes Formed within the PUREX Process: A Proposal of a Plutonium Surrogate in Fire Conditions". In: J. Phys. Chem. A 118 (2014), pp. 10073–10080.

[133] Tom Ziegler and Arvi Rauk. "On the calculation of bonding energies by the Hartree Fock Slater method". In: Theoretica chimica acta 46.1 (1977), pp. 1–10. DOI: 10.1007/BF02401406.

[134] RF Nalewajski, AM Köster, and K Jug. "Chemical valence from the two-particle density matrix". In: Theoretica chimica acta 85.6 (1993), pp. 463–484.

[135] Roman F. Nalewajski and Janusz Mrozek. "Modified valence indices from the two-particle density matrix". In: International Journal of Quantum Chemistry 51.4 (1994), pp. 187–200. DOI: 10.1002/qua.560510403.

[136] Slawomir M. Cybulski and Marion L. Lytle. "The origin of deficiency of the supermolecule second-order Møller-Plesset approach for evaluating interaction energies". In: The Journal of Chemical Physics 127.14 (2007), p. 141102. DOI: 10.1063/1.2795693.

[137] C. David Sherrill, Tait Takatani, and Edward G. Hohenstein. "An Assessment of Theoretical Methods for Nonbonded Interactions: Comparison to Complete Basis Set Limit Coupled-Cluster Potential Energy Curves for the Benzene Dimer, the Methane Dimer, Benzene-àíMethane, and Benzene-àíH2S". In: The Journal of Physical Chemistry A 113.38 (2009), pp. 10146–10159. DOI: 10.1021/jp9034375.

[138] P. Gotcu-Freis et al. "Mass spectrometric studies of the vapour phase in the (Pu+O) system". In: The Journal of Chemical Thermodynamics 43.8 (2011), pp. 1164 –1173. ISSN: 0021-9614. DOI: https://doi.org/10.1016/j.jct.2011.02.024.

[139] V.P. Glushko et al. Thermodynamic Properties of Individual Substances. Ed. by V.P. Glushko (Ed.) Vol. 1-4. Nauka, Moscow, 1978-1982.

[140] E. H. P. Cordfunke and R. J. M. Konings. "Thermochemical data for reactor materials and fission products: The ECN database". In: Journal of Phase Equilibria 14.4 (1993), pp. 457–464. ISSN: 1054-9714. DOI: 10.1007/BF02671964.

[141] Rudy J. M. Konings et al. "The Thermodynamic Properties of the f-Elements and their Compounds. Part 2. The Lanthanide and Actinide Oxides". In: Journal of Physical and Chemical Reference Data 43.1 (2014), p. 013101. DOI: 10.1063/1.4825256.

[142] R. J. Ackermann, R. L. Faircloth, and M. H. Rand. "A Thermodynamic Study of the Vaporization Behavior of the Substoichiometric Plutonium Dioxide Phase1". In: The Journal of Physical Chemistry 70.11 (1966), pp. 3698–3706. DOI: 10.1021/j100883a055.

[143] PARDUE WILLIAM M. and KELLER DONALD L. "Volatility of PuO2 in Nonreducing Atmospheres". In: Journal of the American Ceramic Society 47.12 (), pp. 610–614. DOI: 10.1111/j.1151-2916.1964.tb13116.x.

[144] D. R. Messier. "Evaporation of Hypostoichiometric Plutonium Dioxide from 2070° to 2380°K". In: Journal of the American Ceramic Society 51.12 (), pp. 710–713. DOI: 10.1111/j.1151-2916.1968.tb15933.x.

[145] C Ronchi et al. "Volatile molecule PuO3 observed from subliming plutonium dioxide". In: J. Nucl. Mat. 280.1 (2000), pp. 111–115. ISSN: 0022-3115. DOI: 10.1016/S0022-3115(00)00058-1.

[146] Oscar H. Krikorian et al. "Transpiration studies on the volatilities of PuO3(g) and PuO2(OH)2(g) from PuO2(s) in the presence of steam and oxygen and application to plutonium volatility in mixed-waste thermal oxidation processors". In: Journal of Nuclear Materials 247 (1997). Thermodynamics of Nuclear Materials, pp. 161 –171. ISSN: 0022-3115. DOI: https://doi.org/10.1016/S0022-3115(97)00043-3.

[147] Katharina Boguslawski et al. "On the multi-reference nature of plutonium oxides: PuO22+, PuO2, PuO3 and PuO2(OH)2". In: Phys. Chem. Chem. Phys. 19 (6 2017), pp. 4317–4329. DOI: 10.1039/C6CP05429C.

[148] Attila Kovács. "Relativistic Multireference Quantum Chemical Study of the Electronic Structure of Actinide Trioxide Molecules". In: J. Phys. Chem. A, 121.12 (2017), pp. 2523–2530. DOI: 10.1021/acs.jpca.7b01344.

[149] Meng Sheng Liao, Tapas Kar, and Steve Scheiner. In: The Journal of Physical Chemistry A 108.15 (2004), pp. 3056–3063. DOI: 10.1021/jp036927d.

[150] E. F. Archibong and A. K. Ray. "An ab initio study of PuO$_2$ and of PuN$_2$". In: J. Mol. Struct. (THEOCHEM) 530 (2000), pp. 165–170. DOI: 10.1016/S0166-1280(00)00332-8.

[151] G. La Macchia et al. "A theoretical study of the ground state and lowest excited states of $PuO^{0/+/+2}$ and $PuO_2^{0/+/+2}$". In: Phys. Chem. Chem. Phys. 48 (2008), pp. 7278–7283.

[152] Lyudmila V. Moskaleva et al. "The heat of formation of gaseous PuO22+ from relativistic density functional calculations". In: Phys. Chem. Chem. Phys. 8 (32 2006), pp. 3767–3773. DOI: 10.1039/B607292E.

[153] Arie Landau et al. "Intermediate Hamiltonian Fock-space coupled-cluster method: Excitation energies of barium and radium". In: The Journal of Chemical Physics 113.22 (2000), pp. 9905–9910. DOI: 10.1063/1.1323258.

[154] Lucas Visscher, Ephraim Eliav, and Uzi Kaldor. "Formulation and implementation of the relativistic Fock-space coupled cluster method for molecules". In: The Journal of Chemical Physics 115.21 (2001), pp. 9720–9726. DOI: 10.1063/1.1415746.

[155] Arie Landau et al. "Intermediate Hamiltonian Fock-space coupled cluster method in the one-hole one-particle sector: Excitation energies of xenon and radon". In: The Journal of Chemical Physics 115.15 (2001), pp. 6862–6865. DOI: 10.1063/1.1405005.

[156] H.-J. Werner et al. MOLPRO, Version 2015.1, A Package Of Ab Initio Programs. 2015.

[157] Veryazov Valera, Malmqvist Per Åke, and Roos Björn O. "How to select active space for multiconfigurational quantum chemistry?" In: International Journal of Quantum Chemistry 111.13 (), pp. 3329–3338. DOI: 10.1002/qua.23068.

[158] Kerstin. Andersson et al. "Second-order perturbation theory with a CASSCF reference function". In: The Journal of Physical Chemistry 94.14 (1990), pp. 5483–5488. DOI: 10.1021/j100377a012.

[159] N. Forsberg and P.-Å. Malmqvist. "Multiconfiguration perturbation theory with imaginary level shift". In: Chem. Phys. Lett. 274 (1997), p. 196.

[160] J. Patrick Zobel, Juan J. Nogueira, and Leticia González. "The IPEA dilemma in CASPT2". In: Chem. Sci. 8 (2 2017), pp. 1482–1499. DOI: 10.1039/C6SC03759C.

[161] C. Angeli et al. "Introduction Of N-Electron Valence States For Multireference Perturbation Theory". In: J. Chem. Phys. 114 (2001), pp. 10252–10264.

[162] Kenneth G. Dyall. In: The Journal of Chemical Physics 102.12 (1995), pp. 4909–4918. DOI: 10.1063/1.469539.

[163] Per Åke Malmqvist, Björn O. Roos, and Bernd Schimmelpfennig. "The restricted active space (RAS) state interaction approach with spin–orbit coupling". In: Chemical Physics Letters 357.3 (2002), pp. 230 –240. ISSN: 0009-2614. DOI: https://doi.org/10.1016/S0009-2614(02)00498-0.

[164] Branko Ruscic et al. In: The Journal of Physical Chemistry A 110.21 (2006), pp. 6592–6601. DOI: 10.1021/jp056311j.

[165] J D Cox, Donald D Wagman, and V A Medvedev. CODATA key values for thermodynamics. New York: Hemisphere Pub. Corp., 1989.

[166] R.J. Lemire, NEA Data Bank, and OECD Nuclear Energy Agency. Chemical Thermodynamics o Chemical thermodynamics. Elsevier, 2001. ISBN: 9780444503794.

[167] National Institute of Standards and Technology data base, http://www.nist.gov/chemistry (accessed on March 13, 2014).

[168] A. D. Becke. "Density-functional thermochemistry. III. The role of exact exchange". In: J. Chem. Phys. 98 (1993), pp. 5648–5653.

[169] P. J. Stephens et al. "Ab Initio Calculation of Vibrational Absorption and Circular Dichroism Spectra Using Density Functional Force Fields". In: J. Chem. Phys. 98 (1994), pp. 11623–11627.

[170] M. J. Frisch et al. Gaussian 09, Revision C.02. Gaussian, Inc., Wallingford, CT, 2004.

[171] Xiaoyan Cao, Michael Dolg, and Hermann Stoll. "Valence basis sets for relativistic energy-consistent small-core actinide pseudopotentials". In: J. Chem. Phys. 118.2 (2003), pp. 487–496.

[172] B. O. Roos et al. "Main group atoms and dimers studied with a new relativistic ANO basis set". In: J. Phys. Chem. A 108 (2004), pp. 2851–2858. DOI: 10.1021/jp031064+.

[173] Björn O. Roos et al. "New Relativistic ANO Basis Sets for Actinide Atoms". In: Chem. Phys. Lett. 409 (2005), pp. 295–299.

[174] E. F. Archibong and A. K. Ray. "An ab initio study of PuO_2 and of PuN_2". In: J. Mol. Struct. (THEOCHEM) 530 (2000), pp. 165–170. DOI: 10.1016/S0166-1280(00)00332-8.

[175] "The molecular mean-field approach for correlated relativistic calculations." In: J. Chem. Phys. 131.12 (Sept. 2009), p. 124116. ISSN: 1089-7690. DOI: 10.1063/1.3239505.

[176] L. Visscher, T. J. Lee, and K. G. Dyall. "Formulation and implementation of a relativistic unrestricted coupled-cluster method including noniterative connected triples". In: J. Chem. Phys. 105.19 (1996), pp. 8769–8776. DOI: 10.1063/1.472655.

[177] L. Visscher, E. Eliav, and U. Kaldor. "Formulation and implementation of the relativistic Fock-space coupled cluster method for molecules". In: J. Chem. Phys. 115 (2001), pp. 9720–9726. DOI: 10.1063/1.1415746.

[178] DIRAC, a relativistic ab initio electronic structure program, Release DIRAC16 (2016), written by H. J. Aa. Jensen, R. Bast, T. Saue, and L. Visscher, with contributions from V. Bakken, K. G. Dyall, S. Dubillard, U. Ekström, E. Eliav,

T. Enevoldsen, E. Faßhauer, T. Fleig, O. Fossgaard, A. S. P. Gomes, T. Helgaker, J. Henriksson, M. Iliaš, Ch. R. Jacob, S. Knecht, S. Komorovský, O. Kullie, J. K. Lærdahl, C. V. Larsen, Y. S. Lee, H. S. Nataraj, M. K. Nayak, P. Norman, G. Olejniczak, J. Olsen, Y. C. Park, J. K. Pedersen, M. Pernpointner, R. di Remigio, K. Ruud, P. Sałek, B. Schimmelpfennig, J. Sikkema, A. J. Thorvaldsen, J. Thyssen, J. van Stralen, S. Villaume, O. Visser, T. Winther, and S. Yamamoto (see http://www.diracprogram.org).

[179] K. G. Dyall. "Relativistic double-zeta, triple-zeta, and quadruple-zeta basis sets for the $7p$ elements, with atomic and molecular applications". In: Theor. Chem. Acc. 131 (2012), pp. 1172–4. DOI: 10.1007/s00214-012-1172-4.

[180] K. G. Dyall. "Relativistic double-zeta, triple-zeta, and quadruple-zeta basis sets for the actinides Ac Lr". In: Theor. Chem. Acc. 117 (2007), pp. 491–500. DOI: 10.1007/s00214-006-0175-4.

[181] R. A. Kendall, T. H. Dunning Jr., and R. J. Harrison. "Electron affinities of the first-row atoms revisited. Systematic basis sets and wave functions". In: J. Chem. Phys. 96 (1992), pp. 6796–6806. DOI: 10.1063/1.462569.

[182] L. Visscher. "Approximate molecular relativistic Dirac-Coulomb calculations using a simple Coulombic correction". In: Theor. Chem. Acc. 98 (1997), pp. 68–70. DOI: 10.1007/s002140050280.

[183] J. D. Watts, J. Gauss, and R. J. Bartlett. "Coupled-cluster methods with noniterative triple excitations for restricted open-shell Hartree-Fock and other general single determinant reference functions. Energies and analytical gradients". In: J. Chem. Phys. 98 (1993), pp. 8718–8733.

[184] David H. Bross and Kirk A. Peterson. "Composite thermochemistry of gas phase U(VI)-containing molecules". In: J. Chem. Phys. 141.24 (2014), p. 244308. DOI: http://dx.doi.org/10.1063/1.4904721.

[185] A Shee et al. "Equation-of-Motion Coupled -Cluster Theory based on the 4-component Dirac–Coulomb(–Gaunt) Hamiltonian. Energies for single electron detachment, attachment and electronically excited states". In: The Journal of Chemical Physics (2018).

[186] Aquilante Francesco et al. "Molcas 8: New capabilities for multiconfigurational quantum chemical calculations across the periodic table". In: J. Comput. Chem. 37.5 (), pp. 506–541. DOI: 10.1002/jcc.24221.

[187] R. G. Denning and I. D. Morrison. "The electronic structure of actinyl ions: the excited-state absorption spectrum of $Cs_2UO_2Cl_4$". In: Chem. Phys. Lett. 180 (1991), p. 101.

[188] L. Bovey and S. Gerstenkorn. "Ground State of the First Spectrum of Plutonium (Pu i), from an Analysis of Its Atomic Spectrum". In: J. Opt. Soc. Am. 51.5 (1961), pp. 522–525. DOI: 10.1364/JOSA.51.000522.

[189] J. Blaise et al. In: C.R. Acad. Sci., Fr. 255 (1962), pp. 2403–2405.

[190] J. Blaise et al. In: Physica Scripta 22 (1980), pp. 224–230.

[191] Attila Kovács. "Relativistic Multireference Quantum Chemical Study of the Electronic Structure of Actinide Trioxide Molecules". In: J. Phys. Chem. A 121 (2017), pp. 2523–2530. ISSN: 1520-5215. DOI: 10.1021/acs.jpca.7b01344.

[192] G. La Macchia et al. "A theoretical study of the ground state and lowest excited states of $PuO^{0/+/+2}$ and $PuO_2^{0/+/+2}$". In: Phys. Chem. Chem. Phys. 48 (2008), pp. 7278–7283.

[193] E. G. Rauh and R. J. Ackermann. "First ionization potentials of some refractory oxide vapors". In: The Journal of Chemical Physics 60.4 (1974), pp. 1396–1400. DOI: 10.1063/1.1681210.

[194] F. Capone et al. "Mass Spectrometric Measurement Of the Ionization Energies and Cross Sections Of Uranium and Plutonium Oxide Vapors". In: The Journal of Physical Chemistry A 103.50 (1999), pp. 10899–10906. DOI: 10.1021/jp992405f.

[195] Marta Santos et al. "Gas-Phase Oxidation Reactions of Neptunium and Plutonium Ions Investigated via Fourier Transform Ion Cyclotron Resonance Mass Spectrometry". In: The Journal of Physical Chemistry A 106.31 (2002), pp. 7190–7194. DOI: 10.1021/jp025733f.

[196] F. Capone et al. "Controversy on the First Ionization Potential of PuO2 (Nearly) Settled by New Experimental Evidence". In: The Journal of Physical Chemistry A 109.51 (2005), pp. 12054–12058. DOI: 10.1021/jp055452i.

[197] E. R. Batista et al. "Density functional investigations of the properties and thermochemistry of UF_6 and UF_5 using valence-electron and all-electron approaches". In: J. Chem. Phys. 121 (2004), pp. 2144–2150. DOI: 10.1063/1.1768518.

[198] E. H. P. Cordfunke and R. J. M. Konings. "Thermochemical data for reactor materials and fission products: The ECN database". In: Journal of Phase Equilibria 14.4 (1993), pp. 457–464. ISSN: 1054-9714. DOI: 10.1007/BF02671964.

[199] Oscar H. Krikorian et al. "Transpiration studies on the volatilities of PuO3(g) and PuO2(OH)2(g) from PuO2(s) in the presence of steam and oxygen and application to plutonium volatility in mixed-waste thermal oxidation processors". In: Journal of Nuclear Materials 247 (1997). Thermodynamics of Nuclear Materials, pp. 161 –171. ISSN: 0022-3115. DOI: https://doi.org/10.1016/S0022-3115(97)00043-3.

[200] Attila Kovács et al. "Quantum Chemical Calculations and Experimental Investigations of Molecular Actinide Oxides". In: Chem. Rev. 115.4 (2015), pp. 1725–1759. DOI: 10.1021/cr500426s.

[201] Faoulat Miradji et al. "Thermodynamic Properties of Gaseous Ruthenium Species". In: J. Phys. Chem. A 119.20 (2015), pp. 4961–4971. DOI: 10.1021/acs.jpca.5b01645.

[202] Wanyi Jiang et al. "Comparative Study of Single and Double Hybrid Density Functionals for the Prediction of 3d Transition Metal Thermochemistry". In: Journal of Chemical Theory and Computation 8.11 (2012), pp. 4102–4111. DOI: 10.1021/ct300455e.

[203] Lars Goerigk and Stefan Grimme. "Efficient and Accurate Double-Hybrid-Meta-GGA Density Functionals—Evaluation with the Extended GMTKN30 Database for General Main Group Thermochemistry, Kinetics, and Noncovalent Interactions". In: Journal of Chemical Theory and Computation 7.2 (2011), pp. 291–309. DOI: 10.1021/ct100466k.

[204] Stefan Grimme. "Semiempirical hybrid density functional with perturbative second-order correlation". In: The Journal of Chemical Physics 124.3 (2006), p. 034108. DOI: 10.1063/1.2148954.

[205] Emmanuel Fromager. "Rigorous formulation of two-parameter double-hybrid density-functionals". In: The Journal of Chemical Physics 135.24 (2011), p. 244106. DOI: 10.1063/1.3671384.

[206] Julien Toulouse et al. "Communication: Rationale for a new class of double-hybrid approximations in density-functional theory". In: The Journal of Chemical Physics 135.10 (2011), p. 101102. DOI: 10.1063/1.3640019.

[207] Kamal Sharkas, Julien Toulouse, and Andreas Savin. "Double-hybrid density-functional theory made rigorous". In: The Journal of Chemical Physics 134.6 (2011), p. 064113. DOI: 10.1063/1.3544215.

[208] Tobias Schwabe and Lars Goerigk. "Time-Dependent Double-Hybrid Density Functionals with Spin-Component and Spin-Opposite Scaling". In: Journal of Chemical Theory 13.9 (2017), pp. 4307–4323. DOI: 10.1021/acs.jctc.7b00386.

[209] Stefan Grimme and Frank Neese. "Double-hybrid density functional theory for excited electronic states of molecules". In: The Journal of Chemical Physics 127.15 (2007), p. 154116. DOI: 10.1063/1.2772854.

[210] Tobias Schwabe and Stefan Grimme. "Double-hybrid density functionals with long-range dispersion corrections: higher accuracy and extended applicability". In: Phys. Chem. Chem. Phys. 9 (26 2007), pp. 3397–3406. DOI: 10.1039/B704725H.

[211] Juan Aragó, Enrique Ortí, and Juan C. Sancho-García. "Nonlocal van der Waals Approach Merged with Double-Hybrid Density Functionals: Toward the Accurate Treatment of Noncovalent Interactions". In: Journal of Chemical Theory and Computation 9.8 (2013), pp. 3437–3443. DOI: 10.1021/ct4003527.

[212] Tobias Benighaus et al. "Semiempirical Double-Hybrid Density Functional with Improved Description of Long-Range Correlation". In: The Journal of Physical Chemistry 112.12 (2008), pp. 2702–2712. DOI: 10.1021/jp710439w.

[213] Eric Brémond and Carlo Adamo. "Seeking for parameter-free double-hybrid functionals: The PBE0-DH model". In: The Journal of Chemical Physics 135.2 (2011), p. 024106. DOI: 10.1063/1.3604569.

[214] Jeng-Da Chai and Shan-Ping Mao. "Seeking for reliable double-hybrid density functionals without fitting parameters: The PBE0-2 functional". In: Chemical Physics Letter 538 (2012), pp. 121 –125. ISSN: 0009-2614. DOI: https://doi.org/10.1016/j.cplett.2012.04.045.

[215] Jeng-Da Chai and Martin Head-Gordon. "Long-range corrected hybrid density functionals with damped atom–atom dispersion corrections". In: Phys. Chem. Chem. Phys. 10 (44 2008), pp. 6615–6620. DOI: 10.1039/B810189B.

[216] Bun Chan and Leo Radom. "Obtaining Good Performance With Triple-Type Basis Sets in Double-Hybrid Density Functional Theory Procedures". In: Journal of Chemical Th 7.9 (2011), pp. 2852–2863. DOI: 10.1021/ct200396x.

[217] Lars Goerigk and Stefan Grimme. "A thorough benchmark of density functional methods for general main group thermochemistry, kinetics, and noncovalent interactions". In: Phys. Chem. Chem. Phys. 13 (14 2011), pp. 6670–6688. DOI: 10.1039/C0CP02984J.

[218] David C. Graham et al. "Optimization and Basis-Set Dependence of a Restricted-Open-Shell Form of B2-PLYP Double-Hybrid Density Functional Theory". In: The Journal of Physical Chemistry A 113.36 (2009). PMID: 19645437, pp. 9861–9873. DOI: 10.1021/jp9042864.

[219] Amir Karton et al. "Highly Accurate First-Principles Benchmark Data Sets for the Parametrization and Validation of Density Functional and Other Approximate Methods. Derivation of a Robust, Generally Applicable, Double-Hybrid Functional for Thermochemistry and Thermochemical Kinetics". In: The Journal of Physical Chemistry A 112.50 (2008), pp. 12868–12886. DOI: 10.1021/jp801805p.

[220] Sebastian Kozuch and Jan M. L. Martin. "Spin-component-scaled double hybrids: An extensive search for the best fifth-rung functionals blending DFT and perturbation theory". In: Journal of Computational Chemistry 34.27 (), pp. 2327–2344. DOI: 10.1002/jcc.23391.

[221] Sebastian Kozuch, David Gruzman, and Jan M. L. Martin. "DSD-BLYP: A General Purpose Double Hybrid Density Functional Including Spin Component Scaling and Dispersion Correction". In: The Journal of Physical Chemistry C 114.48 (2010), pp. 20801–20808. DOI: 10.1021/jp1070852.

[222] Sebastian Kozuch and Jan M. L. Martin. "DSD-PBEP86: in search of the best double-hybrid DFT with spin-component scaled MP2 and dispersion corrections". In: Phys. Chem. Chem. Phys. 13 (45 2011), pp. 20104–20107. DOI: 10.1039/C1CP22592H.

[223] Afshan Mohajeri and Mojtaba Alipour. "B2-PPW91: A promising double-hybrid density functional for the electric response properties". In: The Journal of Chemical Physics 136.12 (2012), p. 124111. DOI: 10.1063/1.3698284.

[224] Roberto Peverati and Martin Head-Gordon. "Orbital optimized double-hybrid density functionals". In: The Journal of Chemical Physics 139.2 (2013), p. 024110. DOI: 10.1063/1.4812689.

[225] J. C. Sancho-García and A. J. Pérez-Jiménez. "Assessment of double-hybrid energy functionals for conjugated systems". In: The Journal of Chemical Physics 131.8 (2009), p. 084108. DOI: 10.1063/1.3212881.

[226] Tobias Schwabe and Stefan Grimme. "Towards chemical accuracy for the thermodynamics of large molecules: new hybrid density functionals including non-local correlation effects". In: Phys. Chem. Chem. Phys. 8 (38 2006), pp. 4398–4401. DOI: 10.1039/B608478H.

[227] Sidi M. O. Souvi, Kamal Sharkas, and Julien Toulouse. "Double-hybrid density-functional theory with meta-generalized-gradient approximations". In: The Journal of Chemical Phy 140.8 (2014), p. 084107. DOI: 10.1063/1.4865963.

[228] Alex Tarnopolsky et al. "Double-Hybrid Functionals for Thermochemical Kinetics". In: The Journal of Physical Chemistry A 112.1 (2008), pp. 3–8. DOI: 10.1021/jp710179r.

[229] Julien Toulouse et al. "Communication: Rationale for a new class of double-hybrid approximations in density-functional theory". In: The Journal of Chemical Physics 135.10 (2011), p. 101102. DOI: 10.1063/1.3640019.

[230] Igor Ying Zhang et al. "Doubly hybrid density functional xDH-PBE0 from a parameter-free global hybrid model PBE0". In: The Journal of Chemical Physics 136.17 (2012), p. 174103. DOI: 10.1063/1.3703893.

[231] Igor Ying Zhang and Xin Xu. "Reaching a Uniform Accuracy for Complex Molecular Systems: Long-Range-Corrected XYG3 Doubly Hybrid Density Functional". In: The Journal of Physical Chemistry Letters 4.10 (2013), pp. 1669–1675. DOI: 10.1021/jz400695u.

[232] Ying Zhang, Xin Xu, and William A. Goddard. "Doubly hybrid density functional for accurate descriptions of nonbond interactions, thermochemistry, and thermochemical kinetics". In: Proceedings of the National Academy of Sciences (2009). ISSN: 0027-8424. DOI: 10.1073/pnas.0901093106.

[233]   Igor Ying Zhang et al. "A fast doubly hybrid density functional method close to chemical accuracy using a local opposite spin ansatz". In: Proceedings of the National Academ 108.50 (2011), pp. 19896–19900. DOI: 10.1073/pnas.1115123108.

[234]   Lars Goerigk and Stefan Grimme. "Double-hybrid density functionals". In: Wiley Interdisciplinary Reviews: Computational Molecular Science 4.6 (), pp. 576–600. DOI: 10.1002/wcms.1193.

[235]   Liam Wilbraham, Carlo Adamo, and Ilaria Ciofini. "Communication: Evaluating non-empirical double hybrid functionals for spin-state energetics in transition-metal complexes". In: The Journal of Chemical Physics 148.4 (2018), p. 041103. DOI: 10.1063/1.5019641.

[236]   Miho Isegawa, Frank Neese, and Dimitrios A. Pantazis. "Ionization Energies and Aqueous Redox Potentials of Organic Molecules: Comparison of DFT, Correlated ab Initio Theory and Pair Natural Orbital Approaches". In: Journal of Chemical Theory and Computation 12.5 (2016), pp. 2272–2284. DOI: 10.1021/acs.jctc.6b00252.

[237]   Tomasz Seidler, Katarzyna Stadnicka, and Benoît Champagne. "Evaluation of the Linear and Second-Order NLO Properties of Molecular Crystals within the Local Field Theory: Electron Correlation Effects, Choice of XC Functional, ZPVA Contributions, and Impact of the Geometry in the Case of 2-Methyl-4-nitroaniline". In: Journal of Chemical Theory and Computation 10.5 (2014), pp. 2114–2124. DOI: 10.1021/ct5001654.

[238]   Kirk A. Peterson. "Correlation consistent basis sets for actinides. I. The Th and U atoms". In: The Journal of Chemical Physics 142.7 (2015), p. 074105. DOI: 10.1063/1.4907596.

[239]   Timofei Privalov et al. "Structure and Thermodynamics of Uranium(VI) Complexes in the Gas Phase: A Comparison of Experimental and ab Initio Data". In: The Journal of Physical Chemistry A 106.46 (2002), pp. 11277–11282. DOI: 10.1021/jp0260402.

[240]   M. Dolg, H. Stoll, and H. Preuss. "Energy Aadjusted ab initio pseudopotentials for the rare earth elements". In: The Journal of Chemical Physics 90.3 (1989), pp. 1730–1734. DOI: 10.1063/1.456066.

[241]   G. V. Girichev et al. "Molecular structure and vibrational characteristics of thorium tetrafluoride". In: Journal of Structural Chemistry 40.2 (1999), p. 207.

[242]   Yu Gong et al. "Infrared Spectroscopic and Theoretical Investigations of the OUF2 and OThF2 Molecules with Triple Oxo Bond Character". In: Inorganic Chemistry 51.12 (2012), pp. 6983–6991. DOI: 10.1021/ic3009128.

[243]   Monica Vasiliu et al. "Reliable Potential Energy Surfaces for the Reactions of H2O with ThO2, PaO2(+), UO2(2+), and UO2(.)" In: J. Phys. Chem. A 119.46 (2015), pp. 11422–11431. DOI: 10.1021/acs.jpca.5b08618.

[244] Georg Schreckenbach, P. Jeffrey Hay, and Richard L. Martin. "Density functional calculations on actinide compounds: Survey of recent progress and application to [UO2X4]2-(X=F, Cl, OH) and AnF6 (An=U, Np, Pu)". In: Journal of Computational Chem 20.1 (), pp. 70–90. DOI: 10.1002/(SICI)1096-987X(19990115)20:1<70::AID-JCC9>3.0.CO;2-F.

[245] R. D. Wesley and C. W. DeKock. "Geometry and Infrared Spectra of Matrix-Isolated Rare-Earth Halides. I. LaF3, CeF3, PrF3, NdF3, SmF3, and EuF3". In: The Journal of Chemical Physics 55.8 (1971), pp. 3866–3877. DOI: 10.1063/1.1676673.

[246] Roger L. De Kock et al. "A theoretical study of the linear versus bent geometry for several MX2 molecules: MgF2, CaH2, CaF2, CeO2 and YbCl2". In: Polyhedron 9.15 (1990), pp. 1919 –1934. DOI: https://doi.org/10.1016/S0277-5387(00)84004-8.

[247] V. G. Solomonik, A. Yu. Yachmenev, and A. N. Smirnov. "Structure, force fields, and vibrational spectra of cerium tetrahalides". In: Journal of Structural Chemistry 49.4 (2008), pp. 613–620. DOI: 10.1007/s10947-008-0085-5.

[248] Tanya Mikulas et al. "Reactions of Lanthanide Atoms with Oxygen Difluoride and the Role of the Ln Oxidation State". In: Inorganic Chemistry 53.1 (2014), pp. 446–456. DOI: 10.1021/ic402422h.

[249] V. Yu. Buz'ko, G. Yu. Chuiko, and Kh. B. Kushkhov. "Ab initio study of the structure and stability of AcF n (3 -àí n)+ of complexes (n = 1-àí7)". In: Russian Journal of Inorganic Chemistry 57.6 (2012), pp. 838–842.